



Terms and Conditions of Use of Digitised Theses from Trinity College Library Dublin

Copyright statement

All material supplied by Trinity College Library is protected by copyright (under the Copyright and Related Rights Act, 2000 as amended) and other relevant Intellectual Property Rights. By accessing and using a Digitised Thesis from Trinity College Library you acknowledge that all Intellectual Property Rights in any Works supplied are the sole and exclusive property of the copyright and/or other IPR holder. Specific copyright holders may not be explicitly identified. Use of materials from other sources within a thesis should not be construed as a claim over them.

A non-exclusive, non-transferable licence is hereby granted to those using or reproducing, in whole or in part, the material for valid purposes, providing the copyright owners are acknowledged using the normal conventions. Where specific permission to use material is required, this is identified and such permission must be sought from the copyright holder or agency cited.

Liability statement

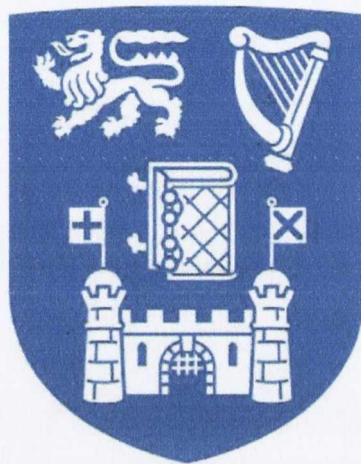
By using a Digitised Thesis, I accept that Trinity College Dublin bears no legal responsibility for the accuracy, legality or comprehensiveness of materials contained within the thesis, and that Trinity College Dublin accepts no liability for indirect, consequential, or incidental, damages or losses arising from use of the thesis for whatever reason. Information located in a thesis may be subject to specific use constraints, details of which may not be explicitly described. It is the responsibility of potential and actual users to be aware of such constraints and to abide by them. By making use of material from a digitised thesis, you accept these copyright and disclaimer provisions. Where it is brought to the attention of Trinity College Library that there may be a breach of copyright or other restraint, it is the policy to withdraw or take down access to a thesis while the issue is being resolved.

Access Agreement

By using a Digitised Thesis from Trinity College Library you are bound by the following Terms & Conditions. Please read them carefully.

I have read and I understand the following statement: All material supplied via a Digitised Thesis from Trinity College Library is protected by copyright and other intellectual property rights, and duplication or sale of all or part of any of a thesis is not permitted, except that material may be duplicated by you for your research use or for educational purposes in electronic or print form providing the copyright owners are acknowledged using the normal conventions. You must obtain permission for any other use. Electronic or print copies may not be offered, whether for sale or otherwise to anyone. This copy has been supplied on the understanding that it is copyright material and that no quotation from the thesis may be published without proper acknowledgement.

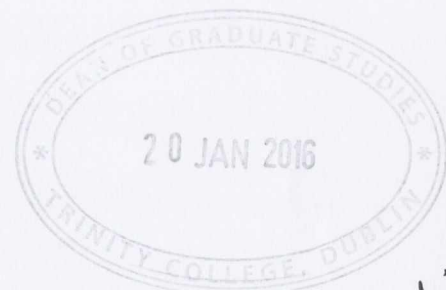
**The role of metabolism, hypoxia and
immunomodulatory therapy in regulating the human
Treg:Th17 cell axis**



Deborah Cluxton, B.A. (Mod.)

2015

Ph.D.

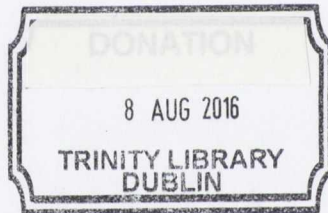


School of Medicine

A thesis submitted to Trinity College Dublin
as completion of a degree in Doctor of Philosophy

Supervisor: Prof. Jean Fletcher

School of Biochemistry and Immunology/ School of Medicine
Trinity Biomedical Science Institute
Trinity College Dublin

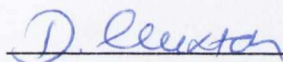


Thesis 11061

Declaration of authorship

This report represents the sole work of the author except where otherwise stated and has not been submitted in whole or in part to any other university or institution as part of a degree or other qualification.

I agree to deposit this thesis in the University's open access institutional repository or allow the library to do so on my behalf, subject to Irish Copyright Legislation and Trinity College Library conditions of use and acknowledgement.

A handwritten signature in blue ink, appearing to read "D. Cluxton", is written over a horizontal line.

Deborah Cluxton

Declaration of authorship

This report represents the sole work of the author except where otherwise stated and has not been submitted in whole or in part to any other university or institution as part of a degree or other qualification.



Abstract

Th17 cells are important pathogenic effector cells in autoimmune diseases such as rheumatoid arthritis (RA), psoriasis and multiple sclerosis (MS). On the other hand, regulatory T (Treg) cells play a crucial role in maintaining tolerance and preventing autoimmunity. Under healthy conditions there is a balance between Treg and effector T cell responses, which may be perturbed in autoimmunity, cancer and other diseases; therefore, it is crucial to understand the factors that regulate this balance. Recently, a role for metabolism and hypoxia in murine T cell differentiation has been identified.

This study examined the metabolism of CD4⁺ T cells expressing the human Th17 lineage cell marker CD161 and found that these cells had an increased glycolytic profile compared with CD4⁺CD161⁻ T cells. Additionally, Th17 cells demonstrated increased GLUT1 expression, mTOR activity, and a reduction in Th17 cell frequencies were observed following glycolytic inhibition via glucose supplementation and rapamycin treatment. CD161⁺ T cells demonstrated increased expression of Bcl-2, Ki67 and HIF-1 α . The RA joint represents a hypoxic environment and demonstrates an increased expression of GLUT1. Additionally, CD161⁺ Th17 lineage cells were increased in the synovial fluid of RA patients and expressed increased GLUT1 in vivo. The study of hypoxia in vitro however, demonstrated a decrease in Th17 cells in hypoxia, with no change in GLUT1 expression and an increase in HIF-1 α for Th17 cells. This suggests an association between the lack of increased glycolytic activity and an inhibition of Th17 cells in hypoxia in vitro. Additionally, human Treg cells demonstrated utilisation of both glycolysis, supported by increased GLUT1 and ECAR via the Seahorse Analyzer, and mitochondrial respiration, supported by increased OCR and an expansion of Treg cells following inhibition of glycolysis. Treg cell frequencies were enhanced in the SFMC of RA patients, in conjunction with increased GLUT1 and HIF-1 α expression. This result was mirrored in hypoxia in vitro. Treg cell expansion in hypoxia in vitro was unchanged following the inhibition of TGF- β 1, HIF-1 α and glycolysis. However, treatment with TEPP-46 and activation of PKM2, known to inhibit glycolysis and HIF-1 α activity, demonstrated a decrease in Treg cell expansion in hypoxia.

Finally, the study of the effect of FumadermTM treatment in vivo on T cell subsets in psoriasis revealed a significant decrease in Th17 and exTh17 cells (highly polyfunctional and pathogenic subset generated from a Th17 cell precursor), and an increase in Treg cells in psoriasis patient blood. Thus FumadermTM treatment appears to favourably modulate the Treg:Th17 axis.

In conclusion, the data suggests that Th17 cells utilise glycolysis, while Treg cells have the capacity to employ both glycolysis and mitochondrial respiration in vitro. Additionally, increased Treg cell frequencies in vivo in RA and in vitro in hypoxia may be orchestrated by both glycolysis and HIF-1 α expression. The Treg/Th17 cell balance is crucial to maintain optimal immunity, and this study provides insight into the possible targeting of the Treg:Th17 cell axis by metabolism and hypoxia in autoimmune and inflammatory disease.

The first part of the document discusses the importance of maintaining accurate records of all transactions. It emphasizes that proper record-keeping is essential for the success of any business and for the protection of the interests of all parties involved. The document outlines the various methods and systems that can be used to ensure the accuracy and reliability of the records.

The second part of the document provides a detailed description of the accounting system that has been implemented. It explains how the system is designed to handle all aspects of the business's financial operations, from the recording of transactions to the preparation of financial statements. The document also discusses the various controls and checks that are in place to ensure the integrity of the system and to prevent any errors or fraud.

The third part of the document discusses the various reports and statements that are generated by the accounting system. It explains how these reports provide valuable information to management and to other stakeholders, and how they can be used to make informed decisions about the business's performance and future prospects.

The final part of the document provides a summary of the key points discussed throughout the document. It reiterates the importance of accurate record-keeping and the role of the accounting system in ensuring the success of the business. The document concludes with a statement of confidence in the system and a commitment to ongoing improvement and innovation.

Acknowledgements

Firstly, I would like to thank my wonderful Mam, who has loved and supported me in everything I've done and whose pride in me studying the immune system has spurred me on when science just doesn't seem to be going my way. To my brother Chris, who introduced me to a career in science and is an absolute inspiration. To Jay, for your continual love, support and encouragement throughout my project and for making me laugh when times get tough. Additionally, I would like to thank all my friends for their support, and apologize for my lack of communication over the last few months.

I would like to thank Professor Kingston Mills for his guidance and wisdom as a mentor. I would like to thank Dr. Aisling Dunne for her ideas and suggestions during lab meetings. To Barry Moran for all his technical support with flow cytometry and cell sorting. To all of the guys in the PRTL group who are always there to help resolve any science problems I may have, with the help of the occasional trip to the pub. I'd like to thank the guys in St. Vincent's. To Mary, Trudy and Wei, for their advice and constantly starting up the hypoxia chamber for me, and to Cheryl and Prof. Brian Kirby for providing psoriasis samples.

To Jamal, who has helped me immensely by taking on the run of the lab in the months leading up to my thesis submission. To the one and only Sharee Basdeo, for teaching me the ropes of human research and filling the lab with laughter. You make flow cytometry look easy and are an absolute inspiration.

Finally, I would like to thank Dr. Jean Fletcher for all her patience and support throughout the project. She has been a truly brilliant teacher, supervisor and PI and I am very excited to see where the research will take us in the future.

I would like to greatly acknowledge the PRTL scheme and the Higher Education Authority for funding my research project.

Publications and Presentations

Basdeo S.A., Moran B., **Cluxton D.**, Canavan M., McCormick J., Connolly M., Orr C., Mills K.H., Veale D.J., Fearon U., Fletcher J.M. Polyfunctional, pathogenic CD161+ TH17 lineage cells are resistant to regulatory T cell-mediated suppression in the context of autoimmunity. *The journal of Immunology*, 2015. 195(2): 528-40

Cluxton D., Basdeo S.A., Moran B., Mills K.H., Fletcher J.M., The role of metabolism and hypoxia in the regulation of human T-cell subsets. *Immunology*, 2014. 143:72-73 (oral presentation abstract publication)

Oral Presentations

The role of metabolism and hypoxia in the regulation of human T cells. *Metabolism and Immunity*, 2014, Trinity Biomedical Sciences Institute, Ireland.

The role of metabolism and hypoxia in the regulation of human T cells. PRTL External Advisory Committee Meeting, 2014, University College Cork, Ireland.

The role of metabolism and hypoxia in the regulation of human T cells. Irish Society for Immunology, 2014, Crowne Plaza, Santry, Ireland.

The role of metabolism and hypoxia in the regulation of human T cells. British Society of Immunology, 2014, Brighton Convention Centre, United Kingdom.

List of abbreviations

2-DG	2-deoxy-d-glucose
ADP	adenosine diphosphate
Akt	protein kinase B
AMPK	AMP-activated protein kinase
APC	antigen presenting cell
ATP	adenosine triphosphate
Bcl	B-cell lymphoma
CCL	CC chemokine ligand
CCR	C-C motif receptor
CD	cluster of differentiation
cDNA	complimentary deoxyribonucleic acid
CFSE	carboxyfluorescein succinimidyl ester
CLR	C-type lectin receptors
CTLA-4	cytotoxic T-lymphocyte antigen 4
CTV	celltrace® violet
CXCR	C-X-C motif receptor
DAMPs	danger-associated molecular patterns
DC	dendritic cell
DMF	dimethyl fumarate
DMOG	dimethyloxaloylglycine
DSS	disuccinimidyl suberate
ECAR	extracellular acidification rate
ELISA	enzyme-linked immunosorbent assay
ETC	electron transport chain
FACS	fluorescence-activated cell sorting
FAO	fatty acid oxidation
FCCP	carbonyl cyanide-4-(trifluoromethoxy)phenylhydrazine
FLC	fibroblast-like synoviocyte
Foxp3	forkhead box P3
GATA3	globin transcription factor 3
GM-CSF	granulocyte-macrophage colony-stimulating factor
HIF	hypoxia-inducible factor
IDO	indoleamine 2, 3-dioxygenase
IFN	interferon
Ig	immunoglobulin
IL	interleukin
IL-2R	interleukin-2 receptor
ITAM	immunoreceptor tyrosine-based activation motif
JAK	janus kinase
JIA	juvenile idiopathic arthritis

Lt1	lectin-like transcript 1
MACS	magnetic-activated cell sorting
MFI	median fluorescence intensity
MHC	major histocompatibility complex
MMP	mitochondrial membrane potential
mRNA	messenger ribonucleic acid
MS	multiple sclerosis
mTOR	mammalian target of rapamycin
mTORC	mTOR complex
NADH	nicotinamide adenine dinucleotide
NK	natural killer
NKT	natural killer T
NKRP1	natural killer receptor protein 1
OCR	oxygen consumption rate
ODD	oxygen-dependent degradation domain
PAMPs	pathogen-associated molecular patterns
PBMC	peripheral blood mononuclear cells
PDK	3-phosphoinositide dependent protein kinase-1
PHD	prolyl hydroxylase
PI3K	phosphatidylinositol-4,5-bisphosphate 3-kinase
PILAR	proliferation-induced lymphocyte-associated receptor
PIP2	phosphatidylinositol 4,5-bisphosphate
PIP3	phosphatidylinositol 3-phosphate
PKM	pyruvate kinase M
PMA	phorbol-12-myristate-13-acetate
PML	progressive multifocal leukoencephalopathy
PRR	pathogen recognition receptor
RA	rheumatoid arthritis
RANKL	Receptor activator of nuclear factor kappa-B ligand
RNA	ribonucleic acid
ROR γ t	RAR-related orphan receptor gamma
ROS	reactive oxygen species
SFMC	synovial fluid mononuclear cells
SLE	systemic lupus erythematosus
STAT	signal transducer and activator of transcription
Tbet	T-box transcription factor
Tc	cytotoxic T cell
TCA	tricarboxylic acid
T _{CM}	central memory T cell
TCR	T-cell receptor
Teff	effector T cell
T _{EM}	effector memory T cell
TGF	transforming growth factor

Th	helper T cell
TLR	toll-like receptor
TNF	tumor necrosis factor
Treg	regulatory T cell
VHL	Von-Hippel Lindau

Table of Contents

Declaration of authorship	i
Abstract	iii
Acknowledgements.....	v
Publications and Presentations.....	vi
List of abbreviations	vii
Chapter 1. Introduction	1
1.1 The immune system	1
1.2 Innate immunity	3
1.3 Adaptive immunity.....	4
1.3.1 B cells	5
1.3.2 T cells.....	5
1.4 Autoimmunity.....	17
1.4.1 Psoriasis.....	18
1.4.2 Rheumatoid Arthritis	21
1.5 Cellular metabolism	25
1.5.1 Immunometabolism.....	25
1.5.2 T cell activation	26
1.5.3 CD4 and CD8 T cell metabolism	29
1.5.4 Metabolism and T cell differentiation; the Th17/Treg balance.....	30
1.6 Hypoxia.....	31
1.6.1 Hypoxia-inducible factors	31
1.6.2 HIF-1 α as a regulator of the Th17/Treg cell balance	34
1.7 Aims.....	37
Chapter 2. Methods	39
2.1 Cell sources	39
2.2 Isolation of PBMC from blood packs.....	39

2.3 T cell purification by Magnetic Activated Cell Sorting (MACS)	39
2.3.1 CD4 ⁺ T cell sorting by positive selection	39
2.3.2 CD4 ⁺ T cell sorting by negative selection	40
2.3.3 Memory CD4 ⁺ T cell sorting by negative selection	41
2.4 Flow-cytometric staining and analysis	41
2.4.1 Surface and intracellular staining	41
2.4.2 Intranuclear staining	42
2.4.3 GLUT1 staining	43
2.4.4. Mitotracker green labelling	43
2.4.5 Cell tracer labelling	44
2.5 Glucose uptake assay	44
2.6 Measurement of glycolysis and oxidative phosphorylation by the Seahorse XF Analyzer	45
2.6.1 The determination of the optimal cell seeding density for memory CD4 ⁺ T cell analysis via the Seahorse XF Analyzer.	46
2.6.2 Optimization of the metabolic compounds required for the measurement of the metabolic activity of memory CD4 ⁺ T cells.....	46
2.7 Protein quantification by Western blotting	48
2.7.1 DSS cross-linking	48
2.7.2 Examination of TEPP-46-induced PKM2 tetramer formation in Jurkat T cells by western blot	48
2.8 Measurement of cytokine production by ELISA	49
2.9 Mitochondrial array	50
2.10 Statistical analysis	50
Chapter 3. The metabolic pathways utilized by human T cell subsets	59
3.1.1 Introduction.....	59
3.1.2 Aims.....	61
3.2 Results	62

3.2.1 The expression of GLUT1 is increased in CD4 ⁺ T cells compared with CD8 ⁺ T cells, and in effector memory versus central memory CD4 ⁺ T cells.	62
3.2.2 Investigation of the mitochondrial mass of CD4 and CD8 T cells	63
3.2.3 mTOR activity in CD4 ⁺ T cells is inhibited by rapamycin treatment	68
3.2.4 Increased mTOR activity in CD161-expressing CD4 ⁺ T cells compared with CD4 ⁺ CD161 ⁻ T cells.	68
3.2.5 GLUT1 expression and glucose uptake is increased in CD4 ⁺ CD161 ⁺ T cells compared with CD4 ⁺ CD161 ⁻ T cells.....	72
3.2.6 Stimulation of memory CD4 ⁺ T cells is required for glycolytic profile generation.	75
3.2.7. The metabolic profiles of memory CD4 ⁺ CD161 ⁺ and CD4 ⁺ CD161 ⁻ T cells.	76
3.2.7a Memory CD4 ⁺ CD161 ⁺ Th17 lineage cells exhibit an increased glycolytic profile compared with CD4 ⁺ CD161 ⁻ T cells.....	76
3.2.7b Memory CD4 ⁺ CD161 ⁺ Th17 lineage cells exhibit a decreased mitochondrial respiration profile compared with CD4 ⁺ CD161 ⁻ T cells.....	79
3.2.8 Examination of mTOR activity in Treg cells.....	81
3.2.9. GLUT1 expression is increased in Treg cells compared with CD4 ⁺ CD161 ⁻ T cells.	83
3.2.10. The metabolic profile of Treg cells compared with CD4 ⁺ CD161 ⁺ and CD4 ⁺ CD161 ⁻ T cells.....	85
3.2.10a Treg cells exhibit an increased basal and maximal glycolytic activity compared with CD4 ⁺ CD161 ⁻ T cells.....	85
3.2.10b Investigation of the mitochondrial metabolic profile of Treg cells	85
3.2.11 A trend towards increased mitochondrial mass in Treg cells.....	86
3.2.12 The effect of inhibiting glycolysis via glucose deprivation on Th17 and Treg cells	90
3.2.12a Glucose deprivation inhibits glycolysis and promotes mitochondrial respiration via the Seahorse Analyzer	90
3.2.12b The effect of inhibiting glycolysis via glucose deprivation on Th17 lineage cells.....	91

3.2.12c Treg cell frequencies are enhanced following inhibition of glycolysis by glucose deprivation.....	91
3.3 Discussion	98
Chapter 4. The role of hypoxia in the regulation of T cell subsets	105
4.1. Introduction	105
4.1.1 Aims	107
4.2 Results.....	108
4.2.1 The characteristics of Th17 lineage cells	108
4.2.1a CD4 ⁺ CD161 ⁺ T cells demonstrate an increased expression of cell survival proteins Bcl-2 and Ki67.....	108
4.2.1b Th17 lineage cells display an increased expression of HIF-1 α	108
4.2.2 The survival characteristics of exTh17 cells.....	109
4.2.3 Culture of CD4 ⁺ T cells in reduced oxygen results in increased HIF-1 α expression.	113
4.2.4. The effect of hypoxia on the expression of GLUT1 by CD4 ⁺ T cells	113
4.2.5 The effect of hypoxia on the expression of mitochondrial genes	114
4.2.6 HIF-1 α expression is increased in CD4 ⁺ CD161 ⁺ T cells in hypoxia.....	120
4.2.7 The effect of hypoxia on T helper cell survival and expansion.....	120
4.2.8 The effect of hypoxia on exTh17 cells	125
4.2.9. CD4 ⁺ IL-17 ⁺ cell frequencies are increased following cytokine stimulations in hypoxia.....	125
4.2.10. IL-17, IFN- γ and IL-10 production by PBMC is decreased in hypoxia	129
4.2.11. The effect of hypoxia on the expression of GLUT1 in CD4 ⁺ CD161 ⁺ T cells.....	129
4.2.12 Treg cell frequencies are increased in hypoxia.....	132
4.2.13 HIF-1 α expression is significantly increased in Treg cells in hypoxia	132
4.2.14 GLUT1 expression is significantly increased in Treg cells in hypoxia.....	135
4.2.15. TGF- β production is significantly increased in hypoxia	135
4.2.16. The effect of TGF- β receptor inhibition on Treg cell generation in hypoxia.	138

4.2.17. Increased frequency of Th17 lineage cells and Treg cells in the inflamed synovial joint of RA patients.	138
4.2.18. Increased expression of GLUT1 in CD4 ⁺ T cells from the synovial joints of RA patients, accompanied by increased GLUT1 expression in Th17 and Treg cells.	144
4.3 Discussion.....	148
Chapter 5. Modulation of the Treg:Th17 cell axis in vitro and in vivo.....	157
5.1.1 Introduction	157
5.1.2 Aims.....	160
5.2 Results.....	161
5.2.1 Inhibition of glycolysis and mTOR by rapamycin results in the inhibition of T helper cells	161
5.2.2 Inhibition of glycolysis and mTOR by rapamycin results in an enhancement of Treg cell frequencies	162
5.2.3. TEPP-46 treatment of human cells promotes PKM2 tetramer formation.	168
5.2.4. The effect of TEPP-46 treatment on CD4 ⁺ T helper cell subsets in normoxia.	171
5.2.5. The effect of TEPP-46 treatment on Treg cells in normoxia.....	171
5.2.6. The effect of inhibiting HIF-1 α via YC-1 treatment on CD4 ⁺ T cell subsets in normoxia.	172
5.2.7. The manipulation of metabolic pathways in hypoxia and the effect on T cell subsets.	178
5.2.8. The effect of TEPP-46 treatment on CD4 ⁺ T cell subsets in hypoxia.	182
5.2.9 The effect of inhibiting HIF-1 α via YC-1 treatment on the frequency of Treg cells in hypoxia.....	185
5.2.10 Details of untreated and Fumaderm TM -treated psoriasis patients	188
5.2.11 CD4 ⁺ CD161 ⁺ cells in psoriasis and the effect of Fumaderm TM treatment.....	188
5.2.12 Increased frequencies of CD4 ⁺ IL-17 ⁺ and CD4 ⁺ IL-17 ⁺ IFN- γ ⁺ T cells in untreated psoriasis patients compared with Fumaderm TM -treated psoriasis patients and healthy controls	189

5.2.13 Th17 lineage cells and exTh17 cells are increased in untreated patients compared with Fumaderm™-treated patients	190
5.2.14 The effect of Fumaderm™ on GM-CSF and IL-22-expressing CD4 ⁺ T cells.	195
5.2.15 The effect of Fumaderm™ on IL-2 and TNF-α-expressing CD4 ⁺ T cells.	195
5.2.16. The effect of Fumaderm™ treatment on regulatory T cell frequencies in psoriasis.	199
5.2.17 The direct effect of Fumaderm™ on CD4 ⁺ CD161 ⁺ T cells in psoriasis	202
5.2.18 The direct effect of Fumaderm™ treatment on IL-17 and IFN-γ cytokine expression by CD4 ⁺ T cells.	202
5.2.19 ExTh17 cells are reduced in psoriasis patients following Fumaderm™ treatment.	205
5.2.20 The direct effect of Fumaderm™ treatment on GM-CSF and IL-22 expressing CD4 ⁺ T cells.....	205
5.2.21 The direct effect of Fumaderm™ treatment on TNF-α and IL-2 cytokine expressing CD4 ⁺ T cells.	208
5.2.22 Treg cells are enhanced in psoriasis patients post-Fumaderm™ treatment.....	208
5.3 Discussion	212
Chapter 6. General discussion and future work	223
6.1 General discussion	223
6.2 Future experiments	231
Appendix 1. Materials	233
References	238

Chapter 1

Introduction

Chapter 1. Introduction

1.1 The immune system

The environment in which most organisms live is one vastly inhabited by microbes, many of which are infectious, and in some cases, result in the development of disease. The immune system provides defence against this ever-present threat. The co-evolution of both organisms and pathogenic agents has pressured the immune system into becoming a fine-tuned, highly specific and adaptable system for the recognition of foreign agents.

The immune system is comprised of a number of organs and processes which function primarily to resist infection to the host caused by pathogens. It consists of layers of defence of increasing specificity for pathogens. Physical barriers prevent pathogens, such as bacteria and viruses, from entering the organism. If a pathogen breaches these barriers, the innate immune system provides an immediate, but non-specific response. If pathogens successfully evade the innate response, vertebrates possess a third layer of protection, the adaptive immune system, which is assisted in its activation by the innate response. Here, the immune system adapts its response during an infection to improve its recognition of the specific pathogen. This response is retained after pathogen elimination in the form of an immunological memory and allows the adaptive immune system to mount faster and stronger attacks each time the pathogen is encountered.

To function accordingly, the immune system must recognise and distinguish between foreign and self-molecules, and be self-tolerant. However, failures of tolerance do occur, resulting in an overreaction or inappropriate response of the immune system to self-antigens. This can cause inflammatory or autoimmune disease if immunity is not appropriately controlled; while at the same time, excessive or over regulation of the immune system can prevent clearance of chronic infections or malignant cells [Figure 1.1]. Therefore, a balance in the immune response to pathogens is required for efficient protection against infection and disease (Murphy, Travers et al. 2008).

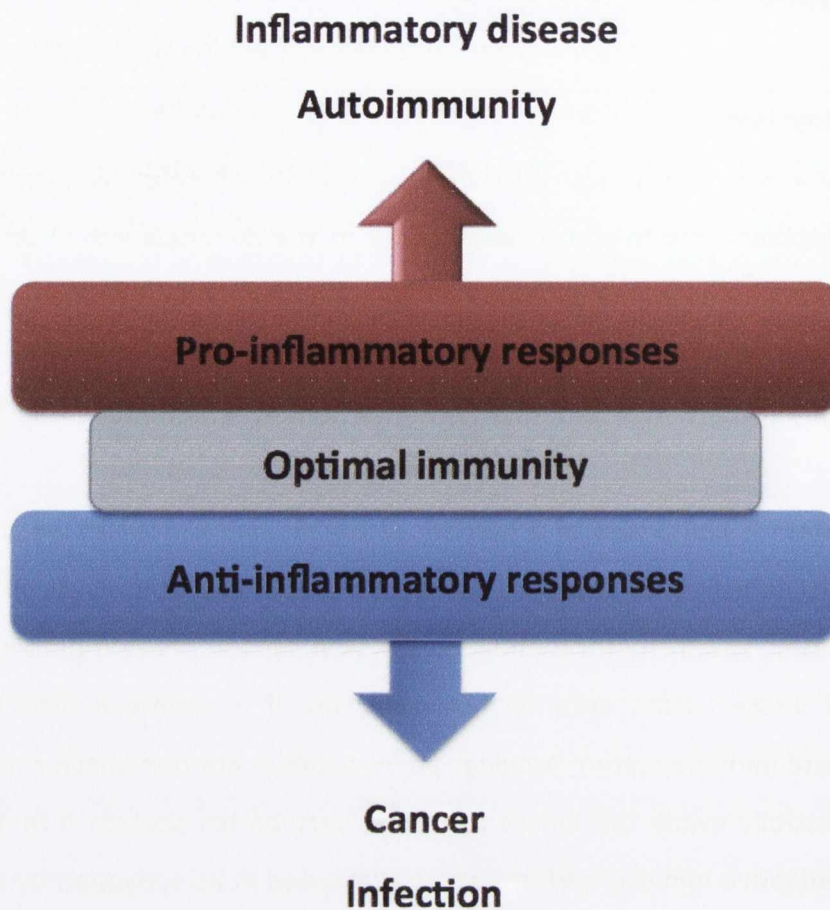


Figure 1.1 The balance between pro-inflammatory and anti-inflammatory immune responses in health and disease.

A healthy state of immune homeostasis is maintained by balancing pro-inflammatory responses with anti-inflammatory or regulatory responses of the immune system. If, however, pro-inflammatory responses outweigh immune regulation, an individual may be more susceptible to inflammatory disease and uncontrolled immune responses may be induced towards self-molecules. Conversely, if immune regulation outweighs immune responses, this can result in the development of cancer or chronic disease.

1.2 Innate immunity

The innate immune system is a broadly-specific system providing the first line of defence against invading pathogens. The cells involved in innate immunity recognise pathogens immediately and respond with antibody-mediated or cell-mediated defences. In almost all types of infection, the pathogen first encounters and must overcome the physical barriers, both fixed and free. The fixed barriers are those of the external epithelia, for example the skin, and the internal or mucosal epithelia, found in the lining of the lungs and gastrointestinal tract. Epithelial cells engulf pathogens providing a clear passage to the underlying tissue; however, these physical barriers are equipped with defensive machinery for the clearance of bacteria and viruses. The movement due to cilia in the respiratory tract aids in the removal of infectious agents. Mucus lining the mucosal epithelia consists of antiseptic enzymes and immunoglobulins (Ig) to assist in pathogen killing. However, pathogens have evolved to evade and adapt to these extreme conditions, breaching the host's physical defences. The physical barriers of the innate immune system are, therefore, not always sufficient to withstand infection, highlighting the need for a more complex immune system.

The innate immune system directly recognises and targets pathogens for destruction through engulfment (phagocytosis) by phagocytic cells, such as macrophages, neutrophils and dendritic cells (DC). These innate immune cells release granules rich in toxins for pathogen killing and mediator proteins, which activate and attract a wave of cells to the infected environment in order to facilitate pathogen clearance. This infiltration of immune cells to the site of infection is known as inflammation (Murphy, Travers et al. 2008).

Pathogen detection is essential for pathogen clearance. Innate immune cells sense molecular patterns expressed on almost all pathogenic cells, known as pathogen-associated molecular patterns (PAMPs). Cells can also recognise danger associated molecular patterns (DAMPs) released by cells following endocytosis of a pathogen. These are recognised by a specific group of receptor proteins, pattern recognition receptors (PRRs) expressed on innate immune cells. PRRs consist of the toll-like receptors (TLRs), NOD-like receptors, RIG-I-like receptors and C-type lectin receptors (Creagh and O'Neill 2006). Specific PRRs recognise specific PAMPs or DAMPS and elicit an immune response

appropriate to the nature of the invader; therefore, the response to a bacterial infection differs to that of a viral infection (Murphy, Travers et al. 2008).

Upon ligation of the PRRs, either membrane-bound or free in the cytosol, a signalling cascade is activated culminating in the translation of defensive proteins such as cytokines (small signalling molecules which mediate the maturation, growth and responsiveness of particular cell populations), chemokines (chemotactic cytokines which guide the migration of cells down a protein gradient to sites of infection or damage), and those involved in the complement cascade (involves the coating of pathogens in antibodies or opsonin proteins and tagging them for destruction by immune cells). Interestingly, it is now emerging that the innate immune system can also exhibit memory, which was previously thought to be the exclusive characteristic of the adaptive immune system. This innate training is thought to be mediated via epigenetic changes (Netea 2013).

Innate immunity has the ability to assist in the activation of the adaptive immune response, providing a 'reminder' of previously encountered pathogens. Upon PRR ligation, professional phagocytes such as DC and macrophages, phagocytose and degrade the pathogenic agent. Peptides processed from pathogenic proteins are loaded onto the major histocompatibility complex (MHC) and displayed at the surface. Peptides are presented to T cells and, in conjunction with the ligation of co-stimulatory molecules and regulatory cytokines, an adaptive immune response is generated. T cells have specificity for one of the two MHC molecules, with $CD4^+$ T cells binding MHC-II and $CD8^+$ T cells interacting with MHC-I. It is the presentation of antigen, along with the ligation of co-stimulatory proteins and the cytokine environment that directs the adaptive immune response (Murphy, Travers et al. 2008).

1.3 Adaptive immunity

The adaptive immune system is a highly specialised and specific system, which adapts to the infectious agents it encounters. Cells of the adaptive immune system generate a vast number of pathogen-specific receptors through gene rearrangements and recombination providing a pool of receptors for the recognition of countless pathogens. Following an infection, a pool of memory cells expressing the definitive receptor for the infectious agent survive, providing a database of effective cells, which promote a faster and

stronger immune response upon re-infection. Immunological memory can be short-term, such as the passing of immunity from mother to baby during pregnancy, or long-term following infection or immunization as a result of vaccination (Murphy, Travers et al. 2008). The two major cell types involved in acquired immunity are T and B lymphocytes. In the bone marrow, T and B cells are derived from a common lymphoid progenitor cell in a process termed lymphopoiesis. They undergo testing of their reactivity towards self-molecules and are eliminated through a process of clonal deletion in their respective primary lymphoid organs before further circulation to the peripheral lymphoid organs, such as the spleen and lymph nodes.

1.3.1 B cells

B cells develop and mature in the bone marrow and circulate in the blood and peripheral lymphoid organs. Each B cell expresses a unique receptor protein, the B-cell receptor (BCR), for a specific pathogen. The BCR is a membrane-bound immunoglobulin protein, which recognises its cognate antigen in its native form. Upon antigen stimulation, B cells can mature into memory B cells, providing a rapid immune response upon re-infection. B cells can also mature into plasma cells producing pathogen-specific antibodies, which coat the pathogen, resulting in the activation of phagocytes and the complement pathway. Antibodies come in five different varieties or isotypes differing in their biological properties, functional locations and ability to deal with different antigens; IgA, IgD, IgE, IgG and IgM. For maximal antibody production, B cell activation requires the assistance of a subset of primed 'helper' T cells, which provide co-stimulation and produce cytokines required for the activation/development of a B cell response (Murphy, Travers et al. 2008).

1.3.2 T cells

Various subsets of T cells exist, including helper, cytotoxic, regulatory, natural killer and $\gamma\delta$ T cells. T cells originate in the bone marrow from their progenitor lymphoid cell precursor and mature in the thymus. T cell precursors, following migration to the thymus, are described as double negative cells lacking the expression of molecules specific to the mature T cell lineage, such as the T cell receptor (TCR). Double negative T cells can give rise to two types of TCR through gene rearrangement, the $\alpha\beta$ -TCR, expressed by 95% of T cells, and the $\gamma\delta$ -TCR (Robey and Fowlkes 1994). The TCR is associated with a collection of

proteins at the cell surface, including CD3. At this stage, the T cell precursor becomes double positive in its expression of co-receptor proteins CD4 (helper) and CD8 (cytotoxic) (Germain 2002). The fate of double positive lymphocytes can be determined by their interaction with the MHC-I (developing into CD8⁺ cells) or MHC-II complexes (developing into CD4⁺ cells) on thymic cortical epithelial cells, which are presenting self-antigens. T cells undergo positive and negative selection; immature cells that interact appropriately with self MHC are selected for maturation and those that interact too strongly are negatively selected and eliminated from the T cell repertoire, as they could contribute to autoimmunity; however, some self-reactive T cells can go undetected and develop into mature T cells (Germain 2002). The cells selected for further development down-regulate either CD4 or CD8, depending upon the MHC molecule engaged, maturing into single positive T cells. These naive T cells migrate to the peripheral lymph nodes and await activation by antigen presenting cells via the TCR. The TCR exists as a complex of several proteins consisting of two CD3 heterodimers ($\epsilon\gamma$ and $\epsilon\delta$) and a CD3 ζ homodimer. Upon TCR/MHC interaction, CD3 proteins become phosphorylated on their ITAMs (immunoreceptor tyrosine-based activation motifs) subsequently recruiting various signalling proteins, ultimately resulting in downstream gene transcription. The TCR requires co-stimulation via CD28 ligation on the T cell with CD80/86 on the APC. Both TCR activation and co-stimulation are required for an effective T cell immune response; in the absence of co-stimulation, the T cell becomes anergic (Murphy, Travers et al. 2008).

CD8⁺ cytotoxic T lymphocytes (Tc) recognise antigen presented in the context of the MHC-I complex and function to combat virally infected and tumour cells. CD4⁺ T helper (Th) lymphocytes recognise antigen loaded onto the MHC-II complex on APCs and assist in fighting various infections and promote the activation of B cells; hence the name 'helper' T cells (Murphy, Travers et al. 2008).

T cell memory

Memory is a hallmark of the acquired immune system. It results from the clonal expansion and differentiation of antigen-specific lymphocytes, following the activation of naïve T cells, which ultimately persist for a lifetime. Vaccinations against disease exploit this feature of the adaptive immune system. Memory lymphocytes provide rapid protection in peripheral tissues and mount recall responses to antigens in secondary

lymphoid organs (Sallusto, Geginat et al. 2004). The memory phenotype has been divided into two subsets: effector memory (T_{EM}) cells, which migrate to inflamed peripheral tissues and display immediate effector function, and central memory (T_{CM}) cells, which home to secondary lymphoid organs (Lanzavecchia and Sallusto 2000). T_{EM} and T_{CM} cells are defined by their expression of homing receptors CCR7 and CD62L. Human T_{CM} cells are CD45RO⁺ (lymphocyte common antigen) memory cells that constitutively express the chemokine receptor 7 (CCR7), required for homing to secondary lymphoid organs, and L-selectin (CD62L), required for extravasation through the endothelia (Forster, Schubel et al. 1999). T_{EM} cells, also CD45RO⁺, lose their expression of CCR7 as they remain in the periphery, and are heterogeneous for CD62L expression. The study of T_{EM} cells can contribute to the knowledge obtained from the site of inflammation.

T helper cell differentiation

CD4⁺ T cells play central roles in the immune system; helping B cells to produce antibody, regulating macrophage function and orchestrating immune responses against a wide variety of pathogenic microorganisms. Many different types of CD4⁺ T cells have been described, each providing a specific role in adaptive immunity. The initial understanding of the existence of distinct CD4⁺ T cell populations came from the work of Mosmann and Coffman on murine CD4⁺ T cell clones (Mosmann, Cherwinski et al. 1986). Two T helper subsets were described, Th1 and Th2, distinguished by their cytokine production and the expression of different patterns of cell surface molecules. In 2003, an additional subset of CD4⁺ T cells producing interleukin (IL) 17, Th17 cells, was discovered (Aggarwal, Ghilardi et al. 2003, Harrington, Hatton et al. 2005). T follicular helper cells were described in 2008 as the major CD4⁺ T cell subset involved in B cell activation (King, Tangye et al. 2008); however, it is unclear whether this is an independent subset or a phenotypic state of each of the three effector subsets already described. Additionally, Th9 and Th22 subsets have been described; however, their role as truly distinct subsets is uncertain (Veldhoen, Uyttenhove et al. 2008, Eyerich, Eyerich et al. 2009).

The major determinant of the differentiated state of the CD4⁺ T cell is the cytokine milieu present during TCR-mediated activation of naive T cells [Figure 1.2]. By binding to their receptors on the naive T cell, polarising cytokines signal via the JAK/STAT pathway to activate specific STAT molecules which induce expression of specific transcription factors

that direct the function of Th cell subsets. Th1 cells are induced by the cytokines IL-12 and interferon (IFN)- γ , which activate STAT1 and STAT4 to promote the expression of the T-box transcription factor TBx21 (T-bet) (Szabo, Kim et al. 2000). Th1 cells produce primarily IFN- γ , a pro-inflammatory cytokine, which further promotes differentiation into the Th1 phenotype via signalling through the JAK-STAT pathway of proteins and subsequently inhibits Th2 cell differentiation (Usui, Preiss et al. 2006). Th1 cells play a key role in macrophage activation and function to combat intracellular pathogens. Th1 cells also provide help to B cells for the production of opsonising IgG antibodies. Th2 cells are induced by the presence of IL-4, which activates STAT6 and promotes expression of the transcription factor GATA3 (GATA binding protein 3) (Usui, Preiss et al. 2006). Differentiated Th2 cells produce IL-4, IL-5, IL-10 and IL-13, which activate mast cells and eosinophils, promote peristalsis and serve to protect against parasites, including helminths. Like how IFN- γ prevents Th2 differentiation, IL-4 inhibits the differentiation of naive CD4⁺ T cells into the Th1 cell lineage.

Murine Th17 cell differentiation is induced by transforming growth factor (TGF)- β and IL-6 (Bettelli, Carrier et al. 2006). The crucial initial cytokines required for Th17 cell differentiation in humans remains somewhat unclear. Chen et al. showed that IL-23 was able to drive Th17 cell differentiation, and Wilson et al. found that culture with either IL-23 or IL-1 stimulated the Th17 cell phenotype, with little or no synergy when both cytokines were present (Chen, Tato et al. 2007, Wilson, Boniface et al. 2007). In contrast, Acosta-Rodriguez et al. identified IL-1 as driving human Th17 cells in vitro, with IL-23 and IL-6 able to potentiate the effects of IL-1 (Acosta-Rodriguez, Napolitani et al. 2007). The role of TGF- β in human Th17 cell differentiation also remains controversial. There is evidence that a high dose of TGF- β abrogates Th17 cell differentiation in human lymphocytes; however, emphasis was placed on the requirement of low doses of this cytokine for Th17-cell differentiation (Manel, Unutmaz et al. 2008). The differentiation of Th17 cells is dependent on STAT3, which promotes expression of RAR-related orphan receptor-gamma t (ROR- γ t) the master regulator of Th17 cell function. Th17 cells produce IL-17A, IL-17F, IL-21, IL-22, IL-26, GM-CSF and TNF- α (Ivanov, McKenzie et al. 2006). Th17 cells provide important defence against extracellular bacteria and fungi.

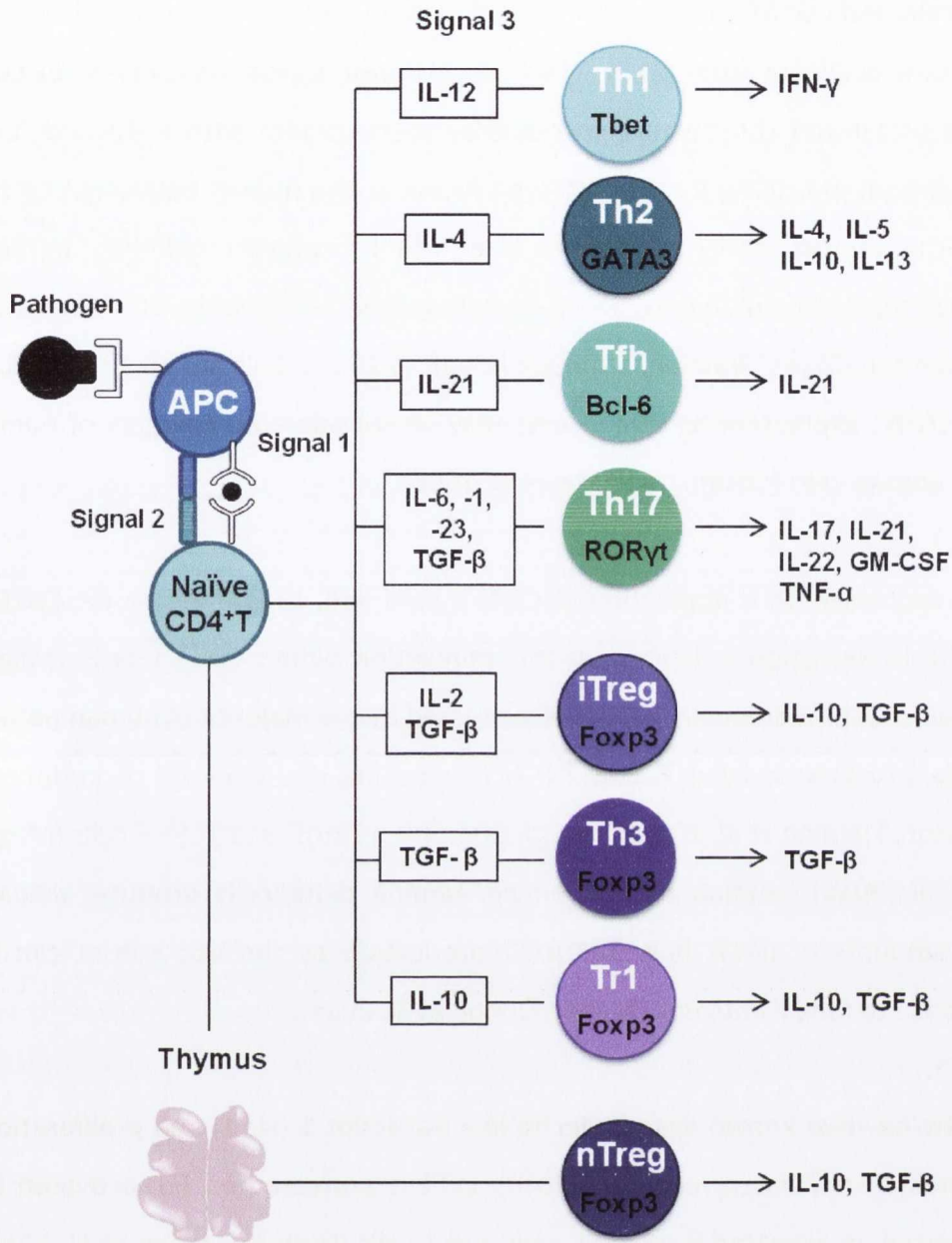


Figure 1.2 CD4⁺ T helper and regulatory cell differentiation

Upon activation of the PRRs on innate immune APCs, the pathogen is phagocytosed and processed. Antigenic peptides are presented on the MHC-II to the TCR of naive T cells within the lymph node (signal 1). In conjunction with co-stimulation through CD28-CD80/86 binding (signal 2), the T cell becomes activated and, depending on the cytokines present in the environment (signal 3), differentiates into one of five T cell subsets. T helper and T regulatory cells express distinct cytokine profiles. Natural/thymic Treg cells develop in the thymus in response to self-antigen. Inducible/peripheral Treg cells, including iTregs, Tr1 and Th3 cells develop in the periphery from naive CD4 T cells in the presence of antigen and specific cytokines.

Human Th17 cells and CD161

Human Th17 cells originate from CD161⁺ CD4⁺ naive T-cell precursors, present in both umbilical cord blood and the thymus, in response to treatment with IL-1 β and IL-23 (Cosmi, De Palma et al. 2008). CD161, a C-type lectin, is the human equivalent to the members of the mouse family of natural killer cell receptor-P1 (NKRP1). In both peripheral blood and inflamed tissues, IL-17A-secreting, RORC-expressing, CD4⁺ T cells are contained within the CD161⁺ fraction, although not all CD161⁺ T cells are able to produce IL-17A. Thus, CD161 expression on CD4⁺ T cells may be considered a hallmark of human memory Th17 lineage cells (Cosmi, De Palma et al. 2008).

CD161 is also expressed on a population of CD8⁺ T cells and, as is the case for CD161⁺ CD4⁺ T cells; IL-17 secretion is limited to this population within CD8⁺ T cells (Maggi, Santarlasci et al. 2010). Additionally, CD161 is expressed by the majority of human natural killer (NK) cells and natural killer T cells (NKT) (composing less than 1% of peripheral blood) (Fergusson, Fleming et al. 2011), and on CD4⁻CD8⁻TCR $\alpha\beta$ ⁺ and TCR $\gamma\delta$ ⁺ cells (Maggi, Santarlasci et al. 2010). Human blood derived gamma delta cells produce virtually undetectable amounts of IL-17, however IL-17 production by the V δ 1 subset can be driven in response to fungal antigens (Maher, Dunne et al. 2015).

CD161 currently has two known ligands; lectin-like transcript 1 (LLT1) and proliferation-induced lymphocyte-associated receptor (PILAR). LLT1 is expressed on TLR activated DC and is up-regulated on activated B cells, NK cells and T cells (Germain, Meier et al. 2011). The ligation of CD161 with LLT1 inhibits IFN- γ production in NK cells and conversely, enhances IFN- γ and IL-17 production by T cells. PILAR is expressed on lymphocytes and its expression is up-regulated in T cells following TCR stimulation. In the absence of co-stimulation via CD28, PILAR increases the proliferation of naïve T cells and induces the production of cytokines, suggesting that CD161 acts as a co-stimulatory molecule (Huarte, Cubillos-Ruiz et al. 2008).

In addition to CD161, the expression of the IL-23 receptor, CCR6 and CCR4 can all be used to identify Th17 cells (Annunziato, Cosmi et al. 2012). Th17 cells are the first adaptive cells to develop during infection, and through the production of IL-17, recruit neutrophils and macrophages to the site of infection (Murphy, Travers et al. 2008). The IL-17 receptor

is widely expressed on epithelial cells and its engagement results in the release of pro-inflammatory cytokine and chemokines and anti-microbial peptides. Th17 cells play a role in the clearance of extracellular bacterial and fungal infections; however, due to their contribution to inflammation, Th17 cells have been implicated in the development and perpetuation of various autoimmune and inflammatory diseases, including rheumatoid arthritis (RA), Crohn's disease, psoriasis and multiple sclerosis (MS) (Sallusto and Lanzavecchia 2009, Fletcher, Lalor et al. 2010). Additionally, CD161⁺ Th17 cells have recently been shown to resist Treg cell suppression in RA and are highly polyfunctional in their cytokine production, suggesting an increased pathogenic profile of Th17 lineage cells in RA (Basdeo, Moran et al. 2015).

Regulatory T cells

Immune responses must be tightly controlled in order to limit potential damage to self-tissue. Thus the immune system must be suppressed following clearance of a pathogen or to prevent an immune response elicited towards self-molecules. This results in a state of unresponsiveness, or tolerance, towards self-molecules. An increase in immune suppression can benefit those suffering from inflammatory disease or undergoing organ transplantation; however, increased immune regulation can compromise the immune system's ability to fight everyday infections and recognise transformed cells. A decrease in immune regulation can result in increased instances of inflammatory and autoimmune disease, and therefore a balance between immune suppression and activation is essential for an appropriate immune response.

A subset of CD4⁺ T cells expressing the interleukin-2 receptor α chain (IL-2R α) were identified in 1995 as mediating immune tolerance through the suppression of other cells (Sakaguchi, Sakaguchi et al. 1995). They were known as regulatory T cells (Treg) and constitutively expressed other activation markers, however not exclusive to Treg cells, including OX40, tumour-necrosis factor (TNF) and the cytotoxic T lymphocyte-associated antigen 4 (CTLA-4), similar to the CD28 protein found on T cells. The transcription factor forkhead box P3 (Foxp3) was identified as an intracellular marker of Treg cells, crucial for their development and functionality (Hori, Nomura et al. 2003). Foxp3⁺ regulatory T cells can develop in the thymus (natural/thymic Treg cells), through IL-2R signalling, or can be induced in the peripheral lymphoid organs from CD4⁺CD25⁻ T cells (induced/peripheral

Treg cells) in response to antigens (allergens, food or the commensal microbiota) in the presence of IL-2 and TGF- β (Apostolou, Sarukhan et al. 2002) [Figure 1.2]. Since there is no one marker that can accurately identify Treg cells, they are currently identified using a panel of markers as CD4⁺CD25⁺CD127^{Lo}FoxP3⁺ cells. FoxP3 expression is often considered to be the hallmark of Treg cells, however since it is an intracellular transcription factor; it cannot be used to sort live Treg cells for functional studies. In addition, the use of both FoxP3 and CD25 can be problematic as these markers can be utilised to identify activated cells. Additional molecules are expressed in subsets of Treg cells including CD39, Helios, HLA-DR, ICOS and GITR (Bin Dhuban, Kornete et al. 2014). Two types of Foxp3⁻ Treg cells which originate in the periphery have been identified; Tr1 cells are characterised by their ability to produce high levels of IL-10, an anti-inflammatory cytokine, and low levels of TGF- β , whereas Th3 cells primarily secrete TGF- β (Roncarolo, Bacchetta et al. 2001, Weiner 2001). A subset of CD8⁺ regulatory T cells were among the first to show induction of immune suppression in the 1970's; however lack of identification of surface markers shifted interest towards the CD4⁺ regulatory T cells (Gershon 1975).

Treg cells require TCR triggering for their suppressive function; however, once activated, their mechanisms of cell suppression are not antigen specific. Treg cells can inhibit effector function directly or indirectly via the APC and inhibition can be mediated via cell-cell contact and/or soluble factors. The binding of CTLA-4 on Treg cells with high affinity to CD80/86 on effector T cells results in the inhibition of T cell responses (Paust, Lu et al. 2004). Ligation of CD80/86 on DC's with CTLA-4 on Treg cells results in the expression and activation of the tryptophan degrading enzyme indoleamine 2,3-dioxygenase (IDO) by the DC. This subsequently acts on neighbouring T cells, halting T cell growth (Munn, Sharma et al. 2002). In addition, CD39 which is expressed on approximately half of human Treg cells, can exert suppressive function by hydrolysing inflammatory adenosine triphosphate (ATP) to adenosine diphosphate (ADP), which is then further catabolised to form anti-inflammatory adenosine (Borsellino, Kleinewietfeld et al. 2007, Deaglio, Dwyer et al. 2007). The production of anti-inflammatory cytokines, IL-10 and TGF- β by Treg cells, also assists in T cell suppression (Taylor, Verhagen et al. 2006).

T cell plasticity

Until recently, the dogma stated that differentiation of naïve CD4⁺ cells into distinct T helper and regulatory cell subsets was an irreversible event; CD4⁺ T cells, which commit to a specific helper lineage, cannot 'switch' towards the phenotype of another. However, over time this concept has been questioned. Although the Th1-Th2 paradigm has provided the essential framework required for the identification of cytokines, transcription factors and surface molecules involved in effector T cell development, it was the first to highlight flexibility within T cell subsets. In 1995, it was revealed that Th2 cells, polarised in the presence of IL-4 for one week, converted to Th1 cells following IL-12 stimulation (Szabo, Jacobson et al. 1995). This flexibility was additionally demonstrated for Th1 cells, which having been polarized in the presence of IL-12 and anti-IL-4 antibodies for one week, converted to the Th2 phenotype after IL-4 stimulation (Murphy, Shibuya et al. 1996). This raised interest as CD4⁺ T cells are rarely exposed to only one polarising cytokine during T cell activation *in vivo*. T cell plasticity is evident across each CD4 T cell subset; Th17 cells exhibit phenotypic switching towards the Th1 and Th2 cell subsets (Lee, Turner et al. 2009) and Treg cells showed plasticity when cultured under Th1 and Th17 polarizing conditions (Oldenhove, Bouladoux et al. 2009, Wei, Wei et al. 2009). It is evident that the cytokine milieu present during T cell activation plays a critical role in both the initial subset differentiation and also the switching between subsets.

In the conventional view, each T cell subset expresses a specific transcription factor; however, recent data has shown this to be far more complicated than originally thought. For example, following viral infection, previously committed Th2 cells can express both T-bet and GATA3 simultaneously, recognised as Th2+1 cells, displaying functional properties of both T cell subsets (Hegazy, Peine et al. 2010). Also, Foxp3⁺ cells can express T-bet, GATA3, ROR γ t and Bcl-6 (the transcription factor specific for follicular T helper cells) retaining functional characteristics of each mediator. It is becoming more acceptable to describe T cell subsets as having co-expression of transcriptional mediators rather than the single master regulator. Other views on the cause of T cell plasticity include roles for micro-RNAs (small non-coding ribonucleic acids, which bind to target messenger RNAs (mRNAs) and lead to mRNA degradation or inhibition of protein translation), epigenetic regulation (the dynamic regulation of specific genes by chromatin and histone modification) and most recently cellular metabolism.

Plasticity of Th17 cells

Human Th17 cells have been extensively studied since their discovery in 2003 and have been characterised as CD161⁺CCR6⁺IL-17⁺ROR γ t⁺. Annunziato et al. first investigated plasticity within the Th17 cell lineage in 2007 in the gut of patients suffering from Crohn's disease, a type of IBD affecting the gastrointestinal tract (Annunziato, Cosmi et al. 2007). The study concentrated on the increased frequency of CD4⁺ IL-17⁺ T cells within the disease-affected areas of the gut. A remarkable proportion, about one third, of IL-17-producing CD4⁺ T cells had the ability to produce IFN- γ (Annunziato, Cosmi et al. 2007). They were referred to as Th17/Th1 cells, or non-classical Th1 cells, as IFN- γ production is characteristic of the Th1 cell phenotype. These Th1-like cells retained their expression of CD161, a marker of all IL-17 producing cells, as they gained the ability to produce IFN- γ (Cosmi, Cimaz et al. 2011). A proportion of CD161⁺ T cells were revealed to primarily express IFN- γ , demonstrating a total of three discrete subpopulations within the CD161⁺ population; bona fide Th17 cells producing IL-17 and retaining no characteristics of Th1 cells, the co-producing IL-17 and IFN- γ cells that upregulate Th1 gene transcription (Th17/Th1, Th17.1 or transitioning exTh17 cells), and finally the fully switched cells no longer producing IL-17 (exTh17 or non-classical Th1 cells) (Annunziato, Cosmi et al. 2012).

ExTh17 cells, along with the bona fide Th17 cells, also express the IL-23 receptor and the chemokine receptor CCR6. CCR6 expression on memory T cells promotes chemotaxis towards sites of infection upon interaction with its ligand CCL20 (Liao, Rabin et al. 1999). Interestingly, CCR6 expression is usually lost on memory T cells following prolonged activation; however, this is not the case for Th17 and exTh17 cells, suggesting steady recruitment in response to CCL20 (Sallusto, Kremmer et al. 1999). This finding has important implications for the long-term maintenance of Th17 cells, and may contribute to their pathogenicity. Additional support for a pathogenic role of Th17 and exTh17 cells comes from studies showing that they exhibit resistance to the suppressive activity of Treg cells (Annunziato, Cosmi et al. 2007, Basdeo, Moran et al. 2015).

Thus far, Th17 and exTh17 cells share similar characteristics, differing only in their cytokine production; however, the subsets do vary in their expression of master transcription factors, with exTh17 cells expressing both Th1- and Th17-related transcription factors Tbet and ROR γ t respectively (Annunziato, Cosmi et al. 2007). CXCR3, a chemokine receptor expressed on Th1 cells, is increased in exTh17 cells compared to

that of Th17 cells (Maggi, Santarlaschi et al. 2012). The mechanism by which Th17 cells 'switch' to IFN- γ ⁺ exTh17 cells is currently under investigation; however it has been suggested that IL-12 cytokine signalling can promote Th17 cell plasticity (Annunziato, Cosmi et al. 2007). Whether this flexibility is exclusive to IL-12 signalling is yet to be explored.

Increased frequencies of the IL-17⁺ IFN- γ ⁺ CD4⁺ T cells have been reported in patients with Crohn's disease (Annunziato, Cosmi et al. 2007, Cosmi, De Palma et al. 2008, Kleinschek, Boniface et al. 2009), in the synovial fluid of juvenile idiopathic arthritis (JIA) (Nistala, Adams et al. 2010, Cosmi, Cimaz et al. 2011) and RA patients (Basdeo et al. unpublished data). Additionally, unpublished data suggests that exTh17 cells are highly polyfunctional in their cytokine production and are resistant to Treg cell suppression, suggesting a pathogenic profile for exTh17 cells in RA (Basdeo et al unpublished). Establishing the functionality of these exTh17 cells and the mechanisms by which Th17 cells switch to IFN- γ producers could potentially unveil a new therapeutic target for inflammatory and autoimmune diseases. Recently, the role of metabolism and how cells utilise their energy supply has become a hot topic in the field of T cell differentiation and plasticity.

An outline of Th17 cell plasticity is presented in Figure 1.3.

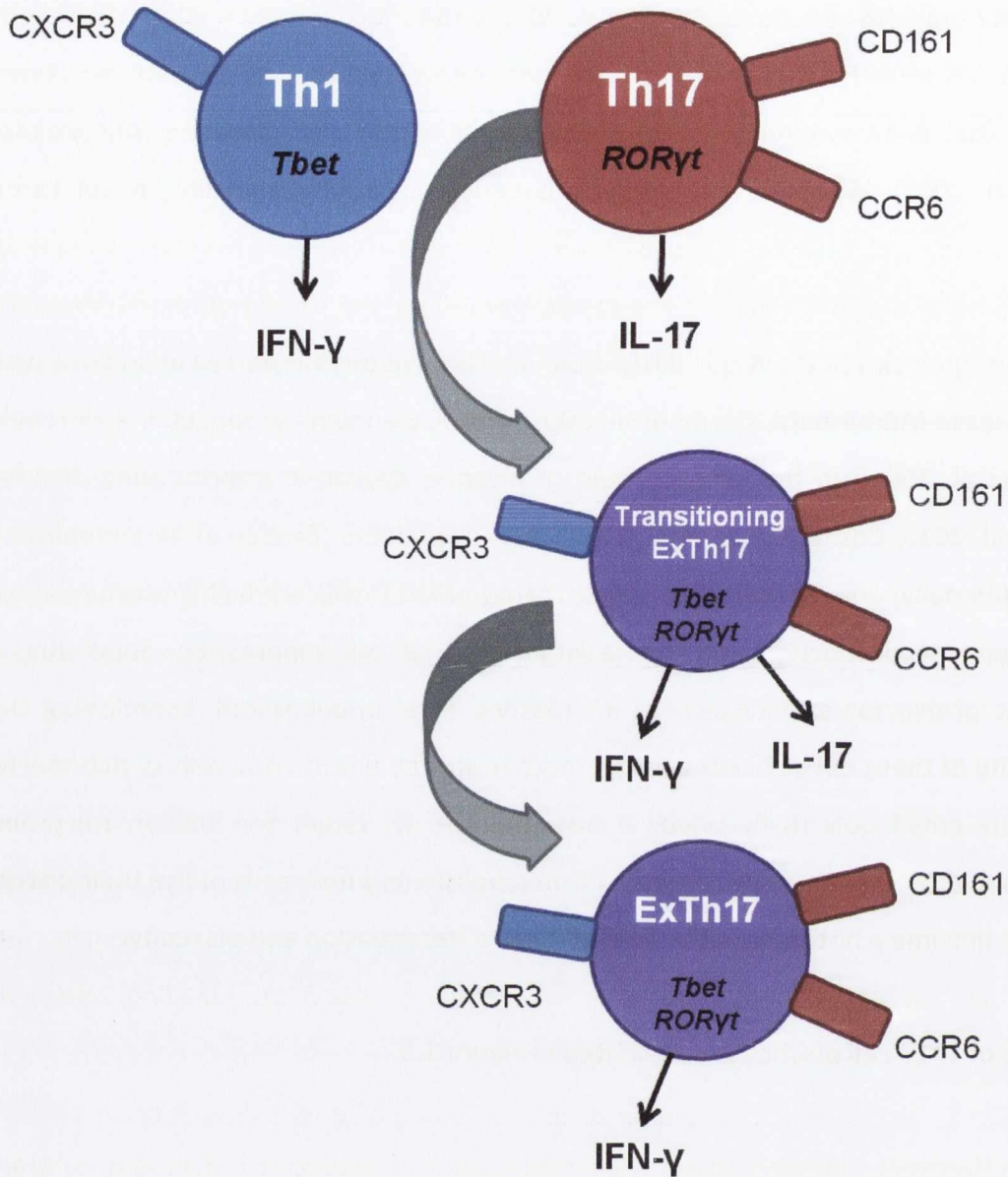


Figure 1.3 Plasticity of Th17 cells

Th1 cells (blue) express CXCR3 on their surface and primarily produce IFN- γ . Th17 cells (red) express CD161 and CCR6 on their surface, and produce IL-17 as their signature cytokine. Th17 cells have the ability to 'switch' to an exTh17 (purple) phenotype. These cells express markers of both Th1, CXCR3, and of Th17 cells, CD161 and CCR6. Transitioning exTh17 (also referred to as Th17/Th1 or Th17.1) initially co-produce IL-17 and IFN- γ , before losing IL-17 production and becoming IFN- γ producing exTh17 cells (also referred to as non-classical Th1 cells).

1.4 Autoimmunity

The immune system functions to maintain host immunity against infection. However, sometimes the immune system generates an immune response towards self-antigens and self-proteins. This can result in the development of autoimmunity, and the diseases related to this breach in self-tolerance. Nobel Laureate Paul Ehrlich, who described it as 'horror autotoxicus', first predicted the concept of autoimmunity. Autoimmune diseases affect approximately 5% of the population in Western countries, with incidences on the rise (Davidson and Diamond 2001). Autoimmunity can arise from auto-reactive T cells as a result of many triggers, with both genetic and environmental factors playing a role. Epidemiological studies have demonstrated that genetic factors are crucial determinants of susceptibility to autoimmune disease, demonstrated by higher concordance of autoimmunity in monozygotic than dizygotic twins (Davidson and Diamond 2001). Environmental changes can trigger auto-reactive cells, demonstrated for instances of MS and type I diabetes, as occurrences differ within a population as members migrate to different countries (Dahlquist 1998, Noseworthy, Lucchinetti et al. 2000). Microbial agents have the potential to initiate auto-reactivity through molecular mimicry, polyclonal activation or the release of previously sequestered antigens. Additionally, the autoimmunity can be associated with a lack of adequate regulation, including defects in Treg cells.

A balance between inflammation and regulation is required to maintain optimal immunity. Subsequently, a disruption of this balance can contribute to inflammation and the development of autoimmunity. The Th17/Treg cell balance has become a topic of increased interest in the study of autoimmunity. Th17 cells have been implicated in many autoimmune disease, such as RA, systemic lupus erythematosus (SLE), MS, psoriasis, IBD and many others (Maddur, Miossec et al. 2012). Reduced frequencies of Treg cells has been observed in the blood of patients suffering with JIA, SLE, psoriatic arthritis and many more (Dejaco, Duftner et al. 2006). However, the recruitment of Treg cells to sites of infection is increased in many disease states. Thus, it appears that Treg cells often fail to totally suppress inflammation despite local enrichment. This may be due to an imbalance of pro-inflammatory Th17 cells to Treg cells at the site of inflammation, Treg cell dysfunction or a resistance to Treg suppression by pathogenic effector cells. Therefore,

understanding the factors that regulate the Th17/Treg cell balance is critical to our understanding of autoimmunity and for the rational design of future therapies.

1.4.1 Psoriasis

Psoriasis is a common chronic inflammatory skin disorder affecting 2.5% of the worldwide population. Psoriatic lesions, or plaques, are typically distributed symmetrically and are most commonly found on the scalp, knees, elbows and in the body folds. Today, psoriasis vulgaris (also known as plaque psoriasis) - the most common form of the disease affecting 80-90% of patients - is recognized as one of the most prevalent autoimmune diseases caused by inappropriate cellular immune responses. Although psoriasis can present at any age, the onset of disease often begins in late adolescence or young adulthood, and usually persists for life (Lebwohl 2003). Psoriasis can be treated in 3 ways, depending on disease severity: topical treatments, including creams containing corticosteroids, phototherapy, consisting of controlled ultraviolet A or B exposure, and systemic treatments.

Immunopathogenesis of Psoriasis

Psoriasis is defined by the thickening of the epidermis, due to increased proliferation of keratinocytes. The abnormal differentiation of keratinocytes results in poor cell adherence within the epidermis, accounting for the characteristic scaling or flaking of psoriatic lesions (Bowcock and Krueger 2005). Psoriasis has also been described as a T cell-mediated disease. The first evidence implicating T cells in this disease demonstrated the successful treatment of psoriasis in patients following treatment with cyclosporine A, an immunosuppressive drug targeting T cell proliferation and cytokine production (Mueller and Herrmann 1979). Additionally, other T cell-targeting drugs, including anti-CD4 and CTLA-4 monoclonal antibodies, have had a successful therapeutic effect on psoriasis patients (Nicolas, Chamchick et al. 1991, Abrams, Kelley et al. 2000). The origin for the initial activation of T cells observed in psoriasis is still unclear in the majority of cases; however, studies have suggested a role for streptococcal antigens via molecular mimicry (Telfer, Chalmers et al. 1992). Once activated, T cells enter the bloodstream and traffic towards the skin. Migration into the dermis requires the tethering of many chemokine receptors and glycoproteins on the T cell surface with adhesion molecules on the endothelium. In previous studies, E-selectin on endothelial cells and ICAM-1 on T cells

is increased in both lesional and non-lesional psoriatic skin (de Boer, Wakelkamp et al. 1994) suggesting an increased infiltration of T cells into the dermis.

T helper cells in psoriasis pathogenesis

Both in the lesions and the peripheral blood of psoriasis patients, a significantly large population of Th1 CD4⁺ T cells exists, along with increased levels of IFN- γ (Schlaak, Buslau et al. 1994). This resulted in the definition of psoriasis as a Th1 cell-mediated disease, suggesting that a Th1/dendritic cell interaction creates a type 1 response by secreting many Th1-related cytokines, including IFN- γ and IL-12, resulting in the progression of psoriasis (Lew, Bowcock et al. 2004). However, as more information emerged about Th17 cells, these were also implicated in psoriasis and many other autoimmune diseases. Th17 cells and their downstream effector cytokines, including IL-17A, IL-17F, IL-21, GM-CSF, IL-22 and TNF- α , were found in abundance in psoriatic skin and blood (Kagami, Rizzo et al. 2010). Additionally, psoriatic lesions exhibited increased IL-23 mRNA and protein levels compared with normal skin (Lee, Trepicchio et al. 2004). As mentioned previously, IL-23 functions to maintain the survival and development of both murine and human Th17 cells, thus implicating Th17 cells in the pathogenesis of psoriasis (Volpe, Servant et al. 2008). Th17-related cytokines have also been shown to act upon keratinocytes and promote increased inflammation through immune cell migration towards the psoriatic environment. IL-22, another Th17 cell-related cytokine, induces hyperproliferation and abnormal differentiation of keratinocytes, a characteristic event in psoriatic disease (Zheng, Danilenko et al. 2007). The above evidence has made Th17 cells an obvious target for the development of therapies for the treatment of psoriasis. Three main molecules target the Th17 cell-specific cytokine IL-17, including: secukinumab, a fully human antibody directed against IL-17A, ixekizumab, a humanized anti-IL-17A monoclonal antibody, and brodalumab, a fully human antibody against the IL-17 receptor. Each has shown great promise thus far in clinical trials, with clinical responses to secukinumab resulting in a decreased frequency of IL-17-producing T cells (Hueber, Patel et al. 2010). Other successful systemic therapies have targeted TNF α (infliximab, etanercept and adalimumab) (Tobin and Kirby 2005) and IL-12/23p40 (ustekinumab).

Regulatory T cells in psoriasis

Regulatory T cells play a key role in immune surveillance and suppression of inappropriate immune responses. The absence of Treg cells has been shown to result in the increased instances of autoimmune disorders in murine models of disease (Ochs, Gambineri et al. 2007). Available literature studying Treg cells in psoriasis is limited. However, one study revealed an increase in the number of Foxp3⁺ T cells infiltrating psoriatic lesions and this correlated with disease severity (Zhang, Yang et al. 2010). This report also revealed an imbalance in the Th17:Treg cell ratio to be in favour of Th17 cells, which may contribute to an insufficient effectiveness of Treg cells in this highly inflamed environment. In two studies, Treg cell frequencies were unchanged between the peripheral blood of psoriasis patients and healthy controls (Zhang, Yang et al. 2010). Contrastingly, Yan et al. demonstrated that Treg cells were increased in peripheral blood and their level positively correlates with disease severity (Yan, Fang et al. 2010). Whilst Treg cell frequencies in psoriasis are under debate, Treg cells from the peripheral blood of psoriasis patients have been shown to have a decreased ability to suppress control effector T cells (Sugiyama, Gyulai et al. 2005), which may in turn have a positive effect on disease progression and inflammatory cell activity in psoriasis. Treatment of psoriasis with infliximab, an anti-TNF α treatment, and a combination of psoralen with UVA exposure, resulted in an increased frequency of Treg cells (Quaglino, Ortoncelli et al. 2009, Saito, Maeda et al. 2009). This data suggests a role for Treg cells in the improvement of psoriasis through inflammatory modulation.

Treatment of psoriasis with fumaric acid esters

A relatively new drug therapy has emerged for the treatment of psoriasis, in the form of a fumaric acid ester. Fumaderm™ is a combination of monomethyl and dimethyl fumarate (DMF), which has been used in Germany since 1994 for the treatment of psoriasis. The first usage was proposed in 1959 by Schweckendiek, a biochemical doctor affected by psoriasis, who used fumaric acid esters to cure himself (Schweckendiek 1959). According to Schweckendiek, psoriasis was a metabolic disease which required replacement of fumaric acid due to insufficient levels recorded in patients. This theory, however, has never been confirmed. Nonetheless, DMF has been shown to have a range of anti-inflammatory and cytoprotective effects in vitro; however, the mechanism of action of this treatment in psoriasis patients is unknown. In experimental models of MS, DMF was

shown to deplete intracellular glutathione levels, resulting in the activation of the stress responsive heme oxygenase 1 (HO-1) via NRF-2 transcriptional activity (Linker, Lee et al. 2011). Additionally, Fumaric acid esters have recently been utilized for treatment of other autoimmune diseases. For example Tecfidera™, an oral agent consisting of dimethyl fumarate, has recently been approved by the European Medicines Agency (EMA) for the treatment of relapsing forms of MS. Even though fumarates have been used in Germany for a number of years, their mechanism of action has not been extensively investigated. However with the recent licensing of Tecfidera™, there is new interest in understanding the immunomodulatory effects of these drugs. Investigating the in vivo effects of Fumaderm™ on immune cells, particularly T cells, could provide insight into the therapeutic effects of Fumaderm™ in psoriasis.

1.4.2 Rheumatoid Arthritis

RA is a chronic inflammatory, autoimmune disorder characterized by a persistent inflammation of the synovial joints (Silman and Pearson 2002). The prevalence of RA is relatively constant in many populations, at 0.5-1%. This is consistent with reports from several European and North-American populations. However, there are some exceptions, with the native American-Indian populations recording the highest occurrence of RA (6.8%), while studies in rural African populations, both in South Africa and Nigeria, failing to discover any instances of RA. This descriptive epidemiology suggests a role for genetics in the susceptibility to RA. Additionally, environmental factors, such as smoking, and previous encounters with infectious agents, including Epstein-Barr virus and cytomegalovirus, are known to increase the risk of developing RA (Alspaugh, Jensen et al. 1978, Symmons, Bankhead et al. 1997). Joint inflammation results in damage to cartilage and bone, culminating in disability and systemic complications, including cardiovascular and pulmonary disorders (McInnes and Schett 2011). RA typically affects the synovial joints, including the fingers, wrists, elbows, ankles and hips. The inflamed synovium undergoes extensive hyperplasia and an accumulation of synovial fluid causes swelling, severe pain and loss of function. In addition, inflammation triggers bone and cartilage destruction. RA disease progression and improvement is measured using the Disease Activity Score (DAS28). DAS28 ranges from 2.0 to 10.0, with higher values related to higher disease activity.

T helper cells in the immunopathology of RA

CD4⁺ T cells are enriched in the joints of RA patients and play a central role in the pathogenesis of RA through the production of pro-inflammatory cytokines (Astry, Harberts et al. 2011). The Th1 cell-specific cytokine profile has been identified in cells extracted from the synovial fluid of RA patients (Dolhain, ter Haar et al. 1996). Additionally, autoantigen-specific Th1 cells were significantly increased in RA peripheral blood compared with healthy controls (James, Rieck et al. 2014). Likewise, the frequency of Th17 cells was increased in the PBMC of RA patients compared with healthy controls (Shen, Goodall et al. 2009). The levels of the Th17 cell-related cytokine IL-17 are upregulated during the acute and chronic phases of RA (Bush, Walker et al. 2001). IL-17 is known to promote inflammation by several mechanisms; by stimulating fibroblast-like synoviocytes and other local cells in the joint to produce pro-inflammatory cytokines including IL-6, IL-8 and the matrix metalloproteinases (Kehlen, Pachnio et al. 2003, Agarwal, Misra et al. 2008), facilitating cellular infiltration into the synovium via chemotaxis provided by IL-17 and CXCL5 (Shahrara, Pickens et al. 2009), and IL-17 can enhance the recruitment and survival of neutrophils, therefore enhancing the innate immune response within the synovium (Parsonage, Filer et al. 2008). Overall, IL-17 is found to induce extensive inflammatory cell migration, bone erosion and cartilage degradation in both murine and human studies of RA. IL-17 promotes expression of RANKL, which plays a key role in bone and cartilage damage by osteoclasts (Lubberts, Koenders et al. 2005). The percentage of Th17 lineage cells, expressing the human Th17 cell marker CD161, have also been reported as increased in JIA, with a positive correlation to erythrocyte sedimentation rate and levels of C-reactive protein, an inflammatory-related protein (Cosmi, Cimaz et al. 2011). Additionally, CD161⁺ Th17 cells are enriched in the synovial fluid and tissue compared with healthy control peripheral blood (Chalan, Kroesen et al. 2013, Basdeo, Moran et al. 2015). Basdeo et al. also reported an increase in survival characteristics for CD161⁺ T cells in the synovial fluid, suggesting a persistence of Th17 lineage cells in the joint.

As mentioned previously, Th17 CD161⁺ T cells exhibit plasticity and have the ability to switch into another cell subtype, known as exTh17 cells. ExTh17 cells, whilst retaining their CD161 expression, switch from primarily IL-17 producers to an intermediate stage, producing both IL-17 and IFN- γ , to finally producing IFN- γ alone (Annunziato, Cosmi et al.

2013). A study in JIA patients found a significant increase in the frequency of exTh17 cells - both in transitional and fully switched subtype - in the synovial fluid; however, no increase in bona fide Th17 cells was observed (Cosmi, Cimaz et al. 2011). This data combined implicates Th17 and exTh17 cells in the pathogenesis of RA. Similar unpublished data has been shown in RA synovial fluid (Basdeo et al, manuscript in preparation).

Evidence, from both murine models of disease and clinical observations, revealed IL-17 as a target for RA therapy. However, clinical trials of IL-17 and IL-17 receptor targeted drugs, including secukinumab, ixekizumab and brodalumab, demonstrated relatively poor clinical efficacy in RA (Kellner 2013). This suggests that targeting of IL-17 alone is not sufficient to inhibit inflammation. It may also imply a role for exTh17 cells in RA pathogenesis, since Th17 cells having switched from IL-17 producers to now primarily IFN- γ producers would result in the redundancy of IL-17 inhibition.

Treg cells in the immunopathology of RA

Understanding the altered immunity related to autoimmune inflammation is essential to targeting autoimmune disease as a whole. A deficit in Treg cell numbers or defects in cell function are both plausible contributors to increased inflammation observed in RA. In the last decade, a number of studies investigated the number and function of Treg cells in the peripheral blood and synovial fluid of RA patients. Although general agreement exists for Treg cell enrichment in the synovial fluid, conflicting results have been reported concerning the frequency of Treg cell populations in the peripheral blood of patients (Alunno, Manetti et al. 2015). This discrepancy may be due to the highly mobile state of immune cells during inflammation, as they constantly traffic from the blood to the synovial fluid. Inflammation persists in the RA joint, despite the increased frequency of Treg cells, therefore implying a defect in Treg cell suppression. Tregs from RA patients were shown to suppress proliferation of effector T cells; however, they were defective in their ability to suppress pro-inflammatory cytokines (Ehrenstein, Evans et al. 2004, van Amelsfort, Jacobs et al. 2004). The pro-inflammatory cytokine TNF- α , produced dominantly by monocytes and macrophages, is known to abrogate the suppressive activity of human Tregs (van Amelsfort, van Roon et al. 2007). Interestingly, treatment with the TNF- α inhibitor, infliximab, gave rise to an adaptive CD62L⁻ Treg cell population

which was able to suppress cytokine production by effector T cells via TGF- β and IL-10 (Nadkarni, Mauri et al. 2007). Effector T cells in the synovial fluid have additionally been shown to resist suppression by Treg cells in RA, enhancing their survival and amplifying inflammation within the joint (van Amelsfort, Jacobs et al. 2004). A recent study using RA synovial fluid, CD161⁺ Th cells demonstrated a resistance to suppression by Treg cells, whereas CD161⁻ Th cells were effectively suppressed (Basdeo, Moran et al. 2015). Additionally, this study restored the suppressive abilities of Treg cells from the synovial fluid following the depletion of CD161⁺ Th17 lineage cells from the effector cell population. Although some of the data are contradictory, it is increasingly appreciated that established RA therapies could influence Treg cell populations. For example; methotrexate treatment of mouse models of collagen-induced arthritis (CIA) revealed an increased frequency of Treg cells (Xinqiang, Fei et al. 2010), TNF- α inhibitors provide conflicting results in terms of Treg cell populations, and IL-6 inhibition with tocilizumab was shown to skew the Th17/Treg balance more towards a protective status (Pesce, Soto et al. 2013).

Hypoxia and HIF-1 α in RA

The importance of inflammation in RA is well understood. However, what is less well appreciated in RA is the link between inflammation and cellular responses to changes in oxygen tension. Inadequate oxygen supply is termed hypoxia and is a feature of inflamed environments, resulting from increased cellular infiltration and oxygen consumption. Low oxygen tension is a well established feature of RA synovial joints (Lund-Olesen 1970) and the hypoxia-inducible factors (HIF) including HIF-1 α which orchestrate the cellular response to low oxygen, are known to be upregulated in human RA synovium compared with controls (Giatromanolaki, Sivridis et al. 2003). HIF expression correlates with indices of angiogenesis, however, despite increased vascular supply there is a failure to restore tissue oxygen homeostasis due to hyperplasia within the synovium and increased metabolic activity resulting in a hypoxic environment (Ng, Biniiecka et al. 2010). Energy metabolism, consisting of glycolysis and oxidative phosphorylation, is required to generate energy for cellular functions. Oxidative phosphorylation requires oxygen; therefore, in hypoxic conditions cells must utilize glycolysis for their metabolic demands, as oxygen is not a requirement for glycolysis. The activity of glycolytic enzymes was

increased in synovial lining cells of synovial tissue of RA patients (Henderson, Bitensky et al. 1979), suggesting a role for altered metabolism in the pathogenesis of RA.

1.5 Cellular metabolism

Cellular energy metabolism is a process utilised by cells to convert biochemical energy from nutrient uptake into a form used for cellular growth, development, proliferation and function. In these scenarios, metabolism is not seen as a static process, but rather a very dynamic one that functions to meet the bioenergetics demands of any given cell at any point in time. It involves a series of enzyme-catalysed reactions organised into two main pathways; glycolytic respiration, an anaerobic process, and oxidative phosphorylation, an aerobic mechanism.

Glucose enters the cell via glucose transporters and is broken down in the glycolytic pathway to produce pyruvate, via a series of ten enzyme-catalyzed reactions, which can then undergo further breakdown to lactate by the enzyme lactate dehydrogenase (LDH). If oxygen is readily available, pyruvate translocates to the mitochondria and enters the tricarboxylic acid cycle (TCA) as acetyl-coA, providing the acetate molecule that is both consumed and regenerated by the cycle supplying the energy required by the next step in oxidative phosphorylation, the electron transport chain (ETC). Reduced nicotinamide adenine dinucleotide molecules (NADH), produced by the TCA cycle, provide electrons to electron acceptors, like oxygen, facilitated by the proteins of the ETC. The ETC gains energy from electron transport to fuel the translocation of protons across the inner mitochondrial membrane, establishing the mitochondrial membrane potential, which in turn fuels ATP synthesis (adenosine triphosphate). ATP is described as the 'cellular currency', providing energy for all essential cellular processes required for survival and proliferation.

1.5.1 Immunometabolism

The relationship between immunological processes and metabolism has become a topic of increasing interest in the last decade. It has recently become clear that the behaviours of immune cells are controlled on many levels by internal metabolic processes. One of the most fundamental cellular requirements is the ability to access sufficient and appropriate nutrients to support essential cellular functions. As cells are stimulated to grow,

proliferate, or die, their metabolic requirements change, and it is important that cellular metabolism matches these demands. Although immune cells spend a significant amount of time in the blood, where nutrients are abundant, during inflammation these nutrients become limited, and so cells must adjust their metabolism to fit the environment.

Interest in cellular metabolism and its role in the activation and differentiation of immune cells have heightened in recent years, although Otto Warburg first identified it almost a century ago. It was discovered that cancer cells utilised the anaerobic process of glycolysis (producing 2 ATP molecules per cycle) for energy generation over that of mitochondrial respiration (producing 36 ATP molecules per cycle) even if oxygen was readily available (Warburg 1956). Warburg studied the metabolism of leukocytes as well as cancer cells and discovered that they too displayed a preference for glycolysis following cellular activation (Warburg, Gawehn et al. 1958). The examination of macrophages highlighted an importance for glycolysis in their inflammatory activation, revealing an increased uptake of glucose and glutamine, and increased lactic acid production (Newsholme, Curi et al. 1986). Additionally, dendritic cells activate their metabolic switch towards glycolysis following ligation of TLRs and also, the maturation of DCs is dependent upon glycolysis, as evidence following the inhibition of glycolysis with 2-deoxy-glucose failed to develop mature dendritic cells from an immature cell population (Jantsch, Chakravorty et al. 2008). In both innate and adaptive immune cells, states of activation and quiescence exist, resulting in different metabolic demands. As mentioned previously, adaptive T cells exist as naïve and memory cells, adopting different activation states and therefore acquire distinct metabolic pathways.

1.5.2 T cell activation

T cell activation leads to dramatic shifts in cell metabolism in order to protect against pathogens and to orchestrate the action of other immune cells. Activated lymphocytes and cancer cells proliferate rapidly, requiring fast metabolic cycles and increased production of biological precursors, including amino acids and nucleotides for the creation of new building blocks, all of which are provided by glycolysis. Naïve resting T cells involved in immune surveillance in the peripheral lymphoid organs require large amounts of ATP for continual cytoskeleton rearrangements, and so utilise oxidative phosphorylation for energy supply (MacIver, Michalek et al. 2013). Upon TCR activation,

an increase in the membrane-bound glucose transporter GLUT1 is observed. Signalling through CD28 activates the phosphoinositide 3-kinase (PI3K) enzyme, converting phosphatidylinositol 4, 5-biphosphate (PIP₂) to PIP3. PIP3 recruits Akt (protein kinase B) and phosphoinositide dependent kinase 1 (PDK1) to the plasma membrane. Both PDK1 and the mTOR complex 2 (mTORC2) phosphorylate Akt, resulting in its activation. Akt promotes glycolysis through the translocation of GLUT1 transporter to the cell surface (Gerriets and Rathmell 2012) and by increasing glycolytic enzyme phosphorylation in order to increase glycolytic flux (Miyamoto, Murphy et al. 2008) [Figure 1.4].

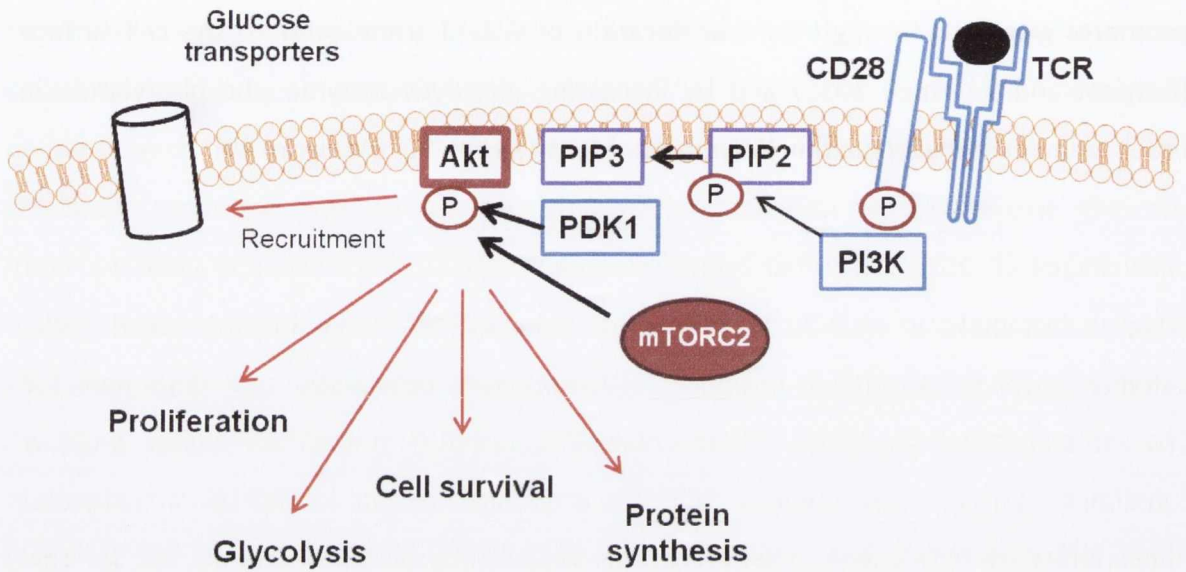


Figure 1.4 T cells switch to glycolysis following TCR activation

The TCR becomes activated following interaction with peptides loaded onto the MHC of APCs. CD28 ligation with CD80/86 on the APC provides essential co-stimulation for T cell activity and the switch in metabolism towards glycolysis. CD28 becomes phosphorylated on its intracellular YMMN motif, recruiting SH2-domain containing protein PI3K. PI3K phosphorylates PIP2 at the plasma membrane, generating PIP3, which in turn recruits Akt and PDK1 via their PH-domain to the plasma membrane. Akt becomes activated following phosphorylation by PDK1 and mTORC2, and acts to regulate many downstream effector proteins, promoting glycolysis and many other cellular processes required for T cell activation and proliferation.

1.5.3 CD4 and CD8 T cell metabolism

CD4⁺ and CD8⁺ T cells differ in function; however, both are capable of producing long-lived memory cells. CD4⁺ T cells respond to specific cytokine signals to differentiate into distinct cell subsets to contribute to immunity or suppress inflammation. Activated CD8⁺ T cells differentiate to provide an antigen-specific cytolytic defence against intracellular pathogens and tumours.

The metabolic requirements of murine naïve CD4⁺ T cells are met by oxidation of glucose and fatty acids via the mitochondrial oxidative phosphorylation pathway (MacIver, Michalek et al. 2013). Upon antigen-stimulation, CD4⁺ T cells become activated and switch their metabolic profile to become more glycolytic. The mechanism by which T cells enhance glycolysis is outlined in figure 1.4, and studies have shown a requirement for CD28 co-stimulation engagement in this metabolic switch (Frauwirth, Riley et al. 2002). A conflicting murine study revealed a reliance of CD4⁺ T cell activation on oxidative phosphorylation following inhibition of glycolysis (Chang, Curtis et al. 2013). This suggested that CD4⁺ T cells could utilise both metabolic pathways during activation if glycolysis is inhibited; however, glycolysis is the preferred pathway. Literature investigating the role of metabolism in memory CD4⁺ T cells, including both effector and central subsets, is scarce. However, hypothesizing from the activity states of each, one could suggest a more glycolytic role for T_{EM} cells and the utilization of mitochondrial respiration, much like naïve T cells, for T_{CM} cells.

Like effector CD4⁺ T cells, resting CD8⁺ T cells undergo dynamic shifts in cell metabolism and switch from oxidative metabolism to aerobic glycolysis upon activation (He, Kato et al. 2011). Memory CD8⁺ T cells were shown to depend upon lipid oxidation (van der Windt, Everts et al. 2012). A study carried out in human CD8⁺ T cells, compared central memory and effector memory cells, demonstrating an increased basal glycolysis for effector memory CD8⁺ T cells compared with central memory cells (Henson, Lanna et al. 2014).

A study directly comparing activated murine CD4 and CD8 T cells reported a greater mitochondrial mass and consistently more oxidative phosphorylation activity in CD4⁺ T cells, whilst CD8⁺ T cells preferentially adopted a more glycolytic metabolism (Cao,

Rathmell et al. 2014). In contrary to this, a study in human CD4 and CD8 T cells, demonstrated both elevated glycolytic and mitochondrial activity as well as an increased proliferative capacity for CD4⁺ T cells compared with CD8⁺ T cells (Renner, Geiselhoringer et al. 2015).

1.5.4 Metabolism and T cell differentiation; the Th17/Treg balance

A relationship between T cell differentiation and metabolism has been established following the discovery of the metabolic switch in T cells as a result of TCR stimulation. The primary focus on the metabolic regulation of CD4⁺ T cell subsets has centred on mTOR, which is activated by the PI3K/Akt pathway to drive the metabolic transition from oxidative phosphorylation to glycolysis. Initial evidence supporting this relationship was recorded in 2007, examining the role of mTOR in the metabolism of murine T cell subsets. In mice, mTOR inhibition following treatment with rapamycin inhibited Th17 cell generation, whilst promoting Treg cell differentiation (Kopf, de la Rosa et al. 2007). This was supported by another study indicating a decrease in IL-17-production by naïve T cells cultured in the presence of glycolytic inhibitors, 2-deoxy-d-glucose (2-DG) and rapamycin (Shi, Wang et al. 2011). Additionally, this study demonstrated an increase in the differentiation of Foxp3⁺ CD4 T cells following inhibition of glycolysis. Michalek et al. performed a study in murine cells focusing on the metabolism utilised by each subset in more detail. This report revealed decreased expression of the glucose transporter GLUT1 in newly differentiated Treg cells, decreased Foxp3 expression by newly differentiated Treg cells following fatty acid oxidation (FAO) inhibition (FAO and oxidative phosphorylation are two separate pathways which share molecules/products) and finally decreased glucose uptake (Michalek, Gerriets et al. 2011). Furthermore, in this study, differentiated Th17 cells demonstrated increased GLUT1 expression and glucose uptake.

Murine regulatory T cells were shown to have less mTOR complex 1 (mTORC1), known to promote glycolysis, and subsequently expressed high AMPK (AMP-activated protein kinase which promotes oxidative phosphorylation as AMP levels increase) (Michalek, Gerriets et al. 2011). Additionally, the mTOR complexes were shown to be differentially expressed in murine effector T cells, with Th17 and Th1 cells expressing mostly mTORC1 and the opposite for Th2 cells, expressing predominantly mTORC2 (Delgoffe, Pollizzi et al. 2011). Further differences were observed between T effector and T regulatory subsets,

suggesting the metabolic switch between glycolysis and oxidative phosphorylation is specific to T cell function. Thus in summary, the above studies indicate that newly differentiated murine Th17 cells utilise glycolysis, whereas Treg cells utilise oxidative phosphorylation and lipid oxidation for their metabolic demands.

Very little is known about the role of metabolism in human helper T cells and Treg cells. A report in 2009 demonstrated an increase in CD4⁺CD25⁺ Treg cells in response to rapamycin treatment (Strauss, Czystowska et al. 2009). However, Foxp3 expression was not taken into account in this study and thus Treg cells may not have been correctly identified. Data presented for both murine and human cells suggests that metabolic pathways could regulate the Th17/Treg cell balance. One such regulator of metabolism, and an orchestrator of the switch towards glycolysis following T cell activation, is HIF-1 α .

1.6 Hypoxia

Oxygen is a molecule that is central to cellular respiration and proliferation. During inflammation, as a consequence of increased cellular migration to the site of infection, oxygen supply to immune cells is diminished producing a hypoxic environment. For example, hypoxia can be found within arthritic joints, atherosclerotic plaques and within the tumour environment (Shay and Celeste Simon 2012). Given the metabolic challenges encountered by cells in a hypoxic environment, hypoxia elicits a range of adaptive cellular responses to promote cell survival and proliferation. One such measure involves the metabolic switch towards glycolysis, as glycolytic metabolism does not require oxygen. This switch, along with other adaptive responses, is mediated by members of the family of HIFs.

1.6.1 Hypoxia-inducible factors

Metabolic reprogramming and changes in gene expression are necessary for the adaptation to decreased oxygen availability. This is mediated in part by HIF transcription factors. HIFs are heterodimeric transcription factors, which are primarily regulated by post-translational modification and stabilization (Semenza 2009). HIF consists of two alpha subunits, HIF-1 α and HIF-2 α , and one beta subunit, HIF-1 β (or aryl hydrocarbon receptor nuclear translocator, ARNT). HIF-1 α is constitutively expressed, while HIF-2 α expression is more tissue-specific (Patel and Simon 2008). Functional HIF consists of two

subunits; one of the oxygen sensing α subunits and a constitutively expressed β subunit. HIFs are expressed under both hypoxia and normal oxygen levels (normoxia). However, in the presence of oxygen two proline residues within the oxygen-dependent degradation (ODD) domain of the α subunit become hydroxylated by prolyl hydroxylase domain (PHD) proteins, members of the 2-oxoglutarate-dependent dioxygenase superfamily. It is important to note that oxygen sensing does not occur through HIFs, but through the PHD proteins, a group of oxygen-dependent enzymes that regulate the stability of the α subunit of HIF (Schofield and Ratcliffe 2004). Following hydroxylation of the ODD domain of HIF- α , recruitment of the von Hippel-Lindau (VHL) protein, an E3 ligase, polyubiquitinates the α subunit and results in its proteasomal degradation (Cockman, Masson et al. 2000). During hypoxia, the PHD proteins become inactive, thus the α subunit is free to translocate to the nucleus and dimerise with its obligate partner, HIF- β , producing its active form and transcribing various genes involved in metabolism, angiogenesis and inflammation (Majmundar, Wong et al. 2010) [Figure 1.5].

HIF-1 α can also be regulated by nonoxygen-dependent pathways, which disrupt the PHD/VHL/HIF proteolytic cascade. The interference of PHDs and their cofactors, such as 2-oxoglutarate and iron, can result in HIF-1 α stabilization. Iron can be removed by chelators, such as desferrioxamine (Wang and Semenza 1993). Additionally, PHD activity is known to be regulated by metabolites as well as oxygen levels, therefore elevated levels of succinate and fumarate can inhibit PHD activity (Isaacs, Jung et al. 2005, Selak, Armour et al. 2005). Furthermore, TCR stimulation results in robust HIF-1 α stabilization, mediated by the PI3K/Akt/mTOR pathway (Nakamura, Makino et al. 2005). HIF-1 α stabilization can additionally be driven by signalling via the pro-inflammatory IL-6 cytokine (Jung, Kim et al. 2008) [Figure 1.5].

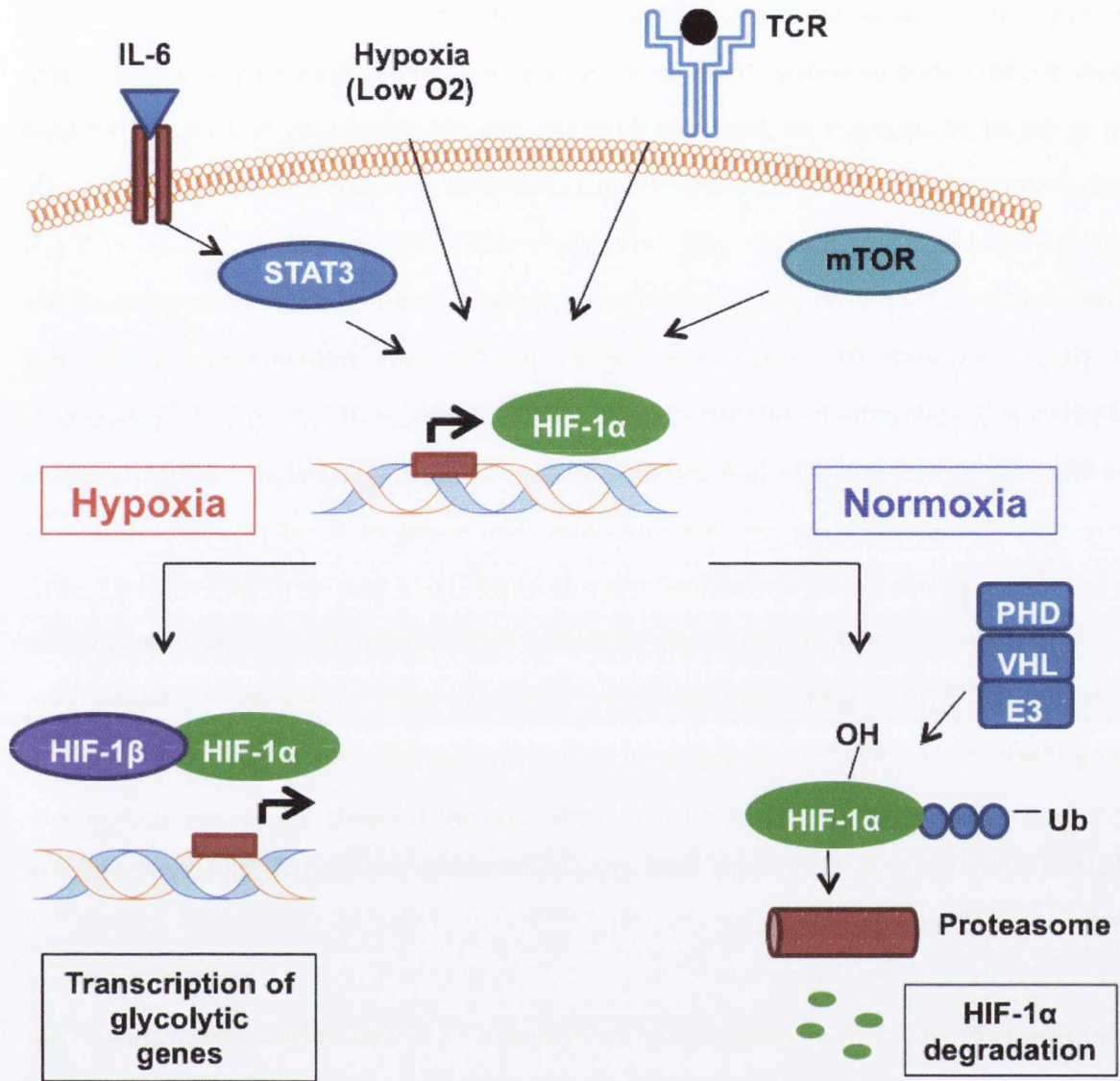


Figure 1.5 Regulation of HIF-1 α stabilization and degradation

HIF-1 α expression is consistently upregulated via TCR, mTOR and IL-6 signalling; however, during normal oxygen supply (normoxia), PHD proteins hydroxylate the ODD domains on HIF-1 α . This subsequently recruits the VHL protein and results in the polyubiquitination of HIF, targeting it for degradation via the proteasome. The PHD proteins are oxygen sensors and are only active when oxygen is present. In hypoxic conditions, HIF-1 α becomes stabilized due to the absence of the PHD-VHL complex and translocates to the nucleus. HIF-1 α forms a heterodimer with the constitutively expressed β subunit and transcribes various genes involved in the cellular adaptation to hypoxia; including glycolysis.

1.6.2 HIF-1 α as a regulator of the Th17/Treg cell balance

Given the likelihood of immune cells experiencing low oxygen levels during inflammation, the effect of hypoxia on immune cell function and differentiation is a highly relevant topic. Studies assessing the role of HIF-1 α in T cells have been advanced most significantly through the analysis of murine cells, primarily investigating the role of HIF-1 α in T cell differentiation. Distinct murine T cell subsets reveal differential expression levels of the HIF-1 α protein, with HIF-1 α expressed highest in Th17 cells, followed by Th2, Th1 and Treg cells expressing the lowest HIF-1 α protein (Shi, Wang et al. 2011). Linking glycolysis and hypoxia in T cells, there is a strong decrease in glycolytic enzyme mRNA levels in naïve CD4⁺ T cells from HIF-1 α knockout mice (Shi, Wang et al. 2011). Two studies in accordance with one another examined the role of HIF-1 α in murine differentiated T cells, revealing similar results. HIF-1 α is required for Th17 differentiation, indicated by impaired expression of Th17 specific cytokines IL-17, IL-22 and IL-23 during HIF-1 α knockdown (Dang, Barbi et al. 2011, Shi, Wang et al. 2011). In contrast, these studies revealed an increased expression of Foxp3 in HIF-1 α ^{-/-} cells, skewed towards a Treg cell population. Treg cells inversely displayed very little glycolytic activity in terms of glycolytic enzyme expression (Shi, Wang et al. 2011).

In murine cells, HIF-1 α has been shown to promote Th17 cell differentiation over Treg cells through direct interactions with T cell subset-specific transcription factors. During low oxygen supply, HIF-1 α promotes ROR γ t gene expression via its interaction with a conserved binding site, the hypoxia response element (HRE), located in the proximal region of the ROR γ t promoter (Dang, Barbi et al. 2011). Additionally, HIF-1 α promotes ROR γ t function through the recruitment of transcriptional co-activator p300, which possesses histone acetyltransferase (HAT) activity required for 'opening' of the DNA to allow access to ROR γ t and HIF-1 α , in order to facilitate expression of Th17 specific genes, including the IL-17A cytokine (Dang, Barbi et al. 2011)[Figure 1.6A]. Knowing that HIF-1 α is stabilized during low oxygen tension and promotes IL-17 production, it has been indicated in murine studies that the hypoxia-induced pathway is activated by IL-17 (Hot, Zrioual et al. 2011). This suggests that the HIF-1 α pool can be sustained through IL-17 signalling, and therefore maintain the Th17 immune response within the inflamed tissue. Contrary to the effects on Th17 cells, HIF-1 α inhibits murine Treg cell differentiation via the down-regulation of Foxp3 protein levels in T cells, skewed under both Th17 and Treg

determining conditions. The Foxp3 binding domain, located at the N-terminal of the HIF-1 α protein, interacts with the HIF-1 α binding domain mapped to the C-terminal of Foxp3. Foxp3 is subsequently targeted for ubiquitination and proteasomal degradation via the PHD/VHL system, also responsible for HIF-1 α degradation during normoxic conditions (Dang, Barbi et al. 2011) [Figure 1.6B]. This is supported by a study examining the E3 ligase Deltex1, as knockdown of Deltex1 resulted in increased HIF-1 α protein stabilization and a subsequent decrease in Foxp3 expression in murine T cells (Hsiao, Hsu et al. 2015). In contrast to this, studies in murine and human cells demonstrate increased frequencies of Treg cells in hypoxic conditions (Clambey, McNamee et al. 2012) (Ben-Shoshan, Maysel-Auslender et al. 2008).

Studies have illustrated the profound effects metabolism and HIF-1 α has on influencing T helper and regulatory cell differentiation profiles, predominantly in the murine species. Th17 cell differentiation demonstrates a requirement for HIF-1 α expression, whilst the effect of hypoxia on Treg cell differentiation is under debate in both murine and human studies. Few studies, in this field, focus on human T cells, with human Th17 cells completely unexplored. Therefore, this study aims to elucidate the role for metabolism and hypoxia in mediating the survival and expansion of human T helper and regulatory cell subsets.

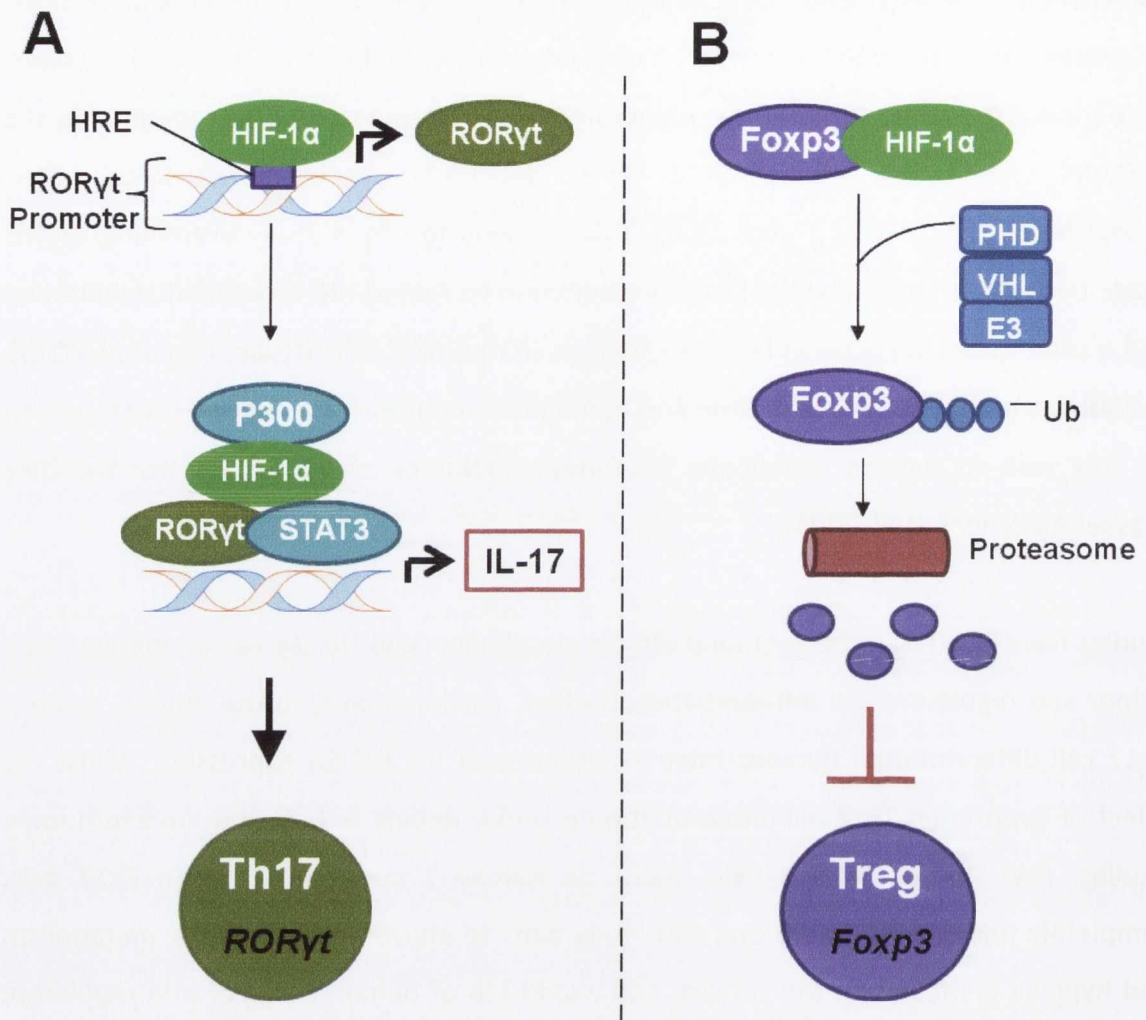


Figure 1.6 Direct effect of HIF-1 α on murine Th17 and Treg cell differentiation

HIF-1 α directly promotes the generation of Th17 cells and subsequently inhibits Treg cell differentiation during hypoxic conditions. Following translocation to the nucleus, HIF-1 α interacts with the hypoxia response element on the ROR γ t gene promoter, resulting in the direct transcription of ROR γ t. HIF-1 α recruits the transcriptional co-activator P300, which via its histone acetyltransferase activity provides access to Th17 cell specific genes, including IL-17. IL-17 is a pro-inflammatory cytokine providing a positive feedback loop for the stabilisation of HIF-1 α . Adversely, HIF-1 α interacts with the Foxp3 protein at the HIF-binding domain found at the c-terminal of Foxp3, targeting it for ubiquitination via the PHD-VHL complex. Foxp3 is degraded by the proteasome and Treg cell generation is therefore inhibited.

1.7 Aims

- **Determine the metabolic pathways utilized by human CD4⁺ T cell subsets.**

The expression of glycolytic correlates will be examined in human T cell subsets by flow cytometry. The metabolic profile of sorted T cell subsets will be investigated via the Seahorse Analyzer. Additionally, the survival, expansion or inhibition of T cell subsets will be examined following the hindrance of glycolysis.

- **Investigate the effect of hypoxia on T cell subset survival and expansion**

Metabolites and resources are diminished in hypoxic and inflamed environments; therefore the effect of hypoxia in vitro on T cell subset survival will be examined. T cell frequencies will be investigated following cultured in an oxygen controlled chamber set at a hypoxic oxygen level. The effect of hypoxia on metabolism will be examined also. Additionally, the RA joint represents a hypoxic environment; therefore, the frequency of T cell subsets within the synovial fluid of RA patients will be examined.

- **The effect of modulating metabolism and hypoxia on the Treg:Th17 cell axis**

The effects of metabolic compounds, utilized to inhibit or promote metabolic pathways, and hypoxic inhibitors on human T cell subsets will be investigated in vitro. Finally, the in vivo effect of Fumaderm™ on the Treg:Th17 cell axis will be examined for psoriasis patients.

The following information is being provided to you for your information only. It is not intended to constitute an offer of insurance or any other financial product. Please consult your agent for more information.

The information contained herein is for informational purposes only and should not be used as a basis for any investment decision. It is not intended to constitute an offer of insurance or any other financial product.

The information contained herein is for informational purposes only and should not be used as a basis for any investment decision. It is not intended to constitute an offer of insurance or any other financial product. Please consult your agent for more information.

The information contained herein is for informational purposes only and should not be used as a basis for any investment decision. It is not intended to constitute an offer of insurance or any other financial product.

The information contained herein is for informational purposes only and should not be used as a basis for any investment decision. It is not intended to constitute an offer of insurance or any other financial product.

The information contained herein is for informational purposes only and should not be used as a basis for any investment decision. It is not intended to constitute an offer of insurance or any other financial product.

The information contained herein is for informational purposes only and should not be used as a basis for any investment decision. It is not intended to constitute an offer of insurance or any other financial product.

The information contained herein is for informational purposes only and should not be used as a basis for any investment decision. It is not intended to constitute an offer of insurance or any other financial product.

The information contained herein is for informational purposes only and should not be used as a basis for any investment decision. It is not intended to constitute an offer of insurance or any other financial product.

Chapter 2

Methods

Chapter 2. Methods

2.1 Cell sources

Leukocyte enriched buffy coats from anonymous healthy donors were obtained with permission from the Irish Blood Transfusion Board, St. James's Hospital, Dublin and ethical approval was granted by Trinity College Faculty of Health Sciences Research Ethics Committee. Human immortalized T lymphocyte cell line Jurkat were a gift from the lab of Prof. Andrew Bowie and human erythroleukemia K562 cells were a gift from the lab of Dr. Clair Gardiner. Psoriasis samples were obtained from the lab of Prof. Kirby and rheumatoid arthritis patient samples were obtained from the labs of Dr. Fearon and Dr. Veale. All cells were maintained in Roswell Park Memorial Institute (RPMI) medium, supplemented with 10% (v/v) foetal calf serum (FCS), L-glutamine (2 mM) (LG), 100 µg/ml penicillin and 100 µg/ml streptomycin.

2.2 Isolation of PBMC from blood packs

Healthy donor blood was removed from blood packs and diluted 1 in 2 with sterile PBS and centrifuged at 1250 g for 10 minutes at room temperature with the brake off. The buffy coat layer containing leukocytes was removed using a Pasteur pipette, diluted in 200 ml of sterile PBS and layered over lymphoprep (25 ml of diluted blood and 20 ml of lymphoprep per tube). PBMC were isolated by density-gradient centrifugation at 900 g for 20 minutes at room temperature, with the brake off. The PBMC layer was removed using a Pasteur pipette, washed in sterile PBS and centrifuged at 650 g for 10 minutes. The supernatant was removed, the pelleted PBMC washed again in sterile PBS and centrifuged at 290 g for 10 minutes in order to remove platelets. PBMC were resuspended in complete RPMI (Biosera) and counted.

2.3 T cell purification by Magnetic Activated Cell Sorting (MACS)

2.3.1 CD4⁺ T cell sorting by positive selection

PBMC were isolated from blood packs as previously described (2.2). Cells were washed in MACS buffer and pelleted by centrifugation at 650 g for 10 minutes. The supernatant was completely aspirated and the pellet was resuspended in 80 µl of MACS buffer (see appendix) per 10 million cells. CD4 magnetic beads (Miltenyi Biotec) were added to the

cells at 20 μ l per 10 million cells. The cell/bead solution was mixed thoroughly and incubated for 15 minutes at 4°C. The cell solution was then washed in MACS buffer and pelleted by centrifugation at 650 g for 10 minutes. The pellet was resuspended in 500 μ l (for up to 100 million cells) of MACS buffer. An LS magnetic column (Miltenyi Biotec) was placed in the magnet and washed with MACS buffer (3 ml). The cell sample was then loaded onto the column followed by 3 washes of MACS buffer (3 ml per wash). The eluent of the CD4-depleted fraction was collected and discarded. The column was removed from the magnet and the CD4⁺ T cells were expelled using a plunger in 5 ml of MACS buffer. Purified CD4⁺ T cells were washed in complete RPMI (Biosera), pelleted by centrifugation at 340 g for 10 minutes and counted. The purity of the sorted CD4⁺ T cells was assessed by flow cytometry and was routinely > 90%.

2.3.2 CD4⁺ T cell sorting by negative selection

PBMC were isolated from blood packs as previously described (2.2). Cells were washed in MACS buffer and pelleted by centrifugation at 650 g for 10 minutes. The supernatant was completely aspirated and the pellet was resuspended in 40 μ l of MACS buffer per 10 million cells. A biotin conjugated antibody cocktail was added to the cells at 10 μ l per 10 million cells. The solution was mixed thoroughly, allowed to incubate for 10 minutes at 4°C then washed in MACS buffer and pelleted by centrifugation at 650 g for 10 minutes. The supernatant was completely discarded and the pellet was resuspended in 30 μ l of MACS buffer per 10 million cells. CD4⁺ T cell MicroBead Cocktail (Miltenyi Biotec) was added to the cells at 20 μ l per 10 million cells and incubated for 15 minutes at 4°C. The cell solution was then washed in MACS buffer and pelleted by centrifugation at 650 g for 10 minutes. The pellet was resuspended in 500 μ l (for up to 100 million cells) of MACS buffer. An LS magnetic column (Miltenyi Biotec) was placed in the magnet and washed with MACS buffer (3 ml). The cell sample was then loaded onto the column followed by 3 washes of MACS buffer (3 ml per wash). The eluent of the CD4⁺ enriched fraction was collected. Purified CD4⁺ T cells were washed in complete RPMI (Biosera), pelleted by centrifugation at 340 g for 10 minutes and counted. A sample of cells were stained with a fluorochrome-conjugated antibody for CD4 and analysed by flow cytometry to check the purity of the sort (Figure 2.1 A)

2.3.3 Memory CD4⁺ T cell sorting by negative selection

PBMC were isolated from blood packs as previously described (2.2). Cells were washed in MACS buffer and pelleted by centrifugation at 650 g for 10 minutes. The supernatant was completely aspirated and the pellet was resuspended in 40 μ l of MACS buffer per 10 million cells. A memory CD4⁺ T cell biotin conjugated antibody cocktail was added to the cells at 10 μ l per 10 million cells. The solution was mixed thoroughly, allowed to incubate for 10 minutes at 4°C then washed in MACS buffer and pelleted by centrifugation at 650 g for 10 minutes. The supernatant was completely discarded and the pellet was resuspended in 30 μ l of MACS buffer per 10 million cells. Memory CD4⁺ T cell anti-biotin microbeads (Miltenyi Biotec) was added to the cells at 20 μ l per 10 million cells and incubated for 15 minutes at 4°C. The cell solution was then washed in MACS buffer and pelleted by centrifugation at 650 g for 10 minutes. The pellet was resuspended in 500 μ l (for up to 100 million cells) of MACS buffer. An LS magnetic column (Miltenyi Biotech) was placed in the magnet and washed with MACS buffer (3 ml). The cell sample was then loaded onto the column followed by 3 washes of MACS buffer (3 ml per wash). The eluent of the memory CD4⁺ enriched fraction was collected. Purified memory CD4⁺ T cells were washed in complete RPMI (Biosera), pelleted by centrifugation at 340 g for 10 minutes and counted. A sample of cells were stained with a fluorochrome-conjugated antibody for CD4 and analysed by flow cytometry to check the purity of the sort (Figure 2.1 B)

2.4 Flow-cytometric staining and analysis

2.4.1 Surface and intracellular staining

In order to stain for cytokine production, cells were stimulated with PMA (50 ng/ml) and Ionomycin (500 ng/ml), in the presence of Brefeldin A (5 μ g/ml) for 5 hours. Every stimulated sample was controlled by an unstimulated sample (Brefeldin A only, at 5 μ g/ml). PMA/ionomycin stimulation of human CD4⁺ T cells down regulates the expression of CD4, therefore CD4 enriched stimulated and control cells were alternatively stained extracellularly for CD3 and CD8; gating on the CD3⁺CD8⁻ population to identify the CD4⁺ population. $\gamma\delta$ T cells are included in this method of gating; however, this population only make up 1% of peripheral blood and produce very little IL-17 following PMA stimulation. After stimulation, cells were washed twice with FACS buffer (see appendix) and

centrifuged at 340g for 5 minutes. The cells were stained with or without a viability dye and incubated for 30 minutes at 4°C. The cells were then washed with FACS buffer and centrifuged again. Supernatants were removed and cells were resuspended in 50 µl of FACS buffer containing antibody-conjugated-fluors against extracellular markers of interest. The samples were incubated for 15 minutes in the dark at room temperature, washed in FACS buffer and pelleted by centrifugation. Supernatants were removed and cells were resuspended in 50 µl of fixative solution (part A of the Caltag Fix and Perm, Biosciences) and incubated in the dark for 10 minutes at room temperature. Cells were then washed, pelleted and resuspended in 50 µl permeabilising buffer (part B) containing the antibody-conjugated-fluors against the desired cytokines and/or other intracellular proteins. Cells were incubated for 15 minutes in the dark at room temperature, washed and acquired on a BD LSRFortessa™ flow cytometer. Compensation beads singly stained with every fluor channel utilised were acquired to adjust for spectral overlap. Fluorescence minus one (FMO) controls were also acquired to set negative gates during analysis and an unstained sample was also run as a control. Unstimulated controls were used to set gates for cytokine staining. Flow cytometric analysis was performed using FlowJo.

2.4.2 Intranuclear staining

In order to stain for transcription factor expression, the nucleus of the cell must be permeabilised. Cells were washed twice with FACS buffer and centrifuged at 340 g for 5 minutes. Supernatants were removed and cells were resuspended in 50 µl of FACS buffer containing antibody-conjugated-fluors against extracellular markers of interest. The samples were incubated for 15 minutes in the dark at room temperature, washed in FACS buffer and pelleted by centrifugation. Supernatants were removed and cells were resuspended in 250 µl of Fix/Perm solution (1 in 4 of concentrate and diluent) from the eBioscience FoxP3 staining buffer kit. Cells were incubated for 30 minutes in the dark at 4°C. Cells were then washed and pelleted twice in 1ml of permeabilisation buffer (diluted 1 in 10 with dH₂O), then resuspended in 50 µl of permeabilisation buffer containing antibody-conjugated-fluors against intranuclear and/or intracellular proteins including FoxP3, HIF-1α, Bcl-2 and Ki67. Cells were incubated for 30 minutes in the dark at 4°C, washed and acquired on a BD LSRFortessa™ flow cytometer. Flow cytometric analysis was performed using FlowJo.

2.4.3 GLUT1 staining

For the examination of GLUT1 expression via flow cytometry, cells were washed twice with warmed GLUT1 staining buffer A (see appendix) and centrifuged at 340 g for 5 minutes. Supernatants were removed and cells were stained with GLUT1-GFP (Metafora Biosystems) and/or with surface markers in GLUT1 staining buffer A and incubated for 20 minutes at 37°C. The cells were then washed with the GLUT1 staining buffer B and centrifuged again. Supernatants were removed and cells were resuspended in 50 µl of GLUT1 staining buffer B and placed in the fridge until acquired by the BD LSRFortessa™ flow cytometer. Cells could additionally be fixed and staining continued for the analysis of intracellular markers.

Initially, the flow cytometric analysis of GLUT1 expression was optimised in total PBMC. Healthy donor PBMC were stimulated in the presence or absence of anti-CD3 (1 µg/ml) for 24 or 48 hours and stained with fluorochrome-conjugated antibodies for CD4 and GLUT1-GFP. The cells were analysed by flow cytometry. The 48 h stimulation was chosen as optimal, as it resulted in the highest median fluorescence intensity (MFI) values for GLUT1 (Figure 2.2).

2.4.4. Mitotracker® green labelling

In order to analyse mitochondrial mass, cells were stained with mitotracker® green FM (Life Technologies). Cells were washed in warm PBS and centrifuged at 340 g for 5 minutes. Supernatants were removed and cells were stained with mitotracker® green FM at a final concentration of 4 nM. Cells were incubated for 30 minutes at 37°C. Cells were washed in warm PBS and centrifuged at 340 g for 5 minutes. Supernatants were removed and cells were acquired immediately by the BD LSRFortessa™ flow cytometer. Mitotracker® green FM staining does not allow for cell fixing, and therefore intracellular staining was not permitted. Surface staining can be performed prior to mitotracker staining.

Mitotracker® green FM staining was optimised for human PBMC cells. Healthy donor PBMC were stimulated in the presence or absence of anti-CD3 (1 µg/ml) for 24 hours. Cells were stained for CD4 and with or without increasing concentrations of Mitotracker® green FM, or DMSO (vehicle control). Cells were analysed by flow cytometry and gated on CD4⁺ T cells. Mitotracker staining was not increased by cell stimulation and a concentration of 4 nM mitotracker was chosen as optimal as it provided the most centred

peak by histogram analysis (Figure 2.3 A and B). To confirm that Mitotracker® green FM was not representative of mitochondrial membrane potential (MMP), cells were stimulated with anti-CD3 and treated with increasing concentrations of carbonyl cyanide-p-trifluoromethoxyphenylhydrazone (FCCP) for 24 hours. FCCP is known to disrupt the MMP, resulting in depolarisation and a subsequent decrease in the MMP. Mitotracker® green FM. Cells were stained for CD4 and with Mitotracker® green FM (4 nM). Cells were analysed by flow cytometry and gated on CD4⁺ T cells. Mitotracker staining was not decreased by FCCP treatment, confirming its use as an indicator of mitochondrial mass and not MMP (Figure 2.3 C).

2.4.5 Cell tracer labelling

Cells for labelling were washed in sterile PBS in order to remove any amine groups as these can quench tracer dyes. Tracer dyes were diluted in warm PBS, to prevent precipitation, and cells were resuspended in an equal amount of warm PBS. The diluted tracer dyes were added to the cells to achieve a final concentration of 0.5 µM (Carboxyfluorescein succinimidyl ester (CFSE)) and 1 µM (CellTrace™ Violet (CTV)). Cells were incubated for 10 minutes at 37°C. 10% FCS was added to stop the labelling and cells were placed on ice for 5 minutes. Cells were then washed twice in complete medium. A sample of both unlabelled and labelled (CFSE and CTV) cells were taken on d0 and fixed with 4% paraformaldehyde (PFA, Santa Cruz Biotech) for use as a positive and negative compensation control.

2.5 Glucose uptake assay

2-NBDG is a fluorescent D-glucose analogue used to monitor glucose uptake in live cells. Human PBMC from healthy donors were stimulated with plate-bound anti-CD3 (1 µg/ml) for 3 days. Cells were washed twice in glucose-free RPMI (see appendix) and centrifuged at 300 g for 5 minutes. Cells were resuspended in glucose-free RPMI and incubated at 37°C for 15 minutes. Cells were washed once again in glucose-free RPMI and resuspended in 200 µl of 100 µM 2-NBDG (Life Technologies) in glucose-free RPMI. Unstained control cells were resuspended in 200 µl of glucose-free RPMI. Cells were incubated for 1 hr at 37°C then washed in pre-cooled PBS. Surface staining was carried out as previously described and cells were incubated for 20 minutes at 4°C. Cells were washed in cold PBS

and acquired immediately on a BD LSRFortessa™ flow cytometer. Flow cytometric analysis was performed using FlowJo.

2.6 Measurement of glycolysis and oxidative phosphorylation by the Seahorse XF Analyzer

The Seahorse XF Analyzer measures both the oxygen consumption rate (OCR), relating to oxidative phosphorylation, and extracellular acidification rate (ECAR), relating to glycolysis, simultaneously, in real time, in the medium directly surrounding a single layer of cells.

The Seahorse cartridge plate, consisting of the dual-analyte sensors, must be soaked in 1 ml of calibrant solution (Seahorse Bioscience) overnight in a non-CO₂ incubator. Seahorse 24-well plates were pre-treated with 50 µl/well Cell-Tak™ (1µg/well) (Seahorse Bioscience) dissolved in 0.1 M sodium bicarbonate (pH 8.0) and incubated at room temperature for a minimum of 30 minutes. Following incubation, the wells were washed twice with dH₂O. Cells were washed and resuspended in XF Assay Medium (Seahorse Bioscience) and seeded at varying densities (100 µl/well) into the culture plate. Blank wells, containing XF Assay Medium only, were loaded in order to subtract the background OCR and ECAR from the cell-containing wells. Cells were adhered onto the Cell-Tak™ within the wells following centrifugation at 40 g for 10 seconds with the brake off. The culture plate is rotated to face the opposing direction and centrifugation is repeated. Cells were incubated in a non-CO₂ environment for 20 minutes. Metabolic compounds were prepared in XF Assay Medium and loaded into the appropriate injection ports (located on the cartridge plate) (75 µl/port) and incubated for 10 minutes in a non-CO₂ environment. The cartridge is placed into the XF Analyzer and the machine is calibrated. XF Assay Medium is gently added to each well of the cell culture plate (400 µl/well), making the total volume 500 µl/well. The culture plate is incubated for a further 15 minutes in a non-CO₂ environment and loaded into the analyzer. Basal OCR and ECAR is measured, followed by 'mixing' of the medium directly surrounding the cell monolayer, facilitated by the probe moving up and down gently within the well. Each compound is added to the well individually, in the appropriate order, and the OCR and ECAR is measured, followed by a mixing step. Upon completion of the protocol, the cells are examined under a microscope to ensure persistent cell adherence to the base of the well.

2.6.1 The determination of the optimal cell seeding density for memory CD4⁺ T cell analysis via the Seahorse XF Analyzer.

The Seahorse XF Analyzer was utilised to determine cellular glycolytic activity and the cellular mitochondrial function in human CD4⁺ T cells for the first time in this study. Initially, the determination of an optimal cell seeding density was required in order to obtain an adequate basal ECAR and OCR reading. Memory CD4⁺ T cells were negatively sorted from PBMC using magnetic beads and seeded at varying densities (2×10^5 – 1×10^6 cells/well) in a Seahorse Biosciences 24-well plate, with K562 cells (1.5×10^5 cells/well) as a positive control for experimental design and cell adherence. Cell-Tak™ (1 µg/well) was utilised to adhere the CD4⁺ T cells to the plate. Within the analyzer, the cells were treated with increasing concentrations of glucose (0.5 – 7 mM) in order to stimulate glycolysis. After each glucose injection, the ECAR and OCR were measured at three time points in each replicate well. The ECAR increased for each cell type and density following the addition of 0.5 and 2.5 mM glucose, however no further increase was observed following addition of 7 mM glucose (Figure 2.4 A). Conversely, the OCR decreased for both cell types and densities following each glucose addition (Figure 2.4 B). After glucose injections, cells were treated with 300 nM FCCP, an ionophore, which transports protons across the mitochondrial membrane, disrupting ATP synthase and thus disturbing the mitochondrial membrane potential. This resulted in increased ECAR and OCR for both cell types and densities as cells attempt to re-establish the MMP. The memory CD4⁺ T cell density displaying the highest ECAR and OCR overall, compared with that of the control, was 1 million cells/well, and therefore this cell seeding density was chosen as optimal. This was also the maximum capacity of the surface area of the well. Glucose at 2.5 mM generated the highest ECAR and was therefore selected for optimal glycolysis stimulation in future experiments (indicated in red).

2.6.2 Optimization of the metabolic compounds required for the measurement of the metabolic activity of memory CD4⁺ T cells.

The metabolic profile of cells can be determined following the addition of inhibitors and stimulators of glycolysis and mitochondrial respiration. These compounds shift the bioenergetics of the cell, distinguishing glycolytic function from mitochondrial respiration. Memory CD4⁺ T cells were negatively sorted from PBMC using magnetic beads and seeded at 1 million cells/well in Cell-Tak™ coated wells. The cells were treated with

various concentrations of compounds required to determine their glycolytic profile; oligomycin A, FCCP and 2-deoxy-d-glucose (2-DG). The ECAR was recorded after the addition of each compound concentration via the Seahorse XF Analyzer. Oligomycin A is an ATP synthase inhibitor, obstructing the transport of protons through the mitochondrial membrane and thus inhibiting ATP production by oxidative phosphorylation. Cellular respiration relies on glycolysis following oligomycin treatment, and so the ECAR is increased. The lowest oligomycin A concentration to induce the maximal ECAR was 0.25 $\mu\text{g/ml}$ (Figure 2.5 A, indicated in red), and so was chosen as the optimal oligomycin A concentration. FCCP is an uncoupler of oxidative phosphorylation and subsequent inhibitor of ATP production through the disruption of ATP synthase. Uncoupling of oxidative phosphorylation results in increased glycolysis and ECAR. The lowest FCCP concentration to induce the maximal ECAR was 450 nM (Figure 2.5 B, indicated in red). This was chosen as the optimal FCCP concentration. 2-Deoxy-D-glucose (2-DG) is a glucose molecule, which has its 2-hydroxyl group replaced by a hydrogen and therefore cannot undergo further breakdown within the glycolytic pathway. 2-DG competes with glucose for cellular uptake via the glucose transporters, and so glycolytic activity decreases. However, following 2-DG treatment, ECAR was not decreased. This was likely due to the fact that resting CD4^+ T cells exhibited relatively low metabolic activity, represented by low ECAR, before the addition of glycolytic inhibitors or stimulators.

Next, compounds involved in the determination of mitochondrial respiration were examined. Memory CD4^+ T cells were negatively sorted from PBMC using magnetic beads, seeded at 1 million cells/well in Cell-Tak™-coated wells and treated with various concentrations of compounds required to determine the mitochondrial respiration of the cells; oligomycin A, FCCP, rotenone and antimycin A. As previously described, oligomycin A is an inhibitor of oxidative phosphorylation, resulting in decreased OCR (Figure 2.6 A). The lowest oligomycin A concentration to induce the lowest OCR was chosen as the new optimal compared with ECAR values (0.5 $\mu\text{g/ml}$) (indicated in red). FCCP, as previously described, disrupts the mitochondrial membrane potential, subsequently increasing both mitochondrial respiration and glycolysis. The OCR was increased following FCCP treatment (Figure 2.6 B). The lowest FCCP concentration to generate the highest OCR was chosen as optimal (450 nM) (indicated in red). Rotenone inhibits complex I in the electron transport chain, preventing the transfer of electrons from the iron-sulphur centres to ubiquinone (coenzyme q). This inhibition of electron transport prevents the conversion of

potential energy, in the form of NADH, to usable energy, ATP. The OCR was decreased following treatment with rotenone (Figure 2.6 C). The lowest concentration of rotenone causing the lowest OCR was chosen as optimal (0.5 $\mu\text{g}/\text{ml}$) (indicated in red). Antimycin A inhibits complex III of the electron transport chain, subsequently preventing ATP production by oxidative phosphorylation and disrupting the formation of the mitochondrial proton gradient. Antimycin A treatment resulted in decreased OCR (Figure 2.6 D). The optimal concentration of antimycin A generating the lowest OCR was 2.5 μM (indicated in red).

2.7 Protein quantification by Western blotting

2.7.1 DSS cross-linking

In order to determine the formation of protein tetramers by western blotting, proteins must be cross-linked prior to cell lysis. Disuccinimidyl suberate (DSS; ThermoFisher Scientific) is a non-cleavable and cell membrane permeable agent, which cross links primary amines in the side chains of proteins. Cells were washed in PBS (pH 8) in order to remove any amines from the culture media, which may quench the DSS. This is repeated twice. Cells were separated into eppendorfs (100 μl). Bring DSS to room temperature and dissolve in DMSO. DSS was added directly to the cells to make a final concentration of 0.5, 1 or 2 mM usually. Cells are resuspended and incubated on ice for 15 or 30 minutes. 5 μl of 1M Tris (see appendix) (pH 7.5) was added to quench the DSS and cells were incubated on ice for a further 15 minutes. Cells were pelleted at 300 g and supernatants were removed completely. Sample buffer (see appendix) was added, cells were boiled at 95°C for 10 minutes and analysed by western blot for protein expression.

2.7.2 Examination of TEPP-46-induced PKM2 tetramer formation in Jurkat T cells by western blot

The Jurkat T cell line was utilised for the optimisation of DSS-linking and TEPP-46-induction of the PKM2 tetramer. TEPP-46 is a small molecule activator of PKM2 and an inducer of the tetrameric form of PKM2. Jurkat T cells were cultured at 1×10^6 cells/ml in a 6-well plate overnight at 37°C. Cells were treated with DMSO or TEPP-46 (10 – 100 μM) for 18 hours. Protein cross linking was performed using the DSS protocol and cells were resuspended in 70 μl of sample buffer. Samples were boiled at 95°C and loaded onto an

8% SDS polyacrylamide gel, along with a prestained protein marker (4-250 kD, SeeBlue® Plus2 Pre-Stained Standard by Invitrogen). Electrophoresis was performed at 130 V for 2 hours. As the proteins of interest are 60 kD (monomeric PKM2) and 260 kD (tetrameric PKM2), smaller proteins were run off the bottom of the gel. Following separation, the proteins were subsequently transferred electrophoretically at 20 v overnight onto a nitrocellulose membrane. Non-specific binding was blocked by incubating the membrane at room temperature for 1 hour (or overnight at 4°C) in PBS-Tween containing 5% (w/v) skimmed milk powder. The membranes were then incubated in primary PKM2 antibody (Cell Signaling) (1:1000) in 5% BSA in PBS-Tween at 4°C overnight. The membranes were washed in PBS-Tween (3 x 10 minutes) prior to incubation with a fluorescently-tagged anti-rabbit IRDye® secondary antibody (LI-COR) (1:1000) for 2 hours in the dark at room temperature. The membranes were washed a further 3 times and proteins were visualised by the Odyssey® Infrared Imaging System (LI-COR). Protein size was determined by comparing to the molecular weight marker. Densitometric analysis was performed using ImageJ software. Jurkat T cells demonstrate an increase in PKM2 tetramer formation following TEPP-46 treatment, with the PKM2 tetramer only detectable in the DSS-treated cells (Figure 2.7).

2.8 Measurement of cytokine production by ELISA

The concentration of human IL-17, IL-10, IFN- γ and TGF- β cytokines in cell culture supernatants were quantified by enzyme-linked immunosorbent assay (ELISA). Capture antibody in coating buffer was applied to high-binding 96-well plates (Greiner Bio-one) in 75 μ l volume. Plates were incubated for 2 hours at 37°C or overnight at 4°C. Plates were then washed in PBS-Tween solution (see appendix) and non-specific binding sites were blocked with 200 μ l of the appropriate blocking solution and incubated at room temperature for 1 hour. After blocking, plates were washed again before the addition of triplicate supernatant samples of 75 μ l into the wells, either neat or diluted 1 in 3 with assay diluent. A standard curve of serially diluted recombinant cytokine standard was also loaded onto the plates (see appendix). Blank wells, containing assay diluents only, were loaded in order to subtract the background absorption from the sample wells. Samples were incubated overnight at 4°C. After washing, 75 μ l of biotinylated detection antibody was added to each well and incubated for 2 hours at room temperature. Plates were washed again and 75 μ l of horseradish-peroxidase (HRP) conjugated to streptavidin was

applied to the wells and the plate was incubated for a further 20 minutes in the dark at room temperature. The plate was thoroughly washed and 75 µl of the substrate tetramethylbenzidine (TMB) was added. Throughout development the enzyme-mediated colour reaction was protected from light and the reaction was stopped with the addition of 37.5 µl (1 in 3 dilution of total volume/well) of 1M H₂SO₄. The absorbance of each well was determined using a microtitre plate reader at 450 nm. Cytokine concentrations were calculated from the standard curve and relevant dilution factors were applied.

2.9 Mitochondrial array

The expression of mitochondrial genes was analysed by RT-PCR and performed by Trudy McGarry (St. Vincent's University Hospital). RNA was first isolated from the cells using the RNeasy Mini Kit from Qiagen. cDNA was synthesized from isolated RNA using the RT² Easy First Strand Reverse Transcription Kit from Qiagen. RT-PCR was performed using the RT² Profiler PCR Array Human Mitochondria (Qiagen) and the plate was applied to the 7500 Fast Real-time PCR machine (Applied Biosystems) and run according to the following PCR cycle conditions; 95°C for 2 minutes to allow for activation, followed by 40 cycles of 95°C for 10 seconds and 60°C for 30 seconds. Quantification was performed using the 7500 Fast System Software v.1.3.1.

2.10 Statistical analysis

Statistical analyses were performed using Prism 5 software. The paired t-test was used to compare variance between 2 groups, while a One-way ANOVA with Tukey's multiple comparison post-test was used for comparing three or more groups. P values of <0.05 were considered significant and denoted with an asterix.

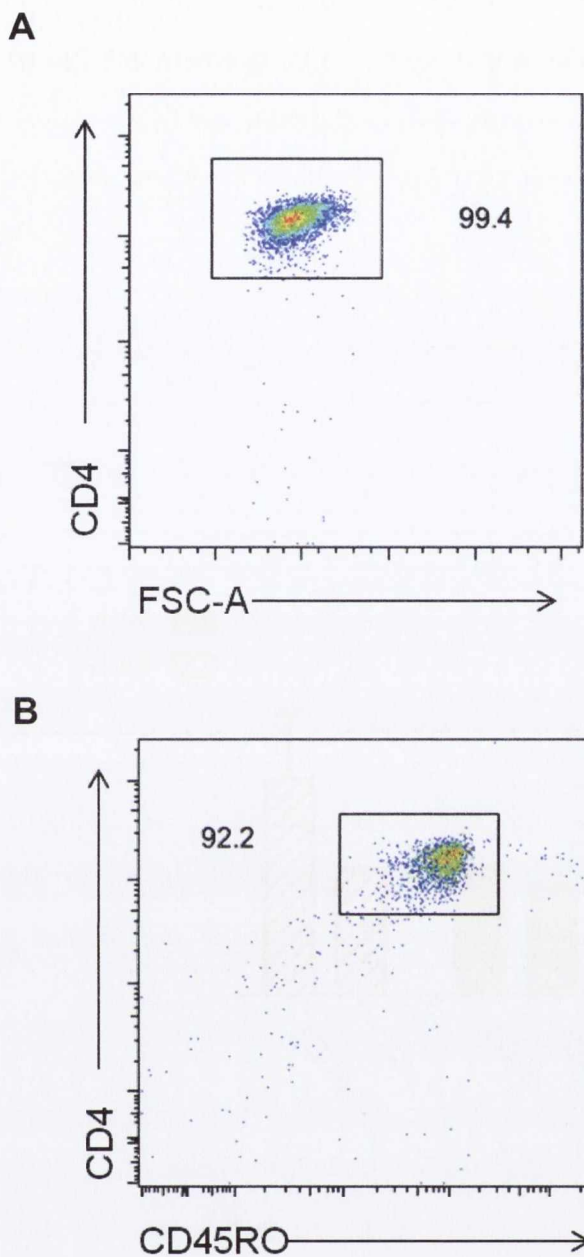


Figure 2.1 Purity check of CD4 and CD45RO MACS sort

PBMC were isolated from healthy donors and labelled with magnetic beads, according to the manufacturer's protocol. The desired CD4⁺ (A) or CD4⁺CD45RO⁺ (B) cells were stained with fluorochrome-conjugated antibodies against CD4 and CD45RO and analysed by flow cytometry. The dot plots represent CD4 vs FSC-A for sorted CD4⁺ cells (A) and CD4 vs CD45RO for sorted memory CD4⁺ T cells (B).

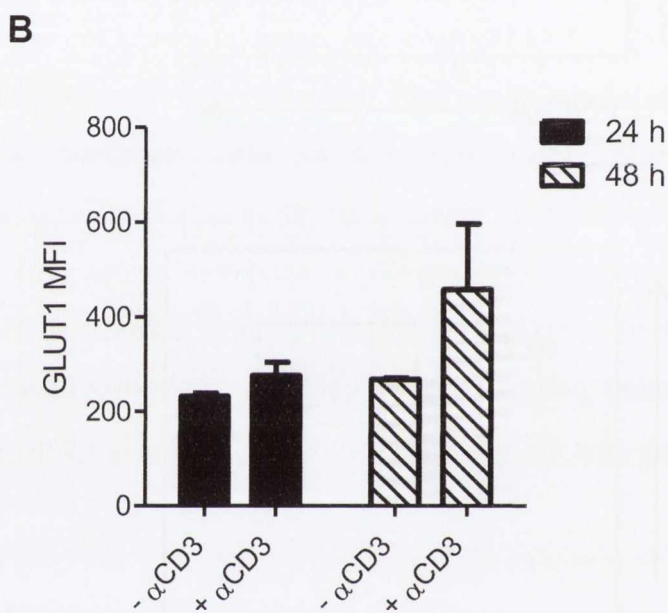
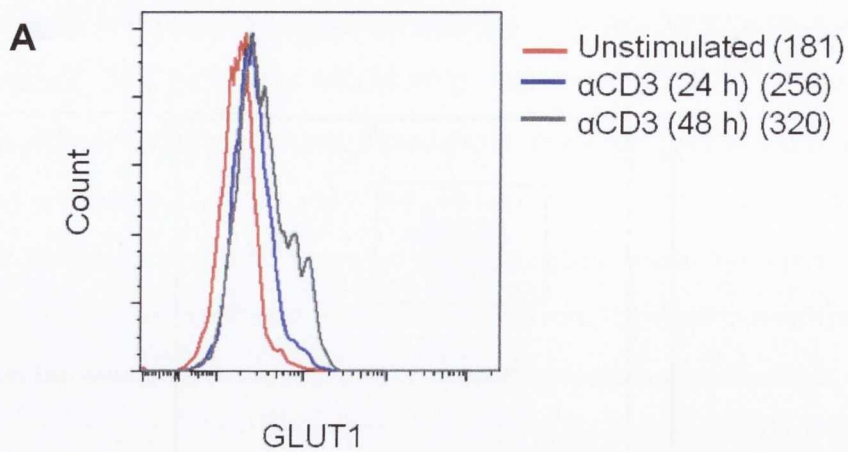


Figure 2.2. Optimisation of the stimulation period for analysis of GLUT1 expression in $CD4^+$ T cells.

PBMC from healthy donors were stimulated in the presence of plate-bound anti-CD3 for 24 or 48 hours. The cells were stained with fluorochrome-conjugated antibodies specific for CD4 and GLUT1, and analysed by flow cytometry, representative histogram gated on $CD4^+$ T cells shown in (A). The graph shows GLUT1 MFI values for $CD4^+$ T cells (n=2) (B).

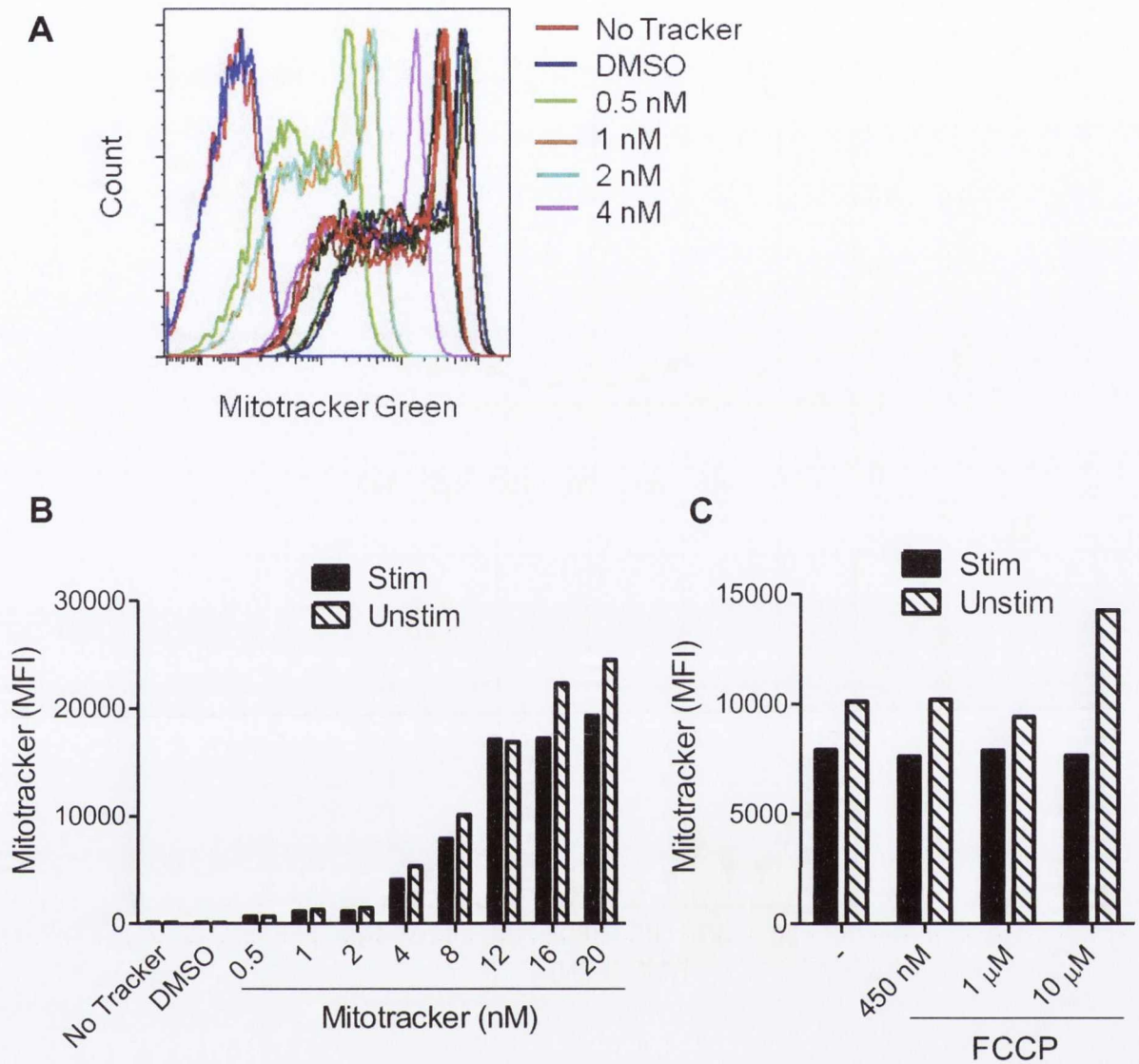


Figure 2.3. Optimization of mitotracker green for flow cytometric analysis of mitochondrial mass.

PBMC from healthy donors were cultured in the presence or absence of plate-bound anti-CD3 and increasing concentrations of FCCP or vehicle (DMSO) for 24 hours. The cells were stained with fluorochrome-conjugated antibodies specific for CD4 and mitotracker green and analysed by flow cytometry. Histograms showing mitotracker staining at increasing concentrations (A) and graphical representation of mitotracker MFI (B) are shown. Mitotracker MFI in the presence or absence of FCCP is shown in (C)

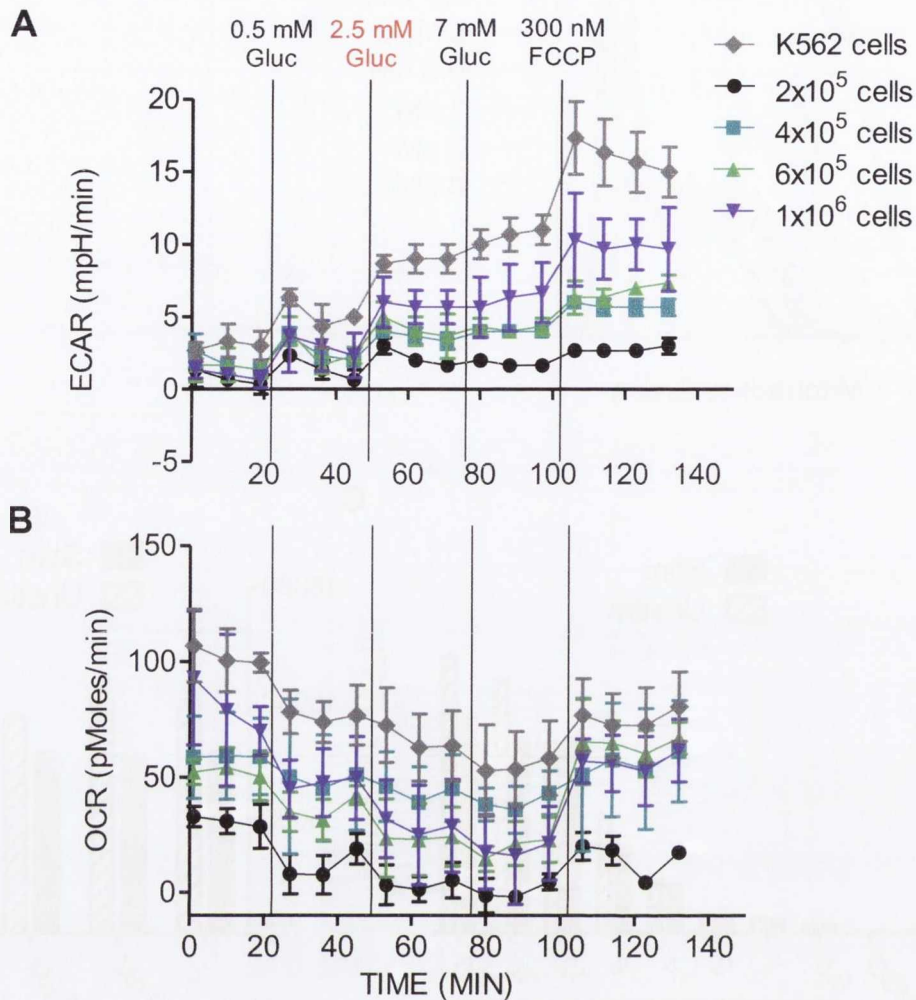


Figure 2.4 Determination of the optimal cell seeding density for the measurement of the metabolic activity of memory $CD4^+$ T cells by the Seahorse XF Analyzer.

Memory $CD4^+$ T cells were negatively sorted from healthy donor PBMC using magnetic beads and seeded at varying densities (2×10^5 - 1×10^6 cells/well) in a Seahorse Biosciences 24-well plate, with K562 cells (1.5×10^5 cells/well) as a positive control. Cell-Tak™ was required to adhere cells to the plate. The extracellular acidification rate (ECAR) (A) and the oxygen consumption rate (OCR) (B) were measured after the addition of 0.5 mM, 2.5 mM and 7 mM glucose, followed by 300 nM FCCP (n=1, performed in triplicate).

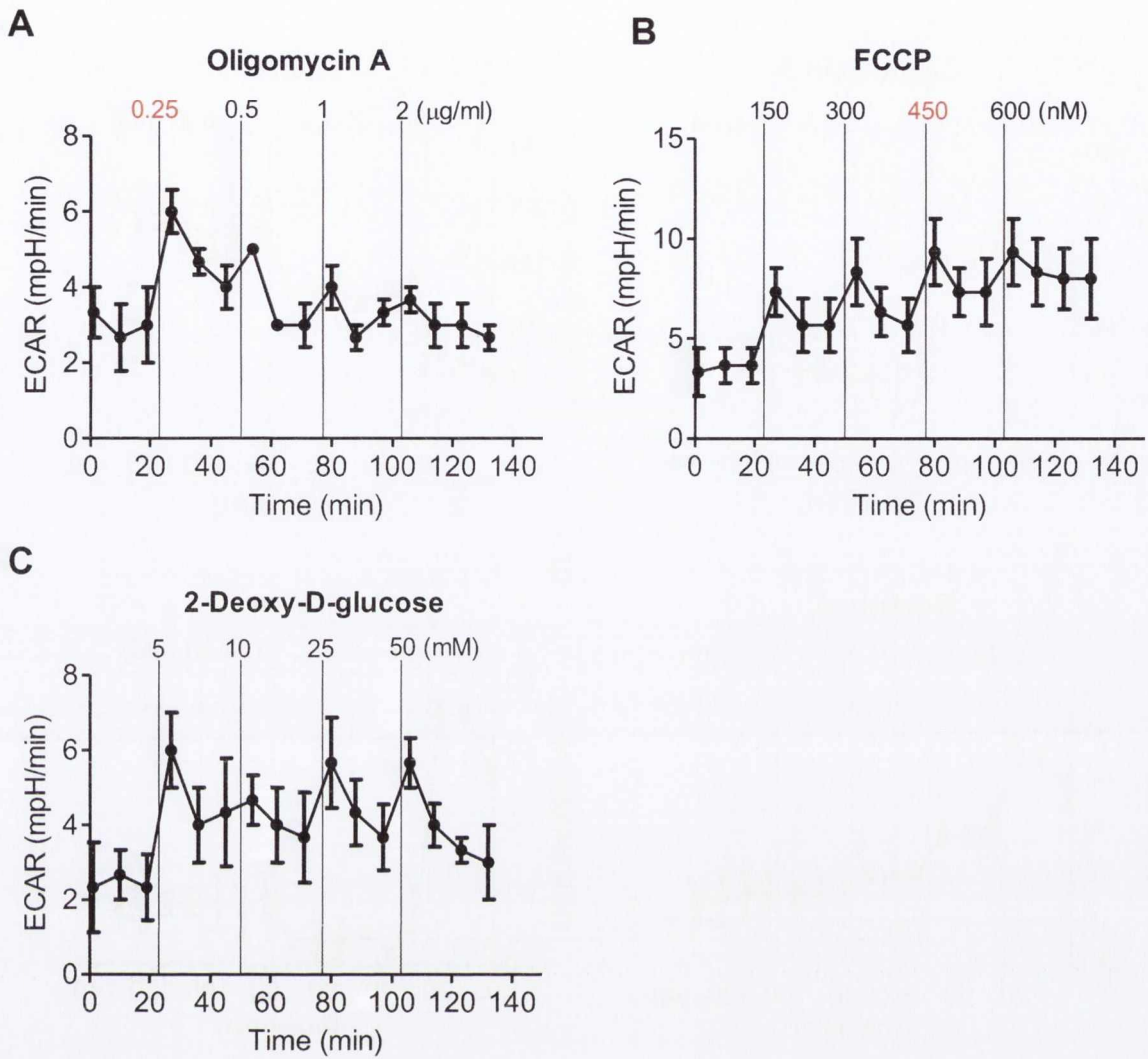


Figure 2.5. Optimization of metabolic compounds used to determine the glycolytic profile of CD4^+ memory cells

Memory CD4^+ T cells were negatively sorted from healthy donor PBMC using magnetic beads and treated with various concentrations of oligomycin A (A), FCCP (B) and 2-deoxy-d-glucose (C). The ECAR was measured after each addition via the Seahorse XF Analyzer ($n=1$, performed in triplicate).

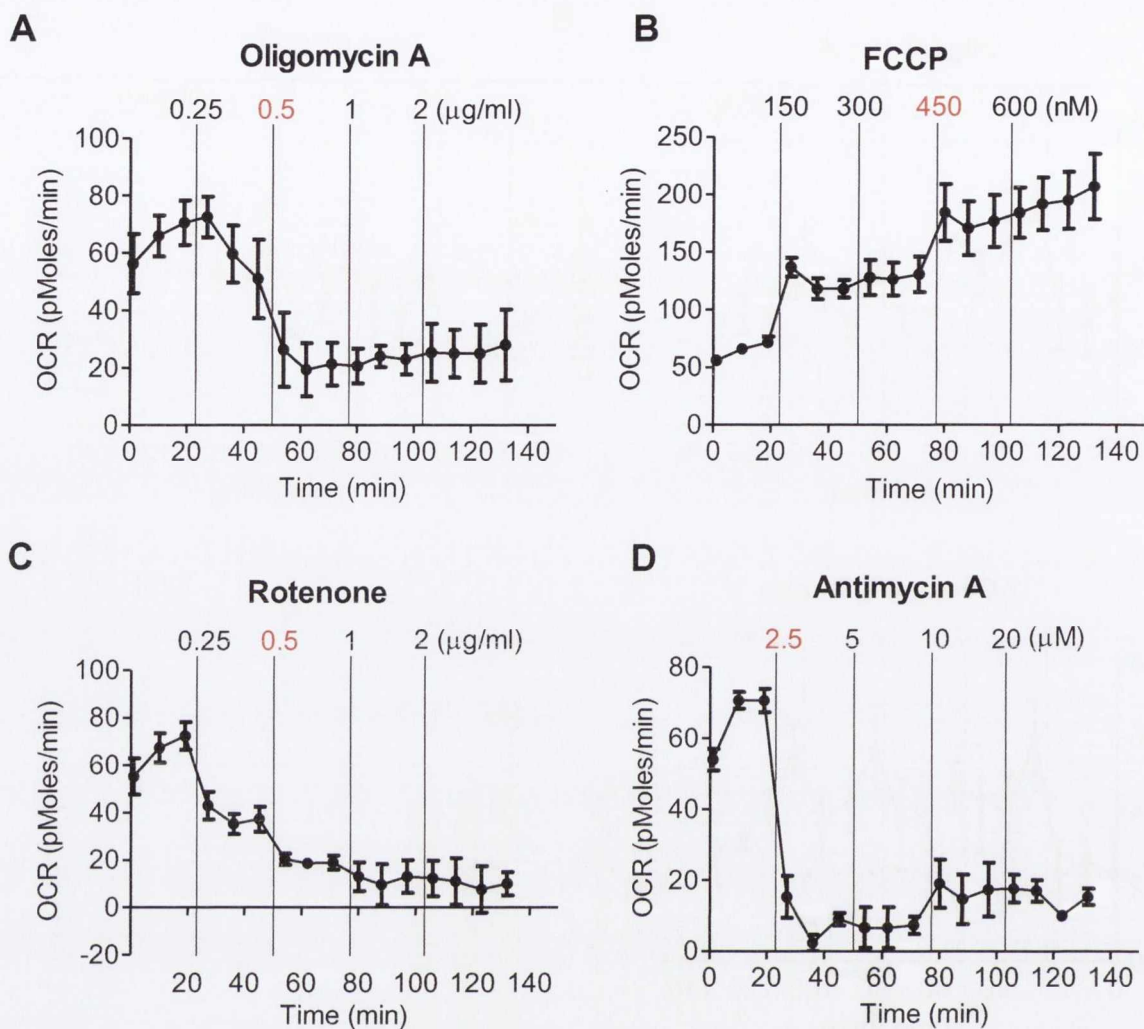


Figure 2.6. Optimization of metabolic compounds used to determine the mitochondrial respiration of CD4^+ memory cells.

Memory CD4^+ T cells were negatively sorted from healthy donor PBMC using magnetic beads and treated with various concentrations of oligomycin A (A), FCCP (B), rotenone (C) and antimycin A (D). The OCR was measured after each addition via the Seahorse XF Analyzer ($n=1$, performed in triplicate).

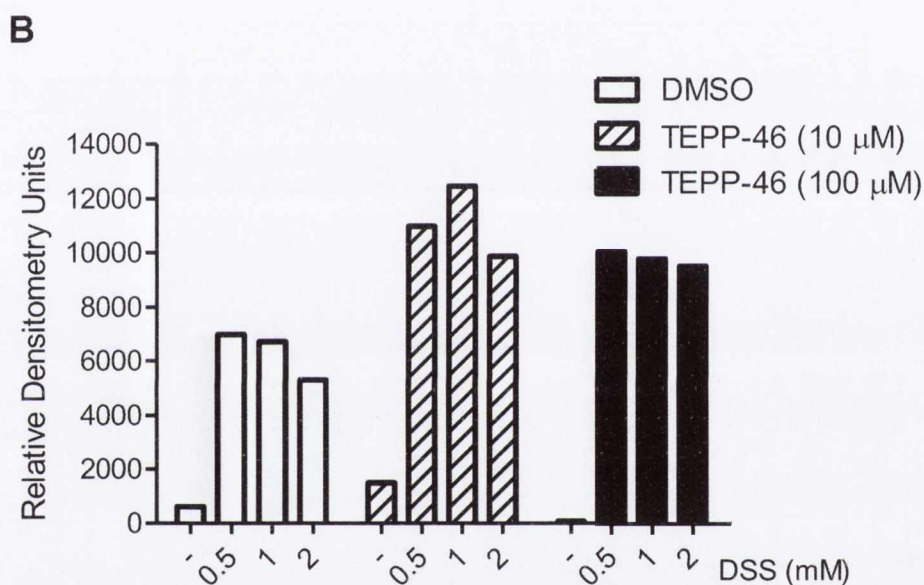
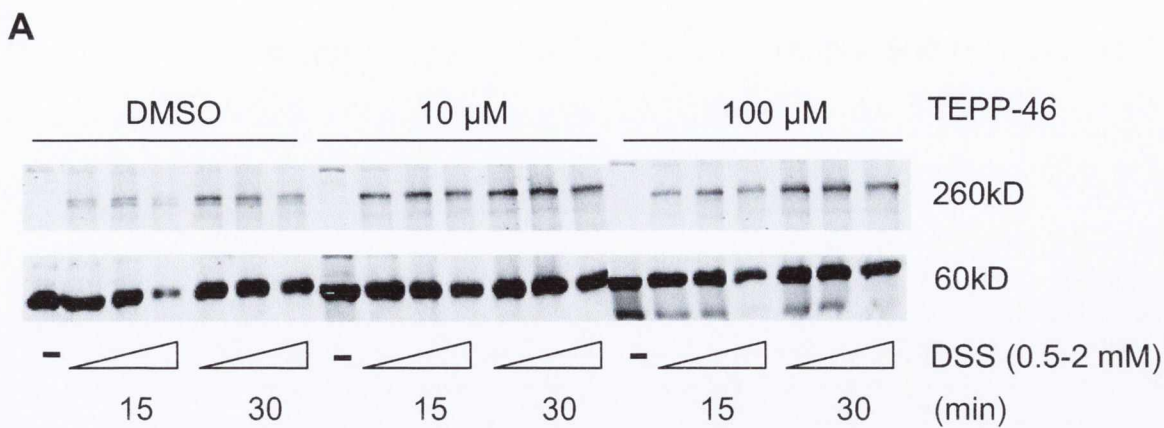


Figure 2.7 TEPP-46 treatment of Jurkat T cells promotes PKM2 tetramer formation.

Jurkat cells were cultured overnight at 37°C and then treated with vehicle (DMSO) or TEPP-46 (0 – 100 μ M) for 18 hrs. DSS-linking was performed on the cells with increasing concentrations of DSS. Western blot was performed for PKM2 (pyruvate kinase M2). The western blot shows both monomeric (60 kD) and tetrameric (260 kD) forms of PKM2 in the presence or absence of TEPP-46 (A). Densitometric analysis was used to compare band intensities for tetrameric PKM2 (B).



Figure 1. Effect of temperature on the formation of 1,2,3,4-tetrahydro-1,2,3,4-tetrahydropyridine (THP) and 1,2,3,4-tetrahydro-1,2,3,4-tetrahydropyridine (THP) at 100°C, 150°C, and 200°C. The amount of starting material was 25, 50, 75, and 100 mg. The amount of product was determined by gas chromatography-mass spectrometry (GC-MS).

Chapter 3

The metabolic pathways utilised by human T cell subsets

Chapter 3. The metabolic pathways utilized by human T cell subsets

3.1.1 Introduction

Autoimmunity results from abnormal and uncontrolled innate and adaptive immune responses, and is often associated with systemic inflammation. CD4⁺ T cells play a key role in autoimmunity and therefore it is important to understand the factors that regulate them during the normal immune response to infection and during aberrant immune responses in autoimmunity. CD4⁺ T cells are required to utilise the available resources in order to survive, proliferate and function under the conditions encountered during infection or autoimmunity. Thus the ability of CD4⁺ T cells, and subsets thereof, to utilise energy sources and metabolic pathways is of key importance and an area of emerging interest in immunology.

Metabolism and pathogen defence are essential for host survival. Naïve T cells in mice exhibit low rates of oxidative metabolism in order to undergo homeostatic proliferation, maintain survival and perform immunosurveillance (Cao, Rathmell et al. 2014); however, upon activation CD4⁺ T cells differentiate into memory T cells and reprogram towards a highly glycolytic metabolic program in order to generate energy and biosynthetic materials for rapid proliferation and differentiation (Sallusto, Geginat et al. 2004). CD4⁺ T cells spend most of their time circulating the blood and secondary lymphoid organs, where nutrients are abundant; however, during infection, T cells migrate to sites of infection, resulting in increased inflammation and subsequent reduction in the availability of resources. Thus T cells must compete with other immune cells for nutrients at sites of inflammation.

Different CD4⁺ T cell subsets fill distinct roles during infection. Understanding the resources and factors which contribute to the balance between Th17/Th1 and Treg cells is key to targeting autoimmunity. One such factor is cellular energy metabolism. The distinctive functions of CD4⁺ T cell subsets suggests that each may require specific metabolic programs to meet their differing energy and biosynthetic demands. Two recent studies in mice have indicated that murine Th17 and Th1 cells are primarily glycolytic, with increased expression of the glucose transporter GLUT1 and inhibition of IL-17 and IFN- γ production following treatment with 2-deoxy-D-glucose (2-DG) and rapamycin

(known inhibitors of glycolysis) (Michalek, Gerriets et al. 2011, Shi, Wang et al. 2011). Increased glucose uptake via glucose transporters is known to be directly proportional to glycolysis (Michalek, Gerriets et al. 2011). In contrast, murine Treg cells primarily use lipid metabolism and oxidative phosphorylation, since treatment with an inhibitor of mitochondrial lipid uptake and oxidation (etomoxir) resulted in a significant decrease in the differentiation of CD4⁺Foxp3⁺ T cells from naïve cells (Michalek, Gerriets et al. 2011).

A number of transcriptional and posttranscriptional mediators control T cell metabolism. Increased glycolysis and metabolic reprogramming following T cell activation is reliant on co-stimulation and signalling through CD28 (Frauwirth, Riley et al. 2002). This in turn activates the PI3K/Akt/mTOR posttranscriptional pathway, which plays a key role in promoting aerobic glycolysis. PI3K becomes activated as a consequence of CD28 ligation and PIP₃ is generated, which recruits Akt and 3-phosphoinositide-dependent protein kinase-1 (PDK1) to the cell membrane. PDK1, together with mTORC2, phosphorylate and activate Akt (Gerriets and Rathmell 2012). Akt is known to promote glycolysis through promoting trafficking of glucose transporters (GLUT1) (Rathmell, Fox et al. 2003) and amino acid transporter proteins to the cell surface (Edinger and Thompson 2002). Akt also initiates a signalling cascade resulting in mTORC1 activation (Chi 2012). mTORC1 stimulates posttranslational events to promote glycolysis; including the phosphorylation of 4EBP and p70S6 kinase (p70S6K) to promote increased protein translation. Activation of p70S6K may mediate many of the glycolytic effects of mTORC1, as p70S6K deficiency prevents increased glycolysis in PTEN-deficient cells (Tandon, Gallo et al. 2011). The phosphorylation of the ribosomal protein S6, the direct phosphorylation target of p70S6K, indicates mTOR activity and can be quantified by flow cytometry. Rapamycin, as mentioned previously, inhibits mTOR and subsequently inhibits glycolysis.

Oxidative phosphorylation occurs within the mitochondria. A recent study investigating the mitochondrial mass and function of murine T cells has shown CD4⁺ T cells to have a larger mitochondrial mass than CD8⁺ T cells through performing mitotracker staining, a mitochondrial membrane dye (Cao, Rathmell et al. 2014). CD8⁺ T cells displayed a higher glycolytic metabolism compared with CD4⁺ T cells in this study, while CD4⁺ T cells demonstrated an increased oxidative metabolism compared with CD8⁺ T cells. An increased mitochondrial mass displayed by CD4⁺ T

cells could potentially promote this increased oxidative phosphorylation in this subset (Cao, Rathmell et al. 2014).

Research carried out thus far on the metabolism of CD4⁺ T cells has focused mainly on the differentiation of T cell subsets from naïve T cells, mostly in mouse models. However, very little, if any, research has centred on differentiated, human memory T cells located at sites of infection and inflammation, where resources such as metabolites and oxygen are in short supply. In this chapter, experiments were aimed at understanding what metabolic pathways could be supporting Th17 and Treg cell populations taken from the blood of healthy individuals.

3.1.2 Aims

The experiments in this chapter aimed to determine the metabolic pathways utilised by human CD4⁺ T cell subsets. The specific objectives were to:

- Establish methods for the investigation of metabolic pathways utilised by human T cells
- Investigate the metabolic profile of human Th17 lineage cells and Treg cells.

3.2 Results

3.2.1 The expression of GLUT1 is increased in CD4⁺ T cells compared with CD8⁺ T cells, and in effector memory versus central memory CD4⁺ T cells.

GLUT1 is a uniporter protein located on the cell surface, which facilitates the movement of glucose molecules through the plasma membrane. GLUT1 expression is essential for the increased glycolytic metabolism shown in activated murine T cells and GLUT1 knockout mice exhibit fewer effector T cells, including Th17 cells (Macintyre, Gerriets et al. 2014). The metabolic pathways utilized by human CD4 and CD8 T cells remains controversial.

Initially, the flow cytometric analysis of GLUT1 expression in total PBMC was optimized, and results are displayed in chapter 2. On the basis of this, the optimal GLUT1 expression was chosen following 48 h stimulation with anti-CD3. First the expression of GLUT1 in total CD4⁺ compared with CD8⁺ T cells was explored, as previous studies in human cells have demonstrated an increase in glucose metabolism for CD4⁺ T cells, using lactate production as a readout of glycolysis (Renner, Geiselhoringer et al. 2015). Healthy donor PBMC were stimulated for 48 h in the presence of anti-CD3 and stained with CD4, CD8 and GLUT1 fluorochrome-conjugated antibodies. The expression of GLUT1 on CD4⁺ T cells was significantly increased, as demonstrated by an increased shift in MFI values for CD4⁺ T cells (Figure 3.1 A), compared with CD8⁺ T cells across five donors ($p < 0.01$) (Figure 3.1 B).

Memory CD4 T cells develop from naïve cells following antigen stimulation and differentiate into one of the various CD4⁺ T cell subsets. Memory cells are divided into two categories; effector memory which home mostly to sites of inflammation and central memory which home to lymph nodes waiting for the recurrence of previous infections (Sallusto, Lenig et al. 1999). The metabolic profile of memory T cells, especially those found at the site of infection, is of interest. Healthy donor PBMC were stimulated for 48 hr in the presence of anti-CD3 and stained for CD4, CD45RO, CCR7 and GLUT1 fluorochrome-conjugated antibodies. The expression of GLUT1 by effector memory (CD4⁺CD45RO⁺CCR7⁻) cells was significantly increased compared with central memory cells (CD4⁺CD45RO⁺CCR7⁺) ($n=6$) ($p < 0.05$) (Figure 3.2).

In summary, these data suggest that CD4⁺ T cells have the ability to take up more glucose than CD8⁺ T cells, as do effector memory relative to central memory CD4⁺ T cells.

3.2.2 Investigation of the mitochondrial mass of CD4 and CD8 T cells

Having examined GLUT1 expression, a correlate of glycolysis, in CD4⁺ and CD8⁺ T cells, the mitochondrial mass was investigated to give an insight into the mitochondrial respiration of these cells. A mitochondrial-specific dye (mitotracker) can be utilised to examine the mass of cellular mitochondria by flow cytometry. Mitotracker green binds the mitochondrial membranes independently of MMP and is used as a quantitative assessment of mitochondrial mass. Mitotracker staining was optimized and results are displayed in chapter 2. Cells did not require stimulation prior to staining and mitotracker at a concentration of 4 nM was chosen as optimal (Figure 2.3 A and B). Additionally, mitotracker staining was confirmed to represent mitochondrial mass rather than MMP, as treatment with FCCP, known to disrupt the MMP, did not affect mitotracker staining (Figure 2.3 C).

Mitotracker green staining was examined *ex vivo* in human CD4 and CD8 T cells. Healthy donor PBMC were stained with fluorochrome-conjugated antibodies specific for the surface markers CD4 and CD8, followed by mitotracker green staining, and cells were analysed by flow cytometry. CD4⁺ T cells revealed a significantly increased mitotracker green staining compared with CD8⁺ T cells ($p < 0.001$) (Figure 3.3).

Additionally, mitotracker green staining was also investigated in naïve, total memory, central memory and effector memory CD4⁺ T cells. Naïve cells (CD4⁺CD45RA⁺) displayed decreased mitotracker staining compared with total memory (CD4⁺CD45RA⁻) cells ($p < 0.001$) (Figure 3.4 A and C). No significant difference in mitotracker MFI values for central memory (CD4⁺CD45RA⁻CCR7⁺) versus effector memory (CD4⁺CD45RA⁻CCR7⁻) cells was observed (Figure 3.4 B and D).

In summary, CD4⁺ T cells had greater mitochondrial mass compared with CD8⁺ T cells, as did naïve CD4⁺ T cells compared with total CD4⁺ memory T cells. This suggested that CD4⁺ T cells may have an overall increased potential to perform mitochondrial respiration, and this is relatively enhanced in memory versus naïve compartments.

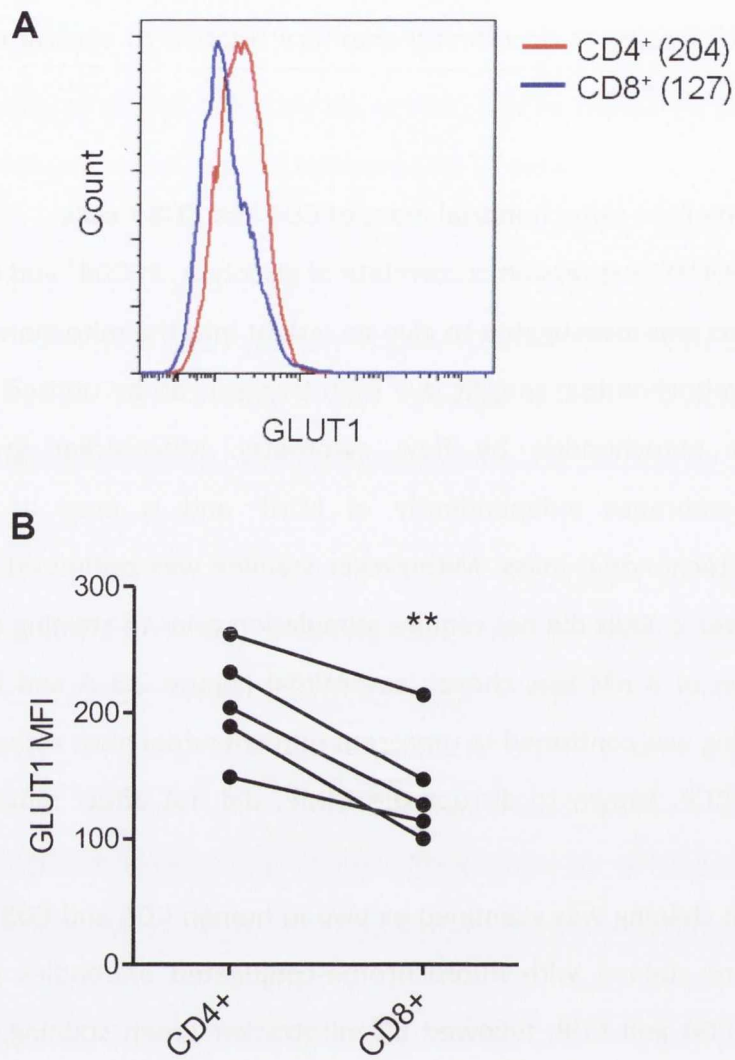


Figure 3.1. GLUT1 expression is increased in activated CD4⁺ T cells compared with CD8⁺ T cells.

PBMC from healthy donors were stimulated in the presence of plate-bound anti-CD3 for 48 h. The cells were stained with fluorochrome-conjugated antibodies specific for CD4, CD8 and GLUT1, and analysed by flow cytometry. The representative histogram shows GLUT1 staining on CD4⁺ and CD8⁺ T cells (A). The graph shows GLUT1 MFI values for CD4⁺ and CD8⁺ T cells (n=5). Statistical differences in the mean between the groups were determined by a paired, two-tailed t test; ** p<0.01.

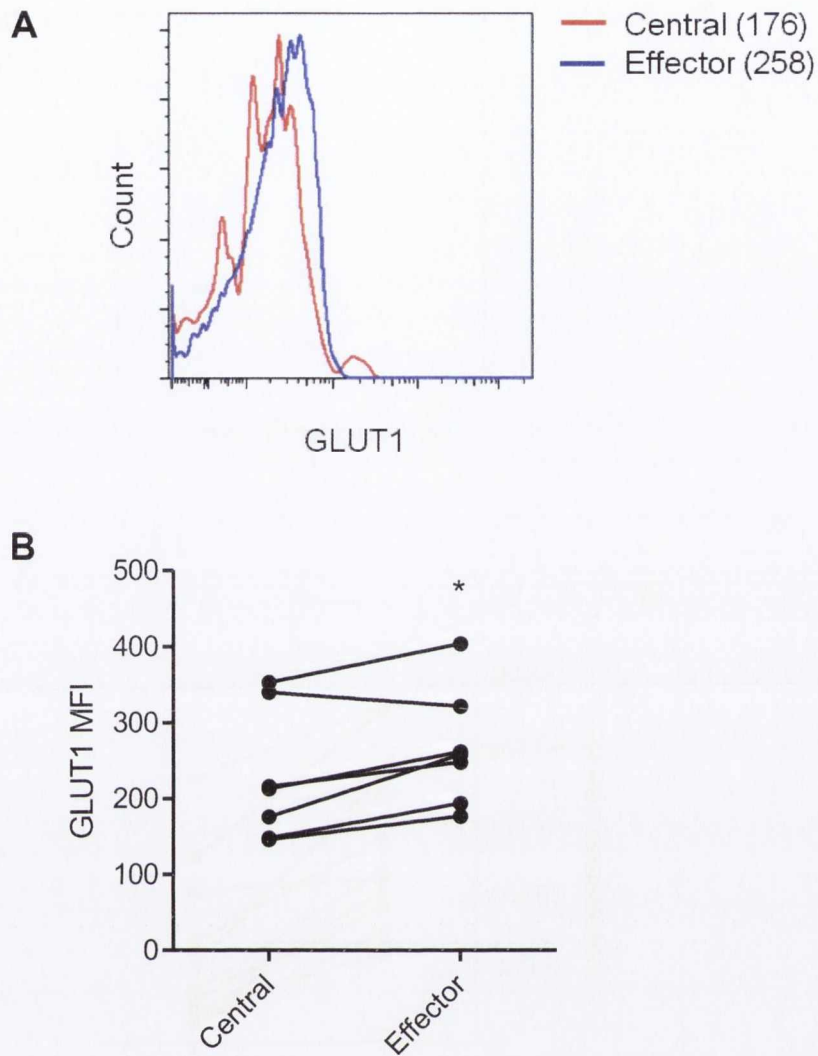


Figure 3.2 GLUT1 expression is increased in effector memory CD4⁺ T cells compared with central memory CD4⁺ T cells.

Human PBMC from healthy donors were stimulated with plate-bound anti-CD3 for 48 h. The cells were stained with fluorochrome-conjugated antibodies specific for CD4, CD45RO, CCR7 and GLUT1, and analysed by flow cytometry. The representative histogram shows GLUT1 staining on CD4⁺CD45RO⁺CCR7⁺ (Central) and CD4⁺CD45RO⁺CCR7⁻ (Effector) memory CD4 T cells (A). The graph shows GLUT1 MFI values for central and effector memory T cells (n=7). Statistical differences in the mean between the groups were determined by a paired, two-tailed t test; * p<0.05.

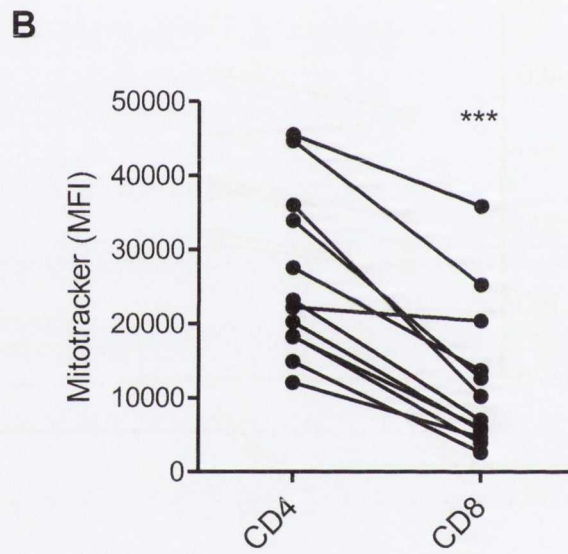
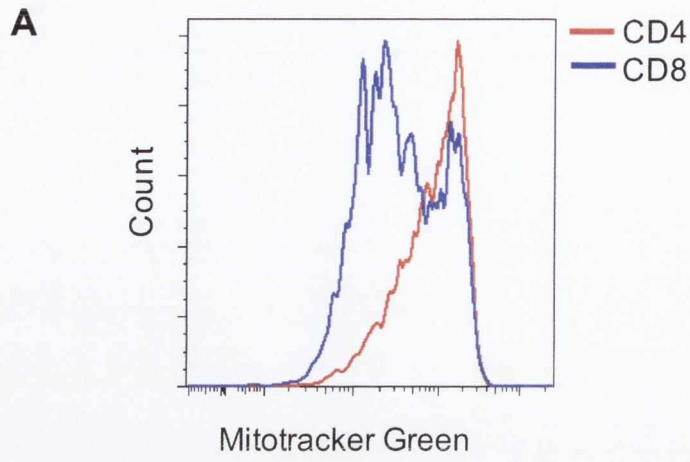


Figure 3.3. Mitotracker intensity is increased in CD4⁺ T cells compared with CD8⁺ T cells. PBMC from healthy donors were stained ex vivo with fluorochrome-conjugated antibodies specific for surface markers CD4 and CD8, and mitotracker green. The cells were analysed by flow cytometry. Representative histograms show mitotracker staining in CD4 and CD8 T cells (A). The graph shows mitotracker MFI values for CD4⁺ and CD8⁺ (B) (n=12, 3 experiments). Statistical differences in the mean between the groups were determined by a paired, two-tailed t test; *** p<0.001.

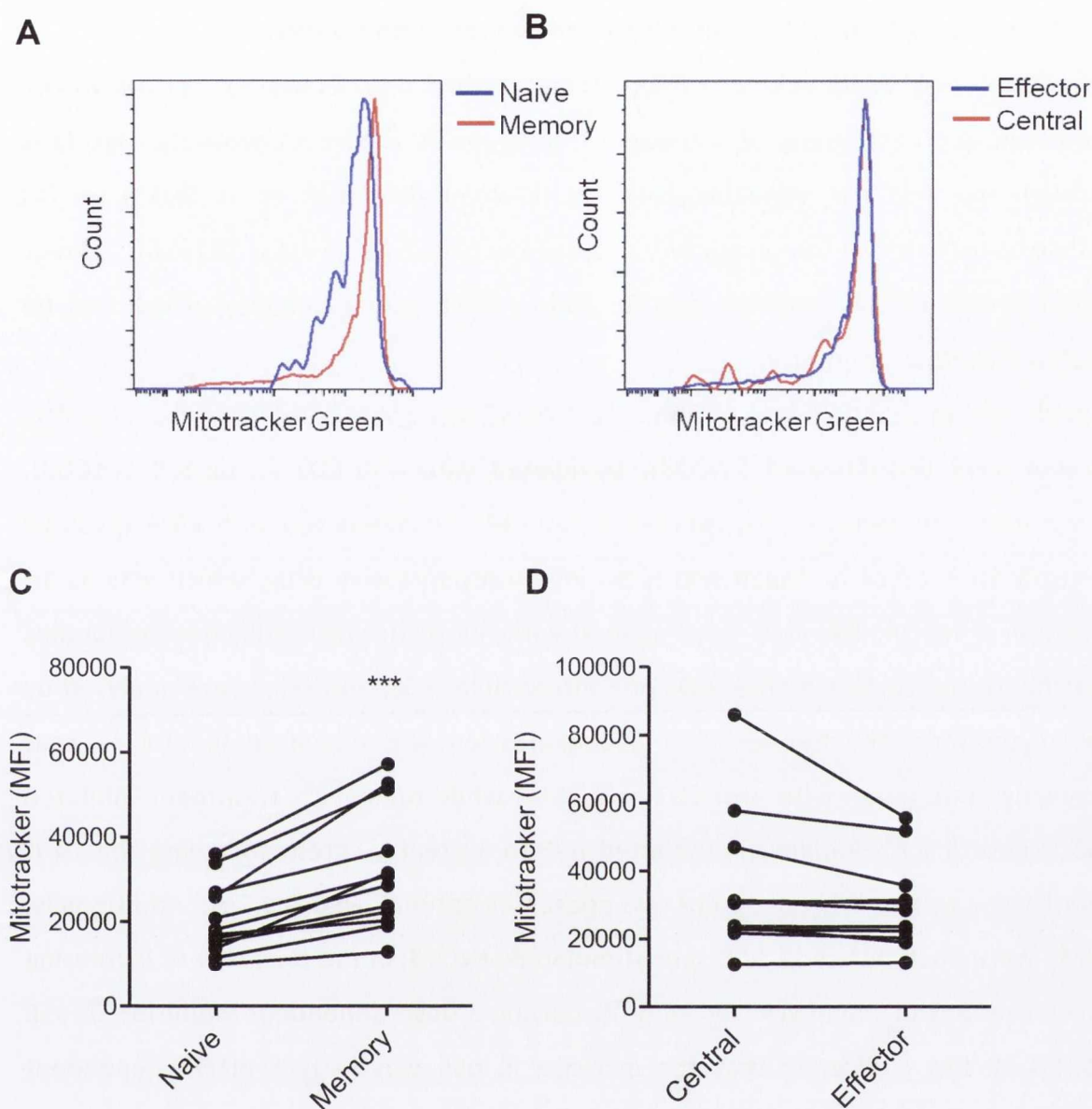


Figure 3.4. Increased mitotracker intensity in memory $CD4^+$ T cells compared with naive $CD4^+$ T cells.

PBMC from healthy donors were stained ex vivo with fluorochrome-conjugated antibodies specific for surface markers CD4, CD45RA, CCR7 and mitotracker green. The cells were analysed by flow cytometry. The histograms represent mitotracker MFI values for $CD4^+CD45RA^+$ (Naive) vs $CD4^+CD45RA^-$ (Memory) (A) and $CD4^+CD45RA^-CCR7^+$ (Central) and $CD4^+CD45RA^-CCR7^-$ (Effector) (B) memory T cells. The graphs show mitotracker MFI values for $CD4^+CD45RA^+$ (Naive) vs $CD4^+CD45RA^-$ (Memory) (C) and $CD4^+CD45RA^-CCR7^+$ (Central) and $CD4^+CD45RA^-CCR7^-$ (Effector) (D) memory T cells (n=12, over 3 experiments). Statistical differences in the mean between the groups were determined by a paired, two-tailed t test; *** p<0.001

3.2.3 mTOR activity in CD4⁺ T cells is inhibited by rapamycin treatment

In addition to glucose uptake, mTOR - a serine/threonine kinase - is central to the metabolic reprogramming of activated T cells and is known to promote glycolysis through the PI3K/Akt signalling pathway (Maclver, Michalek et al. 2013). mTOR activity is reflected in the phosphorylation of the ribosomal protein S6 (pS6), a direct target of the mTOR regulated p70 S6 kinase S6K1 (Sabatini 2006), which can be analysed by flow cytometry.

Initially, the phosphorylation of S6 in total PBMC was optimised. PBMC from healthy donors were unstimulated ($-\alpha$ CD3), stimulated with anti-CD3 (1 μ g/ml) ($+\alpha$ CD3), stimulated with anti-CD3 and rapamycin (20 nM), or stimulated with PMA (positive control) for 6 or 24 h. Rapamycin is an immunosuppressive drug, which acts as an inhibitor of mTOR. The cells were stained with fluorochrome-conjugated antibodies specific for the surface marker CD4 and intracellular pS6, and cells were analysed by flow cytometry. The frequency of pS6 expression was increased in CD4⁺ T cells following stimulation with anti-CD3 and PMA, while rapamycin treatment inhibited pS6 (Figure 3.5 A). Rapamycin inhibited pS6 to a greater extent following the 24 h stimulation, and so this time point was chosen as optimal (Figure 3.5 A). Additionally, PBMC were unstimulated ($-\alpha$ CD3) or stimulated ($+\alpha$ CD3) in the presence of increasing concentrations of rapamycin for 24 h, displaying a dose-dependent inhibition of pS6 from 1-50 nM, indicating that the increase in pS6 was in fact mTOR dependent (Figure 3.5 B).

These data validate the use of pS6 as a direct readout of mTOR activity in CD4⁺ T cells, confirmed by pS6 inhibition following treatment with the known mTOR inhibitor rapamycin.

3.2.4 Increased mTOR activity in CD161-expressing CD4⁺ T cells compared with CD4⁺CD161⁻ T cells.

Th7 lineage cells play a key role in autoimmunity and so it is of importance to understand the metabolic pathways that they utilise in order to identify potential new therapeutic targets. Having established the utility of pS6 as a readout of mTOR activity in total CD4⁺ T cells, mTOR activity in CD161⁺ Th17 lineage cells compared with CD161⁻ (Th1 and Th2) cells as investigated next.

PBMC from healthy donors were stimulated in the presence of anti-CD3 (1 $\mu\text{g}/\text{ml}$) for 24 h, followed by 20 min stimulation with PMA for control cells only (control). The cells were stained with fluorochrome-conjugated antibodies specific for surface markers CD4, CD161 and intracellular pS6, and cells were analysed by flow cytometry. pS6 staining was increased following stimulation with PMA (control) (Figure 3.6 A). Additionally, the results indicate that $\text{CD4}^+\text{CD161}^+$ T cells exhibited a significant increase in pS6 staining, and therefore increased mTOR activity, compared with $\text{CD4}^+\text{CD161}^-$ T cells ($p < 0.001$) ($n = 11$) (Figure 3.6 B). As pS6 expression is directly associated with mTOR activity, these data reveal a significant increase in mTOR activity for Th17 lineage cells ($\text{CD4}^+\text{CD161}^+$) compared with the remaining CD4^+ T cells ($\text{CD4}^+\text{CD161}^-$). This provides support for a glycolytic profile for Th17 lineage cells.

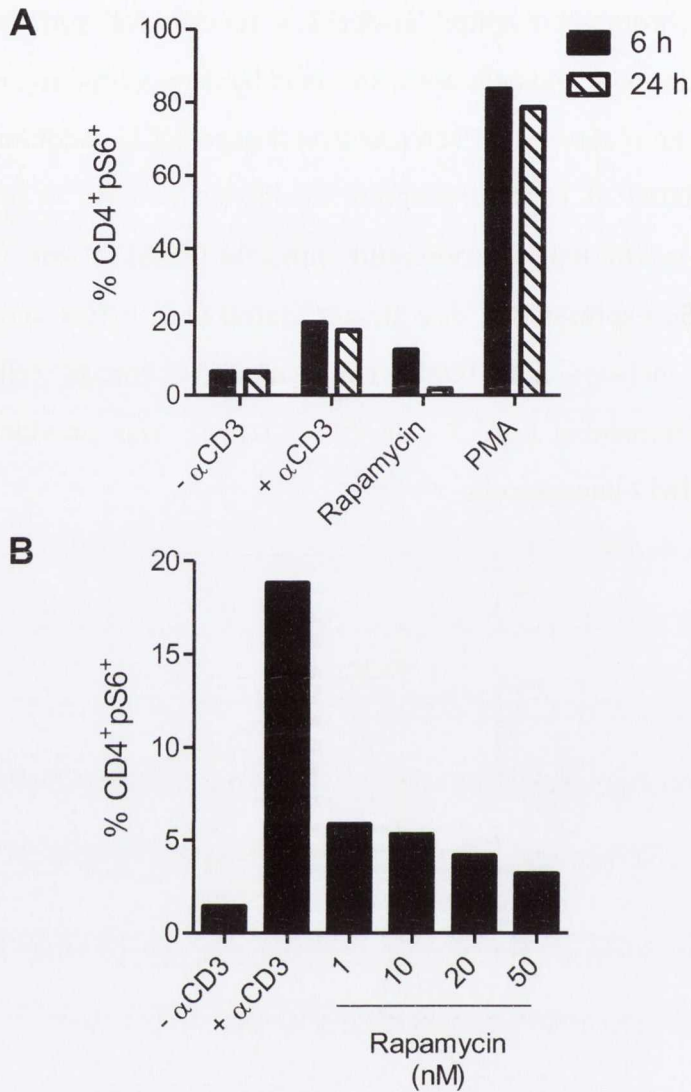


Figure 3.5. pS6 expression is increased following stimulation with α CD3 and is inhibited by rapamycin in a dose-dependent manner.

PBMC from healthy donors were stimulated in the presence or absence of plate-bound anti-CD3 or PMA for 6 or 24 h. Anti-CD3 stimulated cells were also treated with rapamycin (20 nM) for the times indicated (A). Cells were left unstimulated or stimulated with anti-CD3 in the presence of increasing concentrations of rapamycin (B). Cells were stained with fluorochrome-conjugated antibodies specific for the surface marker CD4 and the intracellular protein pS6, and analysed by flow cytometry. The graphs represent the frequency of CD4⁺pS6⁺ T cells (n=2).

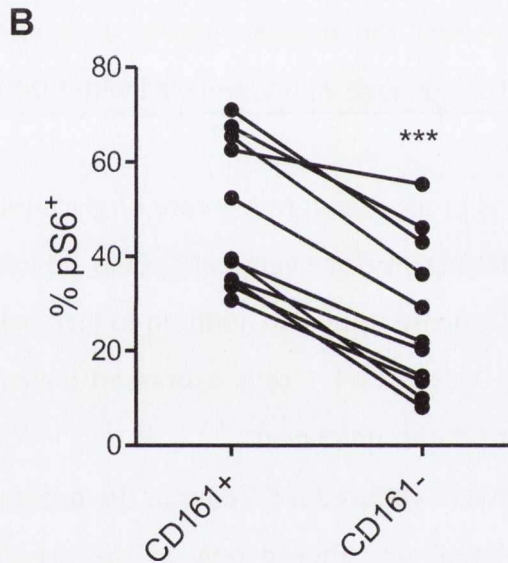
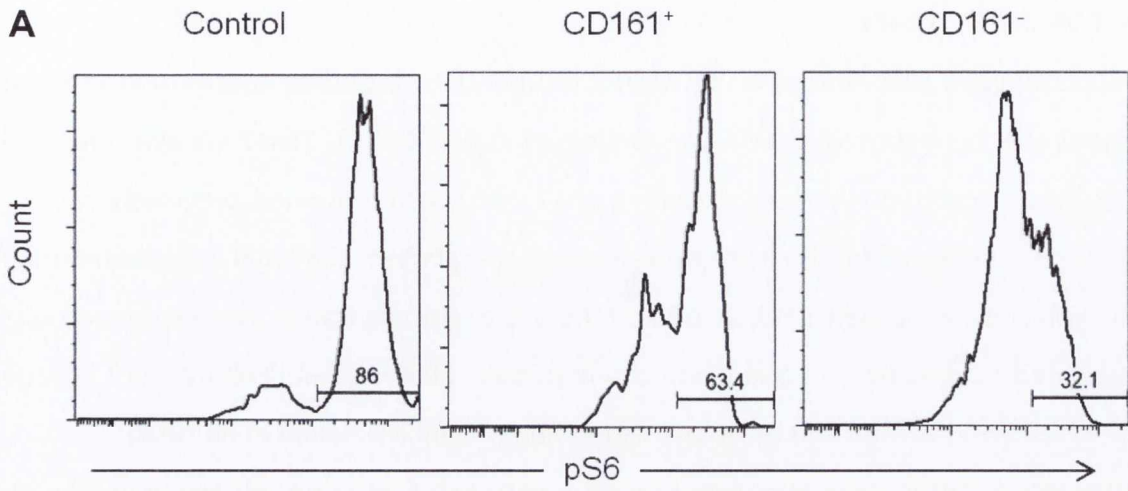


Figure 3.6. Increased pS6 expression in CD4⁺CD161⁺ T cells compared with CD4⁺CD161⁻ T cells.

PBMC from healthy donors were stimulated in the presence of anti-CD3 for 24 h, with control cells stimulated for a further 20 min with PMA as a positive control (Control). The cells were stained with fluorochrome-conjugated antibodies specific for surface markers CD4 and CD161, and the intracellular protein pS6 and analysed by flow cytometry; representative histograms show pS6 expression in total CD4⁺ (Control), CD4⁺CD161⁺ (CD161⁺) and CD4⁺CD161⁻ (CD161⁻) cells in (A). The graph shows the frequency of pS6⁺ T cells within CD161⁻ and CD161⁺ CD4⁺ T cells (n=11 donors over 3 experiments). Statistical differences in the mean between the groups were determined by a paired, two-tailed t test; *** p<0.001.

3.2.5 GLUT1 expression and glucose uptake is increased in CD4⁺CD161⁺ T cells compared with CD4⁺CD161⁻ T cells

Having examined the expression of GLUT1 in CD4 cells, including central and effector memory, the expression of GLUT1 was examined in CD4⁺CD161⁺ (Th17 lineage cells) and CD4⁺CD161⁻ T cells (CD4⁺ T cells excluding Th17 cells). As mentioned previously, GLUT1 expression is essential for the increased glycolytic metabolism shown in activated murine T cells (Macintyre, Gerriets et al. 2014) and therefore, glucose transporter expression was investigated to provide an insight into the metabolic pathways utilized by Th17 lineage cells, which are characterized by CD161 expression (Cosmi, De Palma et al. 2008).

Healthy donor PBMC were stimulated for 48 h with anti-CD3 (1 µg/ml) and stained with fluorochrome-conjugated antibodies specific for CD4, CD161 and GLUT1. The cells were analysed by flow cytometry and the results indicate a significant increase in GLUT1 expression in CD4⁺CD161⁺ Th17 lineage cells compared with CD4⁺CD161⁻ T cells ($p < 0.001$) ($n = 12$) (Figure 3.7 A and B).

The rate of glucose uptake is proportional to the rate of glycolysis, and therefore can be used to study the glycolytic activity of living cells. Cells which exhibit high glycolytic activity will show increased glucose uptake in addition to increased expression of GLUT1. Having demonstrated that CD161⁺ CD4 T cells expressed higher levels of GLUT1, their ability to take up glucose was determined next.

PBMC from healthy donors were cultured for 3 days in the presence of anti-CD3 (1 µg/ml) and IL-2 (20 u/ml) (stimulated) or cultured only in the presence of complete RPMI (unstimulated control). The cells were then incubated with 100 µM fluorescent 2-NBDG in order to measure glucose uptake. 2-NBDG is a fluorescent glucose analogue widely used to study the rate and quantity of glucose uptake in live cells. The cells were surface stained with fluorochrome-conjugated antibodies specific for CD4 and CD161, and analysed by flow cytometry.

Stimulation of PBMC with anti-CD3 was required for 2-NBDG uptake by CD4⁺ T cells (Figure 3.8). The representative histograms show that 44% of CD4⁺CD161⁺ T cells stained positively for 2-NBDG compared to 31% in CD4⁺CD161⁻ T cells ($n = 3$). In summary these data indicated that CD4⁺CD161⁺ T cells expressed more GLUT1 and took up more glucose than CD4⁺CD161⁻ T cells. Th17 lineage cells are characterized by CD161 expression, and therefore, this data provides further support for a glycolytic profile in Th17 lineage cells.

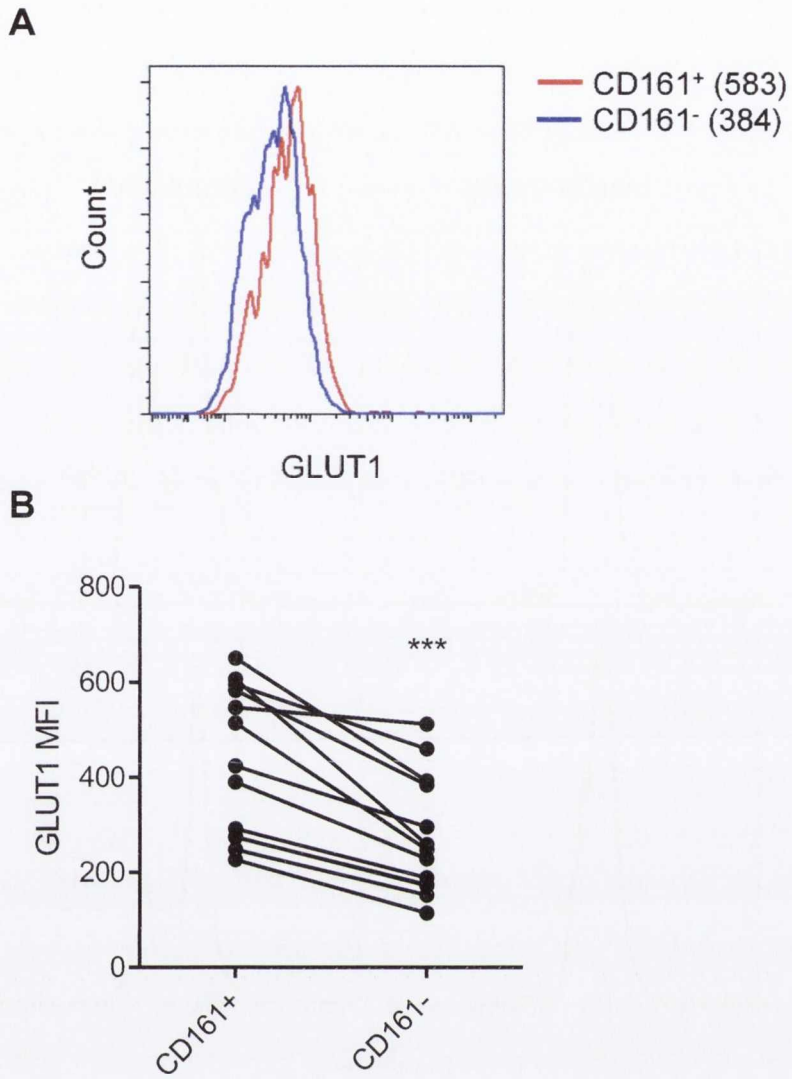


Figure 3.7. GLUT1 expression is increased in CD4⁺CD161⁺ T cells compared with CD4⁺CD161⁻ T cells.

PBMC from healthy donors were stimulated with plate-bound anti-CD3 for 48 h. The cells were stained with fluorochrome-conjugated antibodies specific for CD4, CD161 and GLUT1, and analysed by flow cytometry. The representative histogram shows GLUT1 staining on CD4⁺CD161⁺ and CD4⁺CD161⁻ T cells. MFI values are in parentheses (A). The graph shows GLUT1 MFI values for CD4⁺CD161⁺ and CD4⁺CD161⁻ T cells (n=12). Statistical differences in the mean between the groups were determined by a paired, two-tailed t test; *** p<0.001.

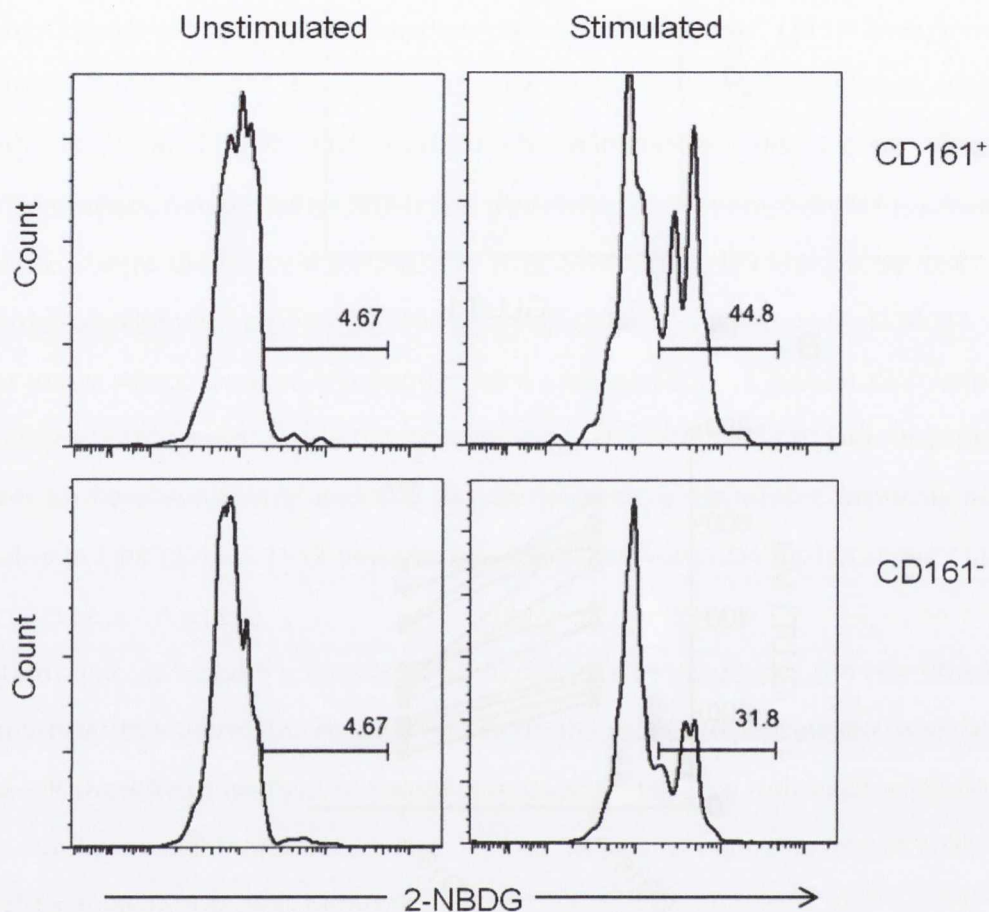


Figure 3.8. 2-NBDG uptake is increased in CD4⁺CD161⁺ Th17 lineage cells compared with CD4⁺CD161⁻ T cells.

PBMC from healthy donors were cultured for 3 days in the presence of plate-bound anti-CD3 and IL-2 (20 u/ml) (stimulated) or cultured only in the presence of complete RPMI (unstimulated). The cells were stained initially with 100 μ M fluorescent 2-NBDG and then surface stained with fluorochrome-conjugated antibodies specific for CD4 and CD161. The histograms represent the frequency of CD4⁺CD161⁺ T cells (CD161⁺) and CD4⁺CD161⁻ T cells (CD161⁻) containing 2-NBDG (data is representative of 3 experiments)

3.2.6 Stimulation of memory CD4⁺ T cells is required for glycolytic profile generation.

In order to further investigate the role of metabolism in regulating T cells it was necessary to measure the type of metabolic activity utilised by particular T cell subsets. The Seahorse XF Analyzer was utilised to determine cellular glycolytic activity, which is measured by proton excretion from cells resulting in the acidification of the surrounding medium, known as the extracellular acidification rate (ECAR), and the cellular mitochondrial function, relating to oxidative phosphorylation and measured by the oxygen consumption rate (OCR). Both the ECAR and OCR are measured simultaneously in real time by solid-state probes residing 200 microns above a cell monolayer within the well of a cell culture plate. The Seahorse allows for the addition of metabolic promoters and inhibitors in order to determine the metabolic profile of the cells under examination. The metabolic profiles of human T cell subsets is of great interest, therefore protocols for the Seahorse were optimized for the examination of metabolism in human T cells for the first time, focusing primarily on memory T cells.

Initially, as outlined in chapter 2, cell seeding density and the concentration of metabolic compounds was optimized for examination via the Seahorse. Next, the necessity of cell stimulation prior to Seahorse experimentation was determined for memory CD4⁺ T cells. CD4⁺ T cells were negatively sorted from PBMC using magnetic beads. The cells were resting (Figure 3.9 A) or stimulated for 18 h with PMA and ionomycin (Figure 3.9 B) and seeded at 1 million cells/well in Cell-Tak™ coated wells of a Seahorse Biosciences™ 24-well plate. The cells were treated with 2.5 mM glucose, stimulating glycolysis, followed by 0.5 µg/ml oligomycin A, inhibiting mitochondrial respiration and promoting glycolytic function, and finally glycolysis was inhibited with 25 mM 2-DG (10-fold the optimal glucose concentration). This protocol is described as the glycolytic stress test (Seahorse Biosciences). It provides three fundamental parameters of cellular glycolysis: basal glycolysis (blue), glycolytic capacity (green) and glycolytic reserve (red) (Figure 3.9 B). Basal glycolysis is the average ECAR measured in response to glucose addition (blue). The total glycolytic capacity is measured as the average ECAR following oligomycin A treatment (green). Finally, the glycolytic reserve of the cell, utilised during cellular stress, is calculated as the glycolytic capacity minus the basal glycolysis rate (red).

Resting CD4⁺ T cells did not show an increase in ECAR after oligomycin treatment (Figure 3.9 A), however activated CD4⁺ T cells did (Figure 3.9 B). The results indicate that human

CD4⁺ T cells require stimulation in order to respond to oligomycin A treatment and to maximise their glycolytic activity.

3.2.7. The metabolic profiles of memory CD4⁺CD161⁺ and CD4⁺CD161⁻ T cells.

Having observed an increase in GLUT1 expression, glucose uptake and mTOR activity in CD161⁺ Th17 cells, the metabolic profile of CD4⁺CD161⁺ T cells compared with CD4⁺CD161⁻ T cells was examined using the Seahorse XF analyser.

3.2.7a Memory CD4⁺CD161⁺ Th17 lineage cells exhibit an increased glycolytic profile compared with CD4⁺CD161⁻ T cells.

CD4⁺ T cells were positively sorted from PBMC using magnetic beads and further sorted via MoFlo into CD161⁺ (CD4⁺CD45RA⁻CD25⁻CD161⁺) and CD161⁻ (CD4⁺CD45RA⁻CD25⁻CD161⁻) effector T cells. The cells were expanded for 7 days in the presence of anti-CD3 (1 µg/ml), irradiated APCs and IL-2 (20 u/ml). Cells were stimulated for 18 h with PMA and ionomycin prior to Seahorse experimentation and seeded at 600,000 cells/well in Seahorse XF Assay Medium in Cell-Tak™ coated wells. The glycolytic stress test was performed on each T cell subset, treating with 2.5 mM glucose, followed by 0.5 µg/ml oligomycin A, and finally 25 mM 2-DG. The glycolytic profile, measured as the ECAR, from both CD4⁺CD161⁺ (CD161⁺) and CD4⁺CD161⁻ (CD161⁻) T cells increased in response to glucose and oligomycin treatment, and decreased after 2-DG addition, although CD161⁺ T cells exhibited higher ECAR throughout (Figure 3.10 A). This experiment was repeated with PBMC from 4 individual donors. The basal glycolysis value, the maximal glycolytic capacity, and the glycolytic reserve were calculated for each T cell subset (Figure 3.10 B-D).

In summary these data indicate that activated memory CD4⁺CD161⁺ Th17 lineage cells have significantly higher basal glycolysis ($p < 0.05$), maximal glycolytic capacity ($p < 0.05$) and glycolytic reserve ($p < 0.05$) compared with memory CD4⁺CD161⁻ T cells ($p < 0.05$).

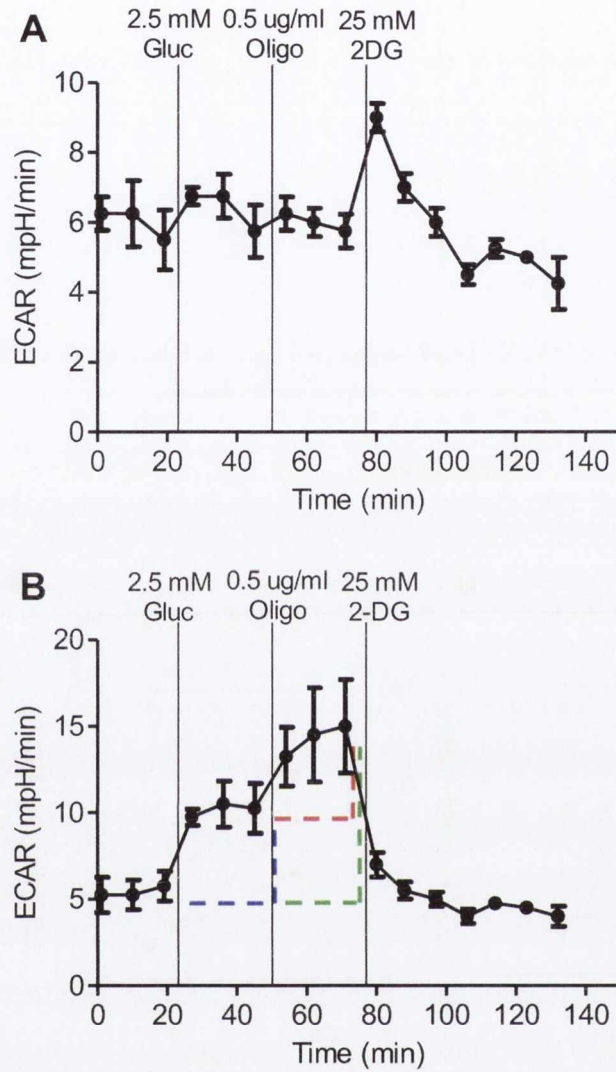


Figure 3.9. Stimulation of memory CD4⁺ T cells is required to determine their glycolytic profile.

Memory CD4⁺ T cells were negatively sorted from healthy donor PBMC using magnetic beads and were treated with 2.5 mM glucose, 0.5 μg/ml oligomycin A and 25 mM 2-DG in order to measure their glycolytic activity. The relative ECAR was measured via the Seahorse XF Analyzer. The cells were resting at the time of Seahorse experimentation (A) or stimulated for 18 h with PMA and ionomycin (B) (n=1, performed in triplicate).

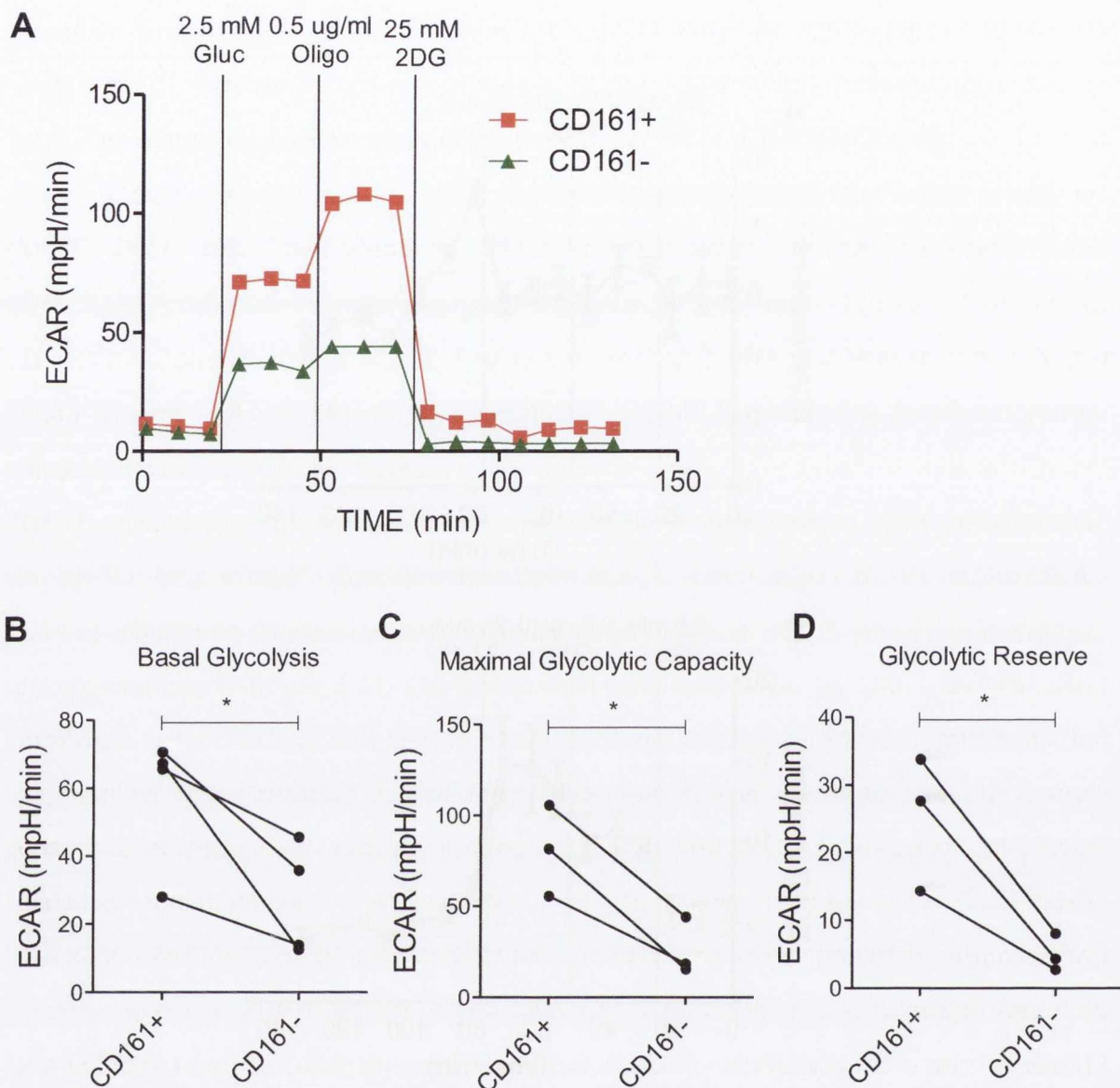


Figure 3.10. Activated CD4⁺CD161⁺ T cells have a higher basal glycolysis, glycolytic capacity and reserve compared to CD4⁺CD161⁻ T cells.

CD161⁺ (CD4⁺CD45RA⁻CD25⁻CD161⁺) and CD161⁻ (CD4⁺CD45RA⁻CD25⁻CD161⁻) cells were sorted from healthy donor PBMC and grown for 7 days in the presence of anti-CD3, irradiated APCs and IL-2 (20 u/ml). Cells were stimulated for 18 h with PMA and ionomycin and metabolic analysis was performed using the Seahorse XF Analyzer. The ECAR was recorded after the addition of glucose, oligomycin A and 2-DG (A). The basal glycolysis (B), maximal glycolytic capacity (C) and glycolytic reserve (D) was calculated for each subset in triplicate from four experiments. Statistical differences in the mean between the groups were determined by paired t-test; *p<0.05.

3.2.7b Memory CD4⁺CD161⁺ Th17 lineage cells exhibit a decreased mitochondrial respiration profile compared with CD4⁺CD161⁻ T cells.

Having established that memory CD4⁺CD161⁺ T cells have a higher glycolytic reserve than that of memory CD4⁺CD161⁻ T cells, the mitochondrial respiration rate, used to investigate oxidative phosphorylation, of each T cell subset was examined next.

CD4⁺ T cells were positively sorted from PBMC using magnetic beads and further sorted via MoFlo for CD161⁺ (CD4⁺CD45RA⁻CD25⁻CD161⁺) and CD161⁻ (CD4⁺CD45RA⁻CD25⁻CD161⁻) effector T cells. The cells were expanded for 7 days in the presence of anti-CD3 (1 µg/ml), irradiated APCs and IL-2 (20 u/ml). Cells were stimulated for 18 h with PMA and ionomycin prior to Seahorse experimentation and seeded at 600,000 cells/well in Cell-Tak™ coated wells in Seahorse XF Assay Medium supplemented with glucose (final concentration of 10 mM). The OCR was recorded following injections of 0.5 µg/ml oligomycin A, 450 nM FCCP, 500 nM rotenone and 2.5 µM antimycin A, and finally 25 mM 2-DG (Figure 3.11 A). This protocol provides three fundamental parameters of mitochondrial function: basal respiration, maximal respiration and the respiratory reserve. Basal respiration (Figure 3.11 B) is the initial OCR before the addition of metabolic compounds. The maximal respiration (Figure 3.11 C) is measured as the average OCR following FCCP treatment. Finally, the respiratory reserve (Figure 3.11 D), utilised during cellular stress, is calculated as the maximal respiratory capacity minus the basal respiration.

CD161⁻ memory T cells displayed a trend towards an increase in basal respiration, maximal respiratory capacity and respiratory reserve compared with CD161⁺ memory T cells. Taken together the data suggests that Th17 lineage cells exhibit reduced mitochondrial respiration in conjunction with increased glycolysis, compared with the remaining memory effector T cells which had the inverse profile.

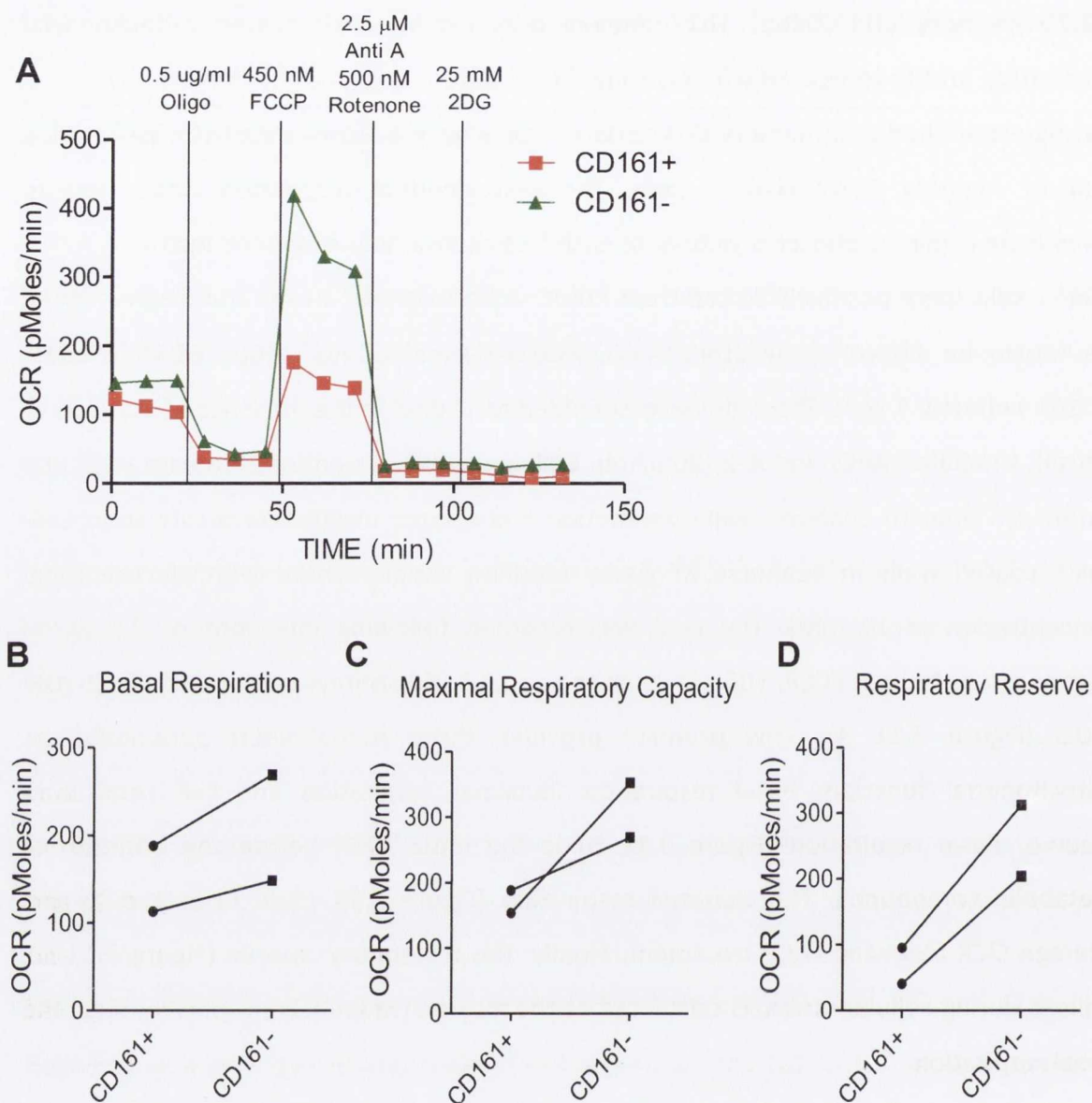


Figure 3.11. Activated $CD4^+CD161^-$ T cells trend towards a higher basal respiration, respiratory capacity and reserve compared to $CD4^+CD161^+$ T cells.

$CD161^+$ ($CD4^+CD45RA^-CD25^-CD161^+$) and $CD161^-$ ($CD4^+CD45RA^-CD25^-CD161^-$) cells were sorted from healthy donor PBMC and expanded for 7 days in the presence of anti-CD3, irradiated APCs and IL-2 (20 u/ml). Cells were stimulated for 18 h with PMA and ionomycin and metabolic analysis was performed using the Seahorse XF Analyzer. Cells were seeded in Seahorse Medium supplemented with 10 mM glucose. OCR was recorded after the addition of oligomycin A, FCCP, rotenone and antimycin A, and 2-DG (A). The basal mitochondrial respiratory capacity (B), maximal respiratory capacity (C) and the respiratory reserve (D) was calculated for each subset (n=2, performed in triplicate).

3.2.8 Examination of mTOR activity in Treg cells

Regulatory T cells are vital to immune regulation, and maintenance of the Th17/Treg cell balance is required to maintain optimal immunity. While murine Th17 cells have previously been demonstrated to utilise glycolysis for their metabolism, in addition it has been shown that regulatory T cells utilised mitochondrial respiration for their metabolic needs (Shi, Wang et al. 2011). Having examined the metabolic profile of human Th17 (CD161-expressing) cells, regulatory T cells were studied next. In previous murine studies, mTOR was shown to be critical for effector T cell activation, while AMP-activated protein kinase (AMPK) is known to be upregulated in Treg cells (Michalek, Gerriets et al. 2011). AMPK is activated when AMP levels rise, promoting metabolism via oxidative phosphorylation and the conversion of AMP to ATP (Towler and Hardie 2007). However, the activity levels of mTOR in human Treg cells have not yet been investigated.

Stimulation of T cells via the TCR results in the sustained activation of the PI3K/Akt/mTOR network (Kane and Weiss 2003) and upregulation of CD25. Therefore, in order to investigate mTOR activity in regulatory T cells, a purified population of Treg cells was required, since identification of Treg cells could be confounded by activation. PBMC from healthy donors were sorted using the Aria Fusion sorter into total CD4⁺ T cells and CD4⁺CD25⁺CD127^{Lo} Treg cells, and stimulated in the presence of anti-CD3 (1 µg/ml) and irradiated APCs for 24 h. The CD4⁺ T cells were stained with fluorochrome-conjugated antibodies specific for CD161 and pS6, while the Treg sorted cells were stained for Foxp3 and pS6. Irradiated APCs were excluded from analysis by CFSE⁻ gating. The data shown in Figure 3.12 represents pS6 expression for CD4⁺CD161⁺ (CD161⁺) and CD4⁺CD161⁻ (CD161⁻) T cells from the sorted CD4⁺ population, alongside sorted Tregs (CD4⁺CD25⁺CD127^{Lo}Foxp3⁺). The data shows a trend towards an increase in the frequency of CD161⁺ cells expressing pS6 compared with both CD161⁻ T cells and Treg cells (Figure 3.12). This result suggests a relative decrease in mTOR activity in Treg cells compared with Th17 lineage cells.

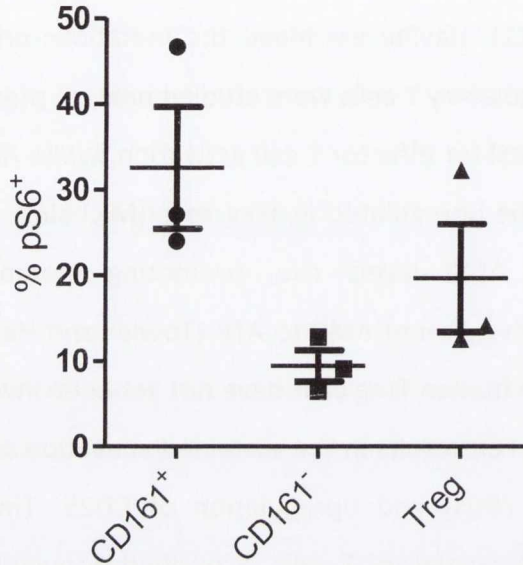


Figure 3.12. pS6 expression in CD4⁺CD161⁺, CD4⁺CD161⁻ T cells compared with sorted Treg cells.

CD4⁺ T cells and Treg (CD4⁺CD25⁺CD127^{Lo}) cells were sorted from PBMC using the Aria Fusion sorter and were cultured in the presence of anti-CD3 and CFSE-labelled irradiated APCs. After 24 h CD4⁺ T cells were stained with fluorochrome-conjugated antibodies specific for surface markers CD161 and pS6, while sorted Treg cells were stained with Foxp3 and pS6, and analysed by flow cytometry. The graph shows the frequency of pS6⁺ cells within CD4⁺CD161⁺ (CD161⁺), CD4⁺CD161⁻ (CD161⁻) and sorted CD4⁺CD25⁺CD127^{Lo}Foxp3⁺ (Treg) T cells (n=3).

3.2.9. GLUT1 expression is increased in Treg cells compared with CD4⁺CD161⁻ T cells.

In order to further investigate the metabolic profile of Treg cells, GLUT1 expression in Treg cells was analysed next and compared with CD4⁺CD161⁺ and CD4⁺CD161⁻ T cells. Healthy donor PBMC were stimulated for 48 h in the presence or absence of anti-CD3 (1 µg/ml) and stained with fluorochrome-conjugated antibodies specific for CD4, CD25, CD127, CD161, GLUT1 and the intranuclear transcription factor Foxp3. In agreement with previous data in this chapter, flow cytometric analysis indicated an increase in GLUT1 MFI values for CD161⁺ (CD4⁺CD161⁺) T cells compared with CD161⁻ (CD4⁺CD161⁻) T cells (p<0.05) (Figure 3.13). The examination of Treg cells (CD4⁺CD25⁺CD127^{Lo}Foxp3⁺) demonstrated a significant increase in GLUT1 MFI values compared with CD4⁺CD161⁻ T cells across 5 individual donors (Figure 3.13). No difference in GLUT1 expression was observed between CD161⁺ Th17 cells and Treg cells. These data suggest potential for glycolytic metabolism in Treg cells in addition to that shown for Th17 lineage cells.

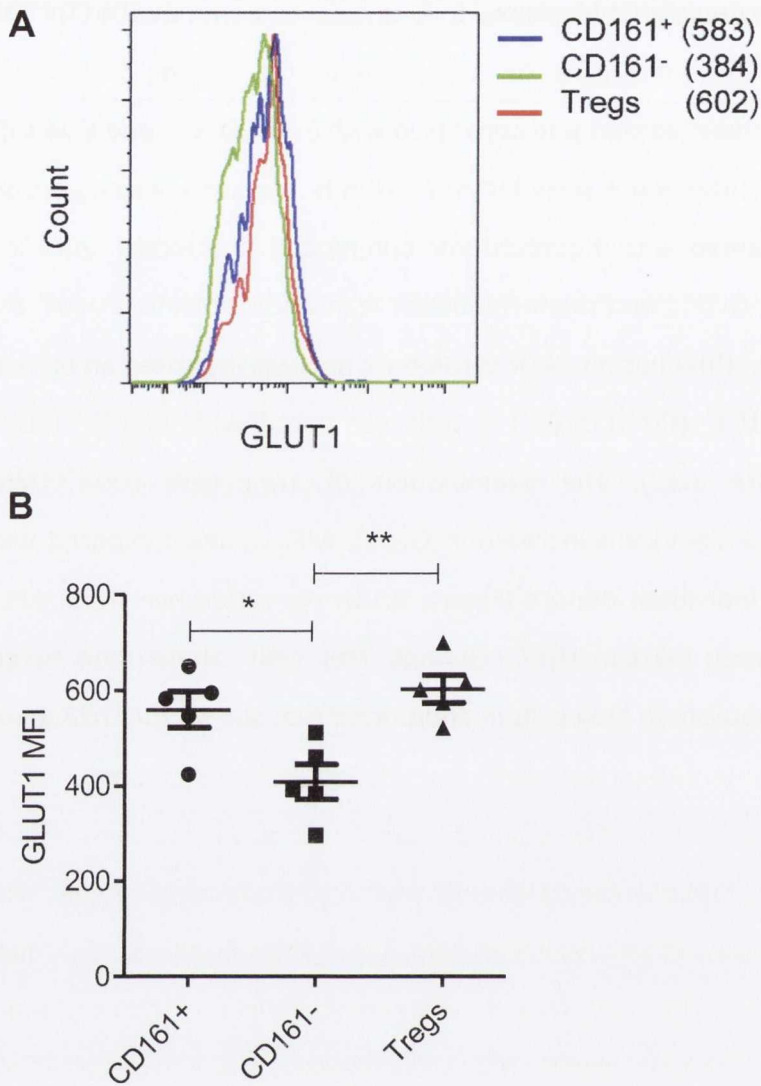


Figure 3.13. GLUT1 expression is increased in CD4⁺CD161⁺ T cells and Treg cells compared to CD4⁺CD161⁻ T cells.

PBMC from healthy donors were stimulated in the presence of plate-bound anti-CD3 for 48 h. The cells were stained with fluorochrome-conjugated antibodies specific for surface markers CD4, CD161, CD25, CD127 and GLUT1, and nuclear transcription factor Foxp3, and analysed by flow cytometry. The representative histogram shows GLUT1 staining on CD4⁺CD161⁺ and CD4⁺CD161⁻ T cells, MFI values are in parentheses (A). The graph shows GLUT1 MFI values for CD4⁺CD161⁺ CD161⁺, CD4⁺CD161⁻ (CD161⁻) and CD4⁺CD25⁺Foxp3⁺CD127^{Lo} (Treg) T cells (n=5). Statistical differences in the mean between the groups were determined by one-way ANOVA with Tukey's Multiple Comparison Test; * p<0.05, **p<0.01.

3.2.10. The metabolic profile of Treg cells compared with CD4⁺CD161⁺ and CD4⁺CD161⁻ T cells.

Having observed an increase in GLUT1 expression and a trend towards a decrease in mTOR activity, the metabolic profile of Treg cells was examined next using the Seahorse Analyser and compared with CD4⁺CD161⁺ and CD4⁺CD161⁻ T cells.

3.2.10a Treg cells exhibit an increased basal and maximal glycolytic activity compared with CD4⁺CD161⁻ T cells.

CD4⁺ T cells were positively sorted from PBMC using magnetic beads and further sorted via MoFlo into CD161⁺ (CD4⁺CD45RA⁻CD25⁻CD161⁺), CD161⁻ (CD4⁺CD45RA⁻CD25⁻CD161⁻) and Treg cells (CD4⁺CD25⁺CD127^{Lo}). The cells were cultured for 7 days in the presence of anti-CD3 (1 µg/ml), irradiated APCs and IL-2 (20 u/ml or 500 u/ml for effector and Treg cells respectively). Cells were stimulated for 18 h with PMA and ionomycin prior to Seahorse experimentation and seeded at 600,000 cells/well in Seahorse XF Assay Medium in Cell-Tak™ coated wells. The glycolytic stress test was performed on each T cell subset, treating with 2.5 mM glucose, followed by 0.5 µg/ml oligomycin A, and finally with 25 mM 2-DG. This experiment was repeated with PBMC from 3 individual donors. The glycolytic profile of both CD161⁺ and Treg T cells remained in sync throughout the experiment (Figure 3.14 A). The basal glycolysis and the maximal glycolytic capacity were significantly increased in Treg cells and CD161⁺ T cells compared with CD161⁻ T cells (Figure 3.14 B and C). Treg cells displayed a trend towards a reduced glycolytic capacity compared with CD161⁺ T cells (Figure 3.14 D).

In summary these data suggest an increased glycolytic profile for Treg cells compared with CD161⁻ T cells. However, Treg cells show a decrease in their glycolytic reserve, suggesting a decreased utilization of glycolysis during stress.

3.2.10b Investigation of the mitochondrial metabolic profile of Treg cells

The mitochondrial metabolic profile of memory Treg cells was examined and compared with CD4⁺CD161⁺ and CD4⁺CD161⁻ T cells. CD4⁺ T cells were positively sorted from PBMC using magnetic beads and further sorted via MoFlo into CD161⁺ (CD4⁺CD45RA⁻CD25⁻CD161⁺), CD161⁻ (CD4⁺CD45RA⁻CD25⁻CD161⁻) and Treg cells (CD4⁺CD25⁺CD127^{Lo}). The cells were cultured for 7 days in the presence of anti-CD3 (1 µg/ml), irradiated APCs and IL-2 (20 u/ml or 500 u/ml for effector and Treg cells respectively). Cells were stimulated for 18

h with PMA and ionomycin prior to Seahorse experimentation and seeded at 600,000 cells/well in Cell-Tak™ coated wells in Seahorse XF Assay Medium supplemented with glucose (final concentration of 10 mM). The OCR was recorded following injections of 0.5 µg/ml oligomycin A, 450 nM FCCP, 500 nM rotenone and 2.5 µM antimycin A, and finally 25 mM 2-DG (Figure 3.15 A).

Treg cells displayed a trend towards an increased basal mitochondrial respiration and maximal respiration, accompanied by CD161⁻ T cells, compared with CD161⁺ T cells (Figure 3.15 B and C). Much like the glycolytic reserve data, Treg cells display a reduction in their mitochondrial respiratory reserve compared with CD161⁻ T cells (Figure 3.15 D).

This data suggests a trend towards the increased utilization of mitochondrial respiration by Treg cells, as was observed for CD161⁻ T cells, compared with CD161⁺ Th17 cells.

3.2.11 A trend towards increased mitochondrial mass in Treg cells

Oxidative phosphorylation occurs in the mitochondria, and as Treg cells display an increase in their mitochondrial respiration, the mitochondrial mass of these cells was investigated next.

PBMC from healthy donors were stained ex vivo with fluorochrome-conjugated antibodies specific for CD4, CD25, CD127, CD161 and mitotracker green. Since mitotracker green staining does not support cell fixation, which is a requirement for intracellular staining, Foxp3 staining was not performed and Treg cells were identified as CD4⁺CD25⁺CD127^{Lo} cells. The data shows a trend towards an increase in mitochondrial mitotracker green staining for Treg cells (CD4⁺CD25⁺CD127^{Lo}) compared with CD161⁺ (CD4⁺CD161⁺) and CD161⁻ (CD4⁺CD161⁻) T cells (Figure 3.16).

This data may suggest an increased potential for Treg cells to utilise mitochondrial respiration due to an increased mitochondrial mass.

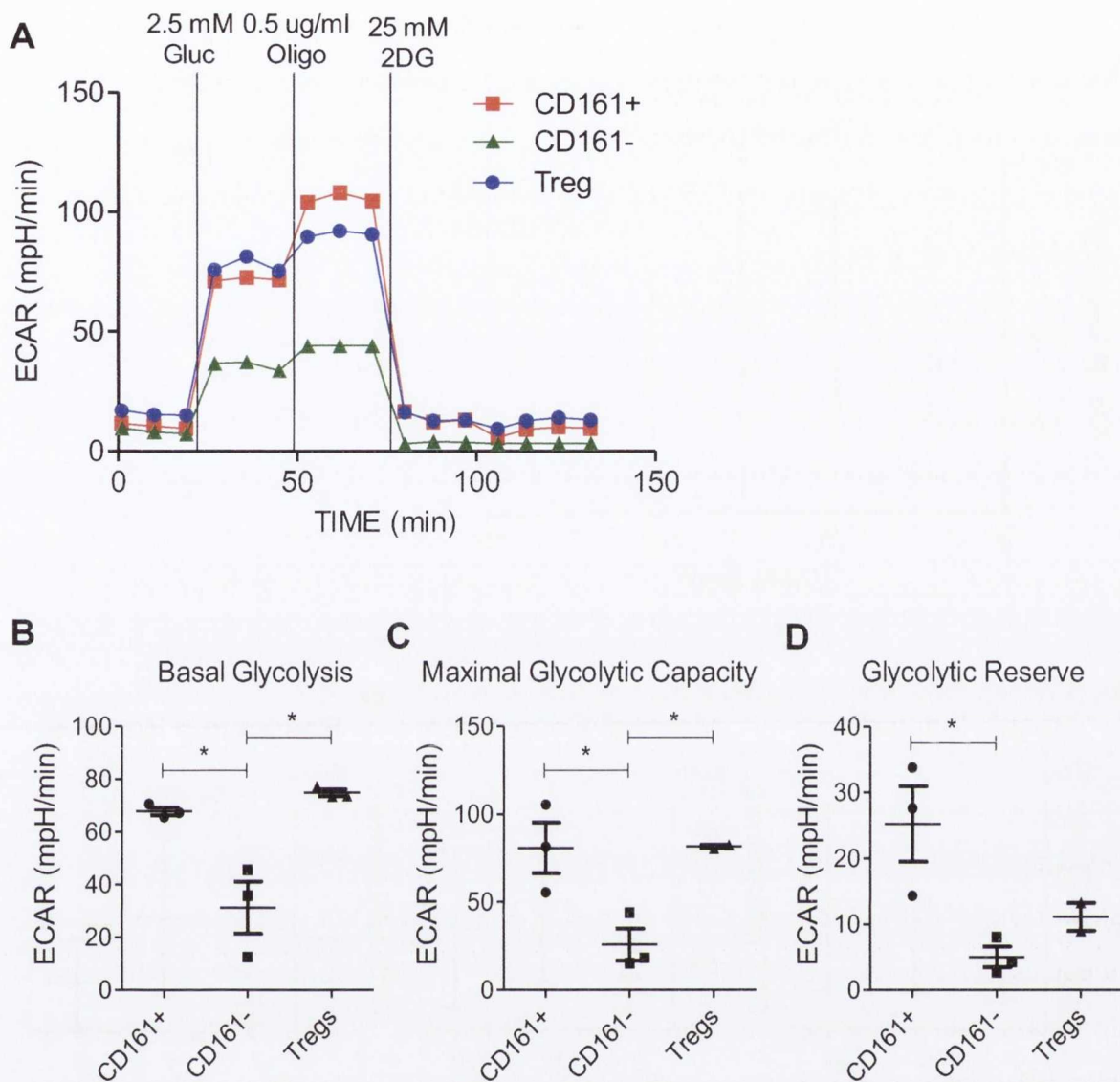


Figure 3.14. Activated Treg cells and CD4⁺CD161⁺ Th17 lineage cells have a higher basal glycolysis and glycolytic capacity compared with CD4⁺CD161⁻ T cells.

CD161⁺ (CD4⁺CD45RA⁻CD25⁺CD161⁺), CD161⁻ (CD4⁺CD45RA⁻CD25⁺CD161⁻) and Treg (CD4⁺CD25⁺CD127Lo) cells were sorted from healthy donor PBMC and grown for 7 days in the presence of anti-CD3, irradiated APCs and IL-2 (20 or 500 u/ml). Cells were stimulated for 18 h with PMA and ionomycin prior to metabolic analysis by the Seahorse XF Analyzer. The ECAR was recorded after the addition of glucose, oligomycin and 2-DG (A). The basal glycolysis (B), maximal glycolytic capacity (C) and glycolytic reserve (D) was calculated for each subset (n=3, performed in triplicate). Statistical differences in the mean between the groups were determined by one-way ANOVA with Tukey's Multiple Comparison Test; * p<0.05.

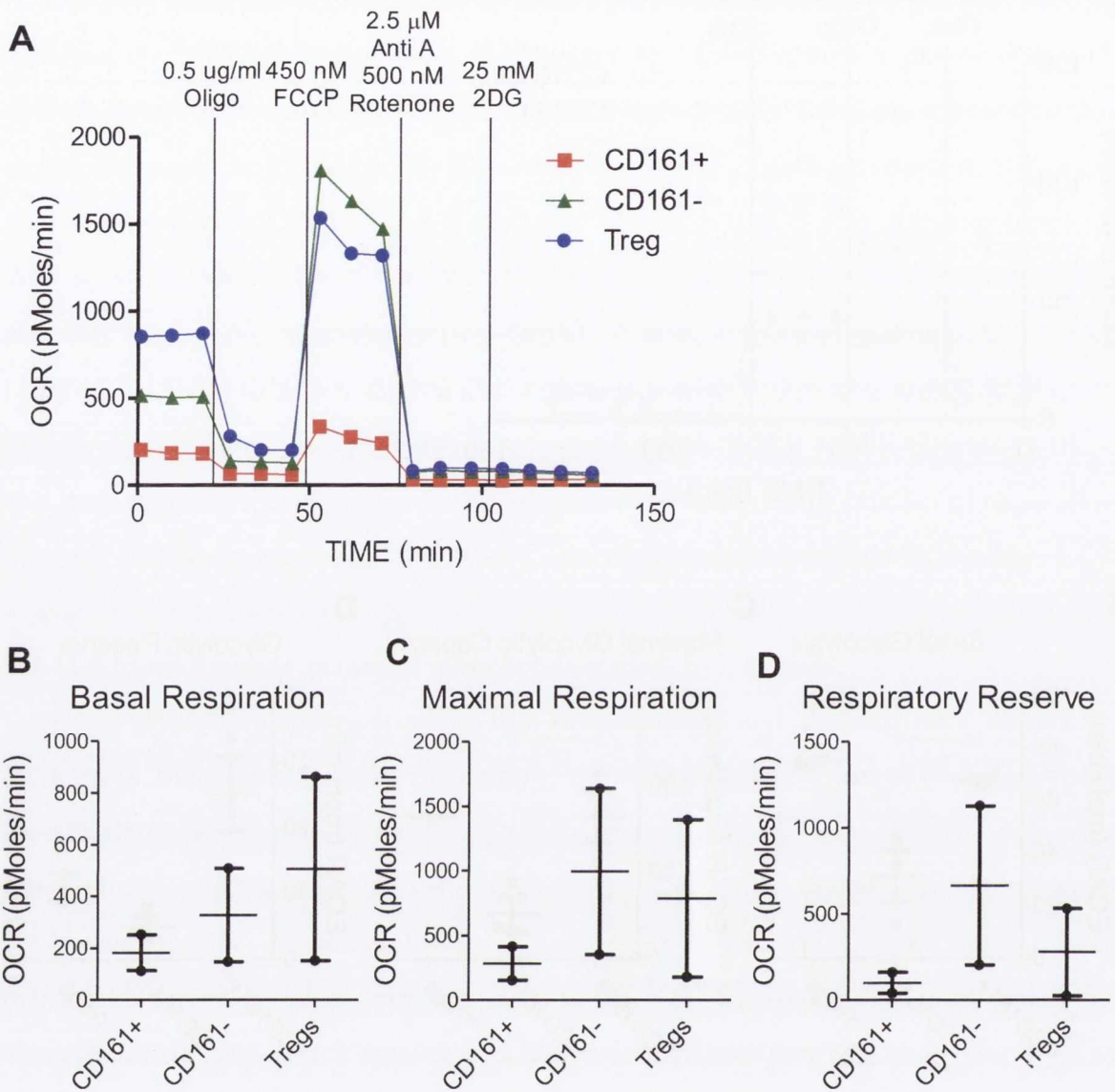


Figure 3.15. The OCR for CD4⁺CD161⁺, CD4⁺CD161⁻ and Treg cells.

CD161⁺ (CD4⁺CD45RA⁻CD25⁻CD161⁺), CD161⁻ (CD4⁺CD45RA⁻CD25⁻CD161⁻) and Treg (CD4⁺CD25⁺CD127^{Lo}) cells were sorted from healthy donor PBMC and grown for 7 days in the presence of anti-CD3, irradiated APCs and IL-2 (20 or 500 u/ml). Cells were stimulated for 18 h with PMA and ionomycin. Cells were seeded in Seahorse Medium supplemented with 10 mM glucose and metabolic analysis was performed using the Seahorse XF Analyzer. The OCR was recorded after the addition of oligomycin A, FCCP, rotenone and antimycin A, and 2-DG (A). The basal mitochondrial respiration (B), maximal capacity (C) and reserve (D) was calculated for each subset (n=2, performed in triplicate).

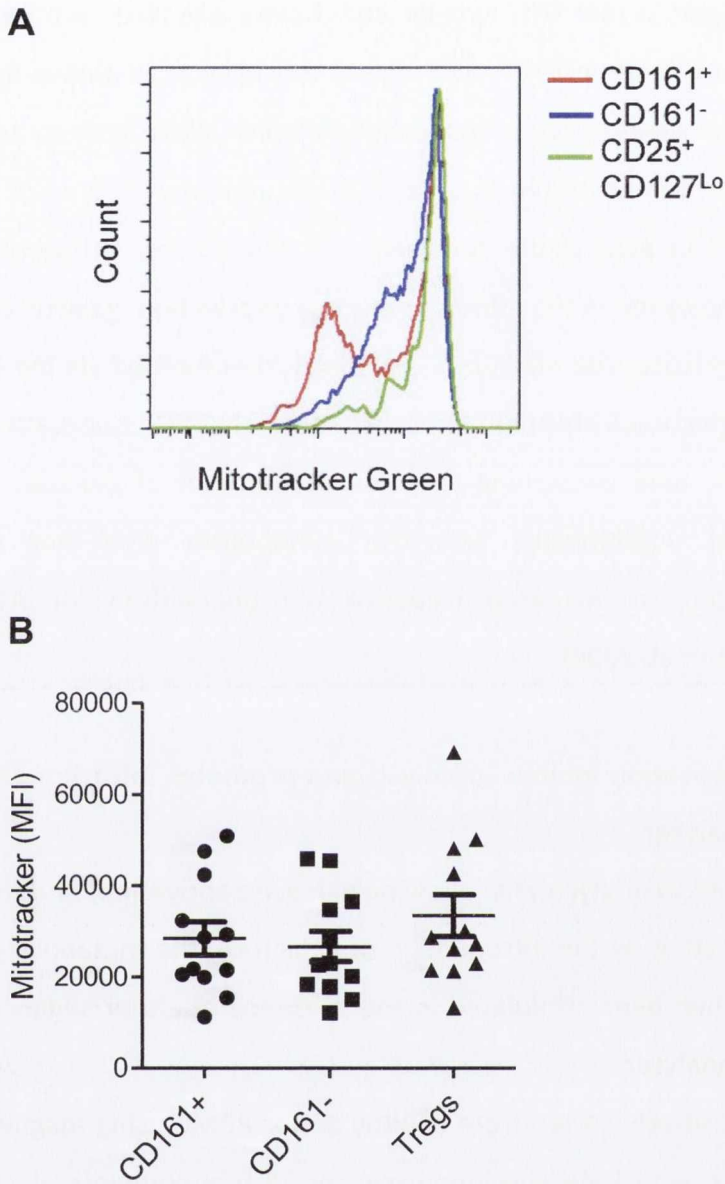


Figure 3.16. Mitotracker staining in CD4⁺ T cell subsets.

PBMC from healthy donors were stained ex vivo with fluorochrome-conjugated antibodies specific for surface markers CD4, CD161, CD25, CD127 and mitotracker green. The cells were analysed by flow cytometry. Representative histograms show mitotracker staining in CD161⁺ (CD4⁺CD161⁺), CD161⁻ (CD4⁺CD161⁻) and (CD4⁺CD25⁺CD127^{Lo}) Treg cells (A). The graphs show mitotracker MFI values for CD161⁺ (CD4⁺CD161⁺), CD161⁻ (CD4⁺CD161⁻) and (CD4⁺CD25⁺CD127^{Lo}) Treg cells (B) (n=12, 3 experiments).

3.2.12 The effect of inhibiting glycolysis via glucose deprivation on Th17 and Treg cells

The data above suggested that Th17 lineage cells have a glycolytic profile; therefore the effect of inhibiting glycolysis on Th17 and Treg cell subsets was examined next.

Glucose is the normal sugar in cell culture medium which allows cells to adopt glycolysis. Previous studies have demonstrated that T cells cultured in the absence of a sugar source have severe defects in gene expression and function (Cham, Driessens et al. 2008). Therefore, in order to examine the effects of glucose deprivation, galactose was used as a sugar substitute in glucose-free medium. Galactose is metabolised via the Leloir pathway of enzymes into D-glucose-6-phosphate, a substrate in the glycolysis pathway. However, this process is more time consuming than the metabolism of glucose, and therefore glycolysis is stalled. Additionally, galactose metabolism does not produce ATP, subsequently resulting in increased oxidative phosphorylation for ATP production (Rossignol, Gilkerson et al. 2004).

3.2.12a Glucose deprivation inhibits glycolysis and promotes mitochondrial respiration via the Seahorse Analyzer

To confirm the inhibition of glycolysis following glucose deprivation, and the induction of mitochondrial respiration by the introduction of galactose, the metabolic profile of total CD4⁺ T cells, which had been stimulated in the presence of either sugar, was evaluated using the Seahorse analyser.

CD4⁺ T cells were positively sorted from healthy donor PBMC using magnetic beads. The cells were stimulated with PMA and ionomycin for 18 h in complete glucose-free RPMI (see appendices) supplemented with 10 mM glucose or 10 mM galactose. Cells were adhered to a Seahorse 24-well plate using Cell Tak™ and metabolic analysis was performed using the Seahorse XF analyzer. The ECAR and OCR were recorded after the addition of oligomycin A, FCCP, rotenone and antimycin A, and 2-DG (see chapter 2 for metabolic functions of compounds used in the Seahorse XF Analyzer).

CD4⁺ T cells deprived of glucose and supplemented with galactose showed a decrease in their overall glycolytic profile (Figure 3.17 A), in their basal glycolysis ($p < 0.05$) (C) and glycolytic capacity (D). Additionally, CD4⁺ T cells stimulated in galactose exhibited a significant increase in their basal mitochondrial respiration compared with glucose treatment (Figure 3.17 B and E). This result validated the use of galactose as a supplemental sugar for the hindrance of glycolysis.

3.2.12b The effect of inhibiting glycolysis via glucose deprivation on Th17 lineage cells

The effect of glucose deprivation on memory CD4⁺ T cell subsets was investigated next. Memory CD4⁺ T cells were negatively sorted from healthy donor PBMC using magnetic beads and stimulated in complete glucose-free medium supplemented with 10 mM glucose or 10 mM galactose in the presence of anti-CD3 (1 µg/ml), CFSE-labelled irradiated APCs and IL-2 (20 u/ml). After 5 days, the cells were stimulated for 5 h with PMA, ionomycin and brefeldin A and stained with fluorochrome-conjugated antibodies specific for surface markers CD3, CD8 and CD161, and the intracellular cytokines IL-17 and IFN-γ. Cells were analysed by flow cytometry and irradiated APCs were selectively excluded from analysis through CFSE⁻ gating.

Following PMA stimulation, surface expression of CD4 is diminished. Therefore in order to examine CD4⁺ T cells in this setting, cells were gated as CD8⁻CD3⁺ T cells. The frequency of CD4⁺(CD8⁻CD3⁺) CD161⁺ T cells cultured in 10 mM galactose trended towards a decrease compared with those cultured in the presence of glucose (Figure 3.18). The expression of IL-17 by CD4⁺ T cells also trended towards a decrease for galactose-treated cells (Figure 3.19). Additionally, the frequency of CD4⁺IFN-γ⁺ T cells was unchanged following inhibition of glycolysis via galactose supplementation (Figure 3.20).

This data collectively suggests a role for glycolysis in the expansion and survival of human memory Th17 cells, as hindrance of the glycolytic pathway, following replacement of glucose with galactose, resulted in a trend towards a decrease in CD161 and IL-17 expression by memory CD4⁺ T cells, both characteristic features of Th17 cells.

3.2.12c Treg cell frequencies are enhanced following inhibition of glycolysis by glucose deprivation.

Having demonstrated a trend towards a decrease in Th17 cell frequencies following the replacement of glucose with galactose in culture medium, the effects of glucose deprivation on regulatory T cells was examined next. Memory CD4⁺ T cells were stimulated in complete glucose-free medium supplemented with 10 mM glucose or 10 mM galactose in the presence of anti-CD3 (1 µg/ml), CFSE-labelled irradiated APCs and IL-2 (20 u/ml). The cells were stained, without restimulation, with fluorochrome-conjugated antibodies specific for surface markers CD4, CD25 and CD127, and the intranuclear transcription factor Foxp3 and analysed by flow cytometry. Irradiated APCs were selectively excluded from analysis through CFSE⁻ gating.

In contrast to Th17 cells, the frequency of Treg (CD4⁺CD25⁺CD127^{Lo}Foxp3⁺) cells was increased in galactose-treated cells compared with glucose-treated cells (Figure 3.21 A), and this was significant across 9 individual donors (p<0.05). This data suggests a reduced requirement of Treg cells for glycolytic metabolism, as Treg cells are enhanced following the hindrance of glycolysis.

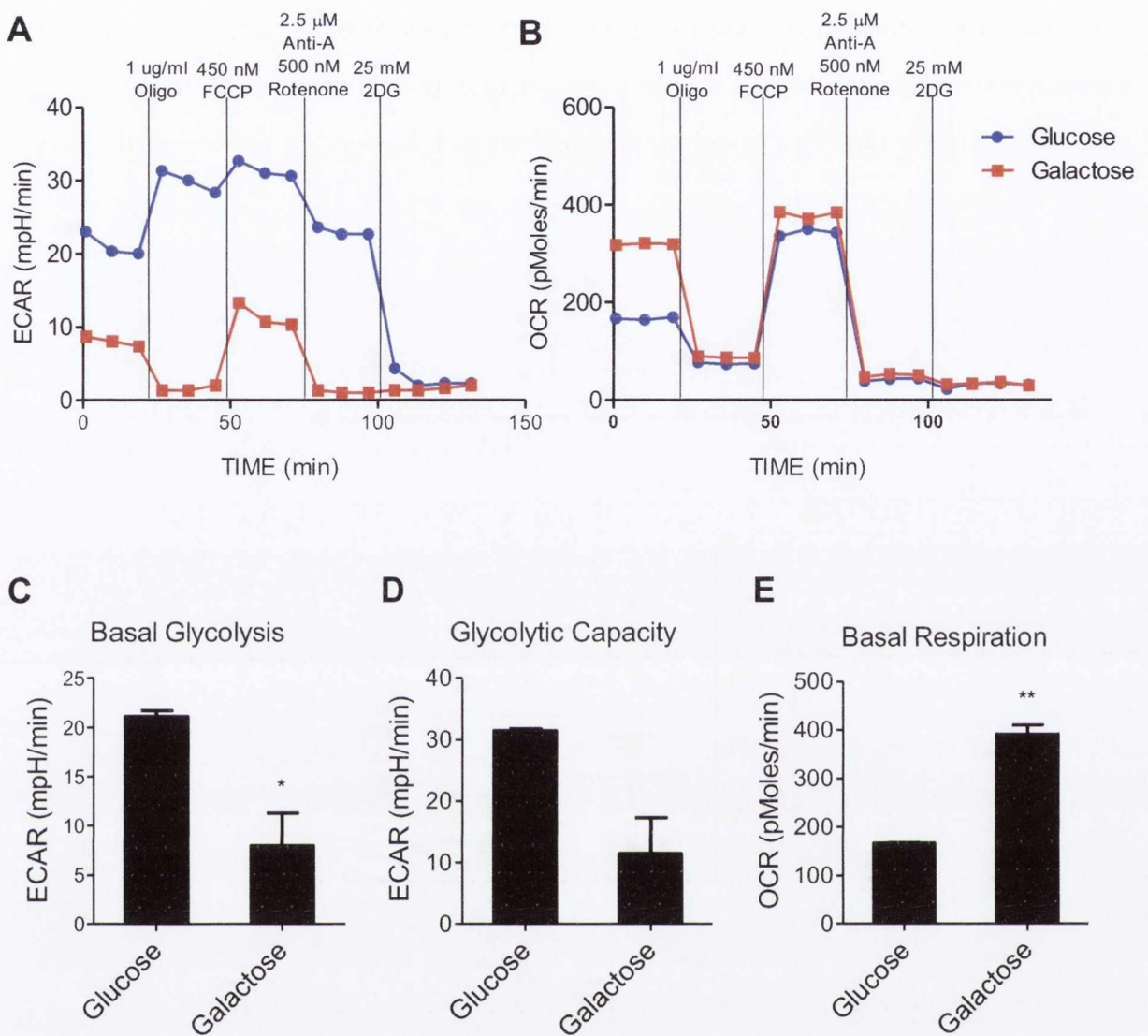


Figure 3.17 Galactose treatment inhibits glycolysis and stimulates mitochondrial respiration.

CD4⁺ T cells were positively sorted from healthy donor PBMC using magnetic beads and stimulated for 18 h with PMA and ionomycin in complete glucose-free medium supplemented with either 10 mM glucose or galactose. Metabolic analysis was performed using the Seahorse XF Analyzer. The ECAR (A) and OCR (B) were recorded after the addition of oligomycin A, FCCP, rotenone and antimycin A, and 2-DG. Basal glycolysis (C), the glycolytic capacity (D) and the basal respiration (E) were calculated. (n=1, performed in triplicate). Statistical differences in the mean between the groups were determined by a paired, two-tailed t test; * p<0.05, ** p<0.01.

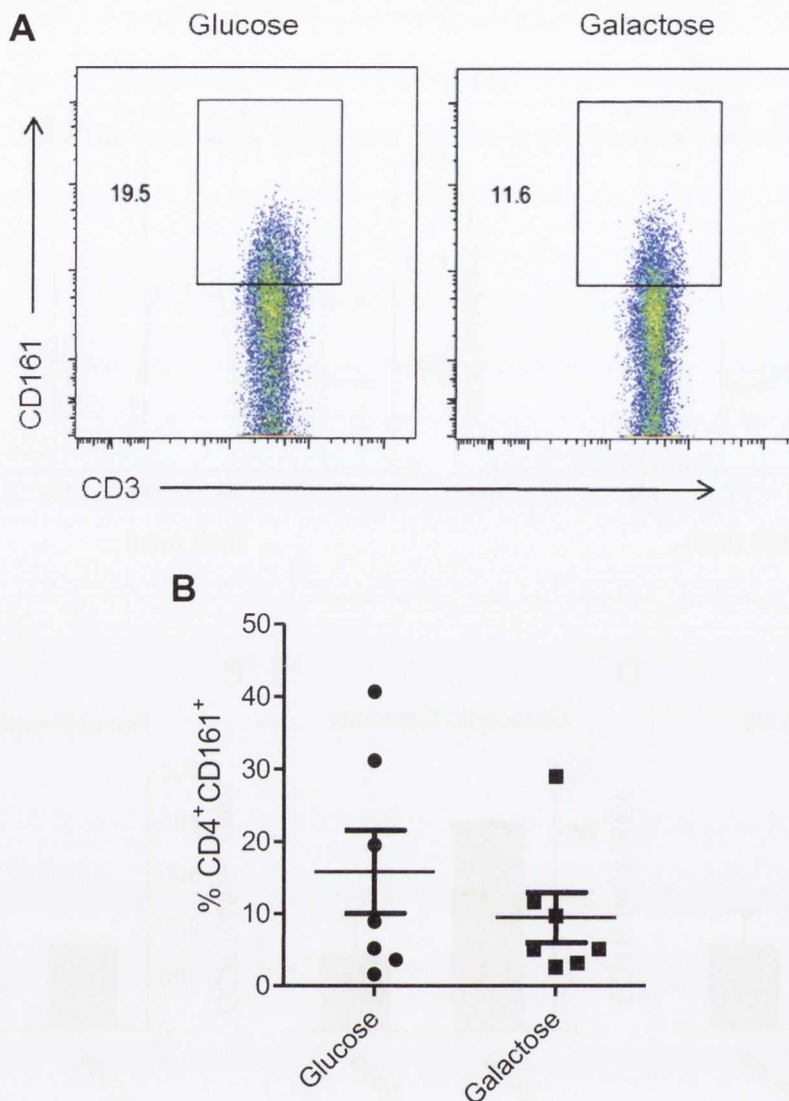


Figure 3.18 CD161 expression by CD4⁺ T cells following inhibition of glycolysis with galactose treatment.

Memory CD4⁺ T cells were negatively sorted from PBMC using magnetic beads and were cultured in complete glucose-free RPMI supplemented with 10 mM glucose or 10 mM galactose for 5 days and in the presence of anti-CD3, CFSE-labelled irradiated APCs and IL-2 (20 u/ml). After 5 days, the cells were stimulated for 5 h with PMA, ionomycin and brefeldin A and stained with fluorochrome-conjugated antibodies specific for surface markers CD3, CD8 and CD161. Cells were analysed by flow cytometry. Irradiated APCs were selectively excluded from analysis through CFSE⁻ gating. Expression of CD161 on CD4⁺ T cells (identified as CD3⁺CD8⁻) is shown in representative dot plots (A). The graph shows the frequency of CD4⁺CD161⁺ T cells in each treatment group (n=7 donors in separate experiments).

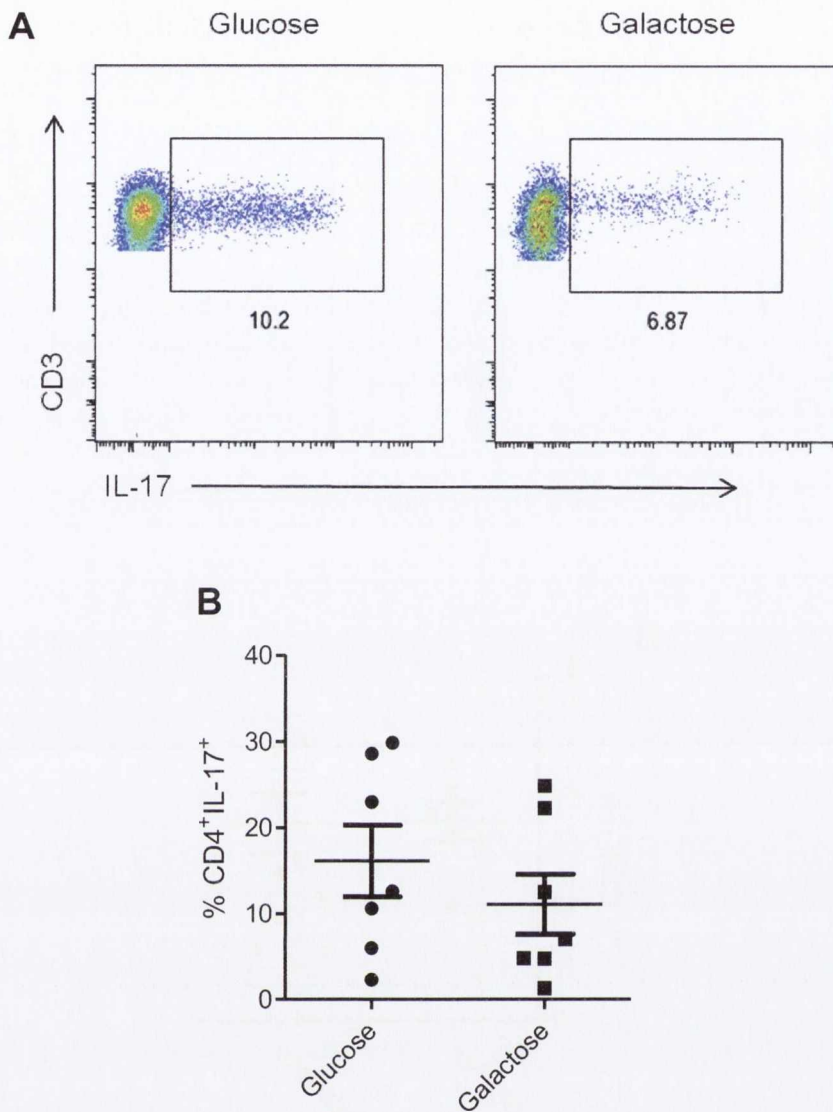


Figure 3.19 IL-17 expression by CD4⁺ T cells following inhibition of glycolysis with galactose treatment.

Memory CD4⁺ T cells were negatively sorted from PBMC using magnetic beads and were cultured in complete glucose-free RPMI supplemented with 10 mM glucose or 10 mM galactose for 5 days and in the presence of anti-CD3, CFSE-labelled irradiated APCs and IL-2 (20 u/ml). After 5 days, the cells were stimulated for 5 h with PMA, ionomycin and brefeldin A and stained with fluorochrome-conjugated antibodies specific for surface markers CD3 and CD8, and intracellular cytokine IL-17. Cells were analysed by flow cytometry. APCs were selectively excluded from analysis through CFSE⁻ gating. Expression of IL-17 by CD4⁺ T cells (identified as CD3⁺CD8⁻) is shown in representative dot plots (A). The graph shows the frequency of CD4⁺IL-17⁺ T cells in each treatment group (n=7 donors in separate experiments).

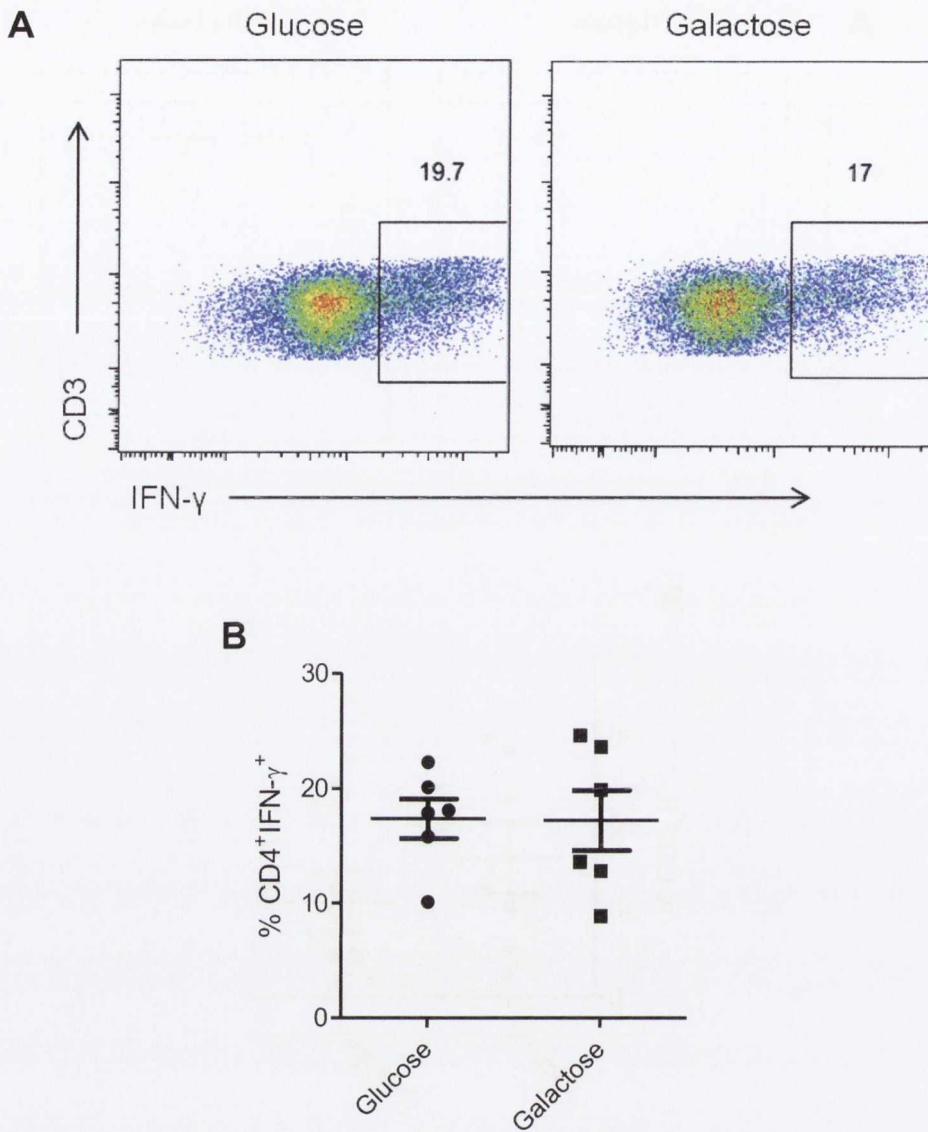


Figure 3.20 IFN- γ expression by CD4⁺ T cells following inhibition of glycolysis with galactose treatment.

Memory CD4⁺ T cells were negatively sorted from PBMC using magnetic beads and were cultured in complete glucose-free RPMI supplemented with 10 mM glucose or 10 mM galactose for 5 days and in the presence of anti-CD3, CFSE-labelled irradiated APCs and IL-2 (20 u/ml). After 5 days, the cells were stimulated for 5 h with PMA, ionomycin and brefeldin A and stained with fluorochrome-conjugated antibodies specific for surface markers CD3 and CD8, and intracellular cytokine IFN- γ . Cells were analysed by flow cytometry. APCs were selectively excluded from analysis through CFSE⁻ gating. Expression of IFN- γ by CD4⁺ T cells (identified as CD3⁺CD8⁻) is shown in representative dot plots (A). The graph shows the frequency of CD4⁺IFN- γ ⁺ T cells in each treatment group (n=6 donors in separate experiments).

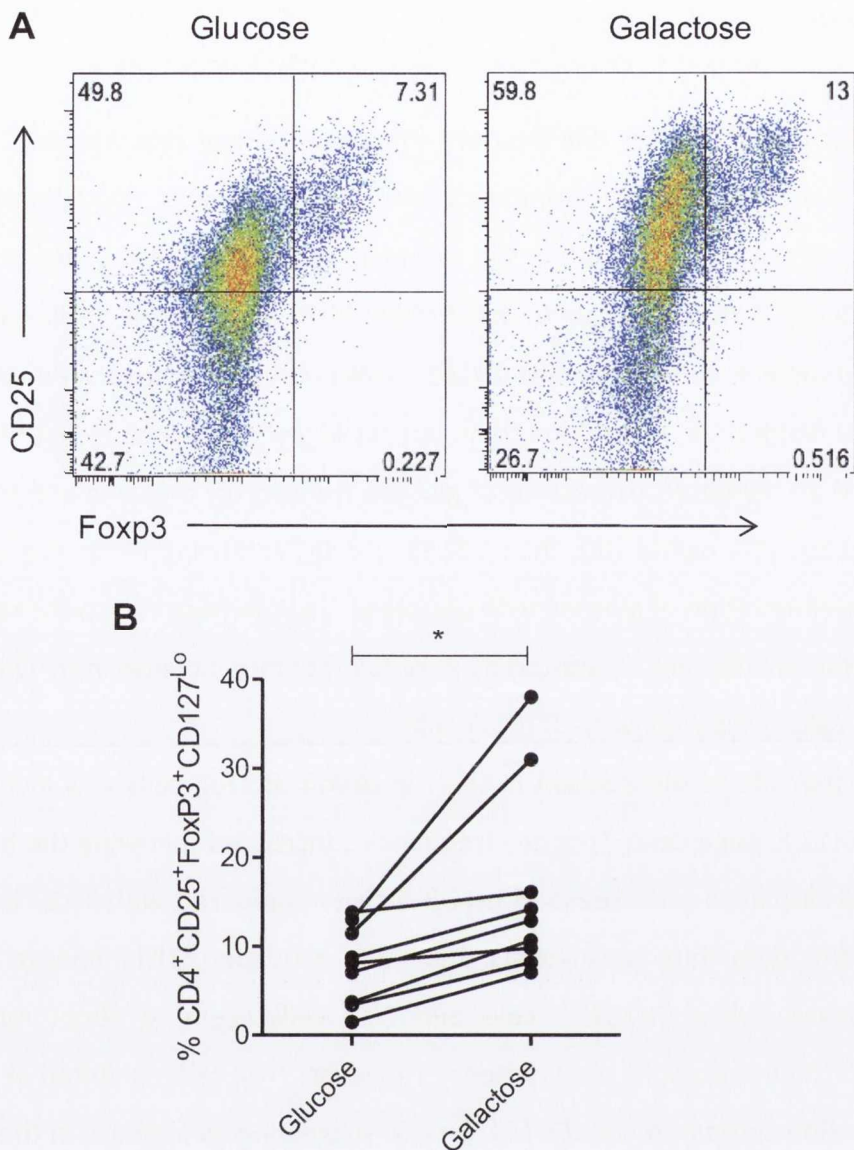


Figure 3.21 Increased frequencies of Treg cells following inhibition of glycolysis with galactose treatment.

Memory CD4⁺ T cells were negatively sorted from PBMC using magnetic beads and were cultured in complete glucose-free RPMI supplemented with 10 mM glucose or 10 mM galactose for 5 days and in the presence of anti-CD3, CFSE-labelled irradiated APCs and IL-2 (20 u/ml). After 5 days the cells were stained with fluorochrome-conjugated antibodies specific for surface markers CD4, CD25 and CD127, and the nuclear transcription factor Foxp3. Cells were analysed by flow cytometry and irradiated APCs were selectively excluded from analysis through CFSE⁻ gating. Representative dot plots show Foxp3 vs CD25 staining in galactose or glucose treated CD4⁺ T cells (A). The graph shows the frequency of CD4⁺CD25⁺CD127^{Lo}Foxp3⁺ Treg cells in each treatment group (B) (n=9 donors in separate experiments). Statistical differences in the mean between the groups were determined by a paired, two-tailed t test; * p<0.05.

3.3 Discussion

The results from this chapter demonstrate the novel finding that human CD161⁺ Th17 lineage cells are more glycolytic compared with CD161⁻ Th cells, consisting primarily of Th1 and Th2 cell subsets. In addition, this research also confirms the findings of previous studies. The present study has shown that CD161⁺ Th17 lineage cells display an increased glycolytic metabolism compared with CD161⁻ T cells, which conversely exhibit increased mitochondrial respiration. In addition to an increased glycolytic profile, Th17 lineage cells demonstrated an increased expression of glucose transporter proteins and the ability to consume glucose at a higher rate than CD161⁻ T cells. Following hindrance of glycolysis through supplementation of glucose with galactose, Th17 lineage cells were subsequently inhibited. These findings are supported by a complementary increase in mTOR activity for Th17 lineage cells compared with CD161⁻ T cells.

Additionally, the role of metabolism in the regulation of Treg cells was investigated. In contrast to Th17 lineage cells, Treg cell frequencies increased following the hindrance of glycolysis and displayed a decrease in mTOR activity compared with Th17 lineage cells. Collectively, this data thus far suggests that upon activation, Th17 lineage cells utilise aerobic glycolysis, while CD161⁻ T cells and Treg cells seem to adopt mitochondrial respiration for their metabolic requirements. However, Treg cells exhibited an increase in GLUT1 expression compared with CD161⁻ T cells, suggesting an increase in their glycolytic metabolism upon stimulation. This may suggest that Treg cells can utilize both metabolic pathways, and this theory is supported by Seahorse data revealing an increase in both glycolysis and mitochondrial respiration for Treg cells compared with CD161⁻ T cells.

The data represented here shows for the first time the expression of glucose transporters in human CD4⁺ T cell subsets. GLUT proteins are expressed in a tissue- and cell-specific manner and GLUT1 provides many cells with their basal glucose requirement (Mueckler 1994). Initially, the expression of GLUT1 by CD4 compared with CD8 T cells was examined, displaying an increased GLUT1 expression by CD4 T cells. A number of studies focus on the metabolism of CD4 and CD8 T cells separately; however, very few studies focus on directly comparing CD4 and CD8 T cell metabolism, and little information is available for human cells. Murine studies have revealed an increased mitochondrial oxidative activity for activated CD4⁺ T cells, whereas CD8⁺ T cells display an increased glycolytic metabolism

following activation (Cao, Rathmell et al. 2014). This increased glycolysis for CD8 T cells correlated with increased proliferation in the latter study. However, in agreement with our current data, a recent study in human T cells has revealed an increase in both mitochondrial metabolism, via oxygen consumption, and glycolysis, via lactate production, for CD4⁺ T cells compared with CD8⁺ T cells (Renner, Geiselhoringer et al. 2015). In addition to GLUT1 expression, differential mitochondrial mass was examined in human CD4 vs CD8 T cells. Mitotracker analysis provides a quantitative measure of cellular mitochondrial mass. Data in the present study revealed a significant increase in mitotracker staining for CD4⁺ T cells compared with CD8 T cells ex vivo. This is in agreement with data published for murine cells, in which CD4⁺ T cells display increased mitochondrial mass both ex vivo and following stimulation with anti-CD3 (Cao, Rathmell et al. 2014). Results shown here demonstrated an increased expression of glucose transporters and an increased mitochondrial mass for human CD4⁺ T cells compared with CD8 T cells, suggesting an increase in glycolysis and a possible link between mitochondrial mass and oxidative phosphorylation for CD4⁺ T cells. While the most prominent role of the mitochondria is to produce ATP via oxidative phosphorylation, it is also heavily involved in controlled cell death (apoptosis) (Zhao, Schlame et al. 1998). Therefore, in linking increased mitochondrial mass to increased mitochondrial respiration, more experiments will need to be performed in the future.

This study shows for the first time, staining for GLUT1 and mitotracker in human memory and naïve CD4⁺ T cells. Human naïve CD4⁺ T cells demonstrated a significant increase in mitotracker staining, correlating with increased mitochondrial mass, compared with total memory CD4 T cells. As naïve cells circulate via the lymph nodes, they remain inactive until they come into contact with antigen, and differentiate into a memory cell phenotype. This result is in agreement with murine studies, revealing that naïve T cells derive most of their ATP from oxidative phosphorylation (Grossman, Min et al. 2004). However, upon activation murine CD4⁺ T cells increase their glycolytic metabolism (Cao, Rathmell et al. 2014). This data is consistent with the increased mitotracker staining displayed for human naïve cells shown here. Activation states play a substantial role in metabolism, and as effector memory (T_{EM}) and central memory (T_{CM}) cells display differential activity states, the expression of GLUT1 in these memory subsets was investigated. The results in this study revealed a significant increase in T_{EM} cell GLUT1

expression compared with T_{CM} . T_{EM} cells reside at sites of infection and inflammation and display a more active profile when compared with T_{CM} cells, which home to the secondary lymphoid organs, much like naïve cells (Sallusto, Geginat et al. 2004). Mitochondrial mass was investigated for memory cell subsets and demonstrated no significant change between T_{EM} and T_{CM} cells. Therefore, this data suggests an increase in glycolysis for total memory cells, particularly effector memory cells, compared with naïve and central memory cells. These data provides an insight into the metabolism utilized by human $CD4^+$ T cells at the site of infection and inflammation, as well as that within the lymph nodes.

$CD4^+$ T cells were dissected further and the metabolism of T helper cell subsets was examined. This study revealed for the first time an increased expression of GLUT1 in Th17 lineage cells, characterized in humans by CD161 expression. This result suggests an increased ability of Th17 cells to consume glucose and perform glycolysis to a higher extent than $CD161^-$ T cells, consisting mostly of Th1 and Th2 cells. This result is consistent with that demonstrated in murine cells, as Th17 cells, differentiated from naïve $CD4^+$ T cells in vitro, displayed increased GLUT1 protein expression compared with Th1, Th2 and Treg cells (Michalek, Gerriets et al. 2011). Furthermore, knockdown of GLUT1 in murine $CD4^+$ T cells resulted in significantly less IL-17 production by $CD4^+$ T cells (Macintyre, Gerriets et al. 2014). Additionally, this study made novel use of a fluorescent glucose analogue (2-NBDG) in the analysis of glucose uptake within human $CD4^+$ T cell subsets. One study examined the effect of adjuvant stimulation on the glucose uptake ability of murine T cells (Sengupta, Chilton et al. 2005); however, 2-NBDG uptake in human $CD4^+$ T cells is, as of yet, unexplored. In the present study, $CD4^+CD161^+$ Th17 lineage cells exhibited an increased uptake of 2-NBDG compared with $CD161^-$ T cells. This increased glucose uptake by Th17 lineage cells is consistent with the GLUT1 data, suggesting Th17 lineage cells exhibit increased glucose uptake and glycolytic activity compared with $CD161^-$ T cells.

The phosphorylation of the ribosomal protein S6 is in direct correlation with mTOR activity. As mentioned previously, mTOR activity is important in promoting glucose metabolism (Duvel, Yecies et al. 2010). The quantification of pS6 by flow cytometry within human $CD4^+$ T cell subsets was performed for the first time in this study. Results demonstrated an increase in pS6 upon T cell activation and its subsequent inhibition

following treatment with rapamycin, the immune-suppressive drug targeting mTOR, indicating that pS6 was a suitable readout for mTOR activity in human CD4⁺ T cells. Additionally, results in this chapter demonstrated a significant increase in the frequency of pS6 expression in Th17 lineage cells compared with CD161⁻ T cells, verifying increased mTOR activity in Th17 cells. This finding compliments previous studies in mice stating that CD4⁺ T cells failed to differentiate into the Th17 lineage under specific skewing conditions following deletion of mTOR (Delgoffe, Kole et al. 2009). Delgoffe et al. have also shown the inability of T cells to differentiate into Th1 and Th2 cells following mTOR deletion. This data additionally suggests an increased glycolytic metabolism for Th17 lineage cells, as mTOR is known to promote the recruitment of glucose transporters to the cell surface and promote glycolytic enzyme activity (Chi 2012).

Having examined the metabolic profile of Th17 lineage cells via glucose transporter expression and glucose uptake, the effect of inhibiting glycolysis on T cell subset survival was investigated. As glucose is the normal sugar in cell culture medium, allowing for the utilization of glycolysis, the removal of glucose would result in decreased glycolytic activity in cells. Glucose was replaced with galactose, which enters glycolysis through the Leloir pathway at a significantly lower rate than glucose enters into glycolysis (Bustamante and Pedersen 1977). Additionally, breakdown of galactose via the Leloir pathway does not produce any net ATP (Marroquin, Hynes et al. 2007). Galactose substitution therefore hinders glycolysis significantly while maintaining cell proliferation through entry into the pentose phosphate pathway. Decreased glycolytic activity and increased mitochondrial activity following galactose treatment was confirmed in CD4⁺ T cells via the Seahorse Analyzer. This study made novel use of galactose supplementation in the examination of human Th cell subset survival and function. The frequency of IL-17-producing and CD161-expressing memory CD4⁺ T cells trended towards a decrease following the supplementation of glucose with galactose in culture medium. The frequency of memory CD4⁺IFN- γ ⁺ T cells was unchanged following galactose treatment. Galactose has previously been shown to promote oxidative phosphorylation in cancer cell lines (Rossignol, Gilkerson et al. 2004, Chang, Curtis et al. 2013), suggesting a requirement of glycolysis for the survival of memory Th17 cells. This is in agreement with a previous murine study reporting a decrease in CD4⁺IL-17⁺ cells following stimulation in the complete absence of glucose (Michalek, Gerriets et al. 2011).

The Seahorse XF technology measures energy utilisation in living cells, simultaneously quantifying mitochondrial respiration and glycolysis in real time. During this study, the use of the Seahorse analyzer on primary human PBMC was a novel application and remains to be the case for human CD4 T cell subsets. This study has demonstrated for the first time the metabolic profiles of differentiated memory CD161⁺ Th17 lineage cells and CD161⁻ Th cells. CD4⁺CD161⁺ Th17 lineage cells demonstrated increased basal glycolysis, maximal glycolytic capacity and glycolytic reserve compared with CD4⁺CD161⁻ T cells. The glycolytic reserve of the cell is relied upon during times of stress, for example during low oxygen levels (hypoxia) or following inhibition of oxidative phosphorylation. Th17 lineage cells display the ability to generate lactate at a high rate following glucose addition and can further elevate their glycolytic rate when required to do so following inhibition of mitochondrial respiration as a result of oligomycin A treatment. Mitochondrial and oxidative metabolism can play a key role in supporting T cell activation and proliferation (Chang, Curtis et al. 2013). Oligomycin A treatment used to inhibit mitochondrial ATP production suppressed oxygen consumption in each subset to an equivalently low level, indicating that oxygen consumption was tightly coupled to ATP generation for all T cell subsets. Upon the addition of FCCP, CD161⁻ T cells displayed an enhanced OCR associated with the maximal mitochondrial respiratory capacity and the respiratory reserve of the cells. A recent study has examined the detailed metabolic phenotype of murine CD4⁺ T cells, comparing effector (Teff) and Treg cells. The ECAR and OCR for Teff (Th1 and Th17) and Treg cells, which were differentiated in vitro from naïve CD4⁺ T cells in the presence of polarizing cytokines, revealed an overall increase in ECAR for Teff cells and a subsequent increase in OCR for Treg cells (Gerriets, Kishton et al. 2015). However, in contrast to the results represented in this chapter, Gerriets et al. focused on murine Th17 and Th1 cells alone, excluding the remaining effector T cells, which were included in the CD4⁺CD161⁻ subset. CD4⁺ T cells and subsets thereof required activation 18 h prior to Seahorse experimentation to enable adequate ECAR and OCR values which ranged above background levels. In agreement with these present findings, a recent study has demonstrated an increase in both glycolysis and mitochondrial respiration following activation of human CD4⁺ T cells via the Seahorse Analyzer (Renner, Geiselhoringer et al. 2015). The results in this chapter demonstrate a clear utilization of glycolysis by Th17 lineage cells compared with non-Th17 lineage cells, as indicated by increased GLUT1 expression, glucose uptake, mTOR activity and Seahorse analysis.

Having investigated the metabolic profile of Th17 lineage cells, regulatory T cells were examined next. The Th17/Treg cell balance is vital to maintaining optimal immunity against infection. This balance is perturbed in autoimmunity; therefore, anything that could manipulate this balance could provide an insight into future targets of inflammatory and autoimmune disease.

Treg cells have previously been described in murine studies as utilizing oxidative phosphorylation for their metabolic demands and needs. For example, murine Treg cell proliferation was significantly reduced following treatment with rotenone, an inhibitor of mitochondrial oxidative phosphorylation via complex inhibition within the electron transport chain (Gerriets, Kishton et al. 2015). In contrast to this, results in this chapter demonstrated an increased expression of GLUT1 by Treg cells, compared with CD161⁻ T cells, and no significant change compared with Th17 cells. This was unforeseen, as previous murine data had also revealed the lowest GLUT1 protein expression by in vitro differentiated Treg cells (Michalek, Gerriets et al. 2011). This result suggests human Treg cells can utilize glycolysis following stimulation. On the other hand however, pS6 expression and mTOR activity trended towards a decrease for Treg cells in this study compared with CD161⁺ T cells. Since GLUT1 and mTOR are both correlates of glycolysis, it would be expected that they would be expressed in parallel and the reason for this discrepancy is unclear. In previous murine studies, mTOR was shown to be critical for effector T cell activation, while AMPK is known to be upregulated in Treg cells (Michalek, Gerriets et al. 2011). AMPK (AMP-activated protein kinase) is activated when AMP levels rise, promoting metabolism via oxidative phosphorylation and the conversion of AMP to ATP (Towler and Hardie 2007). A murine study demonstrates an increased expression of AMPK protein by Treg cells compared with T helper cell subsets (Michalek, Gerriets et al. 2011).

In contrast to Th17 cells, Treg cell frequencies were significantly increased following galactose treatment, suggesting that human Treg cells utilize oxidative phosphorylation following glucose depletion. This is in agreement with a previous study carried out in murine cells demonstrating an increase in CD4⁺Foxp3⁺ cells following stimulation in the complete absence of glucose (Michalek, Gerriets et al. 2011). Treg cells also exhibited decreased glucose uptake in murine studies compared with Th17 cells (Michalek, Gerriets et al. 2011).

Seahorse analysis was performed on Treg cells and compared with CD161⁺ and CD161⁻ T cell subsets, for the examination of both glycolytic metabolism and mitochondrial respiration profiles. This chapter revealed for the first time an increase in basal glycolysis and maximal glycolytic capacity for human Treg cells compared with CD161⁻ T cells. No change was observed between Treg and Th17 cells displaying a simultaneous increase in glycolysis for both subsets. However, Th17 cells demonstrated an increase in their glycolytic reserve, which can be utilized by cells in times of stress, whereas Treg cells revealed a reduction in this reserve. Treg cells additionally demonstrated a significant increase in basal respiration and maximal respiratory capacity compared with Th17 cells. These data conflicts with murine studies demonstrating, via the Seahorse, a decrease in glycolysis for Treg cells compared with Th17 cells (Gerriets, Kishton et al. 2015): However, Treg cells in this study additionally showed an increase in mitochondrial respiration, in agreement with the data presented in this chapter. This suggests Treg cells can potentially utilize both metabolic pathways, and may not require mTOR for increased glycolytic metabolism.

In summary, this chapter has definitively shown for the first time an increased glycolytic metabolism in human Th17 lineage cells. This is supported by an increase in Th17 cell glycolytic profile, glucose transporter expression and increased glucose uptake. These data also demonstrates a decline in Th17 lineage cell frequencies as a result of hindering glycolysis. Additionally, this study provides a further insight into the role of metabolism in Treg cells, shown to withstand glycolytic inhibition, supporting a role for oxidative phosphorylation, whilst also expressing increased frequencies of glucose transporters. Treg cells may have the ability to utilize both pathways of metabolism.

Chapter 4

The role of HIF-1 α and hypoxia in the regulation of human T cell subsets

Chapter 4. The role of hypoxia in the regulation of T cell subsets

4.1. Introduction

Hypoxic conditions are found at sites of inflammation and infection as immune cells infiltrate the surrounding tissue. The RA synovial joint represents such a hypoxic site (Ng, Biniecka et al. 2010). Given the challenges which face immune cells at sites of low oxygen, hypoxia elicits a range of adaptive responses at the cellular, tissue and systemic level to maintain cellular proliferation, function and survival. One such adaptation is the increased expression of HIF-1 α . HIF-1 α , as mentioned previously, is an oxygen-sensing transcription factor, which transcribes specific genes involved in glycolysis and cellular proliferation. HIF-1 α is stabilized at the protein level in hypoxic conditions and recent studies have proclaimed a key role for HIF-1 α in murine T cell subset differentiation.

In mice, T cell subsets displayed differential expression levels of HIF-1 α mRNA, with Th17 cells at the upper-end of the scale. Furthermore, Th17 cell differentiation from naïve CD4⁺ T cells was decreased in HIF-1 α knockout mice, whilst the expression of Foxp3 was increased (Shi, Wang et al. 2011). Additionally, HIF-1 α has been shown to promote Th17 cell differentiation in mice through direct transcriptional activation of the Th17 cell specific transcription factor ROR γ t and through a direct interaction with ROR γ t to activate the transcription of Th17 cell specific genes, such as IL-17A (Dang, Barbi et al. 2011). HIF-1 α can also contribute directly to the inhibition of Treg cell differentiation in mice. Foxp3, the Treg cell specific transcription factor, possesses a HIF-1 α binding domain, allowing HIF-1 α to target Foxp3 for polyubiquitination and proteasomal degradation by the same ligase system which degrades HIF-1 α during normal oxygen levels (Dang, Barbi et al. 2011). Studies thus far have primarily focused on the role of hypoxia and HIF-1 α on T cell differentiation, whilst very little spotlight has been shone on the effect of hypoxia on memory T cell survival and expansion at the sites of inflammation.

A recent study centred on the functional aspects of human Treg and Th17 cells in hypoxia. However, this study failed to reveal the effect of hypoxia on T cell subset survival (Bollinger, Gies et al. 2014). Treg cells in this study displayed a decreased ability to

suppress the proliferation of responder cells. In contrary to previous studies stating an inhibition of Foxp3 in hypoxia, Jurkat T cells exhibited an induction in FOXP3 mRNA levels in hypoxic conditions (Clambey, McNamee et al. 2012). It was revealed that this increased FOXP3 expression was as a result of inducible-Treg cell generation and not the expansion of existing thymic-Tregs.

A key function of HIF-1 α is to promote anaerobic glycolysis in hypoxic conditions. Glycolysis provides a path to continued ATP production in low oxygen tension as oxidative phosphorylation is inhibited. Stabilization of HIF-1 α activates the transcription of glucose transporters, including GLUT1, and many glycolytic enzymes in murine cells (Shi, Wang et al. 2011). However, the expression of glucose specific proteins in human T cells in hypoxia has not yet been elucidated.

A primary role exists for the cytokine environment surrounding naïve T cells during activation and differentiation of T cell subsets. Studies have implicated the requirement for combinations of IL-1 β , IL-6, IL-23 and TGF- β in the differentiation of murine and human Th17 cells (Acosta-Rodriguez, Napolitani et al. 2007, Chen, Tato et al. 2007, Manel, Unutmaz et al. 2008, Stritesky, Yeh et al. 2008, Yang, Anderson et al. 2008). Culture of murine T cells with Th17-skewing cytokines in hypoxia, resulted in increased frequencies of CD4⁺IL17⁺ T cells (Clambey, McNamee et al. 2012). The role of Th17-favouring cytokines on human T cells in hypoxia is yet to be investigated.

Given the key role of Treg cells in constraining effector cells at sites of inflammation, it is important to understand how they might be influenced by hypoxia. Thymic Treg cells, as mentioned in chapter 1, develop in the thymus and upregulate Foxp3 expression following IL-2R signalling. In contrast, peripheral Treg cells develop in the periphery in the presence of IL-2 and TGF- β (Apostolou, Sarukhan et al. 2002). Recently, a study performed in mice revealed that neutralization of TGF- β resulted in a decreased frequency of Foxp3⁺ T cells in hypoxia (Clambey, McNamee et al. 2012). However the role of HIF-1 α in regulating human Treg cells in hypoxia has not yet been investigated.

The rheumatic joint represents a highly inflamed environment (Ng, Biniecka et al. 2010). Th17 cells are thought to play a key role in RA pathogenesis (Astry, Harberts et al. 2011)

and are characterised in humans by CD161 c-type lectin expression (Cosmi, De Palma et al. 2008). CD161⁺ Th17 lineage cells have been shown to be enriched in the RA joint (Chalan, Kroesen et al. 2013, Basdeo, Moran et al. 2015), suggesting they have a pathogenic role in RA. Studies have also reported an increase in Treg cell frequencies in the synovial fluid (SF) extracted from rheumatic joints (van Amelsfort, Jacobs et al. 2004, Basdeo, Moran et al. 2015); however, despite this increase in Treg cell frequencies, the RA joint remains highly inflamed. A recent study reported that CD161⁺ Th17 lineage cells are resistant to Treg-mediated suppression both in the RA joint and healthy controls (Basdeo, Moran et al. 2015). Therefore, this study aimed to elucidate the effect of hypoxia in vitro and in RA patients in vivo on the metabolism, expansion and survival of human CD4⁺ T cell subsets.

4.1.1 Aims

The experiments in this chapter aimed to determine the differential survival and expansion of human T cell subsets in hypoxia and to investigate the mechanisms underlying these effects;

- Examine the survival characteristics of CD4⁺ T cell subsets ex vivo.
- Analyse the ex-vivo expression of HIF-1 α in T cell subsets via flow cytometry
- Investigate the effect of hypoxic conditions on the metabolism and function of T cell subsets.
- Examine HIF-1 α and GLUT1 expression in CD4⁺ T cell subsets ex vivo in RA patient blood and synovial fluid.

4.2 Results

4.2.1 The characteristics of Th17 lineage cells

4.2.1a CD4⁺CD161⁺ T cells demonstrate an increased expression of cell survival proteins Bcl-2 and Ki67.

Th17 cells have recently been described as being long-lived and having stem cell-like features (Kryczek, Zhao et al. 2011, Muranski, Borman et al. 2011). Primary Th17 cells from both peripheral blood and colonic cancer tissue expressed increased Ki67 compared with Th1 cells (Kryczek, Zhao et al. 2011). Ki67 is a specific marker of cellular proliferation. Additionally, polarized Th17 cells from mice were shown to express Bcl2 mRNA to a higher extent than Th1 cells. Bcl-2 is a member of the Bcl-2 family of regulator proteins, which have been describe as playing a role in both cell survival and death; however, Bcl-2 is specifically an anti-apoptotic protein (Czabotar, Lessene et al. 2014). The expression of both Ki67 and Bcl-2 was examined in human Th17 lineage cells, characterized by CD161 expression.

PBMC were isolated from healthy donor blood and stained ex vivo with fluorochrome-conjugated antibodies against CD4 and CD161. Cells were additionally stained intracellularly for Ki67 and Bcl-2 expression and analysed by flow cytometry. Th17 lineage (CD4⁺CD161⁺) cells displayed a significant increase in Bcl-2 (Figure 4.1 A) ($p < 0.001$) and Ki67 (B) ($p < 0.05$) intensity compared with CD161⁻ (CD4⁺CD161⁻) T cells. This data suggests an increased proliferative capacity and survival of resting Th17 lineage cells analysed ex vivo.

4.2.1b Th17 lineage cells display an increased expression of HIF-1 α .

Immune cells frequently encounter a range of oxygen tensions. Most certainly, T cells at sites of inflammation and infection have a high probability of prolonged exposure to hypoxic conditions. The cellular response to hypoxia is mediated in part by the hypoxia-inducible transcription factor HIF-1 α (Ema, Taya et al. 1997). The expression of HIF-1 α by T cell subsets could provide insight into their potential to survive within inflamed environments.

In order to investigate the expression of HIF-1 α in human T cell subsets, PBMC were isolated from healthy donor blood and stained ex vivo with fluorochrome-conjugated antibodies specific for the surface proteins CD4, CD25, CD127, CD161 and Foxp3. Cells

were additionally stained for HIF-1 α expression and analysed by flow cytometry. Th17 lineage (CD4⁺CD161⁺) cells displayed a significant increase in HIF-1 α expression compared with CD161⁻ (CD4⁺CD161⁻) T cells, consisting of mostly Th1 and Th2 cells ($p < 0.001$) (Figure 4.2 A and B). Additionally, Th17 cells expressed significantly increased HIF-1 α when compared with Treg cells (CD4⁺CD25⁺CD127^{lo}Foxp3⁺) ($p < 0.01$) (Figure 4.2 C). This suggests a survival mechanism for Th17 lineage cells in hypoxic environments, and a possible indication of a propensity to switch towards glycolytic metabolism in low oxygen tension.

4.2.2 The survival characteristics of exTh17 cells.

As described in chapter 1, exTh17 cells arise from Th17 cell precursors and retain the expression of CD161 on their cell surface. As mentioned previously, exTh17 cells switch from primarily IL-17 producers, to simultaneously producing IL-17 and IFN- γ , to finally switching fully to IFN- γ only producers (Cosmi, Cimaz et al. 2011). ExTh17 cells are enriched in Crohn's disease, JIA and RA, however very little is known about the pathogenic phenotype of these cells. The expression of survival characteristics in exTh17 cells was examined and compared with Th17 and Th1 cells.

PBMC were isolated from healthy donor blood and stained ex vivo with fluorochrome-conjugated antibodies against CD4, CD161, CXCR3, Bcl-2 and Ki67. HIF-1 α expression in these T cell subsets was investigated. PBMC were isolated from healthy donor blood. Cells were stained ex vivo with fluorochrome-conjugated antibodies against CD4, CD161, CXCR3 and HIF-1 α . The results based on ex vivo staining revealed a trend towards an increase in HIF-1 α expression for Th17 lineage cells (CD4⁺CD161⁺CXCR3⁻) and exTh17 cells (CD4⁺CD161⁺CXCR3⁺) compared with Th1 cells (CD4⁺CD161⁻CXCR3⁺) (Figure 4.3 B).

Additionally, ExTh17 (CD4⁺CD161⁺CXCR3⁺) cells displayed a significant increase in Bcl-2 MFI values compared with Th1 (CD4⁺CD161⁻CXCR3⁺) cells ($p < 0.01$) but not bona fide Th17 cells (CD4⁺CD161⁺CXCR3⁻) (Figure 4.3 C). Ki67 MFI values trended towards an increase in exTh17 cells compared with both Th1 and Th17 (CD4⁺CD161⁺CXCR3⁻) cells (Figure 4.3 D). These data suggest a potential towards increased proliferation and survival of exTh17 cells, which may in part account for their accumulation at sites of inflammation.

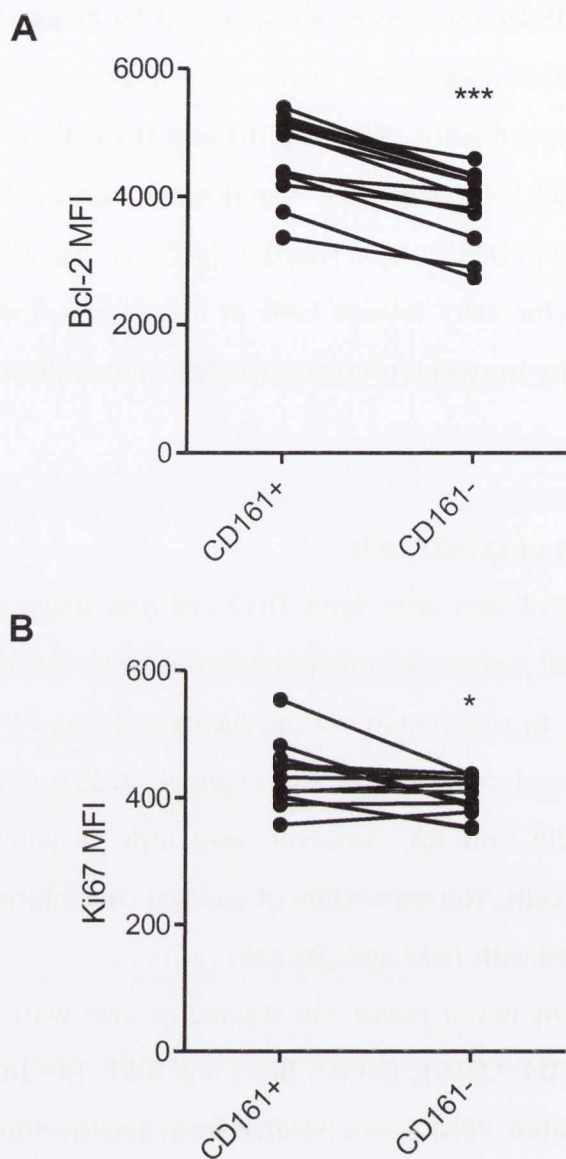


Figure 4.1 Survival characteristics of CD4⁺CD161⁺ T cells.

PBMC from healthy donors were stained with fluorochrome-conjugated antibodies specific for CD4, CD161, and intracellular Bcl-2 and Ki67. Cells were analysed by flow cytometry and results represent Bcl-2 and Ki67 MFI values for CD161⁺ (CD4⁺CD161⁺) and CD161⁻ (CD4⁺CD161⁻) T cells (n=13). Statistical differences in the mean between the groups were determined by a paired, two-tailed t test; *p<0.05, ***p<0.001

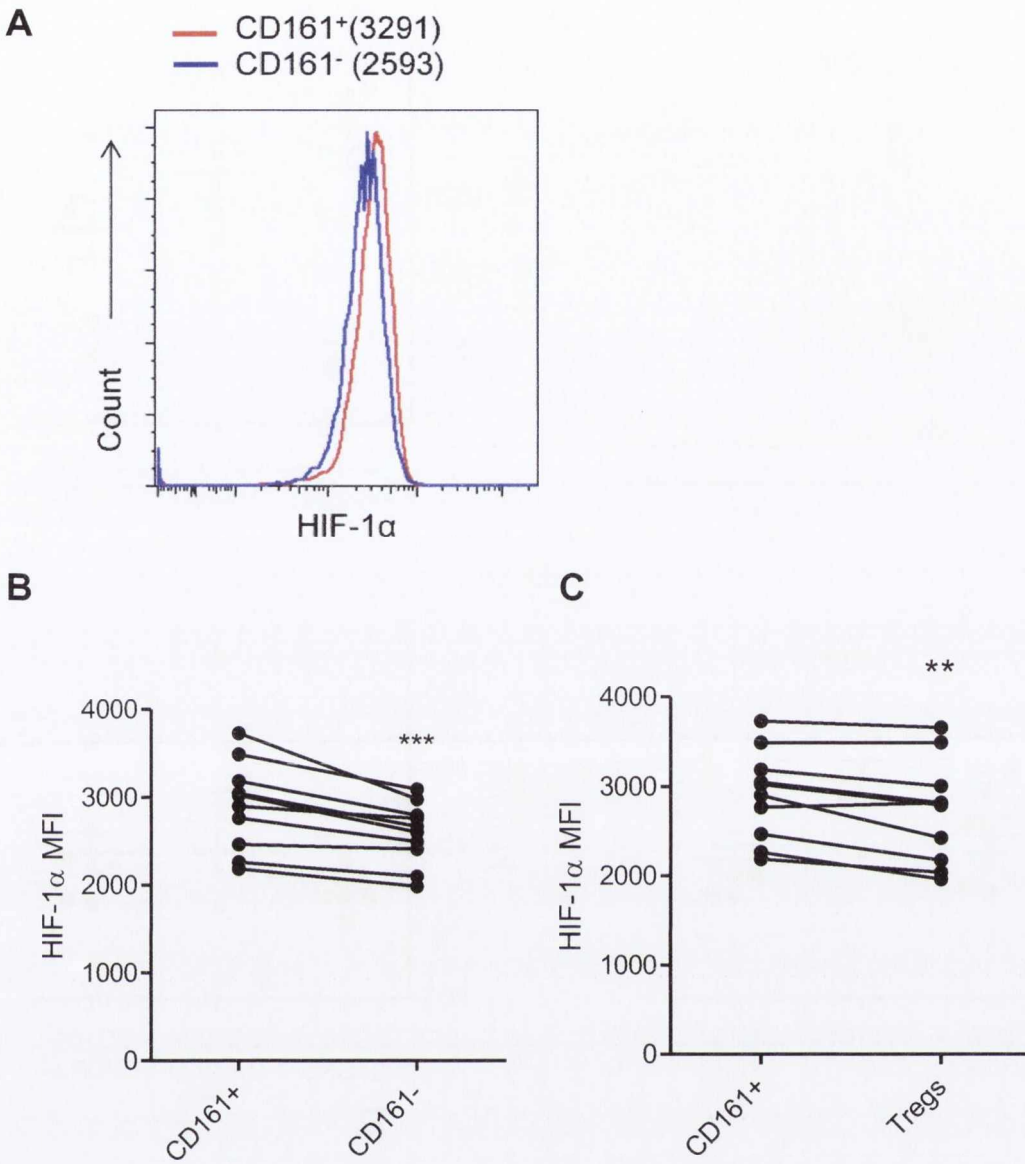


Figure 4.2 Increased frequencies of CD4⁺CD161⁺ T cells expressing HIF-1 α compared with CD4⁺CD161⁻ and Treg cells.

PBMC from healthy donors were stained with fluorochrome-conjugated antibodies specific for CD4, CD161, CD25, CD127, Foxp3 and HIF-1 α . Cells were analysed by flow cytometry. Representative histograms gated on CD4⁺CD161⁺ (CD161⁺) and CD4⁺CD161⁻ (CD161⁻) T cells are shown in (A), with MFI values in parentheses. The graph shows HIF-1 α MFI values for CD4⁺CD161⁺ (CD161⁺) and CD4⁺CD161⁻ (CD161⁻) T cells (A) and for CD4⁺CD161⁺ (CD161⁺) and CD4⁺CD25⁺CD127^{lo}Foxp3⁺ (B) (n=11). Statistical differences in the mean between the groups were determined by a paired, two-tailed t test; **p<0.01, ***p<0.001.

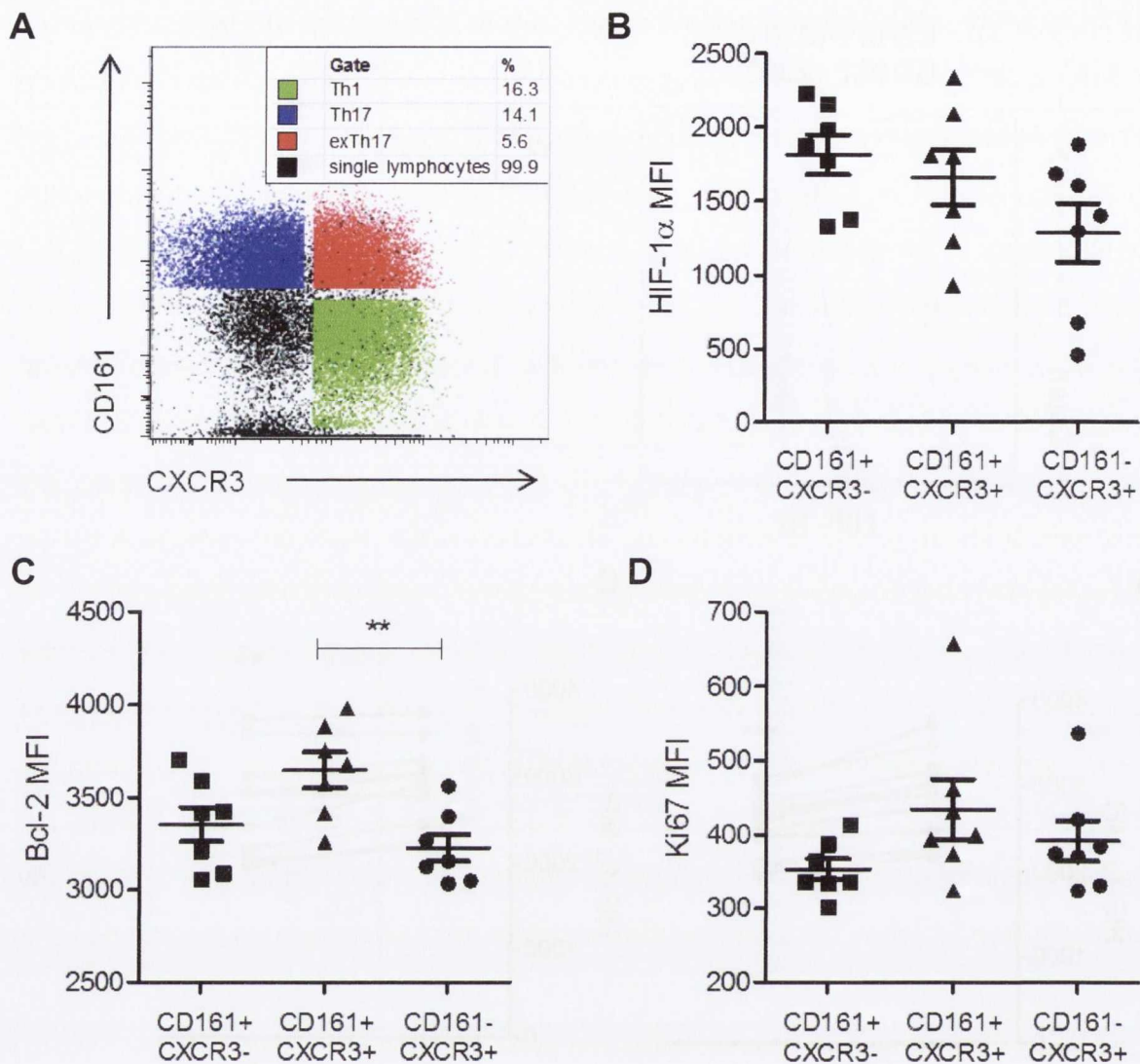


Figure 4.3 Survival characteristics of Th17, exTh17 and Th1 cells.

PBMC from healthy donors were stained with fluorochrome-conjugated antibodies specific for CD4, CD161, CXCR3, the intracellular Bcl-2, Ki67 and HIF-1 α . The cells were analysed by flow cytometry and the representative dot plot is gated on CD4⁺ T cells and demonstrates CD161 vs CXCR3 (A). Results represent HIF-1 α (B), Bcl-2 (C) and Ki67 (D) MFI values for Th17 lineage cells (CD161⁺CXCR3⁻) exTh17 (CD161⁺CXCR3⁺) and Th1 cells (CD161⁻CXCR3⁺) (n=7). Statistical analysis was determined by one-way ANOVA with Tukey's Multiple Comparison test; **p<0.01.

4.2.3 Culture of CD4⁺ T cells in reduced oxygen results in increased HIF-1 α expression.

In order to examine the effects of hypoxic conditions *in vitro*, a specialised cell culture chamber allowing for alteration in oxygen levels was utilized.

To confirm the effects of the low oxygen tension within the hypoxia culture chamber, HIF-1 α expression was examined by flow cytometry, since HIF-1 α protein levels should become stabilized within low oxygen environments. Healthy donor PBMC were stimulated in the presence of anti-CD3 in normoxic (21%) or hypoxic (5%) oxygen levels in an oxygen controlled chamber. After 4 days, the cells were extracted from the chamber and immediately stained with CD4 and HIF-1 α fluorochrome-conjugated antibodies. The cells were analysed by flow cytometry and results revealed a significant increase in HIF-1 α MFI values for CD4⁺ T cells stimulated in hypoxic oxygen levels ($p < 0.001$) (Figure 4.4).

In addition, the effect of hypoxia on total PBMC proliferation was investigated. Healthy donor PBMC were stained with Cell-trace Violet, a cell tracer dye which is diluted out of the cell following each cellular division step, and stimulated with anti-CD3 in normoxic (21%) or hypoxic (5%) oxygen levels. After 4 days, the cells were removed from the chamber and analysed by flow cytometry. PBMC cell proliferation was significantly reduced in hypoxia compared with normoxia controls ($p < 0.001$) (Figure 4.5 A and B).

4.2.4. The effect of hypoxia on the expression of GLUT1 by CD4⁺ T cells

HIFs are known to provide a link between Th cell differentiation and metabolism. Under low oxygen tension, glycolysis provides a path for continued ATP production without the need for O₂-dependent oxidative phosphorylation. HIF-1 α transcribes genes involved in glycolysis, such as glucose transporters and glycolytic enzymes (Semenza 2010). In murine studies, HIF-1 α knockdown resulted in decreased GLUT1 expression and a decrease in the mRNA of many glycolytic enzymes in T cells (Shi, Wang et al. 2011). In order to examine the effects of hypoxia on metabolism, the effect of hypoxia on GLUT1 expression, as a correlate of glycolysis, was measured.

Healthy donor PBMC were stimulated in the presence of anti-CD3 in normoxic (21%) or hypoxic (5%) oxygen levels in a hypoxia chamber. After 48 h, the cells were stained with fluorochrome-conjugated antibodies specific for CD4 and GLUT1. The data shows a trend towards an increase in GLUT1 expression in hypoxia compared with normoxia ($n=4$) (Figure 4.6).

4.2.5 The effect of hypoxia on the expression of mitochondrial genes

The most prominent roles of the mitochondria are to produce the energy currency of the cell, in the form of ATP, and to regulate cellular metabolism. Oxidative phosphorylation occurs in the mitochondria, and having investigated the expression of glucose transporters in hypoxia, the effect of hypoxia on the expression of specific mitochondrial genes was examined next since it might be expected that hypoxia would induce a switch from oxidative phosphorylation to glycolysis.

Healthy donor PBMC were stimulated with anti-CD3 in normoxia (21%) or hypoxia (5%) for 24 h. RNA was extracted from 10×10^6 cells using the Qiagen RNeasy Extraction Kit and cDNA was synthesized and mRNA expression of desired genes was measured via the RT² Profiler™ PCR Array Human Mitochondria. Four housekeeping genes were examined; *ACTB* (β -actin), *B2M* (β -2 microglobulin), *HPRT1* (hypoxanthine phosphoribosyltransferase 1) and *RPLP0* (ribosomal protein, large P0). The fold regulation and fold change is indicated for PBMC in hypoxia, and compared with normoxia (Table 4.1). Genes indicated in blue display a significant reduction in expression, while those indicated in red demonstrate a significant increase in expression in hypoxia compared with normoxia. The expression of the majority of genes in the mitochondrial array was not significantly altered by hypoxia. Genes that were significantly down regulated by hypoxia were *CPT1B* (carnithine palmitoyltransferase 1B), *HSP90AA1* (heat shock protein 90-alpha), *SFN* (stratifin), *SLC25A20* (carnithine carrier protein), *SLC25A5* (adenine nucleotide translocator), *UCP1* (uncoupling protein 1), and *UCP2* (uncoupling protein 2). On the other hand the expression of the following genes were significantly increased by hypoxia; *Bcl-2* (B-cell CLL/lymphoma 2), *BNIP3* (BCL2/adenovirus E1B 19 kDa protein-interacting protein 3), *SLC25A27* (uncoupling protein 4), and *SOD2* (superoxide dismutase 2). Overall the data suggested that hypoxia mostly affected the expression of genes involved in cellular stress and survival, which may have been in due to the oxidative stress imposed on T cells by hypoxia. However, hypoxia did not appear to exert a major effect on the expression of genes involved in mitochondrial energy metabolism.

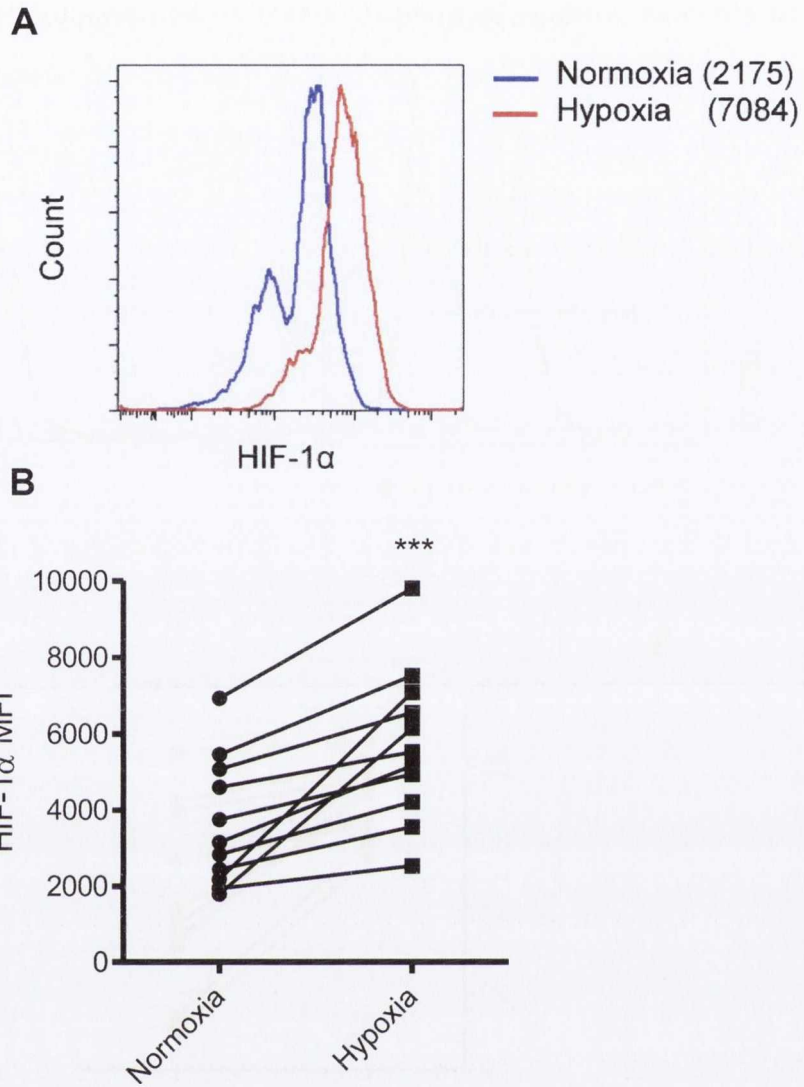


Figure 4.4 Increased HIF-1 α expression by CD4⁺ T cells in hypoxia

Healthy donor PBMC were stimulated in the presence of anti-CD3 in normoxic (21%) or hypoxic (5%) oxygen levels. After 4 days, cells were stained with fluorochrome-conjugated antibodies specific for CD4 and HIF-1 α . The cells were analysed by flow cytometry and representative histograms gated on CD4⁺ T cells are shown in (A), with MFI values in parentheses. The graph shows HIF-1 α MFI values for CD4⁺ T cells in normoxia and hypoxia (n=11). Statistical differences in the mean between the groups were determined by a paired, two-tailed t test; ***p<0.001.

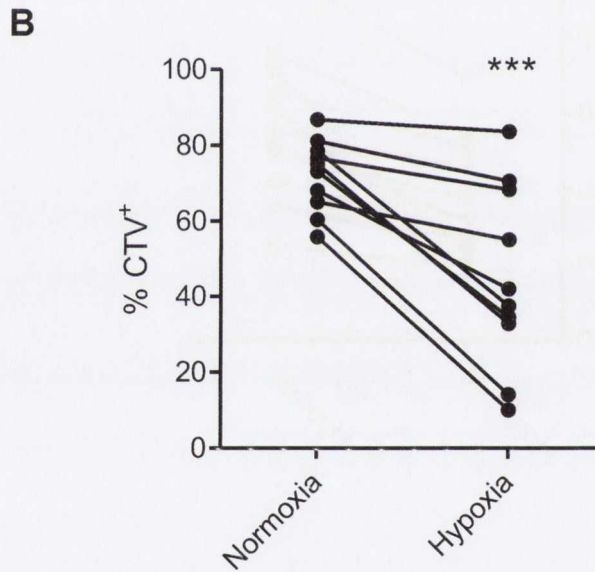
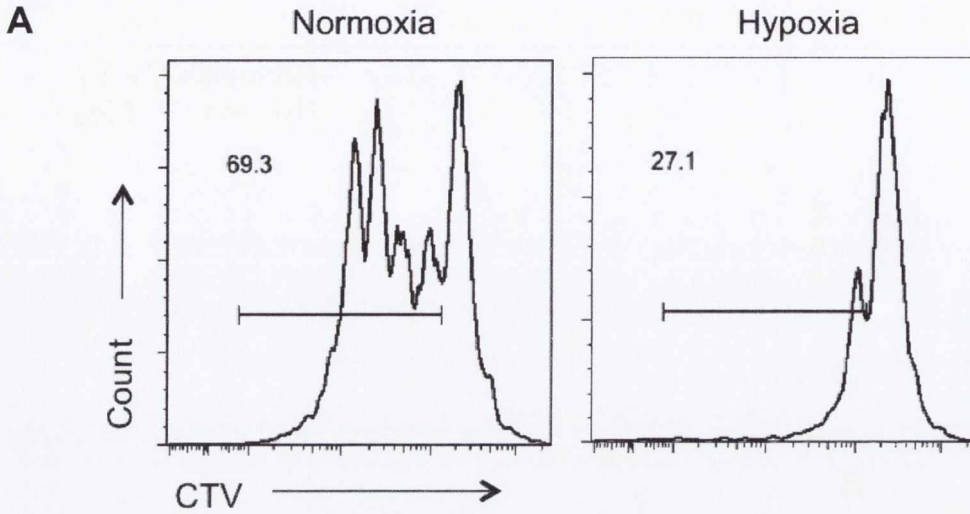


Figure 4.5 Decreased cellular proliferation in hypoxia

Healthy donor PBMC were stained with cell trace violet (CTV) and stimulated in the presence of anti-CD3 in normoxic (21%) or hypoxic (5%) oxygen levels. After 4 days, cells were analysed by flow cytometry. The representative histogram shows CTV dilution for total PBMC (A) and the graph represents the frequency of cell proliferation for total PBMC (B) (n=10). Statistical differences in the mean between the groups were determined by a paired, two-tailed t test; ***p<0.001.

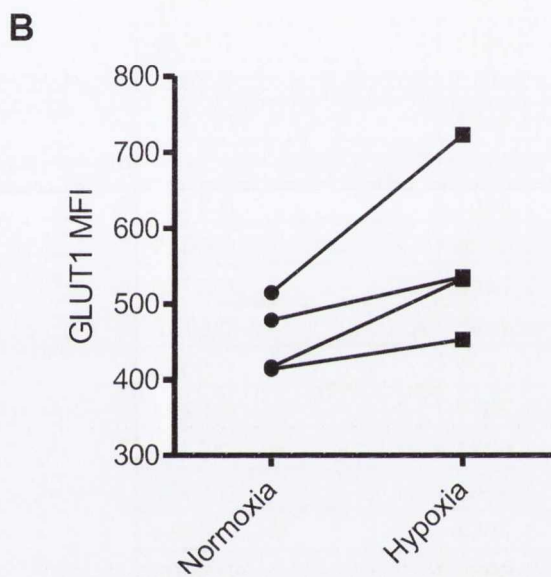
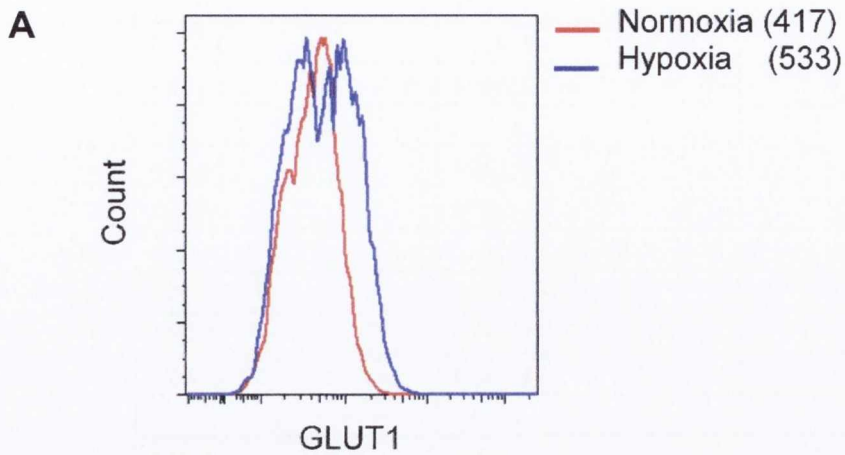


Figure 4.6 The expression of GLUT1 by CD4⁺ T cells in hypoxia compared with normoxia

Healthy donor PBMC were stimulated with anti-CD3 in normoxic (21%) or hypoxic (5%) oxygen levels. After 48 h stimulation, cells were stained with fluorochrome-conjugated antibodies specific for CD4 and GLUT1 and analysed by flow cytometry. Representative histograms gated on CD4⁺ T cells show GLUT1 staining in normoxia and hypoxia (A). The graph shows GLUT1 MFI values for CD4⁺ T cells in normoxia and hypoxia (n=4) (B).

Gene	Fold Regulation	Fold Change
AIP	-1.7291	0.5783
BAK1	-1.7411	0.5743
BBC3	1.2483	1.2483
BCL2	2.0705	2.0705
BCL2L1	-1.2397	0.8066
BID	-1.014	0.9862
BNIP3	5.579	5.579
CDKN2A	-1.6245	0.6156
COX10	-1.0718	0.933
COX18	-1.3379	0.7474
CPT1B	-2.9079	0.3439
CPT2	-1.366	0.732
DNM1L	-1.3287	0.7526
FIS1	1.0425	1.0425
TIMM10B	-1.3013	0.7684
GRPEL1	-1.3472	0.7423
HSP90AA1	-2.4967	0.4005
HSPD1	-1.8661	0.5359
IMMP1L	-1.6586	0.6029
IMMP2L	-1.1408	0.8766
LRPPRC	-1.4845	0.6736
MFN1	-1.2397	0.8066
MFN2	-1.2058	0.8293
MIPEP	-1.6021	0.6242
MPV17	-1.5263	0.6552
MSTO1	-1.7654	0.5664
MTX2	-1.6935	0.5905
NEFL	1.5692	1.5692
OPA1	-1.366	0.732
PMAIP1	-1.1892	0.8409
RHOT1	-1.434	0.6974
RHOT2	-1.366	0.732
SFN	-6.5887	0.1518
SH3GLB1	-1.454	0.6878
SLC25A1	-1.1408	0.8766
SLC25A12	-1.6586	0.6029
SLC25A13	-1.3013	0.7684
SLC25A14	-1.879	0.5322
SLC25A15	-1.6245	0.6156
SLC25A16	-1.4241	0.7022
SLC25A17	-1.5583	0.6417
SLC25A19	-1.4743	0.6783
SLC25A2	-1.2142	0.8236
SLC25A20	-2.7321	0.366
SLC25A22	-1.7411	0.5743

SLC25A23	1.4044	1.4044
SLC25A24	-1.021	0.9794
SLC25A25	-1.5692	0.6373
SLC25A27	3.2266	3.2266
SLC25A3	-1.5583	0.6417
SLC25A30	1.1408	1.1408
SLC25A37	1.6472	1.6472
SLC25A4	-1.1892	0.8409
SLC25A5	-2.6208	0.3816
SOD1	-1.5692	0.6373
SOD2	3.0738	3.0738
STARD3	-1.1728	0.8526
TAZ	-1.6245	0.6156
TIMM10	-1.6472	0.6071
TIMM17A	-1.5911	0.6285
TIMM17B	-1.3472	0.7423
TIMM22	-1.3947	0.717
TIMM23	-1.6586	0.6029
TIMM44	-1.2746	0.7846
TIMM50	-1.2397	0.8066
TIMM8A	-1.5692	0.6373
TIMM8B	-1.366	0.732
TIMM9	-1.5263	0.6552
TOMM20	1.014	1.014
TOMM22	-1.3195	0.7579
TOMM34	1.2397	1.2397
TOMM40	-1.4743	0.6783
TOMM40L	-1.4845	0.6736
TOMM70A	-1.2658	0.79
TP53	-1.1173	0.895
TSPO	-1.1329	0.8827
UCP1	-2.6574	0.3763
UCP2	-2	0.5
UCP3	-1.9862	0.5035
UXT	-1.5052	0.6643

Table 4.1 Fold regulation and fold change of mitochondrial gene expression by stimulated PBMC in hypoxia compared with normoxia.

Healthy donor PBMC were stimulated with anti-CD3 in normoxia (21%) or hypoxia (5%) for 24 h. mRNA expression of desired genes was measured via the RT² Profiler™ PCR Array. Results were normalized to 4 housekeeping genes; *ACTB* (β -actin), *B2M* (β -2 microglobulin), *HPRT1* (hypoxanthine phosphoribosyltransferase 1) and *RPLP0* (ribosomal protein, large P0). The table represents the fold regulation and fold change of the specified gene in hypoxia compared with normoxia (blue-significantly reduced, red-significantly increased).

4.2.6 HIF-1 α expression is increased in CD4⁺CD161⁺ T cells in hypoxia.

Having shown that HIF-1 α expression was increased in total CD4⁺ T cells in hypoxia, the effect of hypoxia on HIF-1 α expression in Th17 lineage cells was examined next. Healthy donor PBMC were stimulated as stated previously and stained with fluorochrome-conjugated antibodies specific for CD4, CD161 and HIF-1 α and analysed by flow cytometry. Results indicate a significant increase in HIF-1 α expression for CD161⁺ T cells (CD4⁺CD161⁺) in hypoxia compared with normoxia ($p < 0.05$) (Figure 4.7 A). Furthermore, Th17 lineage cells expressed higher HIF-1 α in hypoxia compared with CD4⁺CD161⁻ T cells ($p < 0.05$) (Figure 4.7 B). This suggests that Th17 lineage cells may have a relative survival advantage in hypoxic conditions.

4.2.7 The effect of hypoxia on T helper cell survival and expansion

Low oxygen levels have previously been shown to affect T cell subset differentiation. Furthermore in murine studies, T helper cell subsets and regulatory T cells displayed differential expression levels of HIF-1 α (Dang, Barbi et al. 2011, Shi, Wang et al. 2011). Following their differentiation from naïve CD4⁺ T cells in the presence of specific cytokines, Th17 cells revealed the highest HIF-1 α protein levels, followed by Th1 cells, with undetectable levels in Th2 and Treg cells (Shi, Wang et al. 2011). Additionally, a study has revealed an inhibition of Th17 cell differentiation and an enhancement of Foxp3 expression in HIF-1 α knockdown mice (Dang, Barbi et al. 2011). This study also demonstrated that HIF-1 α mitigates FOXP3 expression, by increasing Foxp3 degradation and thereby fostering Th17 lineage commitment. Thus the effect of hypoxia on specific human T helper cell subsets was examined next.

PBMC from healthy donors were stimulated in the presence of anti-CD3 in normoxia (21%) or hypoxia (5%). After 4 days, the cells were stimulated for 5 h with PMA, ionomycin and brefeldin-A and stained for analysis by flow cytometry. The frequency of CD4⁺ T cells expressing CD161 was significantly decreased in hypoxia by more than 50% ($p < 0.01$) (Figure 4.8). Additionally, CD4⁺ T cells expressing IL-17 were significantly decreased in hypoxia ($p < 0.05$) (Figure 4.9). Contrastingly, the examination of CD4⁺ T cells expressing IFN- γ demonstrated a significantly increased frequency in hypoxia compared with normoxia ($p < 0.05$) (Figure 4.10). These data suggests an inhibition of Th17 lineage cells and an increase in IFN- γ -producing T cells in hypoxia.

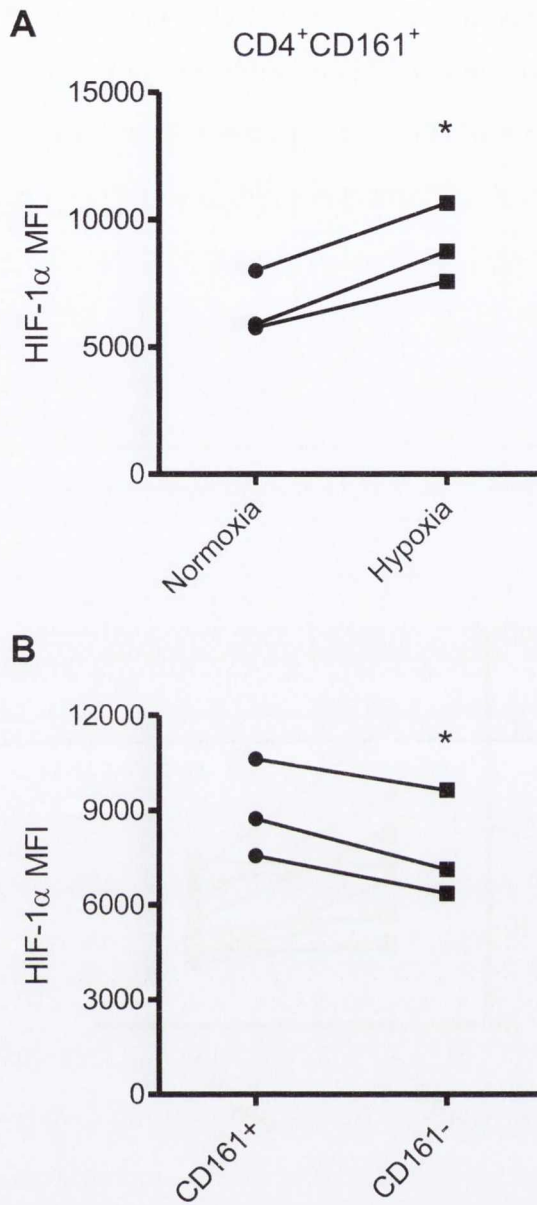


Figure 4.7 Increased HIF-1 α expression by CD4⁺CD161⁺ T cells in hypoxia

Healthy donor PBMC were stimulated in the presence of anti-CD3 in normoxic (21%) or hypoxic (5%) oxygen levels. After 4 days, cells were stained with fluorochrome-conjugated antibodies specific for CD4, CD161 and HIF-1 α . The cells were analysed by flow cytometry and the graphs show HIF-1 α MFI values for CD4⁺CD161⁺ T cells (A) in normoxia and hypoxia, and for CD4⁺CD161⁺ (CD161⁺) and CD4⁺CD161⁻ (CD161⁻) T cells in hypoxia (B) (n=3). Statistical differences in the mean between the groups were determined by a paired, two-tailed t test; *p<0.05.

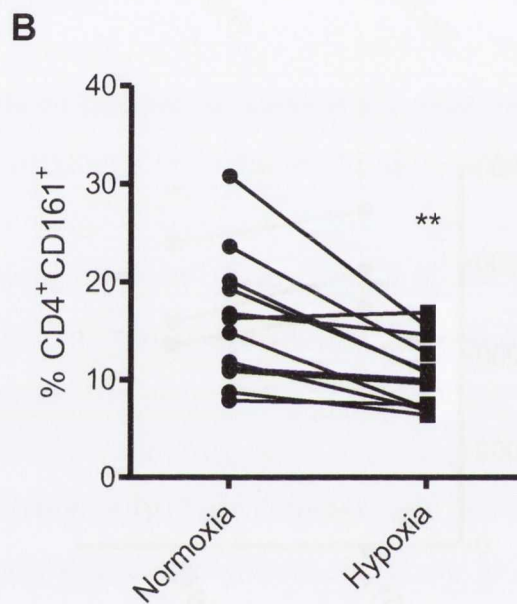
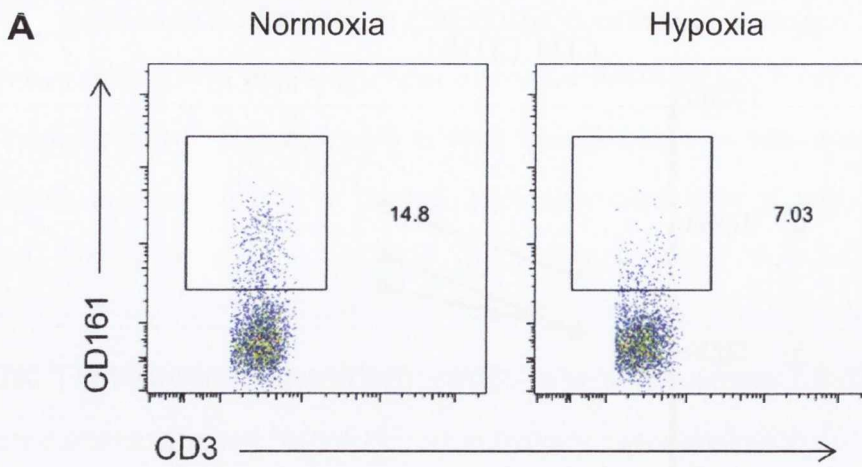


Figure 4.8 Decreased frequencies of Th17 lineage cells in hypoxia.

Healthy donor PBMC were stimulated in the presence of anti-CD3 in normoxic (21%) or hypoxic (5%) oxygen levels. After 4 days, cells were stimulated with PMA, ionomycin and brefeldin-A for 5 hr and stained with fluorochrome-conjugated antibodies specific for CD4, CD161 and intracellular cytokine IL-17. The cells were analysed by flow cytometry. Representative dot plots were gated on CD3⁺CD8⁻ (CD4) T cells and show CD161 vs CD3 staining (A) The graph shows the frequency of CD4⁺CD161⁺ T cells in normoxia and hypoxia (n=9, across multiple experiments). This Statistical differences in the mean between the groups were determined by a paired, two-tailed t test; **p<0.01.

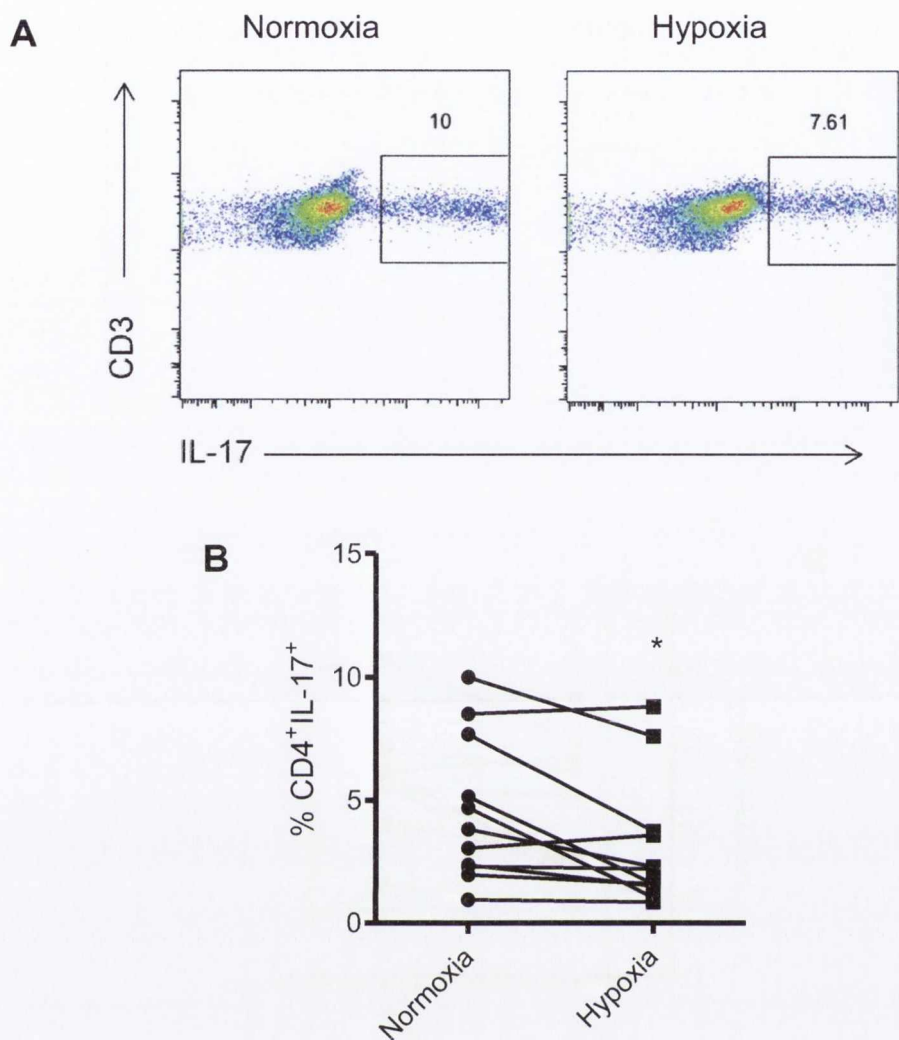


Figure 4.9 Decreased frequencies of CD4⁺ T cells producing IL-17 in hypoxia.

Healthy donor PBMC were stimulated in the presence of anti-CD3 in normoxic (21%) or hypoxic (5%) oxygen levels. After 4 days, cells were stimulated with PMA, ionomycin and brefeldin-A for 5 h and stained with fluorochrome-conjugated antibodies specific for CD3, CD8 and intracellular cytokine IL-17. The cells were analysed by flow cytometry. Representative dots plots were gated on CD3⁺CD8⁻ (CD4) T cells (A). The graph shows the frequency of CD4⁺IL-17⁺ T cells in normoxia and hypoxia (n=10 over multiple experiments). Statistical differences in the mean between the groups were determined by a paired, two-tailed t test; *p<0.05.

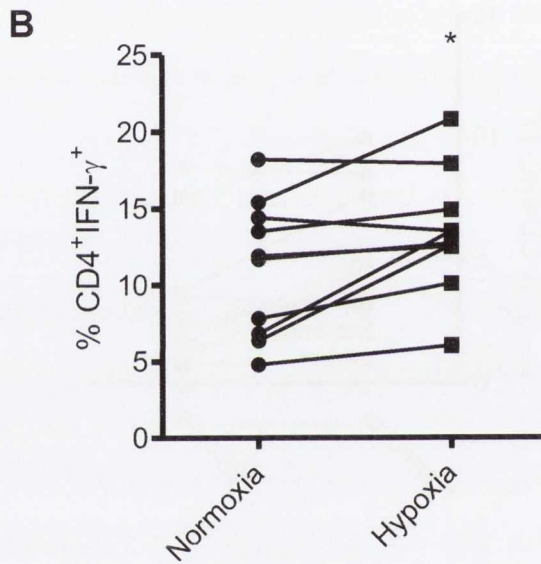
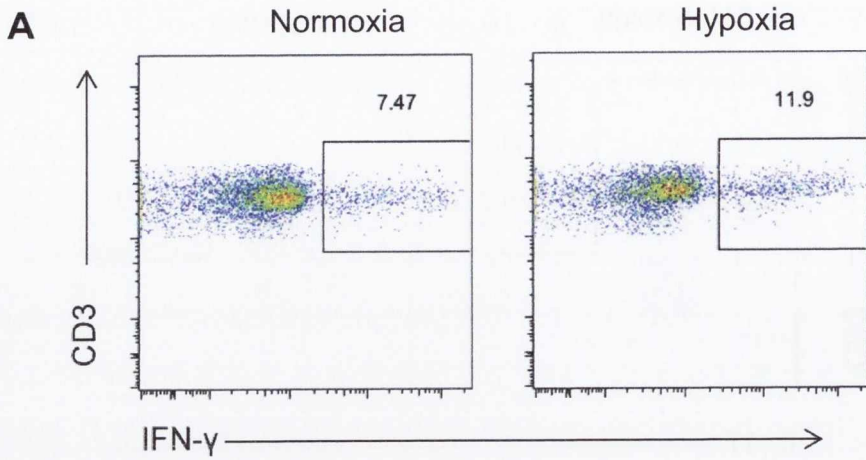


Figure 4.10 Increased frequencies of CD4⁺ T cells producing IFN- γ in hypoxia.

Healthy donor PBMC were stimulated in the presence of anti-CD3 in normoxic (21%) or hypoxic (5%) oxygen levels. After 4 days, cells were stimulated with PMA, ionomycin and brefeldin-A for 5 h and stained with fluorochrome-conjugated antibodies specific for CD4 and intracellular cytokine IFN- γ . The cells were analysed by flow cytometry. Representative dots plots were gated on CD3⁺CD8⁻ (CD4) T cells and show CD3 vs IFN- γ staining (A)The graph shows the frequency of CD4⁺IFN- γ ⁺ T cells in normoxia and hypoxia (n=9 across multiple experiments). Statistical differences in the mean between the groups were determined by a paired, two-tailed t test; *p<0.05.

4.2.8 The effect of hypoxia on exTh17 cells

As mentioned previously, exTh17 cells are derived from a Th17-precursor and express both IL-17 and IFN- γ cytokines before completely switching to primarily IFN- γ producers. The effect of hypoxia in vitro on exTh17 cells was yet to be investigated. PBMC from healthy donors were stimulated in the presence of anti-CD3 in normoxia (21%) or hypoxia (5%). After 4 days, the cells were stimulated for 5 h with PMA, ionomycin and brefeldin A, and stained for analysis by flow cytometry. The frequency of CD4⁺ T cells in transition from Th17 to exTh17 cells, expressing both IL-17 and IFN- γ , was decreased in hypoxic conditions ($p < 0.05$) (Figure 4.11). The examination of exTh17 cells having fully switched to chiefly produce IFN- γ (CD4⁺CD161⁺IFN- γ ⁺) also revealed a significant decrease in hypoxia compared with normoxia ($p < 0.01$) (Figure 4.12). This data suggests an inhibition of both transitioning exTh17 cells and fully switched exTh17 cells in hypoxic conditions.

4.2.9. CD4⁺IL-17⁺ cell frequencies are increased following cytokine stimulations in hypoxia

This study has revealed decreased IL-17⁺ T cell frequencies following the stimulation of PBMC within a hypoxic environment. Studies performed on human cell lines in hypoxia demonstrated an increase in IL-17⁺ cells following stimulation in the presence of Th17 skewing cytokines (Clambey, McNamee et al. 2012).

In order to examine the effect of Th17-skewing cytokines on IL-17 expressing CD4⁺ T cells, healthy donor PBMC were stimulated with anti-CD3 in normoxia (21%) and in the presence of indicated cytokines (IL-1 β , IL-6, IL-23 and TGF- β) in hypoxia (5%). After 4 days, the cells were stimulated for 5 h with PMA, ionomycin and brefeldin-A and stained for analysis by flow cytometry. The frequencies of CD4⁺IL-17⁺ T cells in hypoxia represented in the graph are normalized to those for normoxic levels. The frequency of CD4⁺ T cells expressing IL-17 was significantly increased in hypoxia following treatment with IL-1 β , IL-6 and IL-23 ($p < 0.01$) (Figure 4.13). The further addition of TGF- β did not increase the population of CD4⁺IL-17⁺ T cells compared with hypoxia. This result suggests that IL-17 producing CD4⁺ T cells are inhibited to a lesser extent in hypoxia following stimulation in the presence of appropriate Th17 skewing cytokine milieu.

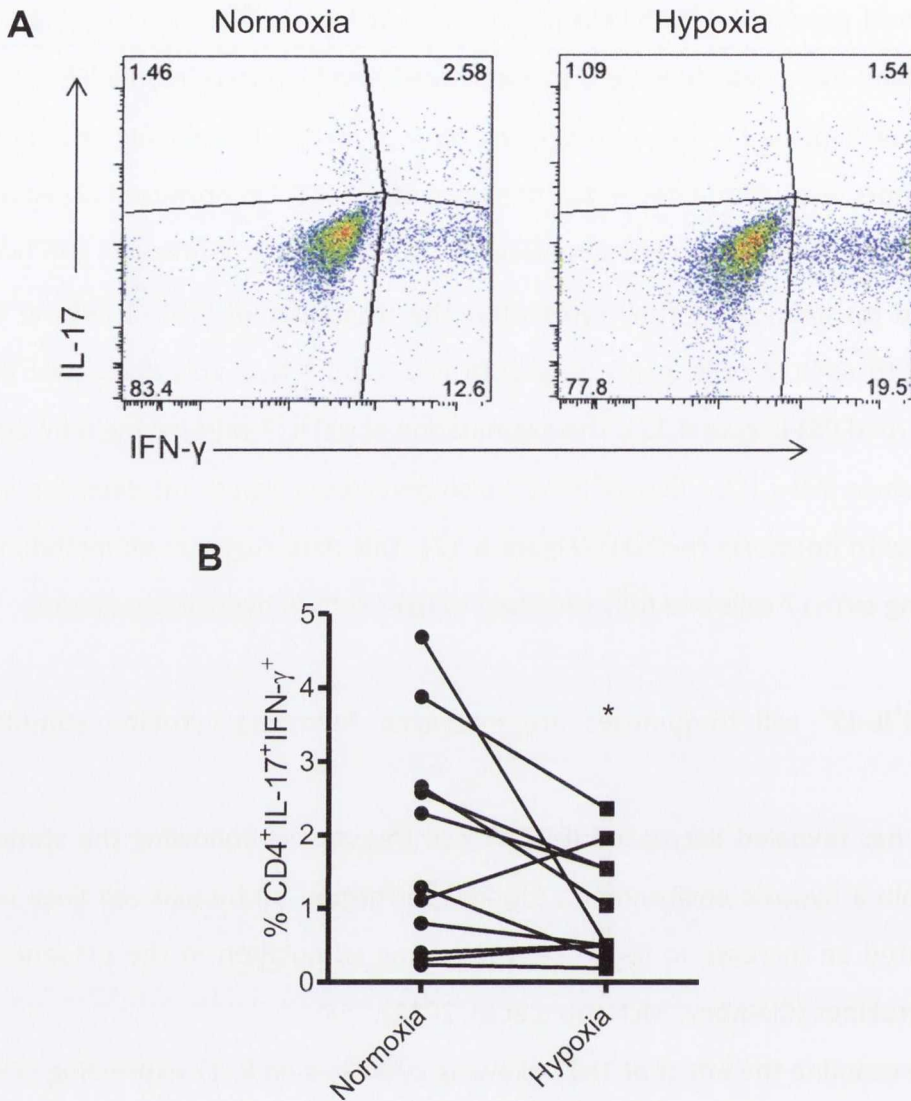


Figure 4.11 A decrease in the frequency of CD4⁺ T cells producing both IFN- γ and IL-17 in hypoxia.

Healthy donor PBMC were stimulated in the presence of anti-CD3 in normoxic (21%) or hypoxic (5%) oxygen levels. After 4 days, cells were stimulated with PMA, ionomycin and brefeldin-A for 5 h and stained with fluorochrome-conjugated antibodies specific for CD4 and intracellular cytokines IL-17 and IFN- γ . The cells were analysed by flow cytometry. Representative dot plots were gated on CD3⁺CD8⁻ (CD4) T cells and show IFN- γ vs IL-17 staining (A). The graph shows the frequency of CD4⁺IL-17⁺IFN- γ ⁺ T cells in normoxia and hypoxia (n=11 across multiple experiments). Statistical differences in the mean between the groups were determined by a paired, two-tailed t test; *p<0.05.

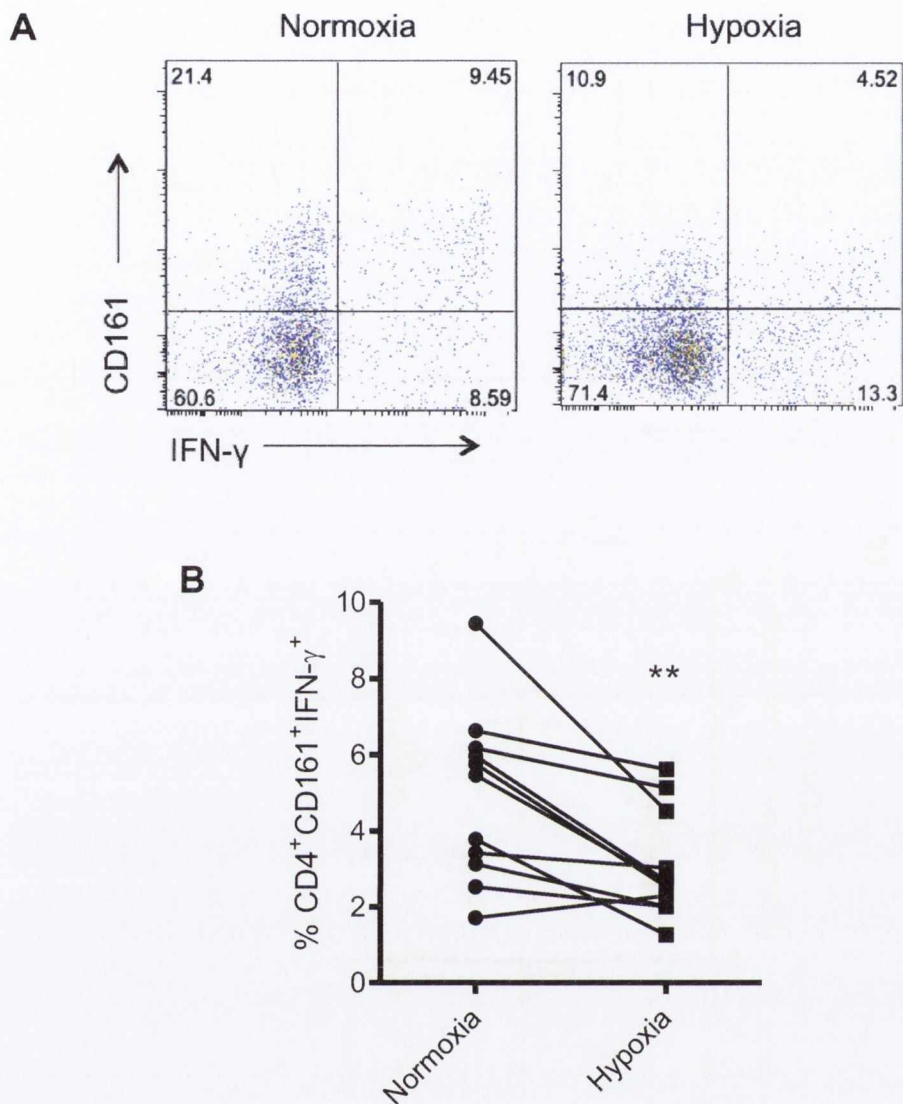


Figure 4.12 The effect of hypoxia on CD4⁺CD161⁺IFN- γ ⁺ exTh17 cells.

Healthy donor PBMC were stimulated in the presence of anti-CD3 in normoxic (21%) or hypoxic (5%) oxygen levels. After 4 days, cells were stimulated with PMA, ionomycin and brefeldin-A for 5 h and stained with fluorochrome-conjugated antibodies specific for CD4 and CD161, and intracellular cytokine IFN- γ . The cells were analysed by flow cytometry. Representative dots plots were gated on CD3⁺CD8⁻ (CD4) T cells and show CD161 vs IFN- γ staining (A). The graph shows the frequency of CD4⁺CD161⁺IFN- γ ⁺ T cells in normoxia and hypoxia (B) (n=11 across multiple experiments). Statistical differences in the mean between the groups were determined by a paired, two-tailed t test; **p<0.01

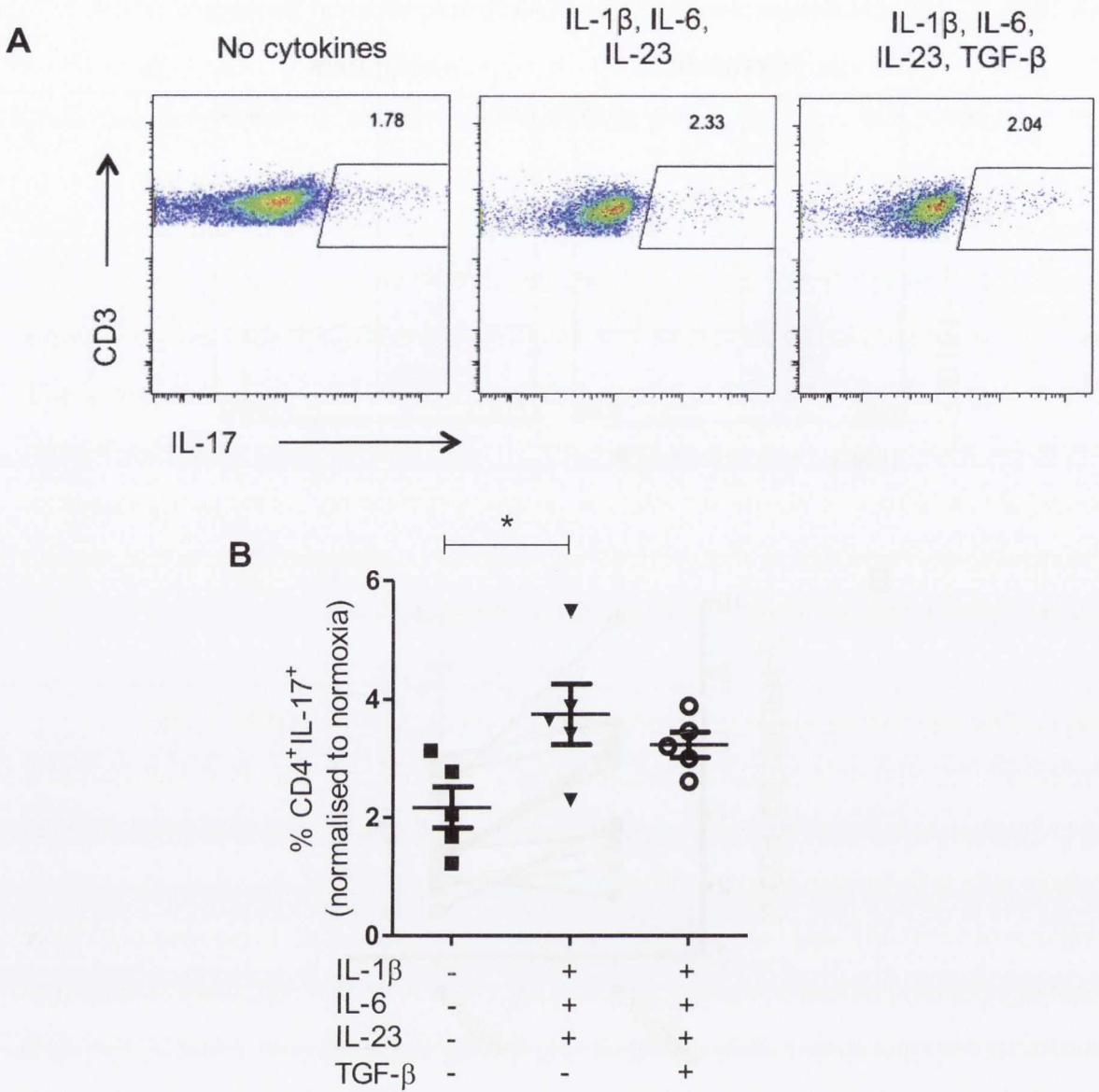


Figure 4.13 Stimulating PBMC in the presence of Th17-skewing cytokines in hypoxia increases the frequency of CD4⁺IL-17⁺ T cells.

Healthy donor PBMC were stimulated with anti-CD3, in the presence of recombinant cytokines IL-1 β , IL-6, IL-23 and TGF- β in normoxic (21%) or hypoxic (5%) oxygen levels. After 4 days, cells were stimulated with PMA, ionomycin and brefeldin-A for 5 hr and stained with fluorochrome-conjugated antibodies specific for CD3, CD8 and IL-17. The cells were analysed by flow cytometry. Representative dot plots were gated on CD3⁺CD8⁻ (CD4) T cells and show CD3 vs IL-17 staining (A). The graph shows the frequencies of CD4⁺IL-17⁺ T cells in hypoxia stimulated in the presence or absence of indicated cytokines, normalised to those for normoxia (n=5 experiments) (B). Statistical analysis was determined by one-way ANOVA with Tukey's Multiple Comparison test; *p<0.05.

4.2.10. IL-17, IFN- γ and IL-10 production by PBMC is decreased in hypoxia

Next, the cumulative production of IL-17A, IFN- γ and IL-10 in supernatants from PBMC cultured in normoxia and hypoxia was assessed by enzyme-linked immunosorbance assay (ELISA) in order to provide an additional readout of cytokine production.

Healthy donor PBMC were stimulated in the presence of anti-CD3 in normoxic (21%) or hypoxic (5%) oxygen levels in a hypoxia chamber. Supernatants were removed after 4 days of culture and analysed by ELISA for cytokines. The results indicate a trend towards a decrease in IL-17A, IFN- γ and IL-10 production by PBMC in hypoxia compared with normoxia (Figure 4.14 A, B and C respectively). It is important to note that hypoxic conditions resulted in a significant decrease in cell proliferation, which may account for the decreased production of IL-17A, IFN- γ and IL-10. It is important to note that hypoxia did not result in the decreased production of all cytokines.

4.2.11. The effect of hypoxia on the expression of GLUT1 in CD4⁺CD161⁺ T cells

Previous data, displayed in chapter 3, demonstrates an increased expression of GLUT1 for Th17 lineage cells in normoxia. Next, the expression of GLUT1 was examined for Th17 lineage cells in an in vitro hypoxia setting.

Healthy donor PBMC were stimulated in the presence of anti-CD3 in normoxic (21%) or hypoxic (5%) oxygen levels in a hypoxia chamber. After 48 h, the cells were stained with fluorochrome-conjugated antibodies specific for CD4, CD161 and GLUT1. The data revealed no significant change in GLUT1 expression for Th17 lineage cells in hypoxia compared with normoxia (n=5) (Figure 4.15 A). However, comparing T cells in hypoxia, CD4⁺CD161⁺ T cells maintained an increased GLUT1 expression compared to CD4⁺CD161⁻ T cells (Figure 4.15 B). These data suggest that the capacity for the Th17 lineage to take up glucose is not increased by hypoxia, although in both hypoxia and normoxia, Th17 lineage cells do have a relatively increased capacity for glucose uptake relative to CD161⁻ Th cells.

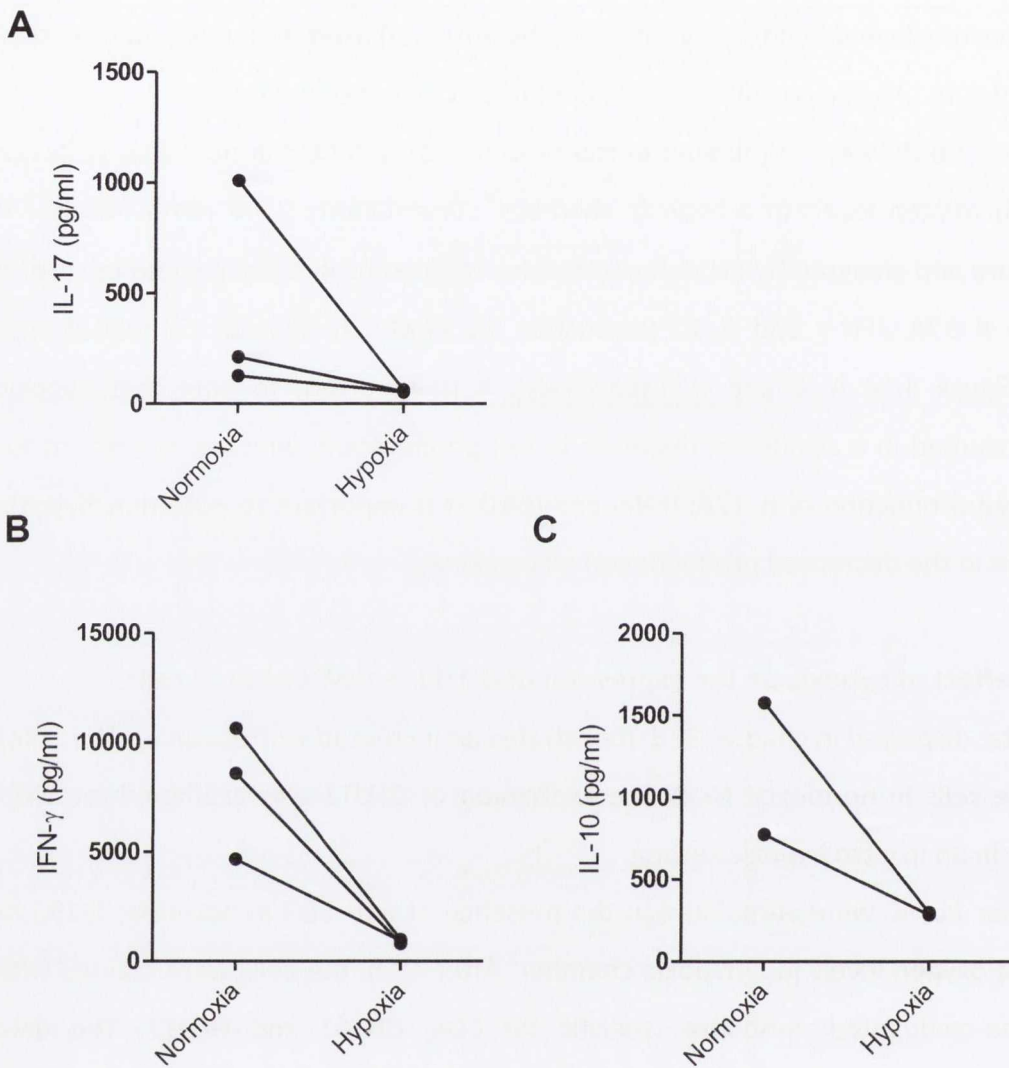


Figure 4.14 The effect of hypoxia on IL-17A, IFN- γ and IL-10 production.

Healthy donor PBMC were stimulated with anti-CD3 in normoxic (21%) or hypoxic (5%) oxygen levels. After 4 days, supernatants were removed and analysed by ELISA for IL-17A (n=3) (A), IFN- γ (n=3) (B), and IL-10 (C) concentrations (n=2).

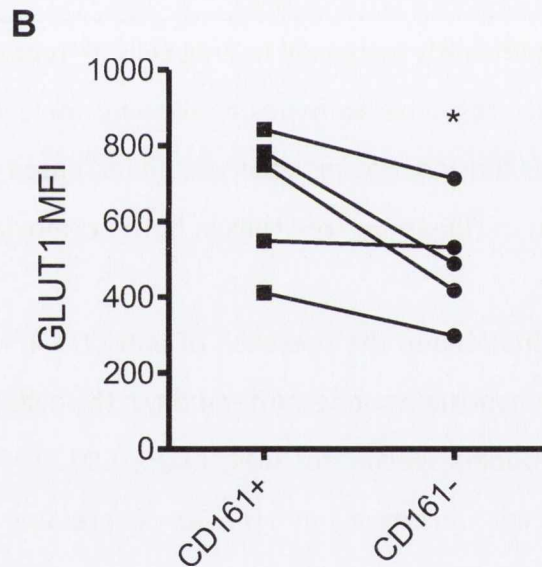
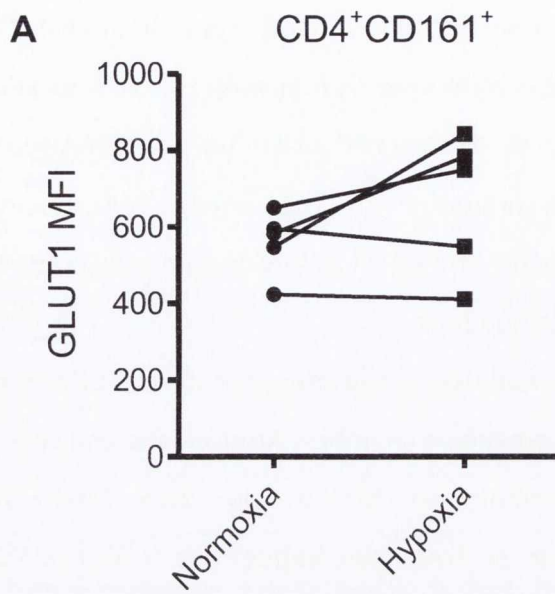


Figure 4.15 The expression of GLUT1 by $CD4^+CD161^+$ T cells in hypoxia compared with normoxia

Healthy donor PBMC were stimulated with anti-CD3 in normoxic (21%) or hypoxic (5%) oxygen levels. After 48 h stimulation, cells were stained with fluorochrome-conjugated antibodies specific for CD4, CD161 and GLUT1 and analysed by flow cytometry. The graphs show GLUT1 MFI values for $CD4^+CD161^+$ T cells in normoxia and hypoxia (A) and for $CD4^+CD161^+$ ($CD161^+$) and $CD4^+CD161^-$ ($CD161^-$) T cells in hypoxia (B). (n=5). Statistical differences in the mean between the groups were determined by a paired, two-tailed t test; *p<0.0.

4.2.12 Treg cell frequencies are increased in hypoxia.

Previous murine studies have revealed a decreased expression of HIF-1 α by Treg cells and a subsequent increase in Foxp3 mRNA levels following HIF-1 α knockdown (Shi, Wang et al. 2011). Previous data in this study revealed a significantly decreased expression of HIF-1 α for Treg cells in normoxia compared with Th17 lineage cells. Having investigated the effect of hypoxia on T helper cells, the effect of low oxygen tension on the expansion and survival of Treg cells was examined next.

Healthy donor PBMC were stimulated in the presence of anti-CD3 in normoxic (21%) or hypoxic (5%) oxygen levels in a hypoxia chamber. After 4 days, the cells were stained with fluorochrome-conjugated antibodies specific for CD4, CD25, CD127 and Foxp3. Results revealed a significant increase in Treg cells frequencies (CD4⁺CD25⁺CD127^{Lo}Foxp3⁺) in hypoxic oxygen levels compared with normoxia (p<0.01) (Figure 4.16).

4.2.13 HIF-1 α expression is significantly increased in Treg cells in hypoxia

HIF-1 α orchestrates the cellular response to hypoxia, allowing for cellular survival and proliferation during low oxygen tension. Having observed an increased frequency of Treg cells in hypoxia, the expression of HIF-1 α by Treg cells in both normoxia and hypoxia was examined next.

Healthy donor PBMC were stimulated in the presence of anti-CD3 in normoxic (21%) or hypoxic (5%) oxygen levels in a hypoxia chamber. After 4 days, the cells were stained with fluorochrome-conjugated antibodies specific for CD4, CD25, CD127, Foxp3 and HIF-1 α . Results revealed a significant increase in HIF-1 α expression by Treg cells (CD4⁺CD25⁺CD127^{Lo}Foxp3⁺) in hypoxic oxygen levels compared with normoxia (p<0.01) (Figure 4.17 A). These data could provide a mechanism whereby hypoxia drives the survival, expansion or induction of Treg cells in vitro.

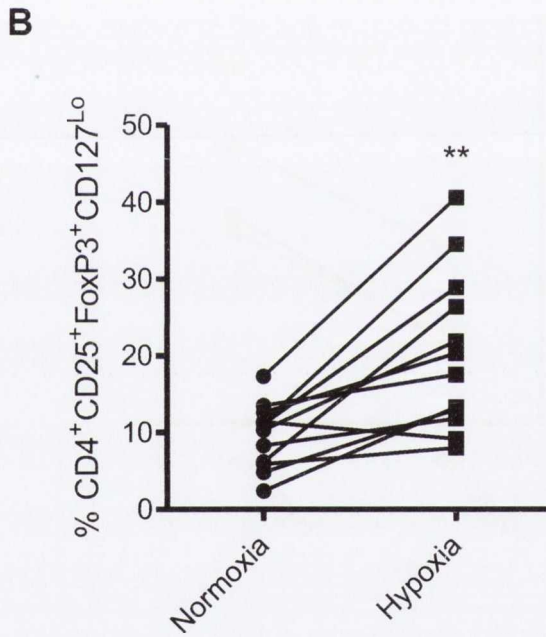
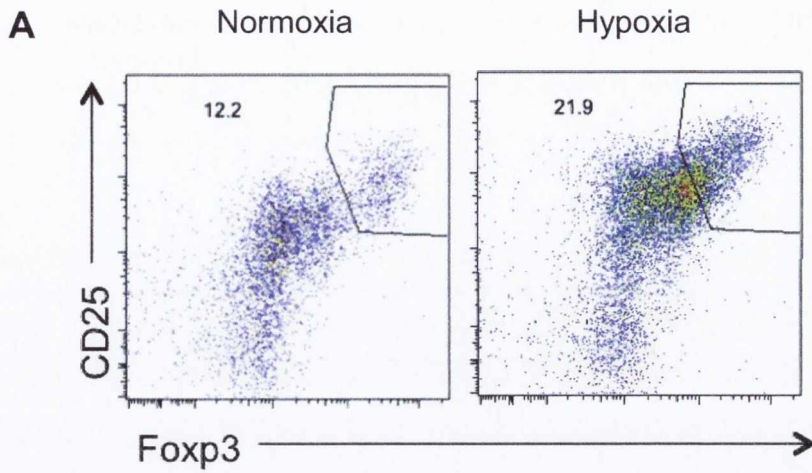


Figure 4.16 Increased frequencies of Treg cells in hypoxia.

Healthy donor PBMC were stimulated in the presence of anti-CD3 in normoxic (21%) or hypoxic (5%) oxygen levels. After 4 days cells were stained with fluorochrome-conjugated antibodies specific for CD4, CD25, CD127 and Foxp3. The cells were analysed by flow cytometry. Representative dots plots were gated on CD4⁺ T cells and show CD25 vs Foxp3 staining (A). The graph shows the frequency of CD4⁺CD25⁺CD127^{Lo}Foxp3⁺ T cells in normoxia and hypoxia (n=11 across multiple experiments). Statistical differences in the mean between the groups were determined by a paired, two-tailed t test; **p<0.01.

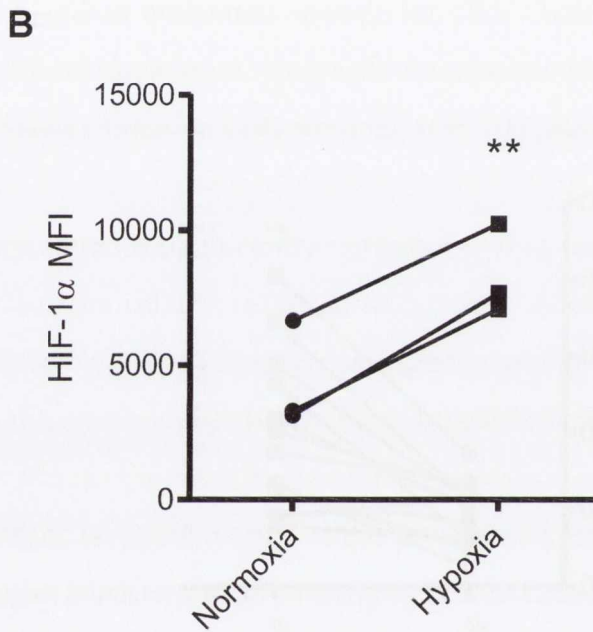
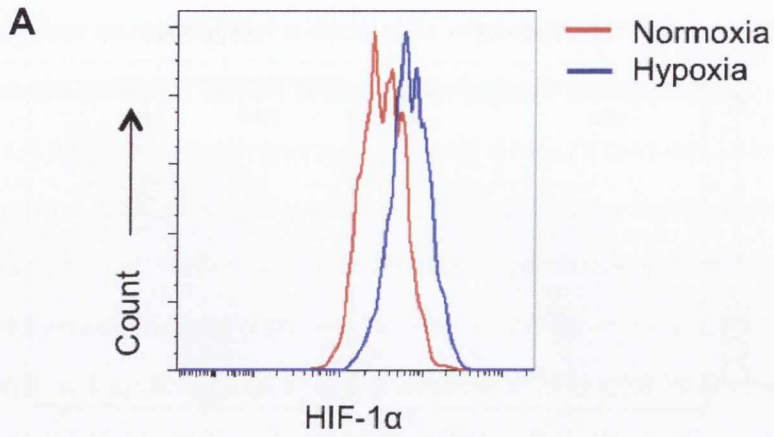


Figure 4.17 The differential expression of HIF-1α by Treg cells in hypoxia compared with normoxia.

Healthy donor PBMC were stimulated in the presence of anti-CD3 in normoxic (21%) or hypoxic (5%) oxygen levels. After 48 h stimulation, cells were stained with fluorochrome-conjugated antibodies specific for CD4, CD25, CD127, Foxp3 and HIF-1A. The cells were analysed by flow cytometry. Representative histograms of HIF-1α staining were gated on CD4⁺CD25⁺CD127^{lo}FoxP3⁺ T cells (A). The graph shows HIF-1α MFI values for Treg (CD4⁺CD25⁺CD127^{lo}Foxp3⁺) cells in normoxia and hypoxia (n=3) (B). Statistical differences in the mean between the groups were determined by a paired, two-tailed t test; **p<0.01.

4.2.14 GLUT1 expression is significantly increased in Treg cells in hypoxia

Having demonstrated a trend towards an increase in GLUT1 expression in hypoxia, the expression of the glucose transporter was examined for Treg cells and compared with that of CD4⁺CD161⁺ and CD4⁺CD161⁻ T cells in hypoxia vs normoxia.

Healthy donor PBMC were stimulated in the presence of anti-CD3 in normoxic (21%) or hypoxic (5%) oxygen levels in a hypoxia chamber. After 48 h, the cells were stained with fluorochrome-conjugated antibodies specific for CD4, CD25, CD127, CD161, Foxp3 and GLUT1. Initially examining Treg cells (CD4⁺CD25⁺CD127^{Lo}Foxp3⁺), the data shows a significant increase in GLUT1 MFI values for Treg cells in hypoxia compared with normoxia ($p < 0.05$) (Figure 4.18 A). Additionally, Treg cells were compared to CD161⁺ (CD4⁺CD161⁺) and CD161⁻ (CD4⁺CD161⁻) T cells, displaying a significant increase in GLUT1 MFI values for Treg cells compared with CD161⁻ T cells ($p < 0.01$) and a trend towards an increase compared with CD161⁺ T cells (Figure 4.18 B). In summary GLUT1 expression was increased in Treg cells in hypoxia and suggests that Treg cells might increase glucose uptake and glycolysis in hypoxia.

4.2.15. TGF- β production is significantly increased in hypoxia

TGF- β is widely known as a suppressive protein, shown previously to inhibit the proliferation of human B and T cells (Kehrl, Roberts et al. 1986, Kehrl, Wakefield et al. 1986). One mechanism by which TGF- β induces suppression of immune cells is through promotion of Treg cell generation. TGF- β was demonstrated to induce the expression of Foxp3 by CD4⁺CD25⁻ human T cells (Fantini, Becker et al. 2004). TGF- β is synthesized in an inactive form, pre-pro-TGF- β , and becomes active when dissociated from latency associated protein. The production of the active form of TGF- β by total PBMC in normoxia and hypoxia was investigated next.

Healthy donor PBMC were stimulated in the presence of anti-CD3 in normoxic (21%) or hypoxic (5%) oxygen levels in a hypoxia chamber. Supernatants were removed after 4 days of culture and TGF- β was analysed by ELISA. The results indicate a significant increase in the production of the active form of TGF- β by PBMC in hypoxia compared with normoxia ($p < 0.05$) (Figure 4.19). These data suggested a possible role for TGF- β in the induction or expansion of Treg cells.

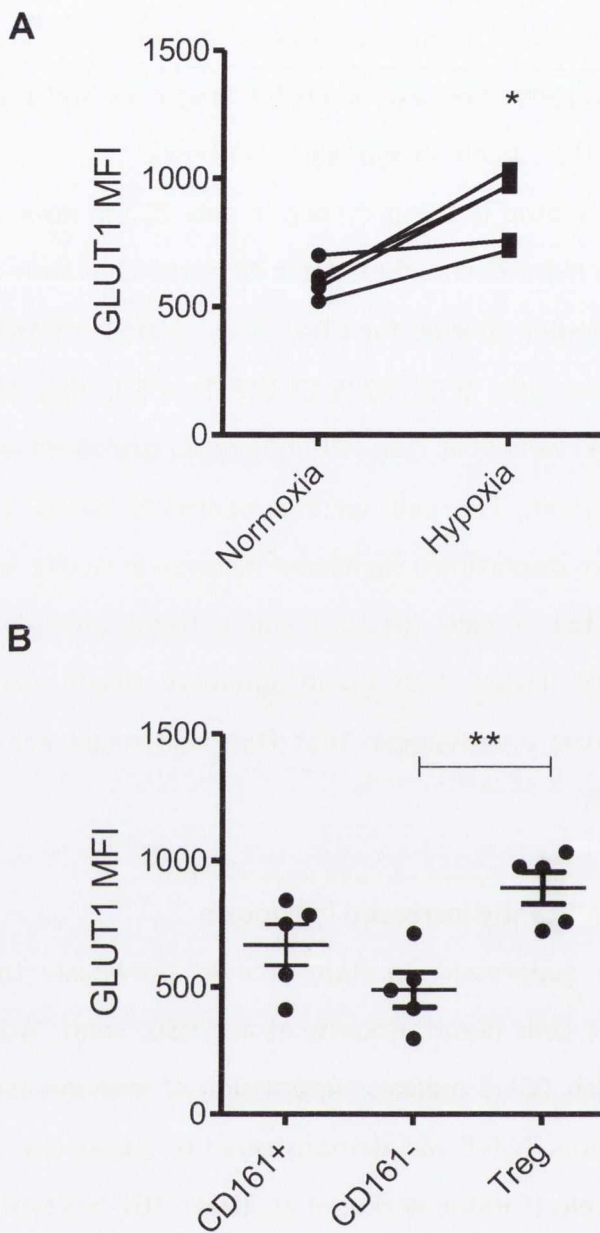


Figure 4.18 The differential expression of GLUT1 by CD4⁺ T cell subsets in hypoxia compared with normoxia.

Healthy donor PBMC were stimulated with anti-CD3 in normoxic (21%) or hypoxic (5%) oxygen levels. After 48 h stimulation, cells were stained with fluorochrome-conjugated antibodies specific for CD4, CD161, CD25, CD127, Foxp3 and GLUT1 and analysed by flow cytometry. The graphs show GLUT1 staining for CD4⁺CD25⁺CD127^{Lo}Foxp3⁺ T cells in normoxia and hypoxia (A) and for CD161⁺ (CD4⁺CD161⁺), CD161⁻ (CD4⁺CD161⁻) and Treg cells (CD4⁺CD25⁺CD127^{Lo}Foxp3⁺) in hypoxia (B) (n=5). Statistical differences in the mean between the groups were determined by a paired, two-tailed t test (A) and a one-way ANOVA (B); *p<0.05, **p<0.01.

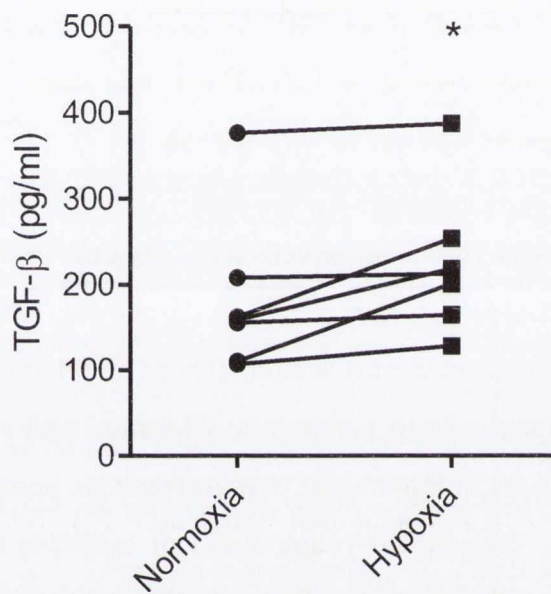


Figure 4.19 Increased active TGF- β production by PBMC in hypoxia.

Healthy donor PBMC were stimulated with anti-CD3 in normoxic (21%) or hypoxic (5%) oxygen levels. After 4 days, supernatants were removed and analysed by ELISA for TGF- β (active form) concentrations (n=7). Statistical differences in the mean between the groups were determined by a paired, two-tailed t test; *p<0.05.

4.2.16. The effect of TGF- β receptor inhibition on Treg cell generation in hypoxia.

Having shown that TGF- β was increased in PBMC cultures during hypoxia, and given the ability of TGF- β to promote Tregs, the effect of blocking TGF- β on Treg cells in hypoxia was examined next.

PBMC from healthy donors were stimulated with anti-CD3 in normoxia (21%) or in the presence of a TGF- β receptor 1 inhibitor (iTGF- β R1) or with recombinant TGF- β in hypoxic (5%) oxygen levels. After 4 days, cells were stained for the analysis of Treg cell frequencies by flow cytometry and results were normalised to normoxia. The results revealed no significant change in Treg (CD4⁺CD25⁺CD127^{Lo}Foxp3⁺) cell frequencies following TGF- β receptor inhibition (Figure 4.20). These data suggested that the increase in Treg cells observed in hypoxia was not TGF- β dependent.

4.2.17. Increased frequency of Th17 lineage cells and Treg cells in the inflamed synovial joint of RA patients.

Metabolites and biosynthetic resources are limited at sites of inflammation. This results in competition amongst immune cells to maintain proliferation and survival. Additionally, increased inflammation results in diminished oxygen levels as immune cells continually infiltrate the inflamed site. Oxygen is a requirement of oxidative phosphorylation and mitochondrial metabolism, without which cells must utilise or 'switch' towards glycolysis for their metabolic demands.

The synovial joint of RA patients represents a highly inflamed site, and thus provided an opportunity to examine the *in vivo* effects of inflammation on the behaviour of T cell subsets. The frequency of T cell subsets within the joint synovial fluid was compared with that found within the blood of RA patients, and the effect of inflammation on T cell metabolism was investigated.

In order to examine T cell subsets, matched PBMC and synovial fluid mononuclear cells (SFMC) were isolated from RA patients with active disease. RA patients consisted of two males and three females, with an average age of 54 and an average DAS28 of 4.19. Additionally, one patient was receiving enbrel and methotrexate treatment at the time of blood sampling. The cells were stained *ex vivo* with fluorochrome-conjugated antibodies specific for the surface markers CD4, CD161 and CD25, and the transcription factor Foxp3. The cells were analysed by flow cytometry. The frequency of CD4⁺CD161⁺ Th17 lineage

cells ($p < 0.001$) (A and B) and $CD4^+CD25^+Foxp3^+$ Treg cells ($p < 0.01$) (C and D) was significantly increased in SFMC compared with PBMC (Figure 4.21).

The expression of HIF-1 α was analysed next as a correlate of hypoxia in vivo. Matched PBMC and SFMC were stained ex vivo with fluorochrome-conjugated antibodies specific for the surface markers CD4, CD25, CD127, CD161, Foxp3 and HIF-1 α , and analysed by flow cytometry. The results demonstrated an increased expression of HIF-1 α by $CD4^+CD161^+$ T cells compared with $CD4^+CD161^-$ T cells in SFMC ($p < 0.05$) (Figure 4.22 C and D). Additionally, examining HIF-1 α expression by $CD161^+$ ($CD4^+CD161^+$) (A) and Treg cells ($CD4^+CD25^+Foxp3^+$) (B) for PBMC and SFMC of RA patients ex vivo, there is a trend towards an increase in HIF-1 α expression for both populations in SFMC compared with PBMC (Figure 4.23).

Having demonstrated that both Th17 and Treg cells are enhanced in the inflamed RA joint compared with peripheral blood, this data suggests a possible role for HIF-1 α in the expansion of these subsets in hypoxic environments in vivo.

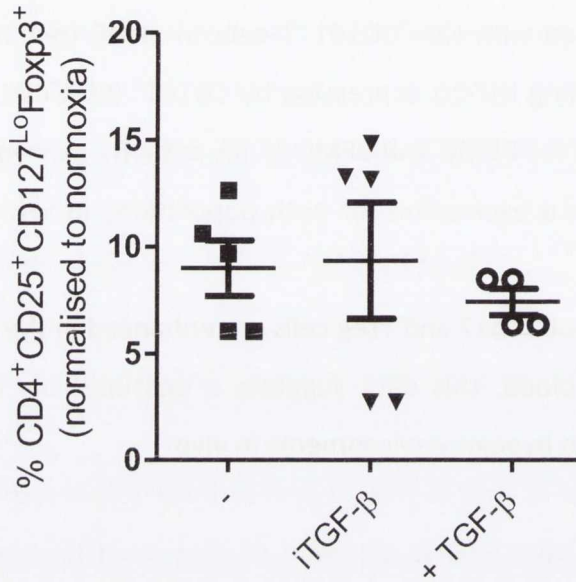


Figure 4.20 The effect of TGF-β1 receptor inhibition on Treg cell frequencies in hypoxia.

PBMC from healthy donors were stimulated with anti-CD3, in the presence of TGF-β receptor 1 inhibitor (iTGF-βR1) or with recombinant TGF-β in normoxic (21%) or hypoxic (5%) oxygen levels. After 4 days, cells were stained with fluorochrome-conjugated antibodies specific for CD4, CD25, CD127 and Foxp3. The cells were analysed by flow cytometry. The graph shows the frequency of Treg (CD4⁺CD25⁺CD127^{Lo}Foxp3⁺) cells in hypoxia in the presence of iTGF-βR1 or TGF-β; normalised to that of normoxia (n=5).

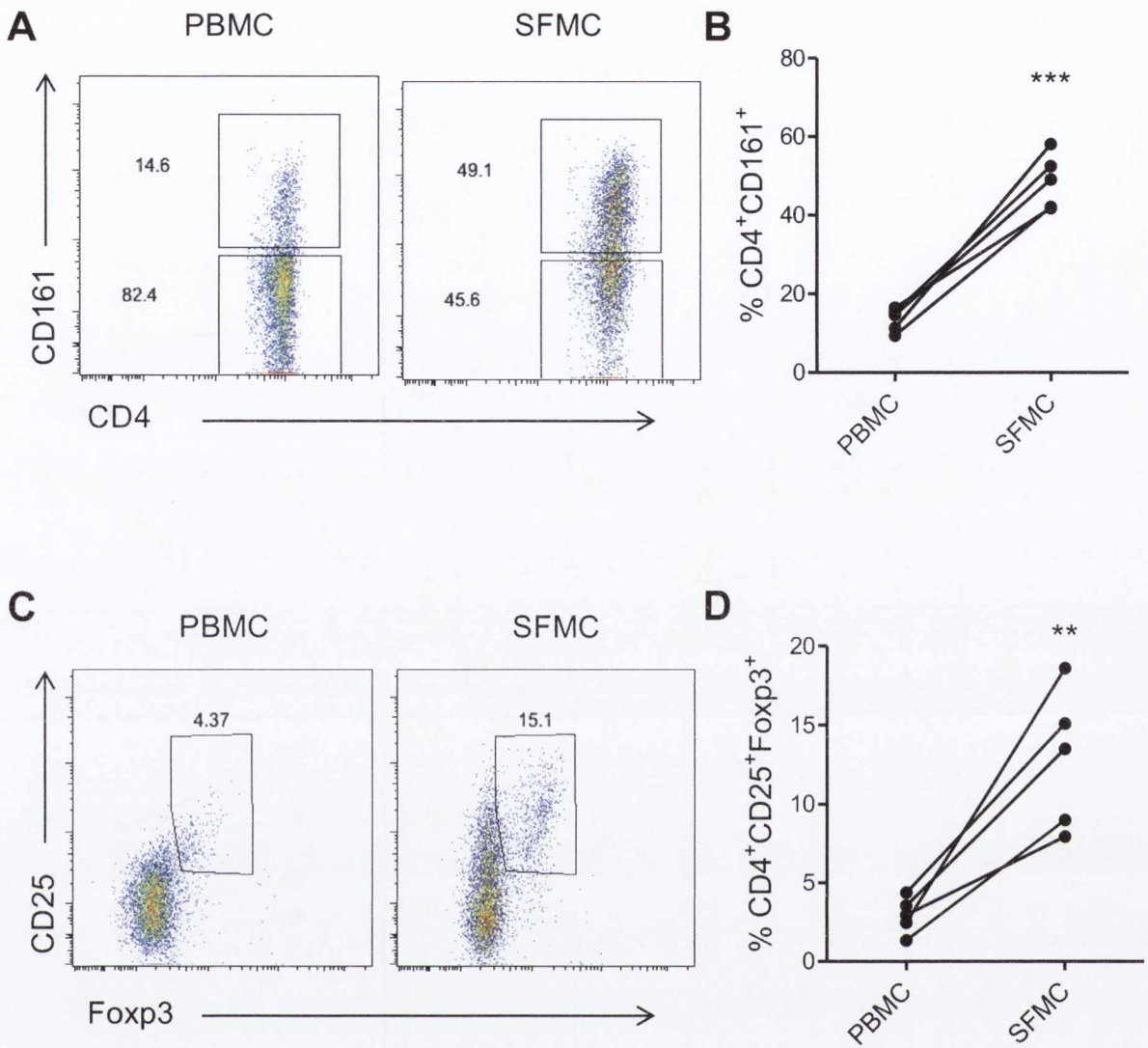


Figure 4.21. Increased frequency of CD4⁺CD161⁺ T cells and Treg cells in RA synovial fluid compared with matched PBMC.

Matched PBMC and SFMC were isolated from RA patients with active disease. Cells were stained with fluorochrome-conjugated antibodies specific for the surface proteins CD4, CD161 and CD25, and the intranuclear transcription factor Foxp3. The cells were analysed by flow cytometry, and gated on CD4⁺ T cells. The frequency of CD4⁺CD161⁺ T cells in RA PBMC and SFMC is shown in the representative dot plots (A) or graph (n=5) (B). The frequency of CD4⁺Foxp3⁺CD25⁺ Treg cells in RA PBMC vs SFMC is shown in representative dot plots (C) or graph (n=5) (D). Statistical differences were determined by paired t-tests with two-tailed p-values; **p<0.01, ***p<0.001.

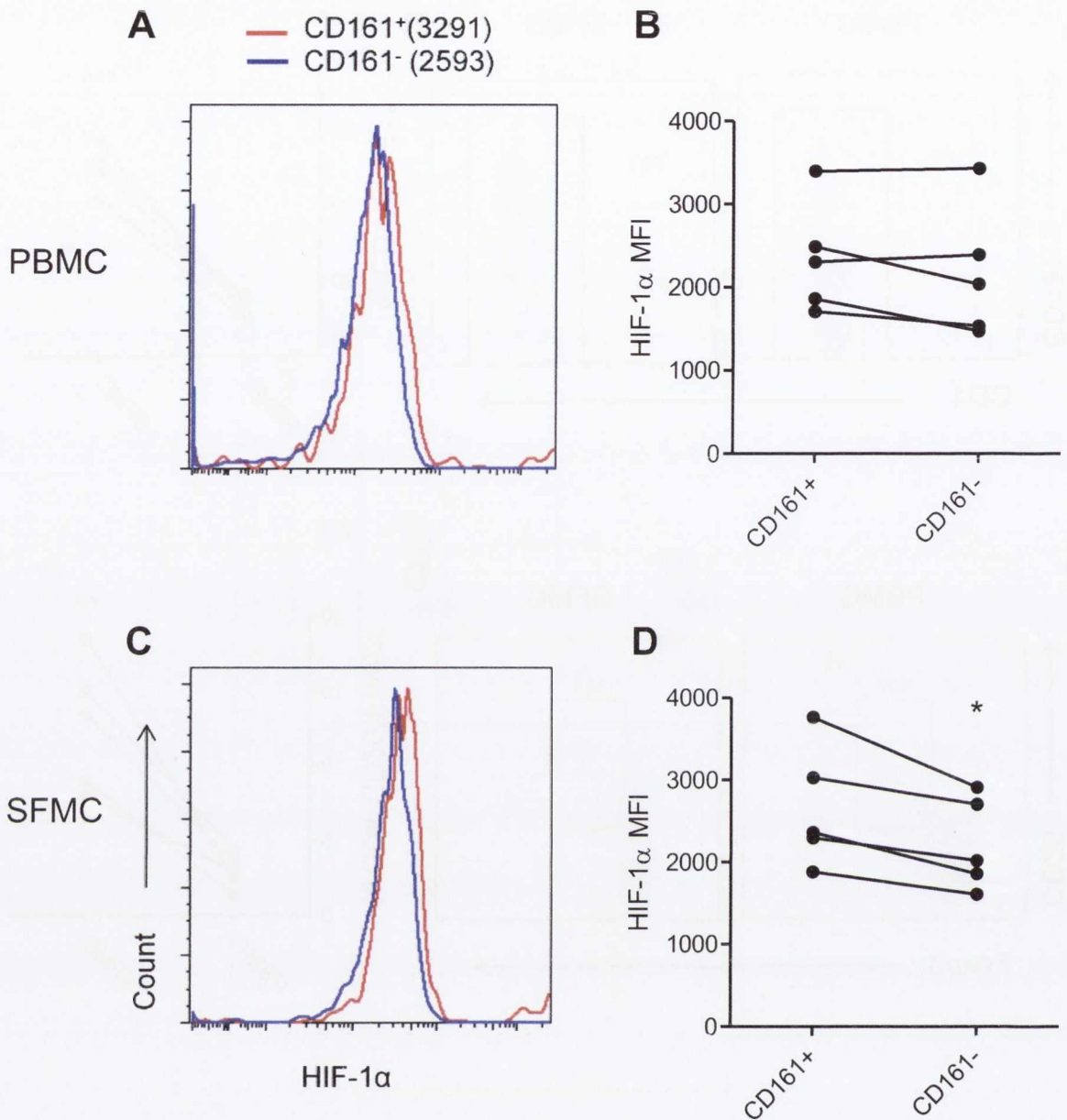


Figure 4.22 HIF-1 α expression in CD4⁺CD161⁺ and CD4⁺CD161⁻ cells in PBMC and SFMC from RA patients.

Matched PBMC and SFMC were isolated from RA patients with active disease. Cells were stained with fluorochrome-conjugated antibodies specific for CD4, CD161, and the transcription factor HIF-1 α . Cells were analysed by flow cytometry. Representative histograms display HIF-1 α MFI values for CD161⁺ (CD4⁺CD161⁺) and CD161⁻ (CD4⁺CD161⁻) T cells in RA PBMC (A) and SFMC (C) (n=5). The graphs represent HIF-1 α MFI values for CD161⁺ (CD4⁺CD161⁺) and CD161⁻ (CD4⁺CD161⁻) T cells in RA PBMC (B) and SFMC (D) (n=5). Statistical differences in the mean between the groups were determined by a paired, two-tailed t test; *p<0.05.

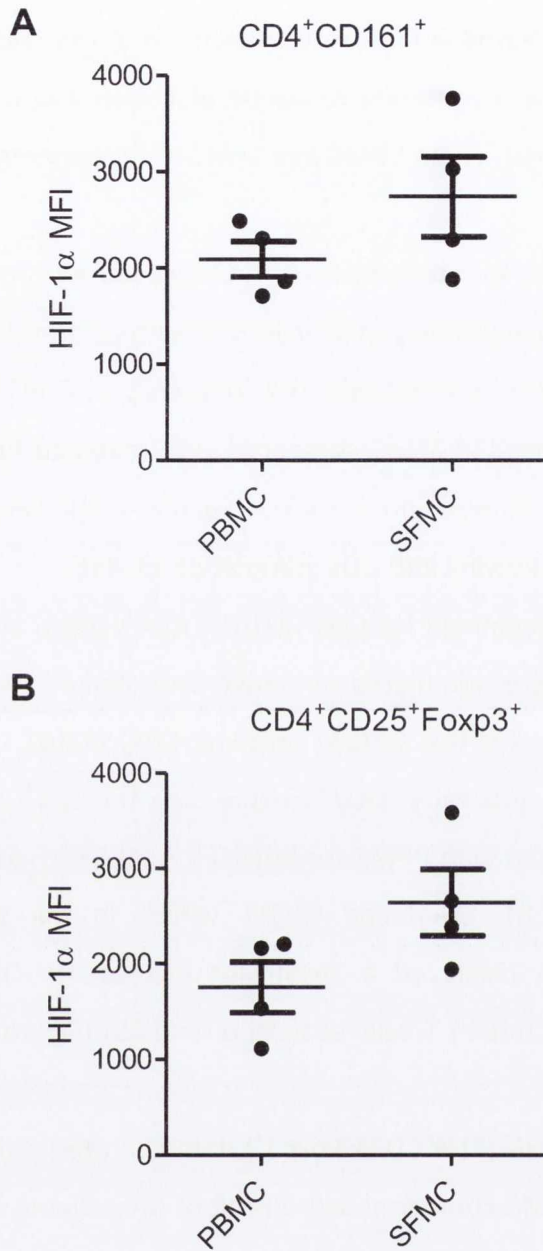


Figure 4.23 The expression of HIF-1 α by Th17 and Treg cells within PBMC and SFMC of RA patients.

Matched PBMC and SFMC were isolated from RA patients with active disease. Cells were stained with fluorochrome-conjugated antibodies specific for CD4, CD161, CD25, and the transcription factors Foxp3 and HIF-1 α . Cells were analysed by flow cytometry and results represent HIF-1 α MFI values for CD4⁺CD161⁺ (A) and Treg (CD4⁺CD25⁺Foxp3⁺) T cells (B) (n=4).

4.2.18. Increased expression of GLUT1 in CD4⁺ T cells from the synovial joints of RA patients, accompanied by increased GLUT1 expression in Th17 and Treg cells.

In order to further investigate the metabolic status of T cells from the inflamed and hypoxic RA joint, GLUT1 was analysed in PBMC and SFMC of RA patients, both ex vivo and in vitro.

Matched PBMC and SFMC were stimulated with anti-CD3 (1 µg/ml) for 0 or 48 h, stained with fluorochrome-conjugated antibodies specific for the surface proteins CD4 and GLUT1 and analysed by flow cytometry. Interestingly, the frequency of CD4⁺ T cells expressing GLUT1 was significantly increased in SFMC compared with matched PBMC both ex vivo ($p < 0.05$) and following 48 h stimulation ($p < 0.01$) (Figure 4.24). SFMC retained their increased GLUT1 expression following anti-CD3 stimulation ex vivo.

Next, GLUT1 expression was examined for CD4⁺CD161⁺, CD4⁺CD161⁻ and Treg cells both ex vivo and in vitro. Cells were stimulated as above and stained with fluorochrome-conjugated antibodies specific for the surface proteins CD4, CD161, CD25, Foxp3 and GLUT1 and analysed by flow cytometry. GLUT1 expression for CD4⁺CD161⁺ T cells was increased in the SFMC compared with PBMC for both 0 h ($p < 0.05$) (Figure 4.25 A) and 48 h time points (Figure 4.25 B). Examining GLUT1 values in the SFMC exclusively, CD4⁺CD161⁺ (CD161⁺) T cells displayed a significant increase in GLUT1 MFI values compared with CD4⁺CD161⁻ (CD161⁻) T cells at both 0 ($p < 0.05$) (Figure 4.25 C) and 48 h ($p < 0.01$) (Figure 4.25 D).

Further examination of Treg cells (CD4⁺CD25⁺Foxp3⁺) demonstrated a significant increase in GLUT1 expression in the SFMC compared with PBMC of RA patients at both 0 ($p < 0.05$) (Figure 4.26 A and B) and 48 h ($p < 0.01$) (Figure 4.26 C and D).

Taken together this data suggests that total CD4⁺ T cells from the inflamed RA joint may be more glycolytic than their counterparts in the blood. Increased GLUT1 expression in synovial fluid vs blood held true for both Th17 lineage and Treg cells, suggesting that both cell types may exhibit increased glycolytic activity in the inflamed joint. Furthermore, within the synovial fluid, Th17 lineage cells expressed relatively more GLUT1 and may therefore be relatively more glycolytic than CD161⁻ Th cells.

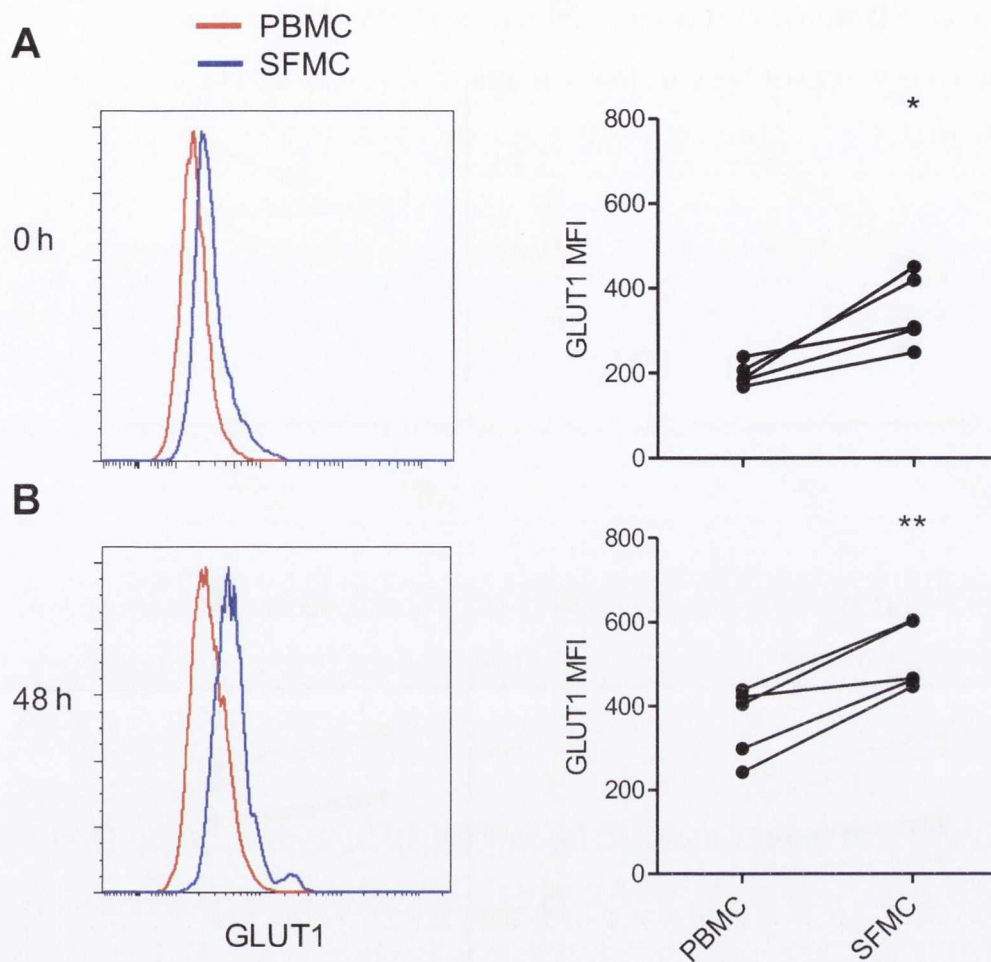


Figure 4.24. Increased frequency of CD4⁺ T cells expressing GLUT1 in the synovial fluid of RA patients compared with PBMC.

Matched PBMC and SFMC were isolated from RA patients (n=5) with active disease. Following a 0 or 48 h stimulation with anti-CD3, cells were stained with fluorochrome-conjugated antibodies specific for CD4 and the glucose transporter GLUT1. The cells were analysed by flow cytometry, representative histograms and graphs showing CD4⁺ GLUT1 MFI at 0 (A) and 48 h (B) are shown. Statistical differences were determined by paired t-tests with two-tailed p-values; *p<0.05.

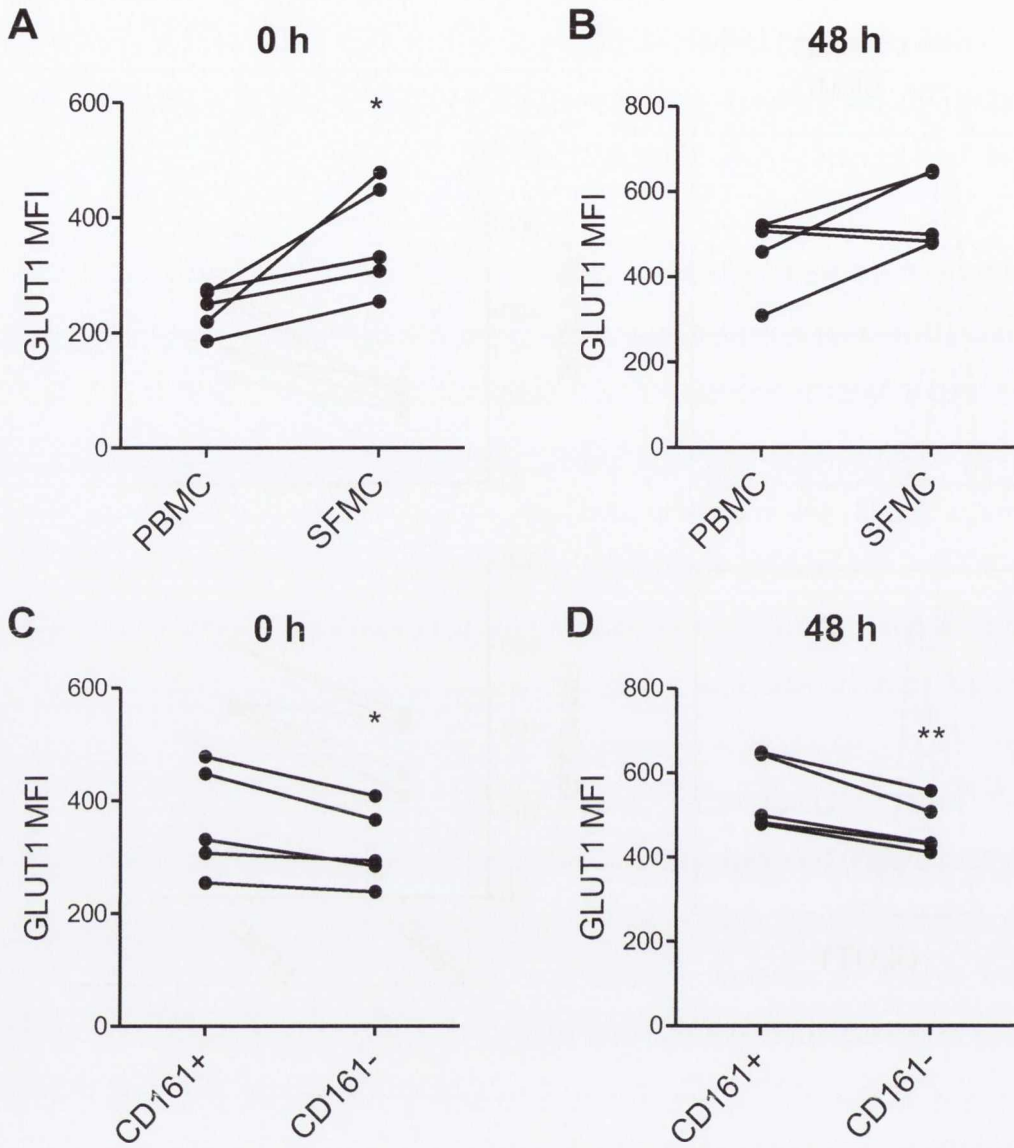


Figure 4.25. Increased frequency of CD4⁺CD161⁺ T cells expressing GLUT1 in the synovial fluid of RA patients compared with PBMC.

Matched PBMC and SFMC were isolated from RA patients (n=5) with active disease. Following a 0 or 48 h stimulation with anti-CD3, cells were stained with fluorochrome-conjugated antibodies specific for CD4 and CD161 and the glucose transporter GLUT1. The cells were analysed by flow cytometry. The graphs represent GLUT1 MFI values for CD4⁺CD161⁺ T cells at 0 h (A) and 48 h (B) for PBMC and SFMC, and for CD4⁺CD161⁺ (CD161⁺) and CD4⁺CD161⁻ (CD161⁻) T cells at 0 (C) and 48 h (D) for the SFMC. Statistical differences were determined by paired t-tests with two-tailed p-values; *p<0.05, **p<0.01.

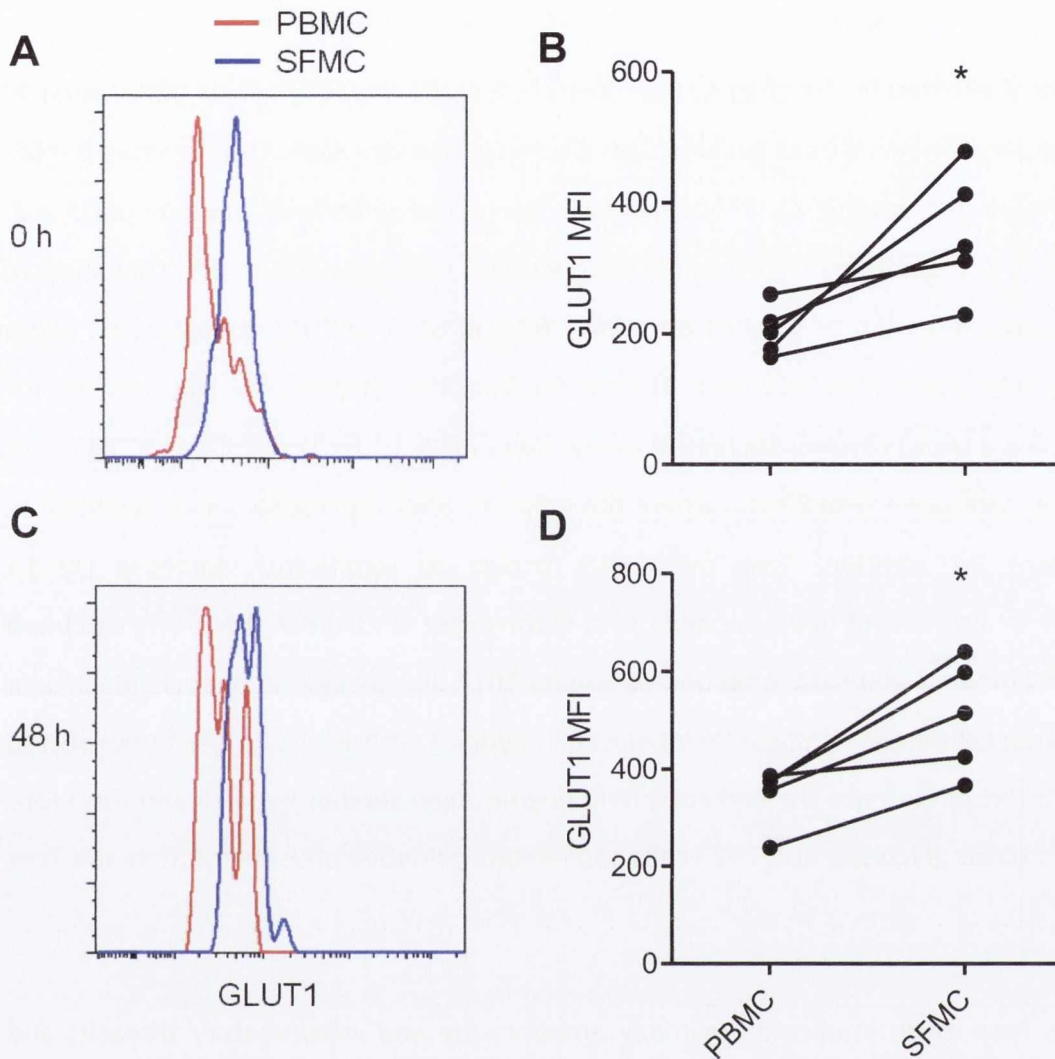


Figure 4.26. Increased expression of GLUT1 in Treg cells from the synovial fluid of RA patients compared with PBMC.

Matched PBMC and SFMC were isolated from RA patients (n=5) with active disease. Following a 0 or 48 h stimulation with anti-CD3, cells were stained with fluorochrome-conjugated antibodies specific for CD4, CD25, Foxp3 and the glucose transporter GLUT1. The cells were analysed by flow cytometry, and representative histograms represent Treg cells (CD4⁺CD25⁺Foxp3⁺) in the PBMC and SFMC at 0 (A) and 48 (C) h stimulations and graphs showing GLUT1 MFI values for CD4⁺CD25⁺Foxp3⁺ cells at 0 (B) and 48 h (D) are shown (n=5). Statistical differences were determined by paired t-tests with two-tailed p-values; *p<0.05.

4.3 Discussion

The results presented in this chapter demonstrate a novel role for hypoxia in the survival and expansion of human T cell subsets. This study has shown a significant increase in HIF-1 α expression for resting Th17 lineage cells compared with Treg cells in normoxia. Additionally, it presents findings broadly in agreement with previous studies that showed an increased expression of survival proteins Ki67 and Bcl-2 in Th17 lineage cells, and a novel increase found in exTh17 cells. The results from this chapter also demonstrate for the first time a trend towards increased expression of HIF-1 α by Treg cells and Th17 cells in RA SFMC compared with PBMC, where the inflamed joint represents an *in vivo* hypoxic environment. In addition, Treg cells were shown to significantly increase HIF-1 α expression *in vitro* under hypoxic conditions. Surprisingly, findings in this study exhibited for the first time a significant inhibition of human Th17 lineage cells in hypoxia *in vitro*. In contrast Treg cells were significantly increased in hypoxia. These results were unexpected and counterintuitive, since the currently held dogma suggests that hypoxia and therefore HIF-1 α promotes glycolysis and Th17 cells and inhibits oxidative phosphorylation and Treg cells.

Th17 cells have been implicated in many autoimmune and inflammatory diseases and therefore, the survival characteristics in Th17 lineage cells were examined. This study presents an increased expression of Ki67, indicative of cellular proliferation, and Bcl-2, an anti-apoptotic protein, in Th17 lineage cells compared with CD161⁻ T cells. This suggests that Th17 lineage cells have the potential to proliferate to a higher extent and are relatively resistant to apoptotic cell death. This is in agreement with previous murine and human studies (Kryczek, Zhao et al. 2011, Czabotar, Lessene et al. 2014, Basdeo, Moran et al. 2015). HIF-1 α orchestrates the cellular response to hypoxia. Although hypoxia is a primary inducer of HIF-1 α protein stabilization, non-hypoxic stimuli can also induce the accumulation of HIF. In T cells in particular, there are two non-conventional ways of stabilizing HIF-1 α : following T cell receptor stimulation and culture with the pro-inflammatory IL-6. Findings in this study support those displayed in murine T cells, with Th17 lineage cells (CD161⁺) expressing increased HIF-1 α compared with CD161⁻ Th cells, consisting mostly of Th1 and Th2 cells, and Treg cells by flow cytometric analysis. Shi et al demonstrated the differential HIF-1 α expression at the protein level by western blot, with

cells differentiated under Th17-skewing conditions expressing HIF-1 α to the highest extent, with undetectable levels found in Treg cells. As mentioned previously, IL-6 plays a role in Th17 cell differentiation and can activate the transcription factor STAT3, which is also described as increasing HIF-1 α protein levels (Demaria, Giorgi et al. 2010). This may be the mechanism by which human Th17 lineage cells express increased HIF-1 α basally in normoxia.

ExTh17 cells, also characterized by CD161 expression, are highly polyfunctional T cells and are enriched in the hypoxic synovial joint of RA patients (Basdeo et al. unpublished data). Results examining the expression of Ki67 and Bcl-2 in exTh17 cells compared with Th17 and Th1 cells demonstrated that exTh17 cells had significantly increased expression of Bcl-2 compared with Th1 cells, and higher Ki67 compared with both Th17 and Th1 cells. This suggests that ExTh17 cells may at least in part account for the increased expression of these proteins within the total CD161⁺ population, and this is not primarily due to bona fide Th17 cells. In addition, HIF-1 α expression in exTh17 cells trended towards an increase compared with Th1 cells, gating on the basis of CD161 and CXCR3. This supports a role for CXCR3 in the increased HIF-1 α expression by exTh17 cells, as previous data in breast cancer cell lines demonstrate a significant increase in CXCR3 expression in hypoxia (Chaturvedi, Gilkes et al. 2013).

Studies focusing on human T cells in hypoxia are scarce; therefore, this chapter examined the expansion and survival of T cell subsets in hypoxia in vitro. The results demonstrated a significant upregulation of HIF-1 α by CD4⁺ T cells in 5% oxygen levels, indicating that the oxygen levels were sufficiently low to stabilise HIF-1 α . 5% oxygen was utilised in this study, since lower oxygen levels did not maintain adequate cell survival and proliferation of human PBMC. Additionally, even 5% oxygen demonstrated a significant decrease in cellular proliferation. As Th17 lineage cells revealed a significant increase in HIF-1 α compared with CD161⁻ T cells in normoxia, the expression of HIF in these subsets was examined in hypoxia in vitro. Th17 cells maintained their increased HIF-1 α expression in hypoxia compared with normoxia, and displayed increased HIF-1 α compared with CD161⁻ T cells once again. The hypothesis was that this increase in the hypoxia-inducible factors in hypoxia could provide a survival mechanism for Th17 cells in hypoxia in vitro. However, the results in this chapter revealed for the first time an inhibition of human Th17 lineage

cells, indicated by decreased CD161 and IL-17 expression by CD4⁺ T cells, in hypoxic conditions. This finding is contrary to past studies which demonstrated that inhibition of HIF-1 α impairs Th17 cell differentiation (Dang, Barbi et al. 2011, Shi, Wang et al. 2011) and the treatment with a hypoxia mimic, DMOG, known to stabilize HIF-1 α at the protein level, additionally resulted in increased ROR γ t and IL-17 expression in Th17 cytokine-skewing conditions in human cells (Bollinger, Gies et al. 2014). However, findings in this chapter are supported partially by a murine study, which demonstrates decreased IL-17 and ROR γ t expression by CD4⁺ T cells under Th17 cell skewing conditions in hypoxia (Clambey, McNamee et al. 2012). Additionally, the novel study of the effect of hypoxia in vitro on exTh17 cells revealed a significant decrease in the frequency of transitioning exTh17 cells and fully switched exTh17 cells. ExTh17 cells have previously been shown to be enriched in chronic inflammatory disorders, including Crohn's disease and juvenile idiopathic arthritis (Cosmi, Liotta et al. 2014), which likely link increased inflammation with hypoxic environments. Therefore, a clear discrepancy is observed between hypoxia in vitro and in vivo for T cell survival and expansion. Th1 cells, characterized by IFN- γ production, were increased in hypoxia in this study. This was unforeseen, as this study and past data has demonstrated a decreased expression of HIF-1 α in Th1 cells compared with Th17 (Shi, Wang et al. 2011) and, exclusively in this study, exTh17 cells. However, in agreement with the finding of this chapter, a murine study demonstrated a significant increase in IFN- γ production by CD4⁺ T cells following stimulation in 1% oxygen levels (Roman, Ranganamy et al. 2010). This study also revealed that this enhancement of cytokine production is independent of HIF-1 α , and is partially dependent on Nrf2. The Nrf-2 transcription factor is known to orchestrate the cellular response to oxidative stress and therefore could be playing a role in the survival of Th1 cells in hypoxia in vitro. These results suggest a failure of HIF-1 α to provide a mechanism for survival for Th17 and exTh17 cells in hypoxic conditions in vitro.

The examination of cytokine accumulation in supernatants by PBMC in hypoxia demonstrated a decrease in IL-17A, the Th17 cell-specific cytokine, IFN- γ , produced mostly by Th1 cells, and the immunosuppressive cytokine IL-10. Secretion of all three cytokines by total PBMC was inhibited, and may have been due to the overall decrease in cell proliferation in hypoxia. Overall proliferation was decreased in PBMC in hypoxia compared with normoxia, however, cell viability remained intact. This is consistent with a

previous study, stating that PBMC in hypoxia, stimulated with PHA, enter into a growth suppressive state by inhibiting the synthesis of mitotic cyclins A and B (Naldini and Carraro 1999). Additionally, a purified CD4⁺ T cell population failed to proliferate after stimulation in hypoxia in vitro; therefore, purified CD4⁺ T cell populations could not be examined in hypoxia. This is suggestive of a role for antigen-presenting cells within the PBMC population in the survival and proliferation of CD4 T cells in hypoxia in vitro.

An attempt to reverse the inhibition of IL-17 producing CD4⁺ T cells within the PBMC population in hypoxia was made via cell stimulation in the presence of Th17 cell-skewing cytokines. This study demonstrates an increased frequency of CD4⁺IL-17⁺ T cells in hypoxia following stimulation of total PBMC in the presence of Th17 skewing cytokines. The frequency of Th17 cells is significantly decreased in hypoxia, however, the addition of IL-1 β , IL-6 and IL-23 cytokines, along with anti-IL-4 and anti-IFN γ , known to promote Th17 cell differentiation, resulted in a decreased inhibition of CD4⁺IL-17⁺ T cells in this study. This is supported by a study in murine cells revealing an increase in IL-17⁺ T cells following stimulation in the presence of Th17 cell skewing cytokines in hypoxia (Clambey, McNamee et al. 2012). There are various possible explanations for this decrease in CD4⁺IL-17⁺ T cell inhibition in hypoxia following the addition of Th17 cytokines. Naïve T cells within the PBMC population may differentiate into Th17 cells as a result of the Th17 cell-skewing cytokines, providing an increased CD4⁺IL-17⁺ population. The introduction of more IL-23 into the system may provide Th17 cells with the appropriate cytokine to maintain cell survival and expansion (Stritesky, Yeh et al. 2008). In conclusion, this finding suggests the potential for human Th17 cell-skewing cytokines in the increased survival of IL-17-expressing cells in hypoxia. Thus at sites of inflammation such as the hypoxic RA joint, the enrichment of Th17 lineage cells could be maintained by the inflammatory cytokine milieu.

Results presented in this chapter suggest a role for metabolism, specifically glycolysis, in T cell survival in hypoxia in vitro. GLUT1 expression trends towards an increase in CD4⁺ T cells in hypoxia compared with normoxia. Hypoxia is strongly linked to glycolysis, as HIF-1 α transcribes genes specific for glycolytic enzymes and glucose transporters (Shi, Wang et al. 2011). This is consistent with a study in humans, stating an increase in lactate production by PBMC in 2% oxygen 2 days after stimulation with PHA (Naldini, Carraro et al. 1997). Additionally, glucose metabolism is known to provide a positive feedback loop

on HIF-1 α , as demonstrated in human glioma cells (Lu, Forbes et al. 2002). This trend towards increased glucose transporter expression in hypoxia could promote HIF-1 α expression further in hypoxia in vitro. The examination of GLUT1 expression in human T cells in hypoxia was performed for the first time in this study. Th17 cells revealed a significant increase in GLUT1 expression compared with CD161⁻ T cells in hypoxia; however, within the CD161⁺ T cell population, GLUT1 was not significantly increased by hypoxia. This could suggest that Th17 cells are not increasing their glycolytic metabolism in vitro in hypoxic conditions, and may provide a reason why Th17 cell frequencies are decreased in hypoxia. Perhaps 5% hypoxia is sufficient to increase HIF-1 α expression but not adequate to completely switch the metabolism of T cells towards glycolysis.

This chapter demonstrates an increased frequency of Treg cells from a total PBMC population cultured in hypoxia compared with normoxia. These data does at the surface appear to conflict with recent high profile murine studies, which demonstrated inhibition of Treg cells by HIF-1 α (Dang, Barbi et al. 2011, Shi, Wang et al. 2011). However these studies examined the role of HIF-1 α rather than hypoxia, although one might have expected that they would have similar effects. However other studies performed under actual hypoxic conditions support the data shown here, having demonstrated an increased frequency of Treg cells in human PBMC cultured in as little as 1% oxygen levels (Ben-Shoshan, Maysel-Auslender et al. 2008). This was also the case for murine studies, as Foxp3⁺ expression within CD4⁺ T cells was increased in hypoxic conditions, although these cells were cultured under Treg cell skewing conditions (Clambey, McNamee et al. 2012). This finding, in partnership with an increased expression of HIF-1 α by Treg cells in hypoxia, suggests an explanation for the fact that Treg cells are enriched in hypoxic and inflamed environments such as the RA joint. Additionally, Treg cells increase HIF-1 α expression in hypoxia to a larger extent than Th17 cells, as shown in this study. A previous study in the human Jurkat T cell line provides evidence that the induction of Foxp3 by hypoxic conditions was dependent on HIF-1 α , as stable knockdown of HIF-1 α resulted in impaired Foxp3 induction in hypoxia (Clambey, McNamee et al. 2012). This suggests a mechanism by which Treg cells survive, expand or are induced in hypoxic conditions in vitro.

The results in this chapter demonstrated for the first time a significant increase in GLUT1 expression for Treg cells in hypoxia in vitro when compared to normoxia levels, and also compared to CD161⁺ T cells in hypoxia. GLUT1 was not significantly increased in Th17 cells; therefore, an increased glycolysis may provide a mechanism by which Treg cells survive within hypoxia and Th17 cells are inhibited.

The regulation of mitochondrial gene expression between normoxia and hypoxia was examined for human PBMC. This study revealed a significant decrease in genes encoding proteins involved in fatty acid oxidation, including *CPT1B*, essential for the beta-oxidation of long chain fatty acids, and *SLC25A20*, encoding an enzyme required for the transport of fatty acids across the mitochondrial membrane (Zhang, Li et al. 2015). Additionally, cells in hypoxia demonstrate a decreased expression of the heat shock protein 90-alpha, known to promote cellular stress adaptation and is fuelled by ATP (Santoro 2000). Furthermore, hypoxia reduces the expression of genes encoding two uncoupling proteins, UCP1, known to disrupt the MMP and reduce oxidative phosphorylation, and UCP2, a dysregulation in which results in increased reactive oxygen species (ROS) (Ricquier and Bouillaud 2000). The examination of mitochondrial genes involved in cell death revealed conflicting results, demonstrating an increase in both the anti-apoptotic protein Bcl-2 and the pro-apoptotic protein BNIP3. Hypoxia additionally promotes the expression of two genes involved in the resistance to ROS-mediated cell death, UCP4 and SOD2. The overexpression of UCP4 in a human neuronal cell line results in an increased survival during increased ROS production (Ramsden, Ho et al. 2012). Therefore, the assessment of mitochondrial gene regulation in hypoxia reveals a complicated scenario. Overall, cells in hypoxia promote the expression of genes involved in the maintenance of cell survival during oxidative stress, while reducing the expression of genes implicated in fatty acid metabolism and the uncoupling and disruption of the MMP. This suggests no known disruption of the MMP or ATP production, but also no promotion of mitochondrial respiration by cells in hypoxia. Additionally, further experimentation will need to be performed to analyse the effect of hypoxia on mitochondrial respiration and also glycolysis.

The production of active TGF- β , another suppressive cytokine produced by every leukocyte lineage, including lymphocytes, macrophages, and dendritic cells, was

increased in hypoxia. TGF- β , along with IL-2 signalling, is required for the generation of induced-Tregs expressing Foxp3 in vitro (Chen, Jin et al. 2003). One murine study has reported an increase in Treg cell populations in hypoxia, owing to de novo Treg induction (Clambey, McNamee et al. 2012). This provides insight into a potential role for TGF- β in the increased frequencies of human Treg cells in vitro and the subsequent suppression of Th17 cells. TGF- β is known to suppress T cell proliferation by inhibiting the production of IL-2 (Brabletz, Pfeuffer et al. 1993) and to induce Treg cells. This theory was tested following TGF- β 1 receptor inhibitor treatment of PBMC in hypoxia. However this revealed no significant change in Treg cell frequencies following iTGF- β 1 treatment in hypoxia, indicating that TGF- β signalling was not required for the increase of Treg cell frequencies in hypoxia. Although TGF- β 1 is the most dominantly expressed within the immune system, inhibition of all isoforms of TGF- β (1,2 and 3) may be required to confirm this.

The RA synovial joint represents a highly inflamed and hypoxic environment in vivo (Ng, Biniecka et al. 2010). Therefore, the role of HIF-1 α in T cell subset survival in RA was investigated. Previous studies have investigated the role of T cell subsets in RA, confirming an increased frequency of Treg cells within the SFMC, but not the PBMC (Cao, van Vollenhoven et al. 2004, Raghavan, Cao et al. 2009, Sempere-Ortells, Perez-Garcia et al. 2009, Basdeo, Moran et al. 2015). This result was confirmed in this study, as was the increased frequency of CD161⁺ Th17 lineage cells within SFMC compared with PBMC (Basdeo, Moran et al. 2015). HIF-1 α expression in Th17 cells was significantly increased compared with CD161⁻ T cells in cells extracted from the hypoxic synovial joint of RA patients compared with the blood. Additionally, examining T cell subsets, both Th17 cells and Treg cells display a trend towards increased HIF-1 α expression in the SFMC compared with the blood of RA patients. This increase in Th17 cells in the hypoxic RA joint was in contrast to the inhibition of Th17 cells cultured in vitro in hypoxia. The reasons for this discrepancy are unclear, but may be due to other factors such as the inflammatory environment of the RA joint. The partial reversal of Th17 inhibition in the presence of inflammatory Th17 skewing cytokines provides support for this.

Finally, as the RA synovial joint represents an environment depleted of metabolites and resources, the metabolic profile of T cells in RA was investigated. The expression of GLUT1 by flow cytometry in SFMC compared with matched PBMC from RA patients was

investigated for the first time in this study, with an increased frequency of CD4⁺ T cells expressing GLUT1 in RA SFMC vs matched PBMC. This result suggests increased glycolysis within the hypoxic and inflamed synovial joint. Additionally, the expression of GLUT1 in CD161⁺, CD161⁻ and Treg cells in the PBMC and SFMC of RA patients was examined for the first time. Th17 lineage cells demonstrated a significant increase in GLUT1 in the SFMC compared with PBMC, and also compared with CD161⁻ T cells in the joint both ex vivo and in vitro. Furthermore, Treg cells displayed a significant increase in GLUT1 expression in the SFMC compared with the PBMC in RA patients. This increase in glycolytic metabolism within the RA joint and an increase in Th17 and Treg cell GLUT1 expression could possibly contribute to the increased frequency of Treg and Th17 lineage cells in the inflamed joint.

In summary, ex vivo Th17 and exTh17 cells exhibited increased survival characteristics, Bcl-2 and Ki67. Th17 cells demonstrated increased HIF-1 α in both normoxia and in vitro in hypoxia. However, despite expressing increased levels of HIF-1 α , CD161 and IL-17-expressing CD4⁺ T cells were inhibited in hypoxia in vitro. This inhibition can be decreased if PBMC are stimulated in the presence of Th17 cell-skewing cytokines. In contrast to this, Treg cells were significantly increased in hypoxia, and additionally demonstrated an increase in HIF-1 α expression. GLUT1 expression trended towards an increase in hypoxia in vitro; however, GLUT1 expression was only significantly increased for Treg cells. This suggests a role for glycolysis in the survival, expansion or induction of Treg cells in hypoxia. Additionally, TGF- β production was significantly increased and hypothesised to be involved in Treg cell expansion in hypoxia and the subsequent inhibition of Th17 cells. However, Treg cell expansion in hypoxia was unchanged following treatment with a TGF- β receptor 1 inhibitor. The increased expression of HIF-1 α for Treg cells, in combination with increased GLUT1 and TGF- β may contribute to Treg survival, induction or expansion in low oxygen tension. Additional research will be required to properly elucidate the mechanism by which hypoxia induces Treg cells in vitro. Furthermore, examination of T cells in a hypoxic environment in vivo demonstrated an increase in both Treg and Th17 cell frequencies, with HIF-1 α expression trending towards an increase for both subsets. These data additionally demonstrate a significant increase in GLUT1 expression in the SFMC compared with PBMC of RA patients, with both Th17 and Treg cells increasing GLUT1 expression also. These data demonstrate a role for glycolysis in the inflamed and

hypoxic environment established in the RA joint, and may contribute to the increased frequencies of both Th17 and Treg cells in RA.

Chapter 5

Modulation of the Treg:Th17 cell axis in vitro and in vivo

Chapter 5. Modulation of the Treg:Th17 cell axis in vitro and in vivo

5.1.1 Introduction

During autoimmune and inflammatory diseases, the balance between pro-inflammatory and regulatory responses is perturbed. Th17 cells are highly pro-inflammatory cells, which, when in excess contribute to disease. On the opposite side of the balance, regulatory T cells function to suppress inappropriate inflammation, which, when in failure also contributes to disease. Therefore, the Th17:Treg axis provides a basis for understanding the immunological mechanisms that induce and regulate autoimmunity and chronic inflammation (Noack and Miossec 2014). RA is a chronic inflammatory and autoimmune disease, characterized by increased Th17 lineage cells and a deficiency in Treg cell-mediated suppression of Th17 lineage cells (Basdeo, Moran et al. 2015). Many RA therapies target pro-inflammatory responses and subsequently enhance Treg cell suppression; including TNF- α inhibitors (infliximab, etanercept and adalimumab) (Valencia, Stephens et al. 2006), anti-IL-6 receptor antibody (tocilizumab) (Pesce, Soto et al. 2013), and inhibition of the Th17 cell specific transcription factor STAT3 (Ju, Heo et al. 2012).

Metabolism and hypoxia are known to play a key role in the manipulation of the murine Th17:Treg cell axis. Inhibition of glycolysis via treatment with known glycolytic inhibitors, 2-deoxy-D-glucose (2-DG) and rapamycin, revealed an inhibition in Th17 cell differentiation and a subsequent increase in Foxp3⁺ T cells (Michalek, Gerriets et al. 2011, Shi, Wang et al. 2011). In accordance with this study, the knockdown of HIF-1 α resulted in a reduction CD4⁺IL-17⁺ T cells and an increase in CD4⁺Foxp3⁺ T cell frequencies (Dang, Barbi et al. 2011, Shi, Wang et al. 2011). Previous studies in humans have focused on the role of rapamycin in the promotion of Treg cells in vitro (Battaglia, Stabilini et al. 2006, Strauss, Czystowska et al. 2009, Battaglia, Stabilini et al. 2012); however, the effect of glycolytic inhibition on human Th17 cells is yet to be investigated.

Pyruvate kinase, the rate-limiting enzyme in glycolysis, which converts phosphoenolpyruvic acid (PEP) to pyruvate, has recently been described as a mediator of HIF-1 α and metabolism. Pyruvate kinase exists as two isoforms: M1 (PKM1) and M2 (PKM2). PKM2 exists as two forms; the enzymatically active tetrameric form, which

promotes the complete conversion of PEP to pyruvate, and the less active dimeric form. Dimeric PKM2 can translocate to the nucleus, where it interacts with HIF-1 α and regulates the expression of numerous pro-glycolytic enzymes, including HIF-1 α itself (Luo, Hu et al. 2011, Luo and Semenza 2011). Additionally, PKM2 is known to regulate metabolism, with the less active PKM2 dimer driving glycolysis, while the active PKM2 tetramer produces pyruvate for oxidative phosphorylation (Christofk, Vander Heiden et al. 2008, Hitosugi, Kang et al. 2009). TEPP-46 is a small-molecule activator of PKM2, which binds PKM2 dimers to promote tetramer formation (Anastasiou, Yu et al. 2012). It has been shown in murine studies that TEPP-46 inhibits HIF-1 α expression in LPS-primed macrophages (Palsson-McDermott, Curtis et al. 2015). It is suggested that the tetramer formation of PKM2 is unable to translocate to the nucleus and interact with HIF-1 α , therefore resulting in decreased HIF-1 α expression. Additionally, YC-1 acts to inhibit HIF-1 α at the transcriptional level. YC-1 was originally developed for circulatory disorders for the inhibition of platelet aggregation and vascular constriction (Teng, Wu et al. 1997). YC-1 is also shown to promote the dissociation of the transcription co-activator p300 from HIF-1 α within the nucleus (Li, Shin et al. 2008).

In this study, investigations into the modulation of the Th17:Treg cell axis in vivo focus on psoriasis. Psoriasis is a chronic inflammatory skin disorder affecting 2.5% of the worldwide population (Nestle, Kaplan et al. 2009). Psoriasis vulgaris is the most common type of psoriasis, affecting 80-90% of psoriasis patients. It manifests as dry, red raised plaques with adherent silvery scales. At a cellular level, psoriasis is characterized by hyperproliferation and abnormal differentiation of keratinocytes, dilated blood vessels as well as an inflammatory infiltration of leukocytes, predominantly into the dermis (Griffiths and Barker 2007).

T cells are known to play a key role in the pathogenesis of psoriasis. The first evidence for this was revealed following the successful treatment of psoriasis patients with cyclosporine A, an immunosuppressive drug targeting T cell proliferation and cytokine production (Mueller and Herrmann 1979). The elevated levels of IFN- γ and IL-12 in both plaques and peripheral blood of psoriasis patients revealed a role for Th1 cells in this disease (Schlaak, Buslau et al. 1994). Increased levels of Th17 cell-related cytokines, including IL-17A, IL-17F, IL-21, IL-22 and TNF- α , are observed in both psoriatic skin and

circulation (Lowes, Kikuchi et al. 2008). These Th17-related cytokines can act upon keratinocytes, causing hyperproliferation and further enhance inflammation through immune cell recruitment.

Psoriasis can be treated in 3 ways, depending on disease severity: topical treatments, phototherapy and systemic treatment. Phototherapy consists of controlled exposure of affected skin to ultra-violet A (UVA) or UVB rays. This, combined with topical treatments, is used to treat moderate to severe psoriasis. Systemic treatments have targeted TNF- α , IL-23 and, most recently, IL-17. Secukinumab, ixekizumab and brodalumab each target IL-17 and have shown excellent results in psoriasis patients thus far in clinical trials (Chiricozzi and Krueger 2013).

An alternative oral treatment, in the form of a fumaric acid ester, is approved for the treatment of psoriasis. FumadermTM is a combination of monomethyl and dimethyl fumarate (DMF), which has been used in Germany since 1994 for the treatment of psoriasis. Originally, Dr. Schweckendiek used fumaric acid to cure himself, as he believed psoriasis to be a metabolic disease which required an input of fumaric acid to replace the insufficient amounts observed in psoriasis patients (Schweckendiek 1959). However, this theory has never been confirmed and the in vivo mechanism of action of FumadermTM is still unknown. DMF has been shown to have a range of anti-inflammatory and cytoprotective effects in vitro. These include anti-inflammatory and protective effects on astrocytes and neurons (Wilms, Sievers et al. 2010, Lin, Lisi et al. 2011, Scannevin, Chollate et al. 2012), inhibition of dendritic cell maturation and inflammatory cytokine production (Litjens, Rademaker et al. 2004, Litjens, Rademaker et al. 2006, Ghoreschi, Bruck et al. 2011), induction of apoptosis in T cells (Treumer, Zhu et al. 2003) and inhibition of T cell cytokine production, proliferation and adhesion molecule expression (Vandermeeren, Janssens et al. 1997, Ockenfels, Schultewolter et al. 1998, Lehmann, Listopad et al. 2007, Rubant, Ludwig et al. 2008, Zoghi, Amirghofran et al. 2011). In experimental models of MS, DMF was shown to deplete intracellular glutathione levels, resulting in the activation of the stress responsive heme oxygenase 1 (HO-1) via NRF-2 transcriptional activity (Linker, Lee et al. 2011). The downstream effects of HO-1 include inhibition of pro-inflammatory cytokine production by PBMC (Lehmann, Listopad et al. 2007) and inhibition of T cell proliferation (Lehmann, Listopad et al. 2007). TecfideraTM, an

oral agent consisting of dimethyl fumarate, has recently been approved by the European Medicines Agency (EMA) for the treatment of relapsing forms of MS.

5.1.2 Aims

The experiments in this chapter aimed to elucidate the modulatory effects of metabolism and hypoxia on the Treg:Th17 cell axis in vitro and the in vivo effects of Fumaderm™ treatment in psoriasis.

- Examine the effect of inhibiting glycolysis on Th17:Treg cell axis in vitro.
- Investigate the role of HIF-1 α inhibition on the Th17:Treg cell axis in vitro.
- Demonstrate the effect of metabolic manipulation within a hypoxic environment on Treg/Th17 cells.
- Analyse T helper cell subsets and Treg cell frequencies in blood from healthy control, untreated psoriasis patients and Fumaderm™-treated patients and in patients pre- and post-Fumaderm™ treatment.

5.2 Results

5.2.1 Inhibition of glycolysis and mTOR by rapamycin results in the inhibition of T helper cells

As previously described, rapamycin is an immunosuppressive drug targeting mTOR, which regulates cell growth and proliferation. mTOR forms two complexes, mTORC1 and mTORC2, the latter of which phosphorylates the protein kinase Akt, which is involved in the translocation of glucose transporters from the cytosol to the cell membrane, promoting glycolysis (Maclver, Michalek et al. 2013). Having demonstrated that CD161-expressing CD4⁺ T cells have increased mTOR activity and glycolytic activity, the effect of inhibiting mTOR and thereby glycolysis, via rapamycin treatment, was addressed next.

Memory CD4⁺ T cells were negatively sorted from PBMC using magnetic beads and stimulated with anti-CD3, CFSE-labelled irradiated APCs and IL-2 (20 u/ml) in the presence or absence of rapamycin (20 nM) for 7 days. Rapamycin stocks were replenished after 3 days of culture together with the replacement of culture medium. The cells were restimulated for 5 h with PMA, ionomycin and brefeldin-A after the 7 day culture and stained with fluorochrome-conjugated antibodies specific for surface markers CD3, CD8 and CD161, and the intracellular cytokines IL-17 and IFN- γ . Cells were analysed by flow cytometry. Irradiated APCs were selectively excluded from analysis through CFSE⁻ gating and CD4⁺ T cells were gated as CD3⁺CD8⁻ T cells following PMA stimulation.

Examining Th17 cells initially, the frequency of CD4⁺CD161⁺ T cells was significantly reduced across 6 donors following treatment with rapamycin ($p < 0.05$) (Figure 5.1) as represented in the dot plots (A) and graphed data (B) ($n = 6$). Additionally, the frequency of CD4⁺IL-17⁺ T cells was significantly decreased following rapamycin treatment ($p < 0.05$) (Figure 5.2).

The frequency of CD4⁺ T cells expressing both IL-17 and IFN- γ , representing the cells transitioning to an exTh17 cell subpopulation, was also significantly decreased following rapamycin treatment ($p < 0.01$) (Figure 5.3 A and B). Additionally, the frequency of fully switched exTh17 cells, now primarily expressing IFN- γ and retaining CD161 expression, was significantly decreased following rapamycin treatment (Figure 5.3C).

Th1 cells are characterized by their expression of IFN- γ and following rapamycin treatment the frequency of IFN- γ -producing CD4⁺ T cells was also significantly decreased ($p < 0.001$) (Figure 5.4).

This data demonstrates an inhibition of Th17, exTh17 and Th1 cells following the inhibition of glycolysis and mTOR via rapamycin treatment. This data reveals an ability to modulate T helper cells by rapamycin and ultimately by metabolism.

5.2.2 Inhibition of glycolysis and mTOR by rapamycin results in an enhancement of Treg cell frequencies

In chapter 3, Treg cells displayed low mTOR activity via pS6 staining and an enhancement in cell frequencies following the hindrance of glycolysis via galactose treatment. Next, the effect of mTOR inhibition on memory Treg cells was determined.

Memory CD4⁺ T cells were negatively sorted from PBMC using magnetic beads and stimulated with anti-CD3, CFSE-labelled irradiated APCs and IL-2 (20 u/ml) in the presence or absence of rapamycin (20 nM) for 7 days. Rapamycin stocks were replenished after 3 days of culture together with the replacement of culture medium. Cells were stained with fluorochrome-conjugated antibodies specific for surface markers CD4, CD25 and CD127, and the nuclear transcription factor Foxp3. The frequency of CD4⁺CD25⁺CD127^{Lo}FoxP3⁺ (Treg) T cells was significantly increased following glycolytic inhibition with rapamycin (n=5) (p< 0.05) (Figure 5.5). This data suggests that Treg cells are not dependent on mTOR and glycolysis and can be modulated by metabolism.

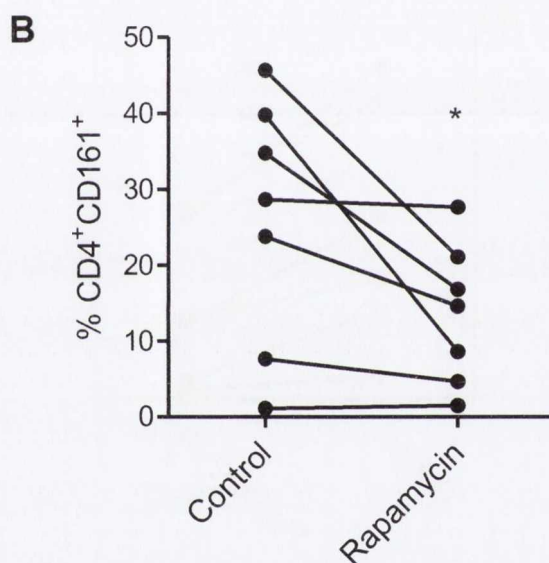
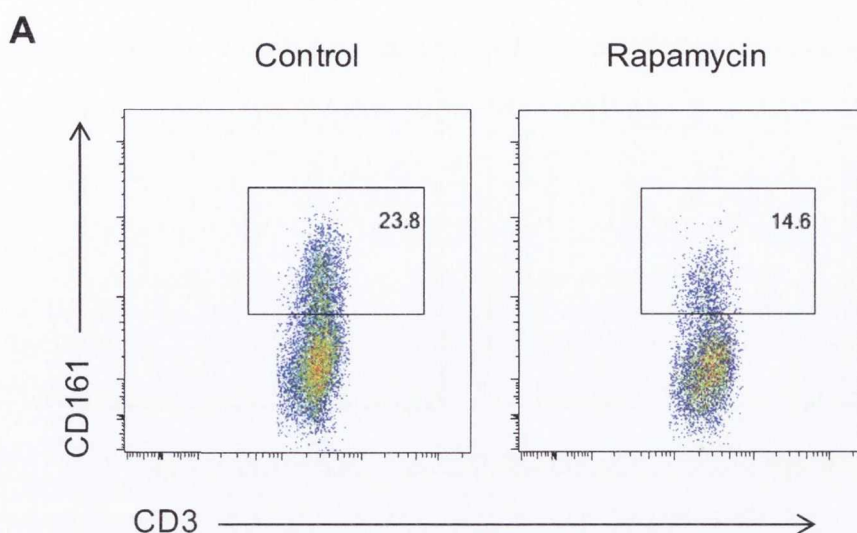


Figure 5.1. Reduction in CD4⁺CD161⁺ T cells following inhibition of glycolysis via rapamycin treatment.

Memory CD4⁺ T cells were negatively sorted from PBMC using magnetic beads and stimulated for 5 days with anti-CD3, CFSE-labelled irradiated APCs and IL-2 (20 u/ml) in the presence or absence of rapamycin. After 5 days, the cells were stimulated for 5 h with PMA, ionomycin and brefeldin A and stained with fluorochrome-conjugated antibodies specific for surface markers CD3, CD8 and CD161. Cells were analysed by flow cytometry and irradiated APCs were selectively excluded from analysis through CFSE⁻ gating. Representative dots plots show CD161 staining in CD3⁺CD8⁻ (CD4) T cells in the presence or absence of rapamycin (A), cumulative data (n=7) is shown in (B). Statistical differences in the mean between the groups were determined by a paired, two-tailed t test; * p<0.05.

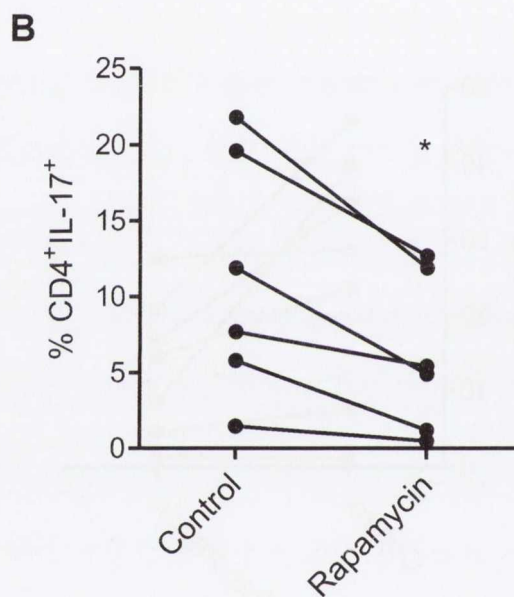
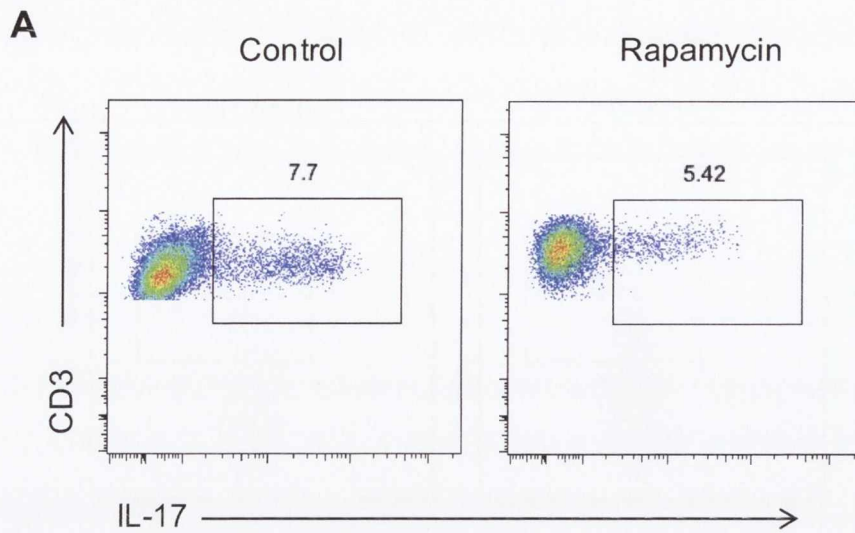


Figure 5.2. IL-17 expressing CD4⁺ T cells are decreased following inhibition of glycolysis via rapamycin treatment.

Memory CD4⁺ T cells were negatively sorted from PBMC using magnetic beads and stimulated for 5 days with anti-CD3, CFSE-labelled irradiated APCs and IL-2 (20 u/ml) in the presence or absence of rapamycin. After 5 days, the cells were stimulated for 5 h with PMA, ionomycin and brefeldin A and stained with fluorochrome-conjugated antibodies specific for surface markers CD3 and CD8, and intracellular cytokine IL-17. Cells were analysed by flow cytometry and irradiated APCs were selectively excluded from analysis through CFSE⁻ gating. Representative dots plots show IL-17 staining in CD3⁺CD8⁻ (CD4) T cells in the presence or absence of rapamycin (A), cumulative data (n=6) is shown in (B) Statistical differences in the mean between the groups were determined by a paired, two-tailed t test; * p<0.05.

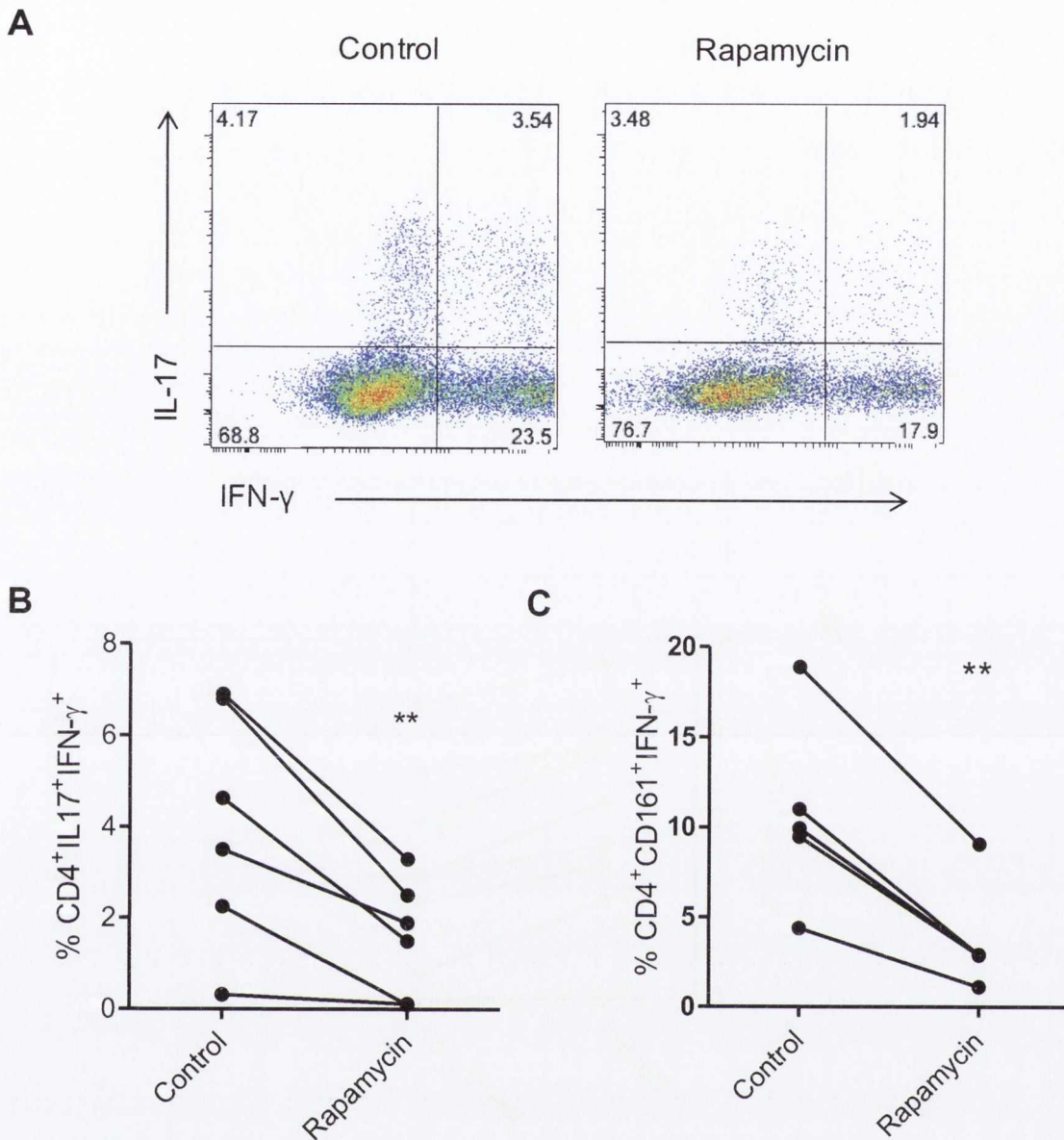


Figure 5.3. Reduction in transitional $CD4^+IL-17^+IFN-\gamma^+$ T cells following inhibition of glycolysis via rapamycin treatment.

Memory $CD4^+$ T cells were negatively sorted from PBMC using magnetic beads and stimulated for 5 days with anti-CD3, CFSE-labelled irradiated APCs and IL-2 (20 u/ml) in the presence or absence of rapamycin. After 5 days, the cells were stimulated for 5 hr with PMA, ionomycin and brefeldin A and stained with fluorochrome-conjugated antibodies specific for CD3, CD8, IL-17 and IFN- γ . Cells were analysed by flow cytometry and irradiated APCs were selectively excluded from analysis through CFSE $^-$ gating. Representative dots plots show IL-17/IFN- γ staining in $CD3^+CD8^-$ ($CD4$) T cells in the presence or absence of rapamycin (A), cumulative data (n=6) is shown in (B). Graph also represents the frequency of $CD4^+CD161^+IFN-\gamma^+$ cells for control and rapamycin treatment (n=5) (C). Statistical differences in the mean between the groups were determined by a paired, two-tailed t test; **p<0.01

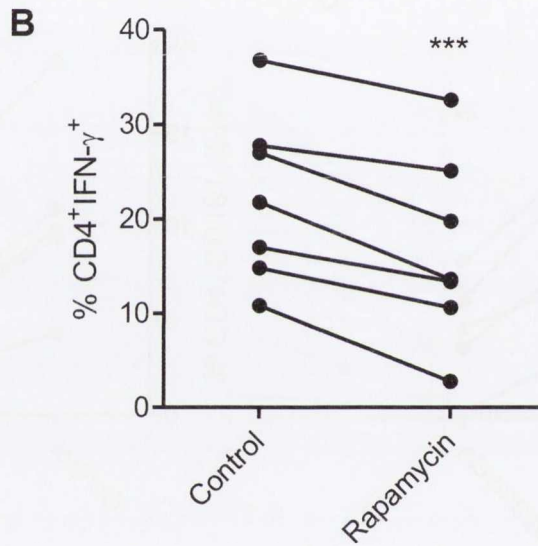
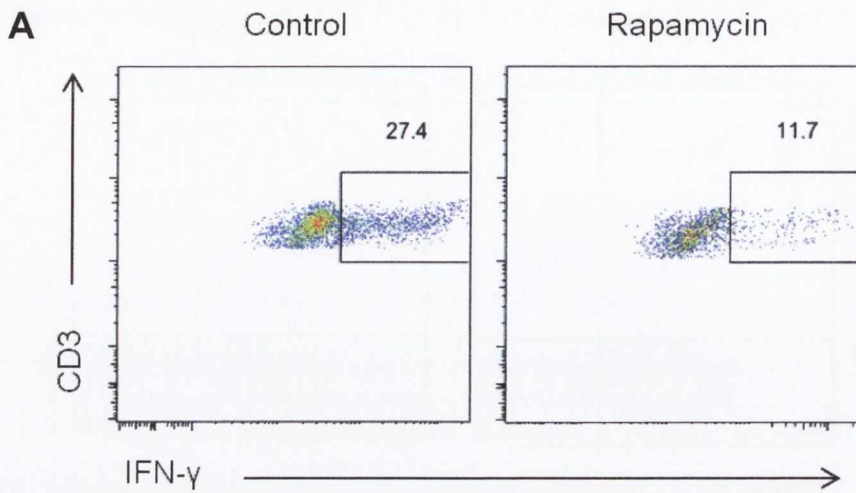


Figure 5.4. Reduction in CD4⁺IFN-γ⁺ T cells following inhibition of glycolysis via rapamycin treatment.

Memory CD4⁺ T cells were negatively sorted from PBMC using magnetic beads and stimulated for 5 days with anti-CD3, CFSE-labelled irradiated APCs and IL-2 (20 u/ml) in the presence or absence of rapamycin. After 5 days, the cells were stimulated for 5 h with PMA, ionomycin and brefeldin A and stained with fluorochrome-conjugated antibodies specific for surface markers CD3 and CD8, and intracellular cytokine IFN-γ. Cells were analysed by flow cytometry and irradiated APCs were selectively excluded from analysis through CFSE⁻ gating. Representative dots plots show CD3/IFN-γ staining in CD3⁺CD8⁻ (CD4) T cells in the presence or absence of rapamycin (A), cumulative data (n=7) is shown in (B). Statistical differences in the mean between the groups were determined by a paired, two-tailed t test; ***p<0.001

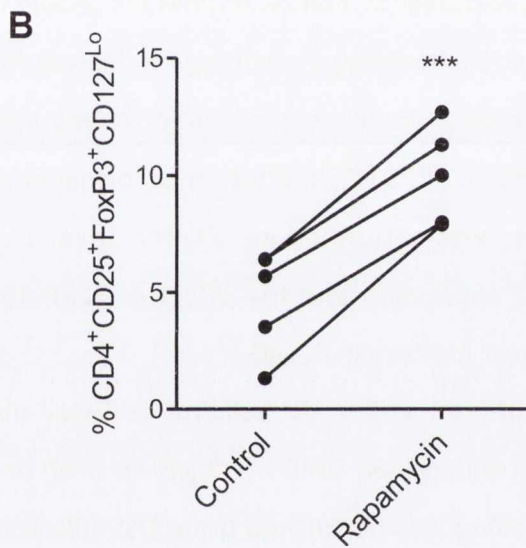
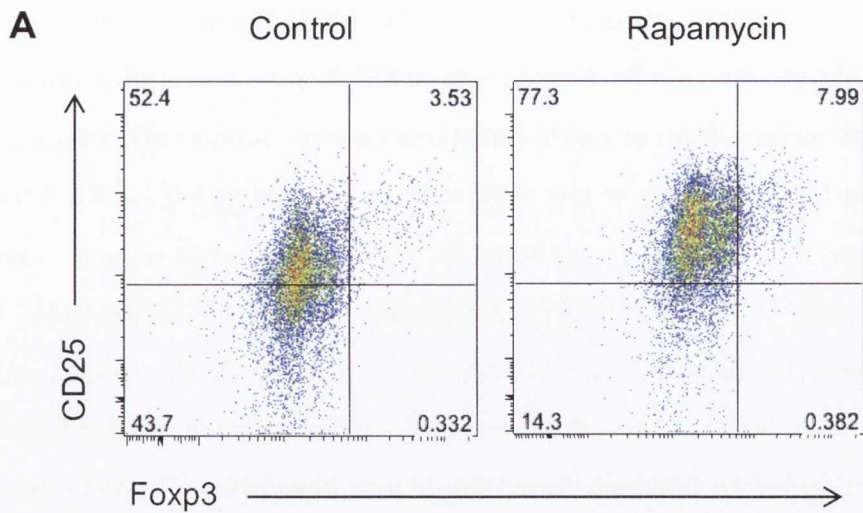


Figure 5.5. Increased regulatory T cells following inhibition of glycolysis via rapamycin treatment.

Memory CD4⁺ T cells were negatively sorted from PBMC using magnetic beads and stimulated for 5 days with anti-CD3, CFSE-labelled irradiated APCs and IL-2 (20 u/ml) in the presence or absence of rapamycin. After 5 days, the cells were stained with fluorochrome-conjugated antibodies specific for surface markers CD4, CD25 and CD127, and nuclear transcription factor Foxp3. Cells were analysed by flow cytometry and irradiated APCs were selectively excluded from analysis through CFSE⁻ gating. Representative dots plots show CD25 vs Foxp3 staining in CD4⁺ T cells in the presence or absence of rapamycin (A), cumulative data for CD4⁺CD25⁺CD127^{Lo}Foxp3⁺ T cells (n=5) is shown in (B). Statistical differences in the mean between the groups were determined by a paired, two-tailed t test; *** p<0.001.

5.2.3. TEPP-46 treatment of human cells promotes PKM2 tetramer formation.

In glycolysis, PKM2 is the rate-limiting enzyme which converts phosphoenolpyruvic acid to pyruvate. The dimeric form of PKM2 can translocate to the nucleus, interact with HIF-1 α and regulate the expression of glycolytic enzymes, including HIF-1 α itself (Luo, Hu et al. 2011, Luo and Semenza 2011). Additionally, PKM2 is known to regulate metabolism, with the less active PKM2 dimer driving glycolysis, while the active PKM2 tetramer produces pyruvate for oxidative phosphorylation (Christofk, Vander Heiden et al. 2008, Hitosugi, Kang et al. 2009). TEPP-46 is a small-molecule activator of PKM2, which binds PKM2 dimers to promote tetramer formation. It has been shown in mice that TEPP-46 inhibits HIF-1 α expression in LPS-primed macrophages (Palsson-McDermott, Curtis et al. 2015). It is suggested that the tetramer formation of PKM2 is unable to translocate to the nucleus and interact with HIF-1 α , therefore resulting in decreased HIF-1 α expression. PKM1 and PKM2 isoforms are differentially expressed in tissues and cells; therefore, in order to determine the expression of PKM2, and tetramer formation resulting from TEPP-46 treatment, western blotting was performed initially for Jurkat T cells, and results are displayed in chapter 2. PKM2 expression and the effect of TEPP-46 on PKM2 tetramer formation were determined next for human PBMC.

Healthy donor PBMC were cultured at 1×10^6 cells/ml in 6-well plates, and incubated overnight at 37°C. Cells were treated with DMSO (vehicle control) or TEPP-46 (10 and 50 μ M) for 18 h. Protein cross-linking was performed using DSS (disuccinimidyl suberate) in order to keep the tetrameric form of PKM2 intact following cell lysis. Western blot was performed for PKM2 (method outlined in chapter 2). Results revealed a dose-dependent increase in PKM2 tetramer formation (260 kD) following TEPP-46 treatment (Figure 5.6), with TEPP-46 at a concentration of 50 μ M displaying the highest increase in tetrameric formation. Tetrameric PKM2 forms basally and can be seen in the DMSO treated lanes.

Additionally, the promotion of PKM2 tetrameric protein expression as a result of TEPP-46 treatment was examined in CD4⁺ T cells. Due to limited cell numbers, DSS-linking was performed at a concentration of 1 mM only. The protein expression of the PKM2 tetramer was increased as a result of TEPP-46 treatment at both 10 and 20 μ M (Figure 5.7).

These data demonstrate the ability of TEPP-46 to promote PKM2 tetrameric formation in human PBMC and CD4⁺ T cells.

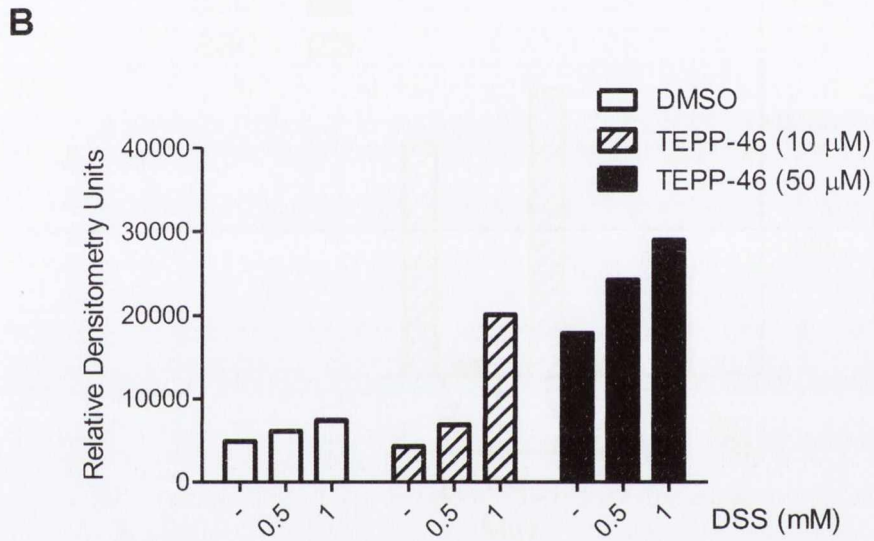
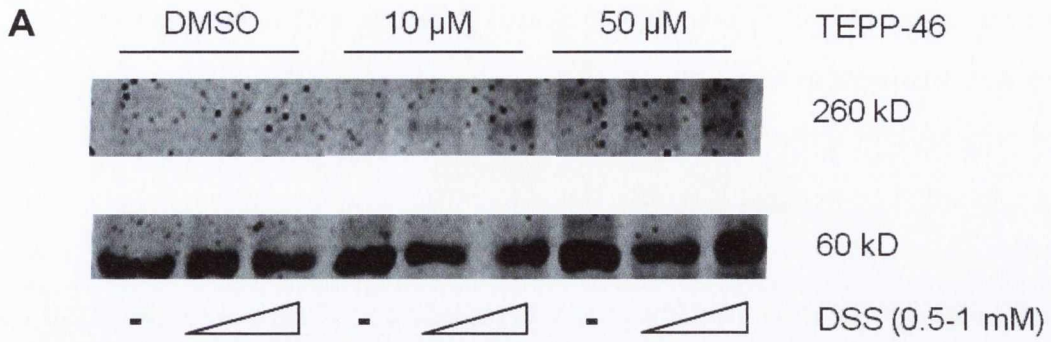


Figure 5.6 TEPP-46 treatment of human PBMC promotes PKM2 tetramer formation.

Healthy donor PBMC were cultured at 1×10^6 cells/ml in 6-well plates and incubated overnight at 37°C. Cells were treated with DMSO or TEPP-46 (10 – 50 μ M) for 18 h. DSS-linking was performed on the cells with increasing concentrations of DSS (0.5-1 mM). Western blot was performed for PKM2 (pyruvate kinase M2) at concentrations specified in appendix. Results show both monomeric (60 kD) and tetrameric (260 kD) forms of PKM2 (A) and densitometric analysis was used to compare band intensities for tetrameric PKM2 (B).

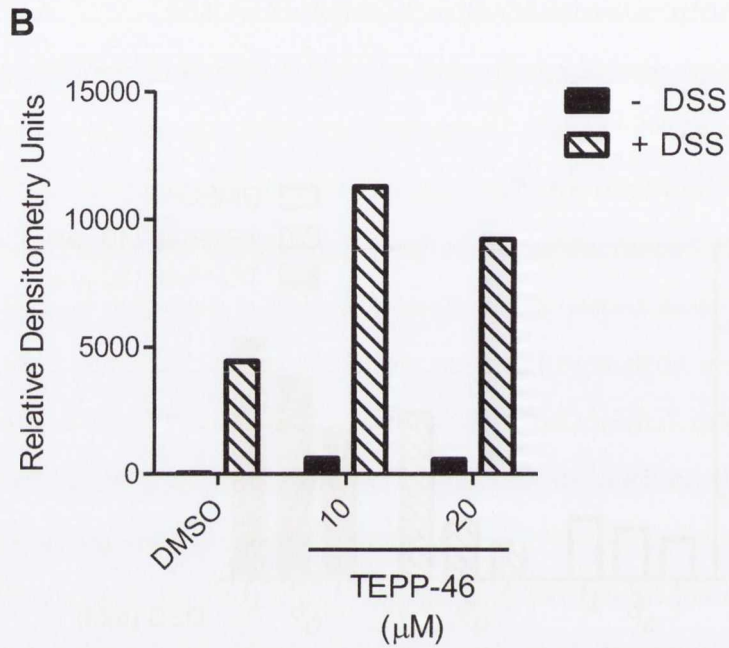
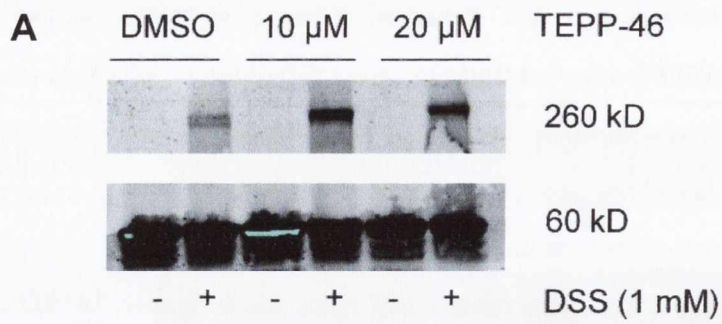


Figure 5.7 TEPP-46 treatment of human CD4⁺ T cells promotes PKM2 tetramer formation.

Total CD4⁺ T cells were positively sorted from healthy donor PBMC incubated overnight at 37°C, and then treated with vehicle (DMSO) or TEPP-46 (10 – 20 μ M) for 18 h. DSS-linking was performed on the cells with 1 mM DSS. Western blot was performed for both monomeric (60 kD) and tetrameric (260 kD) forms of PKM2 (A). Densitometric analysis was used to compare band intensities for tetrameric PKM2 (B).

5.2.4. The effect of TEPP-46 treatment on CD4⁺ T helper cell subsets in normoxia.

As mentioned previously, formation of the tetrameric PKM2, following TEPP-46 treatment, results in the inhibition of HIF-1 α in LPS-primed macrophages. As previous results in this study have indicated, CD161⁺ Th17 lineage cells expressed increased HIF-1 α compared with CD161⁻ and Treg cells in normoxia. Therefore, the effect of HIF-1 α inhibition on T helper cell subsets in normoxia was observed following TEPP-46 treatment. Additionally, tetrameric PKM2 is known to drive metabolism towards oxidative phosphorylation, and subsequently inhibits glycolysis.

PBMC from healthy donors were stimulated in the presence of anti-CD3 and/or TEPP-46 (10 – 20 μ M) for 5 days. Cells were stimulated with PMA, ionomycin and brefeldin-A for 5 h and stained with fluorochrome-conjugated antibodies specific for CD3, CD8, CD161, IL-17 and IFN- γ . The cells were analysed by flow cytometry and CD4 cells are gated as CD8⁻ CD3⁺ T cells. The results revealed a trend towards a decrease in CD4⁺CD161⁺ T cell frequencies in each TEPP-46 treatment group across 6 healthy donors (Figure 5.8). Additionally, the frequency of CD4⁺IL-17⁺ and CD4⁺IL-17⁺IFN- γ ⁺ (transitioning exTh17) cells both trended towards a decrease following TEPP-46 treatment (Figure 5.9 A and B). There was very little change in CD4⁺IFN- γ ⁺ T cell populations across each group (Figure 5.9 C). These results demonstrate a trend towards decreased Th17 and transitioning exTh17 cells following TEPP-46 treatment. TEPP-46 is known to inhibit HIF-1 α related genes in murine macrophages and is known to inhibit glycolysis; therefore, the effect of TEPP-46 on T cell subsets may be as a result of either HIF-1 α inhibition or inhibition of glycolysis.

5.2.5. The effect of TEPP-46 treatment on Treg cells in normoxia.

Previous data in this study has demonstrated a decreased expression of HIF-1 α by Treg cells compared to that of CD161⁺ T cells in normoxia. Additionally, Treg cells revealed less reliance on glycolysis for their metabolic needs. Therefore, the effect of TEPP-46 on Treg cell survival was examined next.

PBMC from healthy donors were stimulated in the presence of anti-CD3 and TEPP-46 (10 – 20 μ M) for 5 days. Cells were stained with fluorochrome-conjugated antibodies specific for CD4, CD25, CD127 and Foxp3. The cells were analysed by flow cytometry and results demonstrate a trend towards an increase in Treg cells (CD4⁺CD25⁺CD127^{Lo}Foxp3⁺) following 20 μ M TEPP-46 treatment compared with untreated cells (Figure 5.10). This data suggests that Treg cells are not inhibited by either function of TEPP-46 for survival or

expansion. As Treg cells display low HIF-1 α expression in normoxia compared with Th17 lineage cells, this may be the reason why Treg cells are not restricted by HIF-1 α inhibition in normoxia.

5.2.6. The effect of inhibiting HIF-1 α via YC-1 treatment on CD4⁺ T cell subsets in normoxia.

The effect of another HIF-1 α inhibitor on T cell subsets in normoxia was examined next. YC-1 (3-(5'-hydroxymethyl-2'-furyl)-1-benzylindazole) is a synthetic compound that has been established as a HIF-1 α inhibitor (Chun, Yeo et al. 2001, Chun, Yeo et al. 2004). This compound was demonstrated to repress the transcriptional activity of HIF-1 α by disrupting p300 binding to HIF-1 α and additionally assisting in the acceleration of HIF-1 α degradation (Kim, Yeo et al. 2006). The effect of inhibiting HIF-1 α via YC-1 on CD4⁺ T cells in normoxia was determined. PBMC from healthy donors were stimulated in the presence of anti-CD3 and YC-1 (10 – 50 nM) for 5 days. Cells were stimulated with PMA, ionomycin and brefeldin-A for 5 h and stained with fluorochrome-conjugated antibodies specific for CD4, CD161, IL-17 and IFN- γ and analysed by flow cytometry. The results show no significant change in Th17 lineage cells (CD4⁺CD161⁺), CD4⁺IL-17⁺ cells, CD4⁺IFN- γ ⁺ cells or transitioning exTh17 cells (CD4⁺IL-17⁺IFN- γ ⁺) following YC-1 treatment (Figure 5.11A-D). Additionally, the inhibition of HIF-1 α in Treg cells was examined. Cells were stimulated as stated and stained immediately for CD4, CD25, CD127 and Foxp3 fluorochrome-conjugated antibodies. The results show no significant change in the frequency of Treg cells (CD4⁺CD25⁺CD127^{Lo}Foxp3⁺) following inhibition of HIF-1 α with YC-1 treatment (Figure 5.12).

In summary, YC-1 appeared to have no effect on CD4⁺ T cell survival or expansion in normoxia. However it is possible that YC-1 does not in fact affect basal HIF-1 α expression levels in T cells.

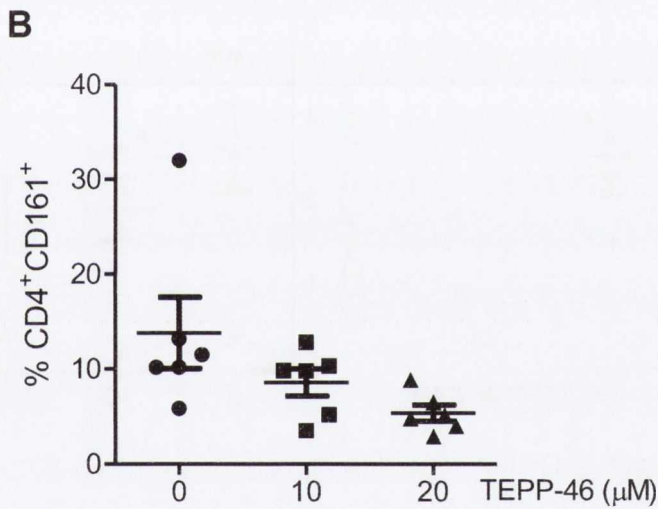
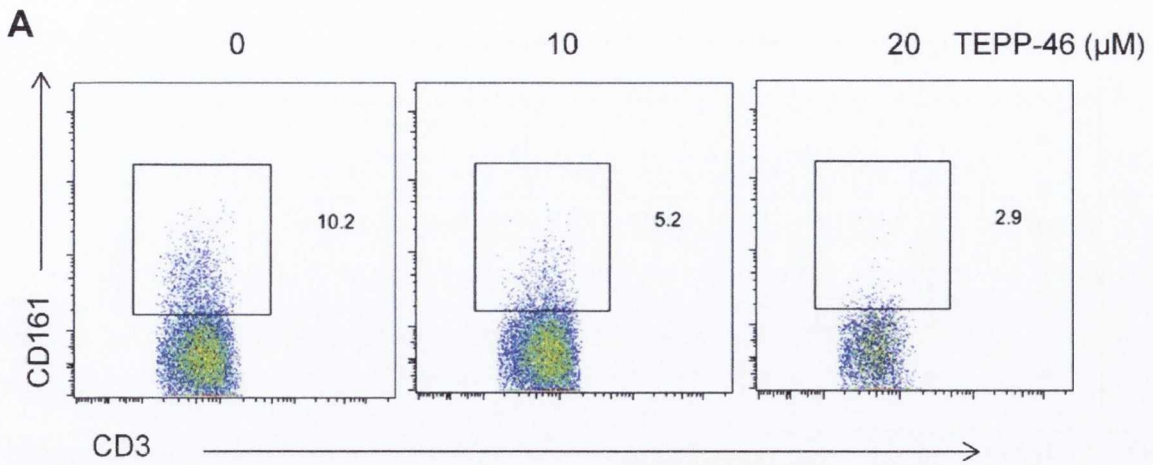


Figure 5.8 The effect of TEPP-46 on the frequency of CD4⁺CD161⁺ T cells.

Healthy donor PBMC were stimulated with anti-CD3 and TEPP-46 (0 – 20 μM) for 5 days. Cells were re-stimulated with PMA, ionomycin and brefeldin-A for 5 h and stained with fluorochrome-conjugated antibodies specific for CD4 and CD161. The cells were analysed by flow cytometry. Representative dot plots gated on CD3⁺CD8⁻ (CD4) T cells show CD3 vs CD161 staining in the presence of TEPP-46 as indicated (A). The graph shows the frequency of CD3⁺CD8⁻CD161⁺ T cells in the presence of TEPP-46 (n=6).

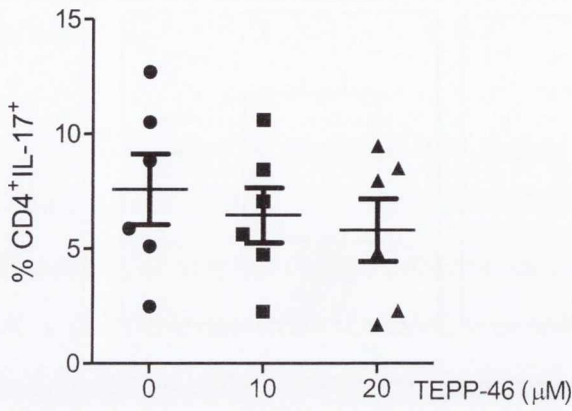
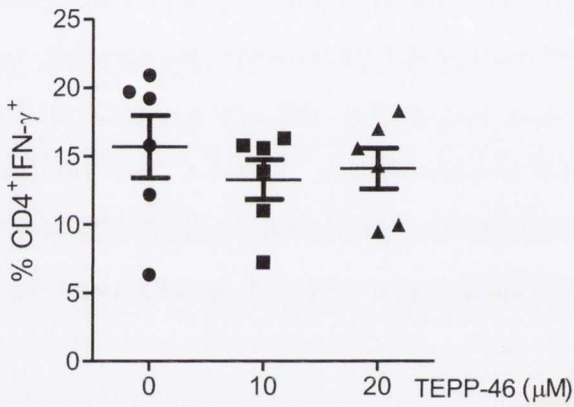
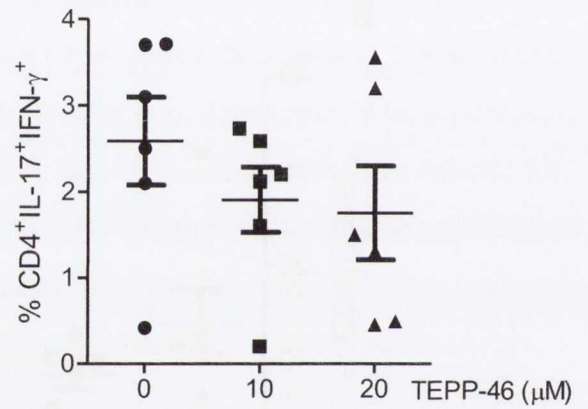
A**B****C**

Figure 5.9 The effect of TEPP-46 on the frequency of CD4⁺IL-17⁺, CD4⁺IFN-γ⁺ and CD4⁺IL-17⁺IFN-γ⁺ T cells.

Healthy donor PBMC were stimulated with anti-CD3 in the presence of TEPP-46 (0 – 20 μM) for 5 days. Cells were re-stimulated with PMA, ionomycin and brefeldin-A for 5 h and stained with fluorochrome-conjugated antibodies specific for CD3, CD8 and intracellular cytokines IL-17 and IFN-γ. The cells were analysed by flow cytometry and gated on CD3⁺, CD8⁻ (CD4) T cells. The results represent the frequency of CD4⁺IL-17⁺, CD4⁺IFN-γ⁺ and CD4⁺IL-17⁺IFN-γ⁺ T cells in the presence or absence of TEPP-46 (n=6 separate experiments).

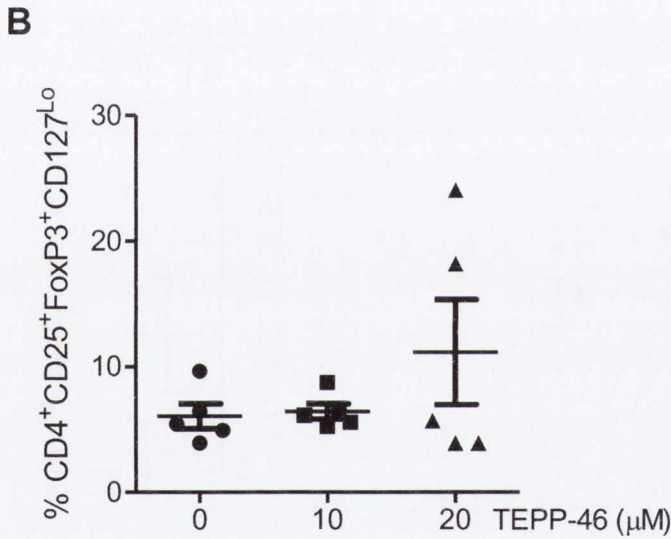
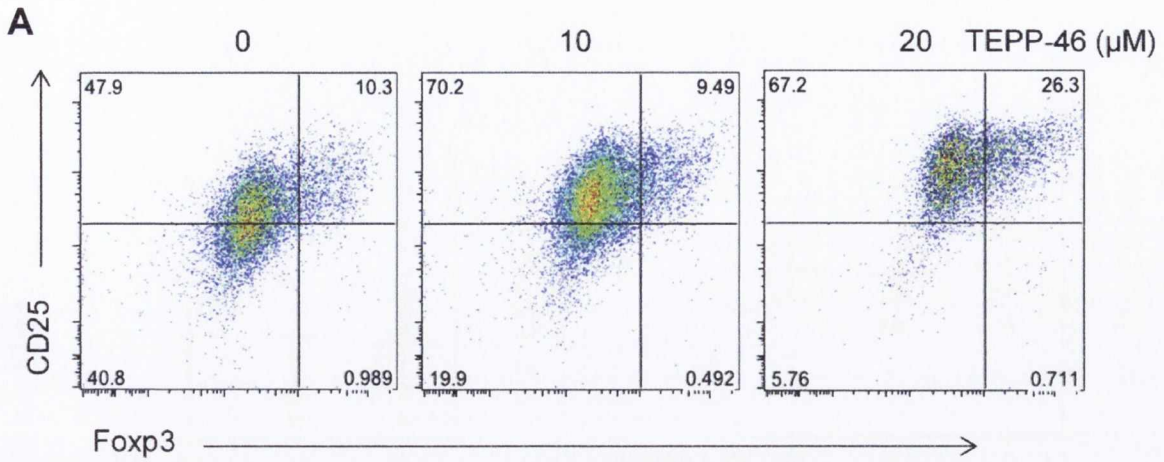


Figure 5.10 The effect of TEPP-46 on the frequency of Treg cells.

Healthy donor PBMC were stimulated with anti-CD3 in the presence of TEPP-46 (0 – 20 μM) for 5 days. Cells were stained with fluorochrome-conjugated antibodies specific for CD4, CD25, CD127 and Foxp3 and analysed by flow cytometry. Representative dot plots gated on CD4⁺ T cells show CD25 vs Foxp3 staining in the presence or absence of TEPP-46 (A). The graph shows the frequency of CD4⁺CD25⁺CD127^{Lo}Foxp3⁺ Treg cells in the presence or absence of TEPP-46 (n=5 separate experiments).

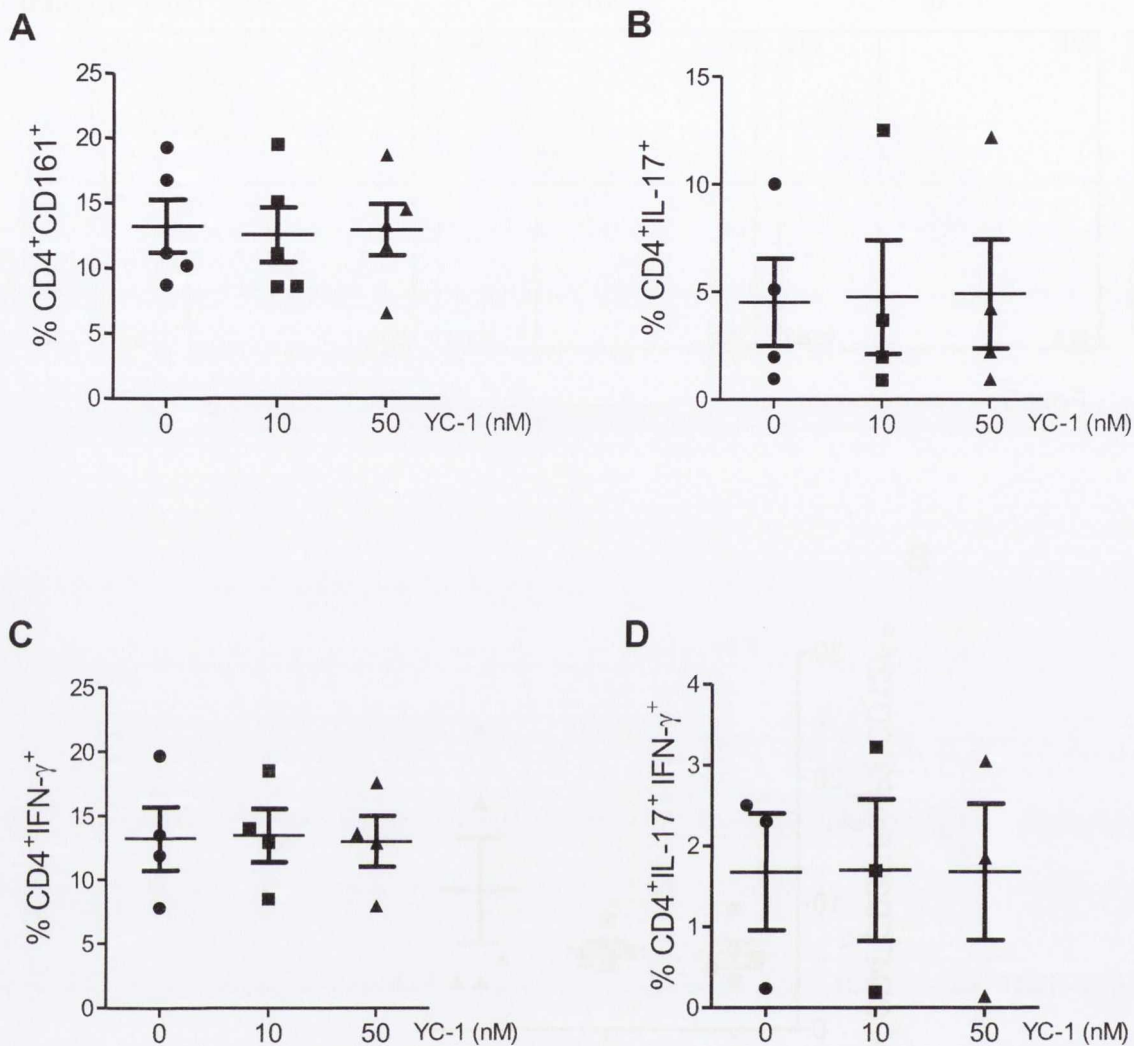


Figure 5.11 The effect of YC-1 on the frequency of CD4⁺CD161⁺, CD4⁺IL-17⁺, CD4⁺IFN- γ ⁺ and CD4⁺IL-17⁺IFN- γ ⁺ T cells.

PBMC from healthy donors were stimulated in the presence of anti-CD3 and YC-1 (10 – 50 nM) for 5 days. Cells were stimulated with PMA, ionomycin and brefeldin-A for 5 h and stained with fluorochrome-conjugated antibodies specific for CD3, CD8, CD161 and intracellular cytokines IL-17 and IFN- γ . The cells were analysed by flow cytometry gated CD3⁺CD8⁻ (CD4) T cells. The graphs show the frequency of CD4⁺CD161⁺, CD4⁺IL-17⁺, CD4⁺IFN- γ ⁺ and CD4⁺IL-17⁺IFN- γ ⁺ T cells in the presence of increasing concentrations of YC-1 (n=3).

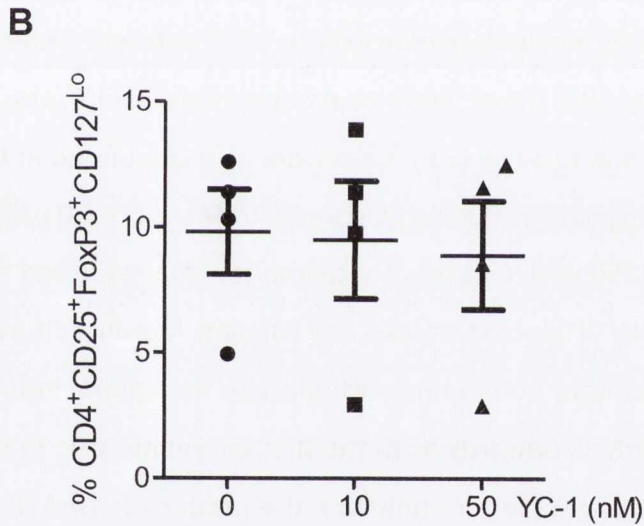
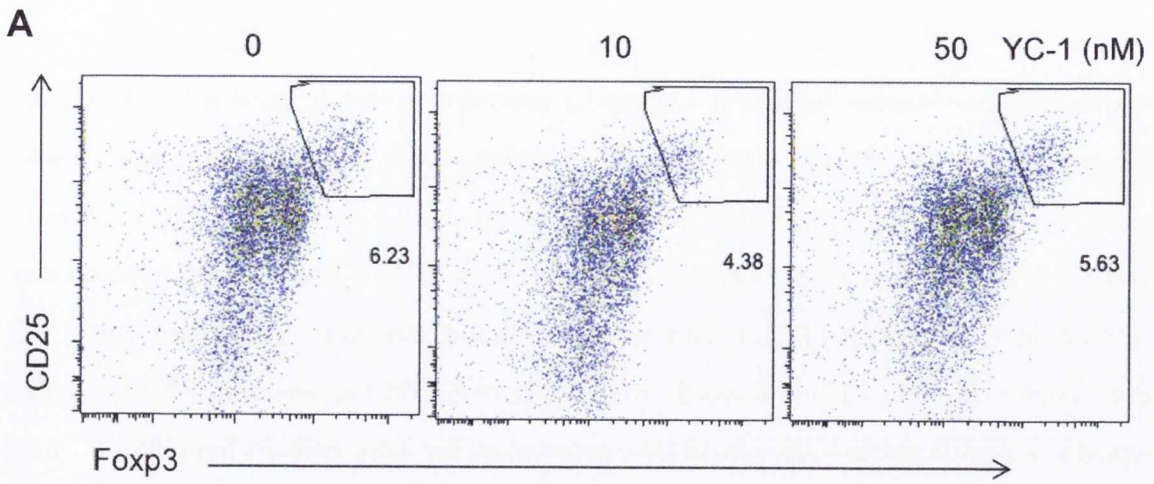


Figure 5.12 The effect of YC-1 on the frequency of Treg cells.

PBMC from healthy donors PBMC were stimulated in the presence of anti-CD3 and YC-1 (10 – 50 nM) for 5 days. Cells were stained with fluorochrome-conjugated antibodies specific for CD4, CD25, CD127 and Foxp3. The cells were analysed by flow cytometry and gated on CD4⁺ T cells. Representative dot plots show CD25 vs FoxP3 staining in the presence or absence of YC-1. The graph shows the frequency of CD4⁺CD25⁺CD127^{Lo}Foxp3⁺ T cells in each treatment group (n=4).

5.2.7. The manipulation of metabolic pathways in hypoxia and the effect on T cell subsets.

As mentioned previously, hypoxia is known to promote a switch towards a glycolytic metabolism through HIF-1 α stabilization. In partnership, low oxygen has been demonstrated to reduce oxidative phosphorylation and Krebs cycle rates, which contribute to a lower respiratory rate (Galkin, Higgs et al. 2007). The effect of hypoxia on the metabolism of human CD4⁺ T cells is understudied. Previous results presented in chapter 3 have revealed a trend towards an increase in GLUT1 expression for CD4⁺ T cells in hypoxia, a significant increase in GLUT1 expression for Treg cells in hypoxia and no significant increase in GLUT1 for CD161⁺ T cells. To further understand the metabolic pathways utilized by T cells in hypoxia, metabolism was manipulated via treatment with metabolic inhibitors and promoters in hypoxia in vitro.

Initially, the effect of metabolic manipulation on CD4⁺IL-17⁺ T cells was examined. Human PBMC were isolated from healthy donor buffy coats and stimulated in the presence of anti-CD3 in normoxia (21%) and hypoxia (5%). Cells were also stimulated in the presence of metabolic compounds in hypoxia, including glucose (25 mM), 2-DG (10 μ M), oligomycin A (50 ng/ml) and rotenone (250 nM). Glucose is required for glycolysis, and extra glucose could stimulate this pathway if glucose stocks are running low in culture. 2-DG is a competitive inhibitor of glycolysis, competing with glucose for uptake into the cell and consequently inhibiting glycolysis onwards from the first enzymatic step in the pathway. Oligomycin A is an ATP synthase inhibitor, inhibiting the production of ATP by oxidative phosphorylation, resulting in its inhibition and a subsequent increase in glycolysis. Finally, rotenone is a complex I inhibitor of the electron transport chain, which inhibits the conversion of NADH to ATP, resulting in an inhibition of oxidative phosphorylation. After 4 days, cells were stimulated with PMA, ionomycin and brefeldin A for 5 h and stained with fluorochrome-conjugated antibodies specific for CD3, CD8 and IL-17. The cells were analysed by flow cytometry and each experiment was normalised to normoxia. The frequency of CD4⁺IL-17⁺ cells was unchanged in the presence of each compound compared to untreated cells (Figure 5.13) (n=6). This data shows that the manipulation of metabolism using the compounds indicated does not affect the inhibition of CD4⁺IL-17⁺ T cells observed in hypoxia in vitro.

The effect of metabolic manipulation on the survival and expansion of Treg cells in hypoxia was examined next. Cells were treated as stated in hypoxia, and stained after 4

days with CD4, CD25, CD127 and Foxp3. This result revealed no significant change in Treg cell frequencies in hypoxia following glucose, 2-DG or oligomycin A treatment (Figure 5.14 A-C). However, rotenone treatment resulted in a significant decrease in Treg cell frequencies (Figure 5.14 D) ($p < 0.05$). This suggests a possible role for oxidative phosphorylation metabolism in the expansion of Treg cell frequencies observed in hypoxia.

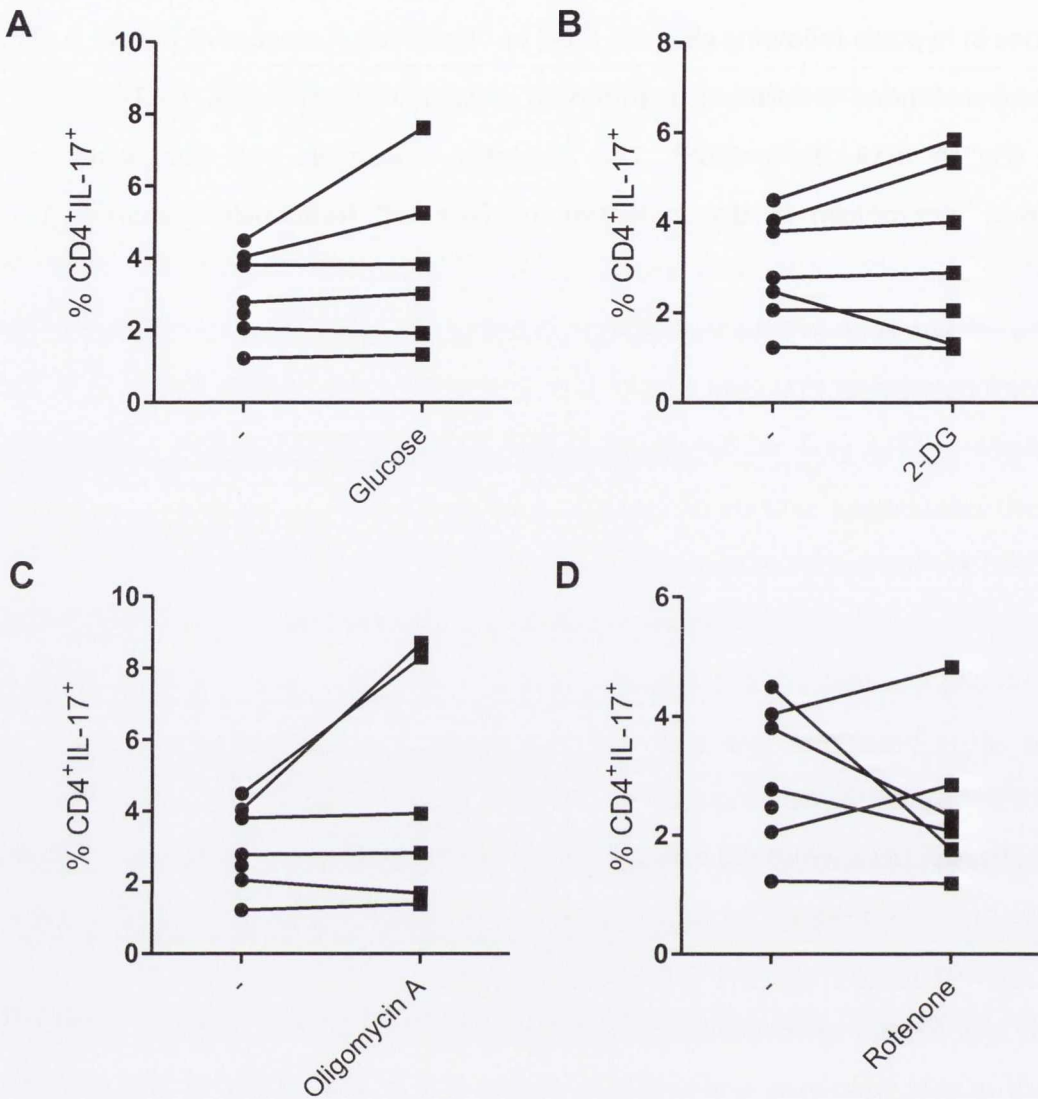


Figure 5.13. The manipulation of metabolism in hypoxia and the effect on CD4⁺IL-17⁺ T cell frequencies.

Healthy donor PBMC were stimulated with anti-CD3 in normoxia (21%) and hypoxia (5%) oxygen levels, with the addition of metabolic compounds in hypoxia: glucose (25 mM), 2-DG (10 μ M), oligomycin A (50 ng/ml) and rotenone (250 nM). After 4 days, cells were stimulated with PMA, ionomycin and brefeldin-A, and stained with fluorochrome-conjugated antibodies specific for CD3, CD8 and IL-17. The cells were analysed by flow cytometry and gated on CD3⁺CD8⁻ (CD4) T cells. The graphs show the frequencies of CD3⁺CD8⁻IL-17⁺ T cells in hypoxia with and without the addition of metabolic compounds; the data was normalised to that for normoxia (n=6).

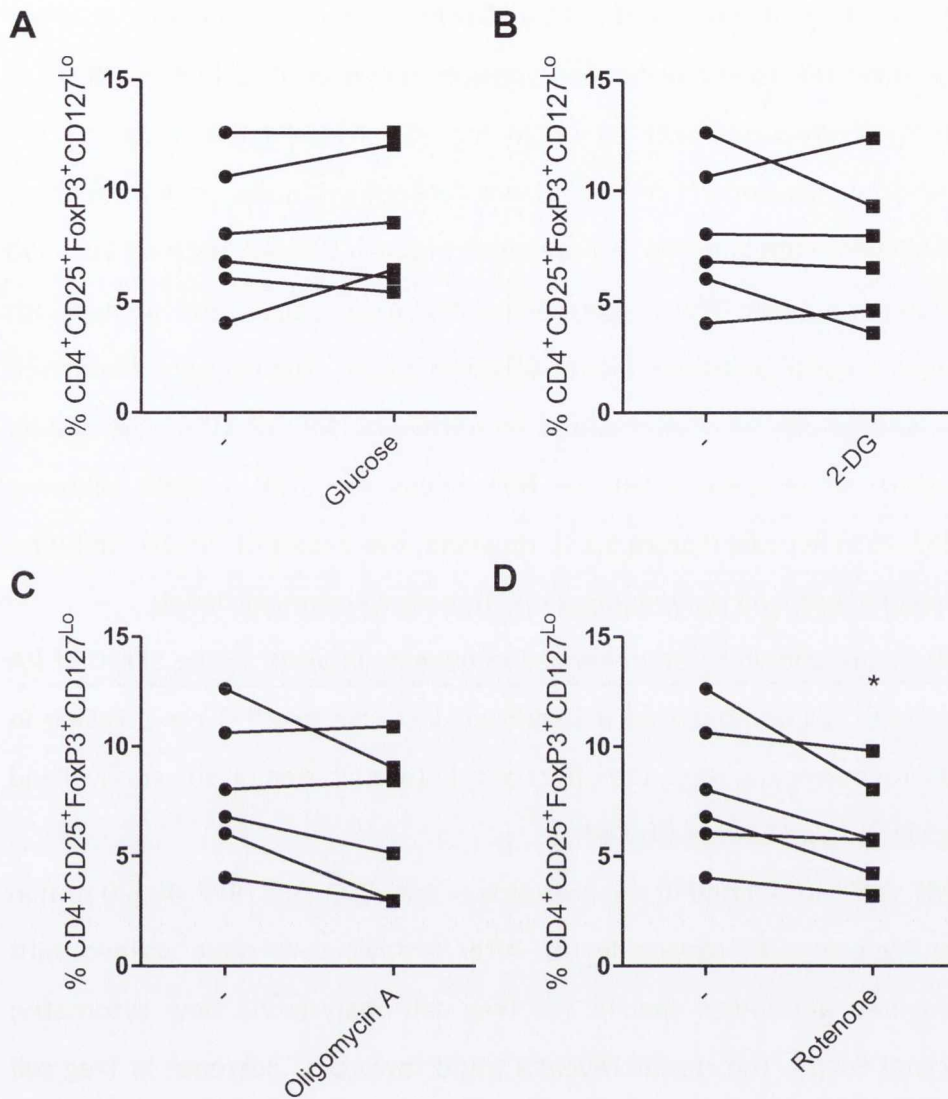


Figure 5.14. The manipulation of metabolism in hypoxia and the effect on Treg cell expansion.

Healthy donor PBMC were stimulated with anti-CD3 in normoxia (21%) and hypoxia (5%) oxygen levels, with the addition of metabolic compounds in hypoxia: glucose (25 mM), 2-DG (10 μ M), oligomycin A (50 ng/ml) and rotenone (250 nM). After 4 days, cells were stained with fluorochrome-conjugated antibodies specific for CD4, CD25, CD127 and Foxp3 and analysed by flow cytometry. The graphs show the frequencies of CD4⁺CD25⁺CD127^{Lo}Foxp3⁺ Treg cells in hypoxia with and without the addition of metabolic compounds; normalized relative to normoxia (n=6). Statistical differences in the mean between the groups were determined by a paired, two-tailed t test; *p<0.05.

5.2.8. The effect of TEPP-46 treatment on CD4⁺ T cell subsets in hypoxia.

HIF-1 α expression is significantly increased in CD4⁺ T cells in hypoxic conditions. TEPP-46 has been shown to inhibit HIF-1 α in murine macrophages; however, its effect on HIF-1 α in human CD4⁺ T cells is unknown. Since HIF-1 α was increased in hypoxia, the effect of TEPP-46 treatment on HIF-1 α expression in CD4⁺ T cells was determined in this environment.

Healthy donor PBMC were stimulated in the presence of anti-CD3 and TEPP-46 (10 – 50 μ M) in normoxic (21%) or hypoxic (5%) oxygen levels. After 4 days, cells were stained with fluorochrome-conjugated antibodies specific for CD4 and HIF-1 α . The cells were analysed by flow cytometry and results were normalized to normoxia (MFI of 100). The results show a trend towards a decrease in HIF-1 α MFI values for CD4⁺ T cells following treatment with TEPP-46 in hypoxia (Figure 5.15). However, the extent of HIF-1 α inhibition with TEPP-46 was insufficient, and only reduced HIF-1 α back to normoxic levels.

Treg cells in this study are shown to be enhanced in hypoxia in vitro, in the SFMC of RA patients and also, Treg cells demonstrate a significant increase in HIF-1 α expression in hypoxia compared with normoxia. Next, the effect of HIF-1 α inhibition on the survival and expansion of Treg cells in hypoxia was studied.

Healthy donor PBMC were stimulated in the presence of anti-CD3 and TEPP-46 (20 μ M) in normoxic (21%) or hypoxic (5%) oxygen levels. After 4 days, cells were stained with fluorochrome-conjugated antibodies specific for Treg cell analysis via flow cytometry; CD4, CD25, CD127 and Foxp3. The results reveal a trend towards a decrease in Treg cell (CD4⁺CD25⁺CD127^{lo}Foxp3⁺) populations when stimulated in the presence of TEPP-46 compared with untreated cells in hypoxia (Figure 5.16). However, this experiment was performed twice and therefore more experimentation will need to be performed in order to elucidate the role of TEPP-46 in Treg cell survival or expansion in hypoxia in vitro. This result may suggest a role for HIF-1 α in the expansion of Treg cells in hypoxia. However, TEPP-46 does not inhibit HIF-1 α significantly in CD4⁺ T cells and therefore may not be an effective HIF-1 α inhibitor in this system. The result observed for Treg cells treated with TEPP-46 in hypoxia could correlate with the ability of TEPP-46 to inhibit glycolysis via PKM2 activation. Alternatively, it could be a combination of both HIF-1 α and glycolytic inhibition.

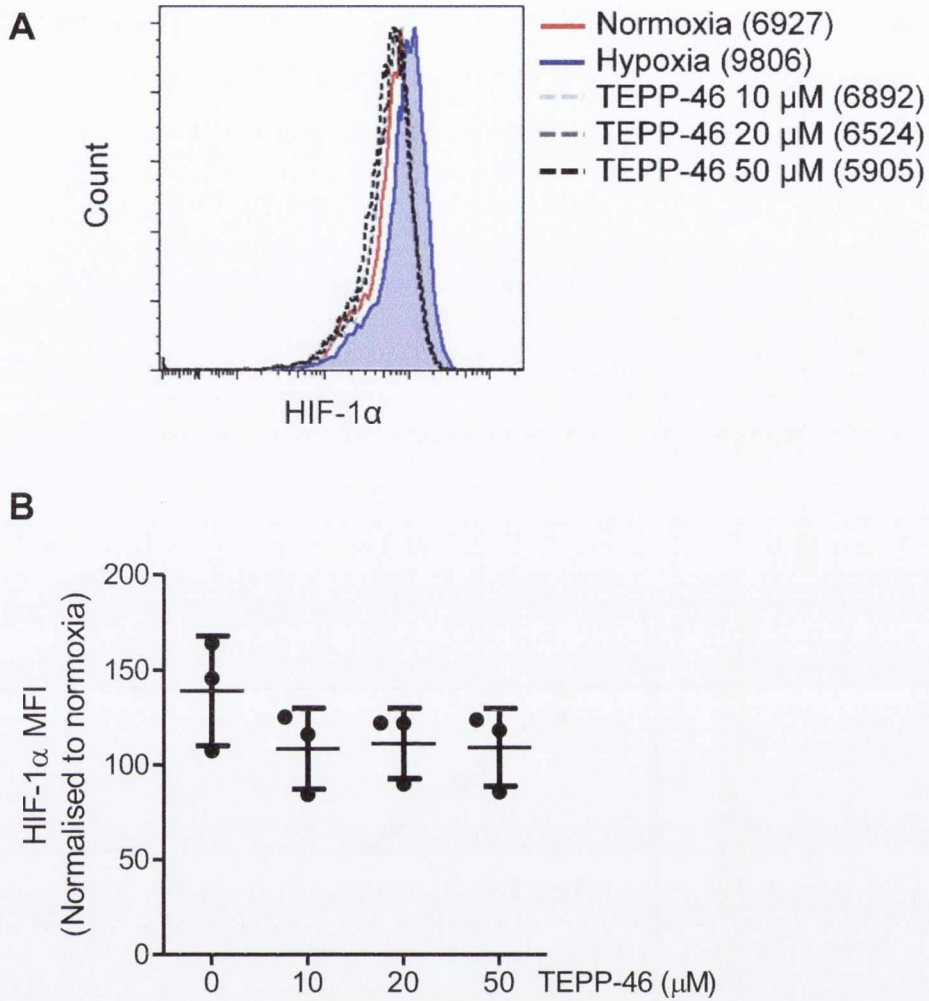


Figure 5.15 The effect of TEPP-46 on HIF-1 α expression by CD4⁺ T cells in hypoxia.

Healthy donor PBMC were stimulated with anti-CD3 in the presence of TEPP-46 (0 – 50 μ M) in normoxic (21%) or hypoxic (5%) oxygen levels. After 4 days, cells were stained with fluorochrome-conjugated antibodies specific for CD4 and HIF-1 α and analysed by flow cytometry. Representative histograms gated on CD4⁺ T cells show HIF-1 α staining in normoxia and in hypoxia in the presence or absence of TEPP-46 (A). The graph shows HIF-1 α MFI values for CD4⁺ T cells in hypoxia with and without TEPP-46, normalised to the those for normoxia (n=3 separate experiments).

5.2.9 The effect of inhibiting HIF-1 α via YC-1 treatment on the frequency of Treg cells in hypoxia.

YC-1 is a known inhibitor of HIF-1 α and has been shown to decrease HIF-1 α protein expression in hypoxia in HT1080 cells (fibrosarcoma cell line) and h1299 cells (non-small lung cell carcinoma cell line) (Li, Shin et al. 2008). However, the effects of YC-1 on human cells have not yet been studied. As HIF-1 α is increased in hypoxia, the effect of YC-1 on HIF-1 α inhibition was examined in this setting by flow cytometry.

PBMC from healthy donors were stimulated in the presence of anti-CD3 in normoxia (21%) and hypoxia (5%). Additionally, cells in hypoxia were treated with increasing concentrations of YC-1 (10 – 100 nM). After 4 days, cells were stained for CD4 cells and analysed by flow cytometry. Each experiment is normalized to CD4⁺HIF-1 α MFI values in normoxia (100 MFI). The frequencies of CD4⁺HIF-1 α ⁺ T cells are significantly decreased following YC-1 treatment at 10 nM ($p < 0.05$) (Figure 5.17). However, much like TEPP46 treatment, HIF-1 α is not completely inhibited. This indicates YC-1 as a moderate inhibitor of HIF-1 α protein expression in CD4⁺ T cells in hypoxia.

As mentioned previously in this study, Treg cells are enriched in hypoxia and display a significant increase in HIF-1 α expression. Therefore, the effect of HIF-1 α inhibition on the increased frequency of Treg cells, observed in hypoxia, was examined. Healthy donor PBMC were stimulated as stated above with YC-1 (10 and 50 nM). Cells were stained with fluorochrome-conjugated antibodies specific for the analysis of Treg cells by flow cytometry; CD4, CD25, CD127 and Foxp3. The frequency of Treg cells (CD4⁺CD25⁺CD127^{Lo}Foxp3⁺) in hypoxia was unchanged following YC-1 treatment (Figure 5.18). This result suggests that HIF-1 α may not play a solitary role in the expansion of Treg cells in hypoxia. However, as YC-1 treatment only moderately inhibits HIF-1 α , the remaining HIF-1 α may be sufficient to maintain the specific transcriptional effects of this protein.

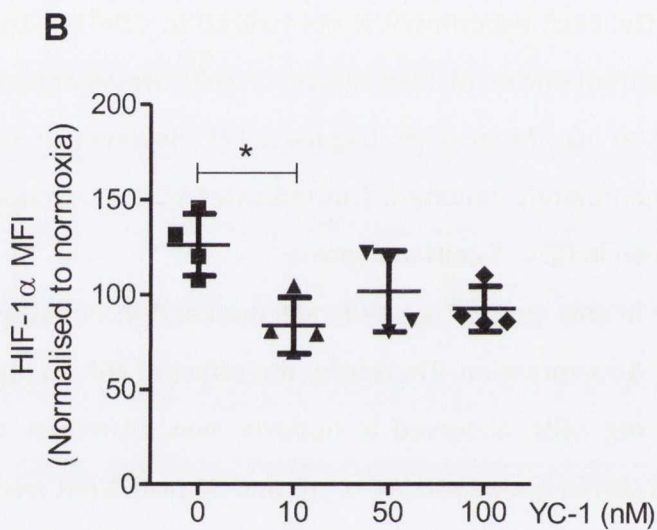
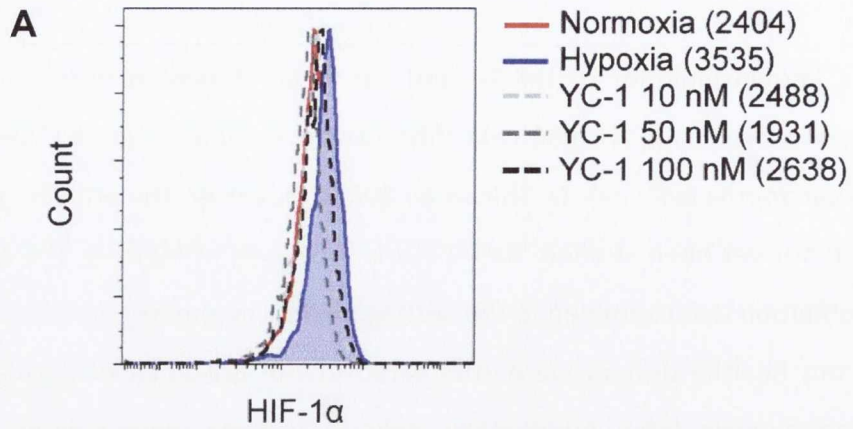


Figure 5.17 The effect of YC-1 on HIF-1 α expression by CD4⁺ T cells in hypoxia.

Healthy donor PBMC were stimulated with anti-CD3 in the presence or absence of YC-1 (0 – 100 nM) in normoxic (21%) or hypoxic (5%) oxygen levels. After 4 days, cells were stained with fluorochrome-conjugated antibodies specific for CD4 and HIF-1 α . The cells were analysed by flow cytometry and results were normalized to those for normoxia. The histogram shows HIF-1 α expression in CD4⁺ T cells in normoxia, or in hypoxia with increasing concentrations of YC-1 (A). The graph shows HIF-1 α MFI values for CD4⁺ T cells cultured in hypoxia with the concentrations of YC-1 indicated (n=4) (B). Statistical differences in the mean between the groups were determined by a One-way ANOVA, with Tukeys Multiple Comparison Test; *p<0.05

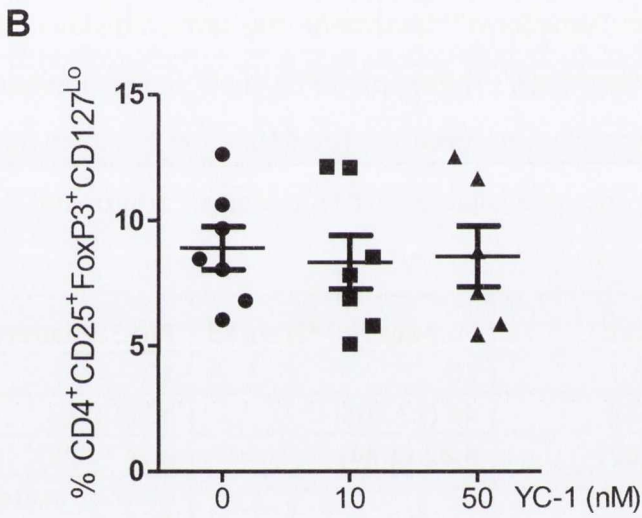
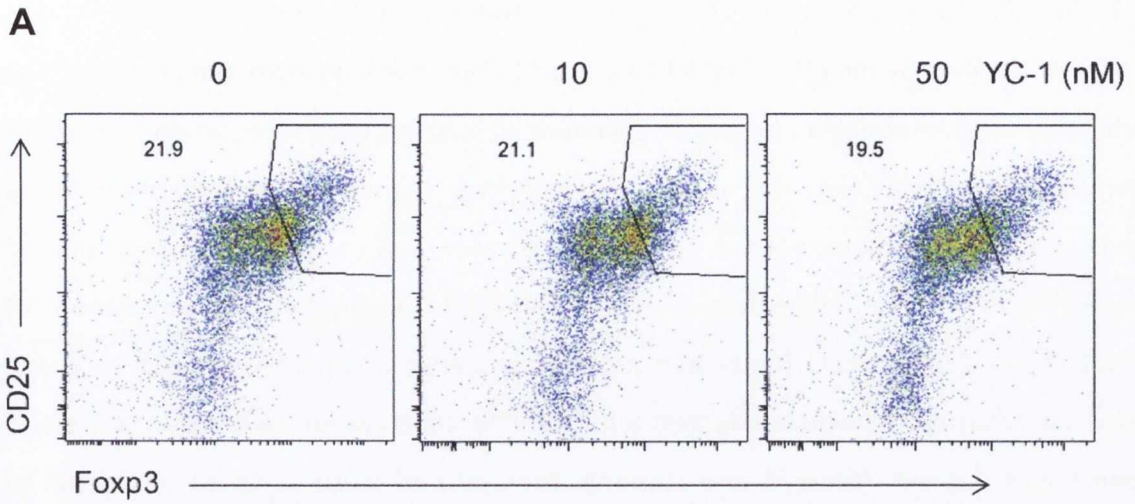


Figure 5.18 The effect of YC-1 on the frequency of Treg cells in hypoxia.

Healthy donor PBMC were stimulated with anti-CD3 in the presence of YC-1 (0 - 50 nM) in normoxic (21%) or hypoxic (5%) oxygen levels. After 4 days, cells were stained with fluorochrome-conjugated antibodies specific for CD4, CD25, CD127 and Foxp3. The cells were analysed by flow cytometry. Representative dot plots show CD25 vs FoxP3 staining on CD4 gated cells cultured in hypoxia with the concentrations of YC-1 indicated (A). The graph shows the frequencies of CD4⁺CD25⁺CD127^{Lo}Foxp3⁺ Treg cells, normalized to those for normoxia (B).

5.2.10 Details of untreated and Fumaderm™-treated psoriasis patients

Fumarate was initially hypothesised to mediate its immunomodulatory effects in part via modulation of metabolism. However following Seahorse experimentation (data not shown) this possibility was discounted. Nonetheless, the in vivo immunomodulatory effects of Fumaderm have not yet been demonstrated and so these were investigated here in the psoriasis patient groups shown in Table 5.1. Initially two separate groups of unrelated psoriasis patients (untreated patients or patients which have been receiving Fumaderm treatment) were compared with healthy controls for reference. Untreated patients had not yet received any systemic therapy and were sampled just prior to commencing phototherapy. In addition, a single group of psoriasis patients were examined both pre- and post-Fumaderm™ treatment (the same individual patient before and after Fumaderm™ treatment). These patients may have previously received phototherapy or systemic therapy in some cases. The PASI score is shown for the patients pre- treatment, scores were not yet available post-Fumaderm™ treatment.

	Untreated	Fumaderm™Treated	Pre-Fumaderm™
Number	8	10	10
Mean Age (SD)	43 (13.70)	49 (17.30)	40 (14.05)
Mean PASI (SD)	8.04 (5.02)	5.82 (2.84)	8.76 (2.26)
Treatment	Nil	Fumaderm™	Methotrexate, 1 wk prior to blood sampling (1 patient)

Table 5.1 Details of psoriasis patient groups

5.2.11 CD4⁺CD161⁺ cells in psoriasis and the effect of Fumaderm™ treatment

Fumaderm™ has been approved for the treatment of psoriasis in Germany since 1994. However its mechanism of action in vivo in patients is yet to be elucidated. The anti-inflammatory effects of Fumaderm™ are thought to act through increased HO-1 via NRF-2 transcriptional activity (Linker, Lee et al. 2011). T cells play a key role in the pathogenesis of psoriasis, and so the effect of Fumaderm™ treatment on the expansion and survival of T cell subsets, in psoriasis patient blood, was investigated in order to inspect a possible role for T cell modulation in the anti-inflammatory effects of Fumaderm™.

Initially, the effect of Fumaderm™ on Th17 lineage cells was examined. Blood from healthy donors, psoriasis patients who have not yet received treatment (Untreated) and

psoriasis patients receiving Fumaderm™ were processed and PBMC were isolated. Cells were stimulated with PMA, ionomycin and brefeldin A for 5 h and stained with fluorochrome-conjugated antibodies specific for CD3, CD8 and CD161, and analysed by flow cytometry. The gating strategy used for analysing cytokine production by CD4⁺ T cells is shown in Figure 5.19.

The frequency of CD4⁺CD161⁺ Th17 lineage cells trended towards an increase in untreated psoriasis patients compared with Fumaderm™-treated patients or healthy controls; however, this was not significant (Figure 5.20).

5.2.12 Increased frequencies of CD4⁺IL-17⁺ and CD4⁺IL-17⁺IFN-γ⁺ T cells in untreated psoriasis patients compared with Fumaderm™-treated psoriasis patients and healthy controls

IL-17 and IFN-γ cytokines have been implicated in psoriasis pathogenesis. Therefore, expression of these cytokines by CD4⁺ T cells was investigated for healthy controls, untreated and Fumaderm™- treated patients.

Blood from healthy donors, untreated psoriasis patients and psoriasis patients receiving Fumaderm™ were processed and PBMC were isolated. Cells were stimulated with PMA, ionomycin and brefeldin A for 5 h to examine cytokine expression. Cells were stained with fluorochrome-conjugated antibodies specific for CD3, CD8, IL-17 and IFN-γ, and analysed by flow cytometry. Representative dot plots were gated on CD3⁺CD8⁻ (CD4) T cells. The frequency of CD4⁺IL-17⁺ T cells (CD3⁺CD8⁻IL-17⁺) was significantly increased in the untreated group compared with healthy donors ($p < 0.05$) and Fumaderm™-treated patients ($p < 0.01$) (Figure 5.21 A and C).

The frequency of CD4⁺ T cells expressing both IL-17 and IFN-γ was also examined in psoriasis patients. These cells, which are in transition to becoming exTh17 cells, have been implicated in autoimmunity. The frequency of CD3⁺CD8⁻IL-17⁺IFN-γ⁺ T cells was significantly increased in the untreated psoriasis patient group compared with both healthy controls ($p < 0.001$) and Fumaderm™-treated patients ($p < 0.001$) (Figure 5.21 B and D).

Psoriasis was originally thought of as a Th1 cell-mediated disease, as increased cytokines from the Th1 cell-phenotype, such as IL-12 and IFN-γ, were observed in psoriasis patients (Lew, Bowcock et al. 2004). Thus the frequency of IFN-γ⁺ T cells in the blood of psoriasis patients and Fumaderm™-treated patients was investigated. Cells were stimulated as

previously stated, stained with CD3, CD8 and IFN- γ , and analysed by flow cytometry. The frequency of CD3⁺CD8⁺IFN- γ ⁺ T cells trended towards an increase in untreated patients compared with healthy donors, and no trend was observed between untreated and total Fumaderm™-treated patients (Figure 5.21 E).

This data collectively suggests a role for IL-17⁺ and IL-17⁺IFN- γ ⁺ CD4 T cells in psoriasis, and a role for Fumaderm™ treatment in the inhibition of these cell subsets.

5.2.13 Th17 lineage cells and exTh17 cells are increased in untreated patients compared with Fumaderm™-treated patients

Having examined cytokine production in untreated and Fumaderm™ treated psoriasis patients, specific T cell subsets were analysed next. Th17 lineage cells (CD4⁺CD161⁺IL-17⁺), exTh17 cells (CD4⁺CD161⁺IFN- γ ⁺) and Th1 cells (CD4⁺CD161⁻IFN- γ ⁺) were examined in the blood of healthy donors, untreated psoriasis patients and Fumaderm™-treated patients. Cells were stimulated as stated previously (5.2.12) and stained for CD3, CD8, CD161, IL-17 and IFN- γ . A significant increase in Th17 lineage cells was observed in untreated patients compared with Fumaderm™-treated patients ($p < 0.05$) (Figure 5.22 A). Interestingly, the frequencies of fully switched exTh17 cells, expressing both CD161 and IFN- γ were markedly and significantly increased in untreated psoriasis patients when compared with healthy donors ($p < 0.001$). The frequencies of ex-Th17 cells in untreated psoriasis patients were far higher than that of bona-fide Th17 cells and similar to that of Th1 cells. Furthermore, ex-Th17 cells were significantly reduced in psoriasis patients treated with Fumaderm™ compared with untreated patients ($p < 0.05$) (Figure 5.22 B). Finally, Th1 cells (CD4⁺CD161⁻IFN- γ ⁺) were unchanged between healthy, untreated and Fumaderm™-treated patients. This data suggest a role specifically for both Th17 lineage cells and exTh17 cells in the pathogenesis of psoriasis. Furthermore the data demonstrates a role for Fumaderm™ in the inhibition of both bona fide Th17 cells and exTh17 cells in psoriasis patients back to the levels observed in healthy controls. In contrast Th1 cells were not enhanced in untreated psoriasis patients compared with healthy controls, nor reduced in Fumaderm treated patients.

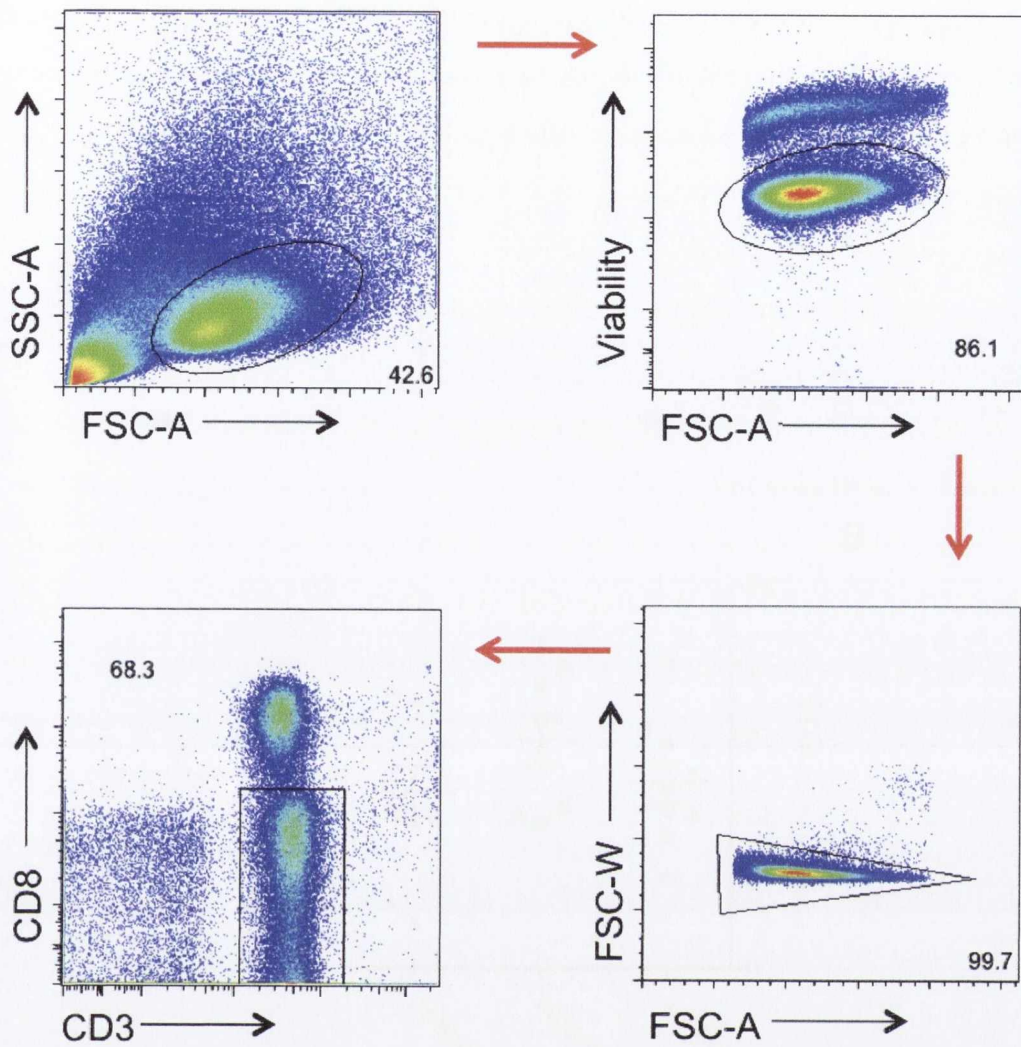


Figure 5.19 The flow cytometric gating strategy for PMA stimulated cells for the analysis of cytokine expression

The lymphocyte population was identified from total PBMC on the basis of SSC-A and FSC-A. Viable cells were gated from the lymphocyte population following gating on the basis of Viability dye and FSC-A. Doublets were removed from the population of interest on the basis of FSC-W and FSC-A. Finally, CD4⁺ T cells were gated on the basis of CD8⁻CD3⁺, since CD4 was down-regulated upon PMA stimulation.

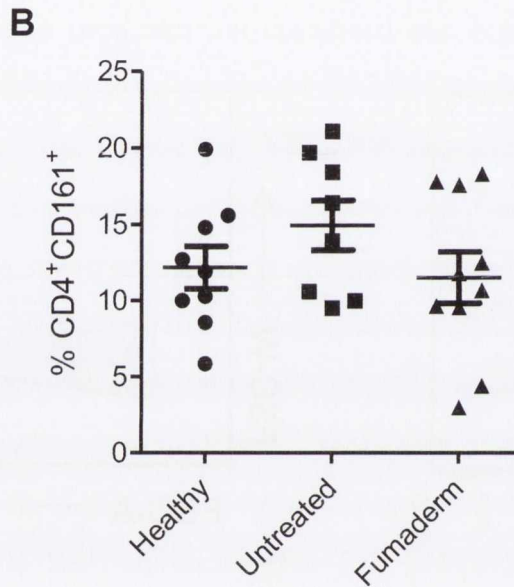
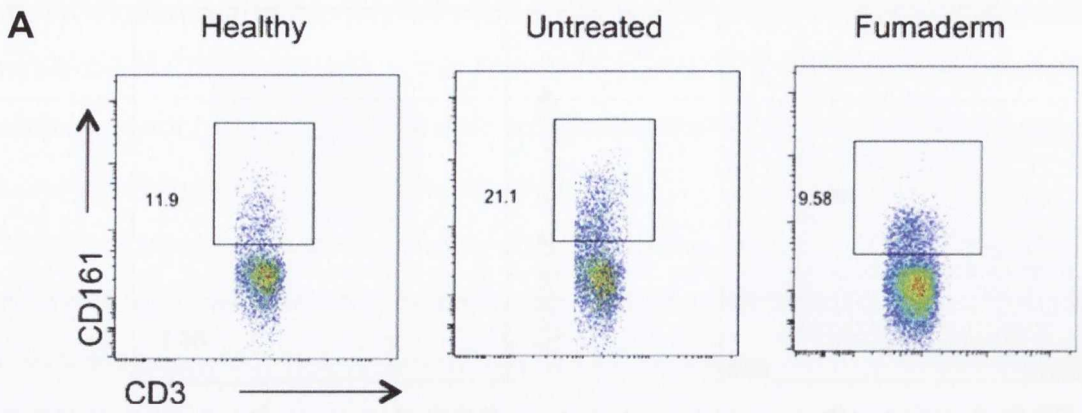


Figure 5.20. The effect of Fumaderm™ on the expression of CD161 in psoriasis patients.

PBMC were isolated from healthy donors, a group of untreated psoriasis patients and a separate group of Fumaderm™-treated psoriasis patients. PBMC were stimulated for 5 h with PMA, ionomycin and brefeldin A, stained with fluorochrome-conjugated antibodies specific for CD3, CD8 and CD161, and analysed by flow cytometry. Representative dot plots are gated on CD3⁺CD8⁻ (CD4) T cells. The frequencies of CD4⁺CD161⁺ cells (A) are presented for healthy, untreated psoriasis patients and Fumaderm™ treated psoriasis patients. The graph represents CD4⁺CD161⁺ cells (B) for healthy, untreated psoriasis patients and Fumaderm™ treated psoriasis patients.

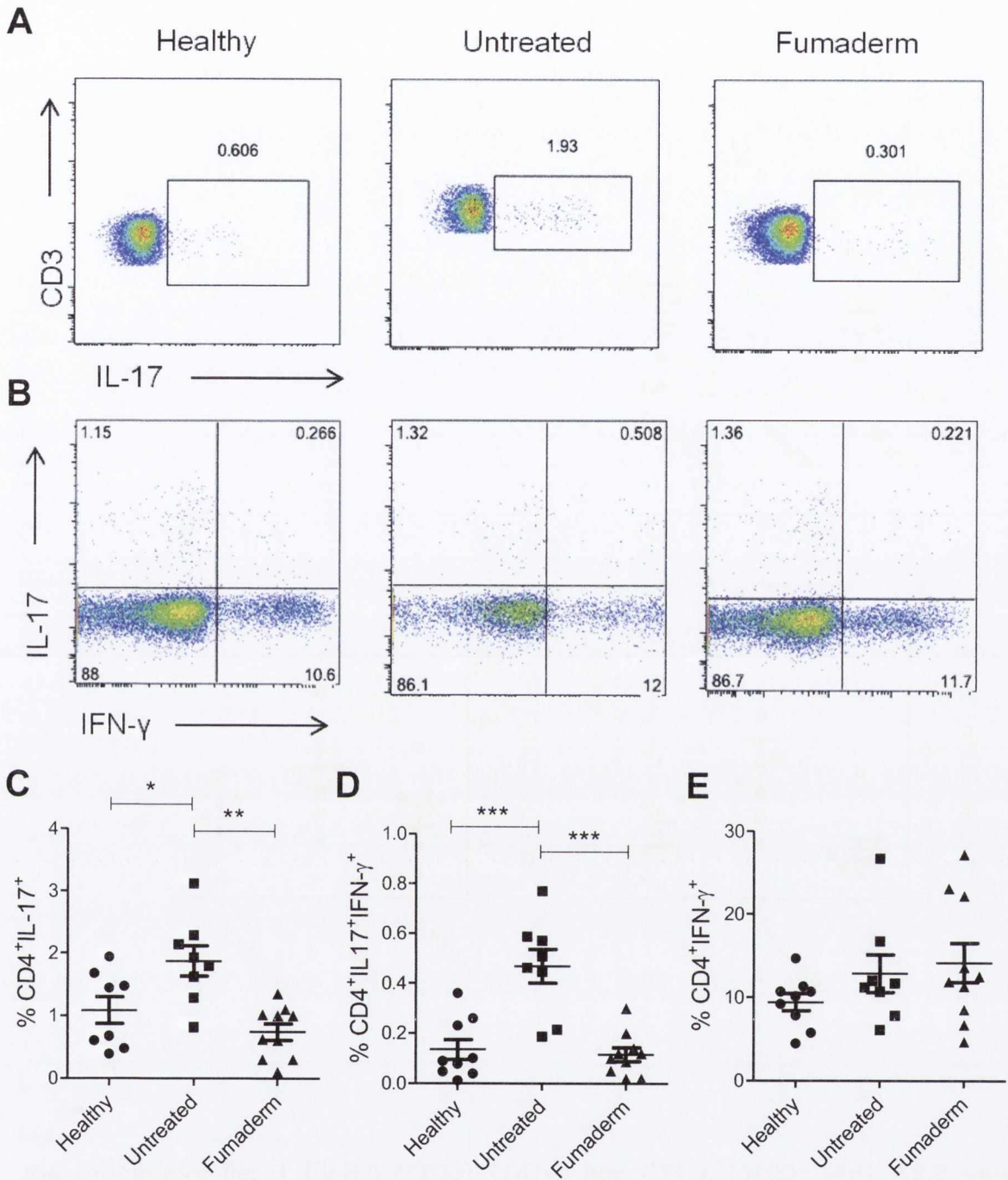


Figure 5.21. The effect of Fumaderm™ treatment on CD4⁺IL-17⁺, CD4⁺IL-17⁺IFN- γ ⁺ and CD4⁺IFN- γ ⁺ T cells in psoriasis patients.

PBMC were isolated from healthy donors, a group of untreated psoriasis patients and a separate group of Fumaderm™-treated psoriasis patients. PBMC were stimulated for 5 h with PMA, ionomycin and brefeldin A, stained with fluorochrome-conjugated antibodies specific for CD3, CD8, IL-17 and IFN- γ , and analysed by flow cytometry. Representative dot plots are gated on CD3⁺CD8⁻ (CD4) T cells. The frequencies of CD4⁺IL-17⁺ cells (A) and CD4⁺T cells examining IL-17⁺ vs IFN- γ ⁺ cells (B) are presented for healthy, untreated psoriasis patients and Fumaderm™ treated psoriasis patients. The graphs represent CD4⁺IL-17⁺ cells (C), CD4⁺IL-17⁺IFN- γ ⁺ cells (D) and CD4⁺IFN- γ ⁺ cells (E). Statistical differences between groups were determined by one-way ANOVA with Tukey's Multiple Comparison test; * $p < 0.05$, ** $p < 0.01$, *** $p < 0.001$.

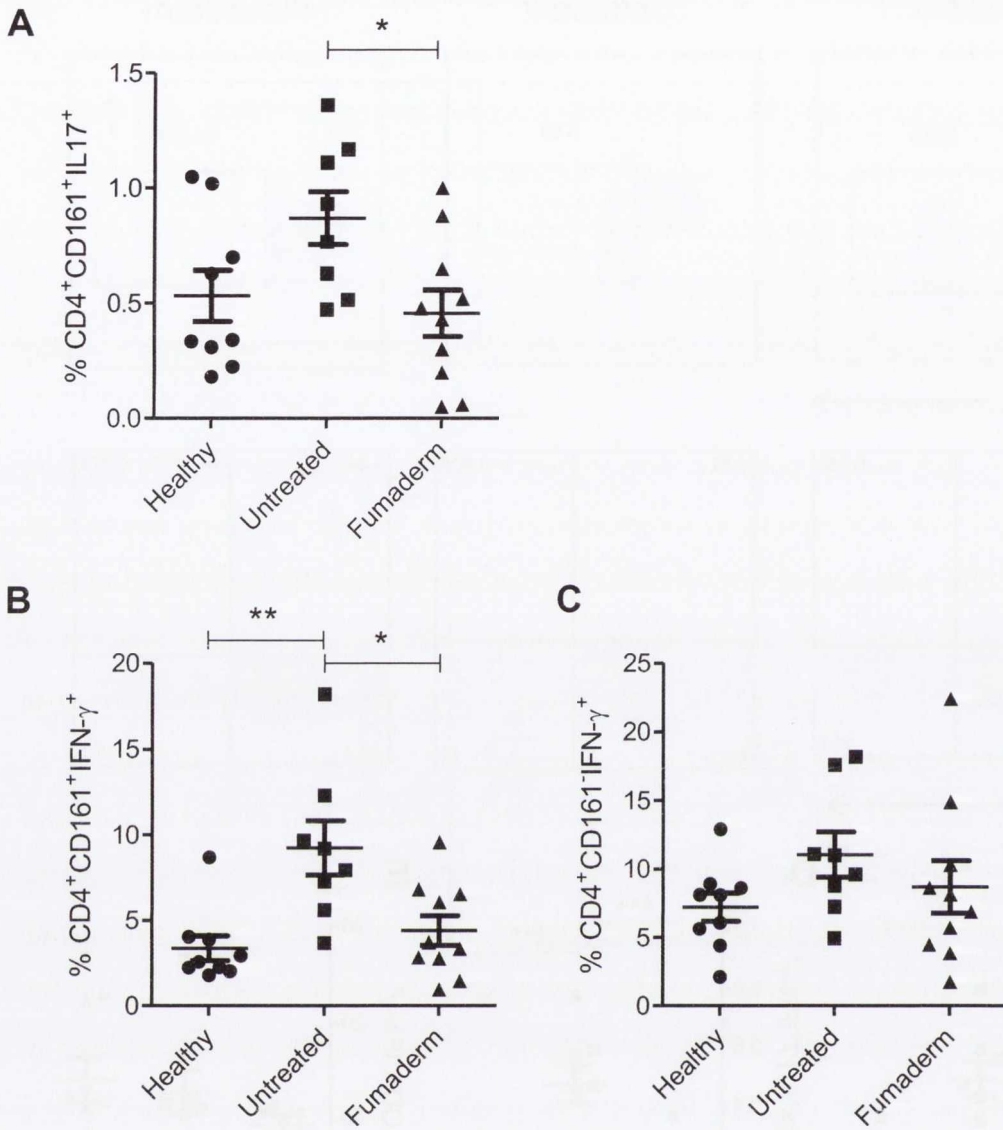


Figure 5.22. Th17 (CD161⁺IL-17⁺) and exTh17 (CD161⁺IFN-γ⁺) T cell frequencies are decreased in Fumaderm[™] treated vs untreated psoriasis patients.

PBMC were isolated from healthy donors, a group of untreated psoriasis patients and a separate group of Fumaderm[™]-treated psoriasis patients and stimulated for 5 h with PMA, ionomycin and brefeldin A. Cells were stained with fluorochrome-conjugated antibodies specific for CD3, CD8, CD161, IL-17 and IFN-γ, and analysed by flow cytometry. CD4 T cells are represented as CD3⁺CD8⁻ T cells. The graphs represent the frequency of Th17 (CD4⁺CD161⁺IL-17⁺) (A), exTh17 (CD4⁺CD161⁺IFN-γ⁺) (B) and Th1 (CD4⁺CD161⁻IFN-γ⁺) T cells (C) for healthy controls, untreated psoriasis patients and Fumaderm[™] treated psoriasis patients. Statistical differences between groups were determined by one-way ANOVA with Tukey's Multiple Comparison test; *p<0.05, **p<0.01.

5.2.14 The effect of Fumaderm™ on GM-CSF and IL-22-expressing CD4⁺ T cells.

Th17 lineage cells produce numerous cytokines, which propagate inflammation in psoriasis. These include GM-CSF (Granulocyte macrophage colony-stimulating factor), known to promote macrophage growth and differentiation, and IL-22, which in conjunction with IL-17 elicits pro-inflammatory effects and results in increased epithelial cell proliferation (Hao 2014). The frequency of CD4⁺ T cells expressing GM-CSF and IL-22 was investigated in healthy donors, untreated psoriasis patients and patients receiving Fumaderm™ treatment.

Healthy donor, untreated patients and Fumaderm™-treated patient PBMC were stimulated with PMA, ionomycin and brefeldin A for 5 h to examine cytokine expression. Cells were stained with fluorochrome-conjugated antibodies specific for CD3, CD8, GM-CSF and IL-22, and were analysed by flow cytometry. The frequency of CD4⁺GM-CSF⁺ T cells trended towards an increase in patients who have not received treatment compared with healthy donors (Figure 5.23 A and C).

The frequency of CD4⁺IL-22⁺ T cells was significantly increased in untreated psoriasis patients compared with both healthy ($p < 0.001$) and Fumaderm™-treated patients ($p < 0.001$) (Figure 5.23 B and D). These data suggest a role for IL-22⁺CD4⁺ T cells in the pathogenesis of psoriasis. Furthermore, the data suggests a role for Fumaderm™ in the inhibition of IL-22-expressing CD4⁺ T cells in psoriasis down to the levels observed in healthy controls.

5.2.15 The effect of Fumaderm™ on IL-2 and TNF- α -expressing CD4⁺ T cells.

The presence of the IL-2 cytokine is increased in skin lesions of psoriasis patients (Uyemura, Yamamura et al. 1993) and targeting of the IL-2 receptor with basiliximab has been shown to successfully treat severe psoriasis (Owen and Harrison 2000). Additionally, increased TNF- α is a hallmark of psoriasis, and many successful treatments have targeted this particular cytokine, including adalimumab, etanercept and infliximab. Although successful, these treatments are expensive and can cause side effects. TNF- α is produced chiefly by activated macrophages, but is also produced by CD4⁺ T cells.

The effect of Fumaderm™ on the frequencies of IL-2 and TNF- α -expressing CD4⁺ T cells was examined. Blood from healthy donors, psoriasis patients who had not yet received treatment (Untreated), and psoriasis patients receiving Fumaderm™ were processed and PBMC were isolated. Cells were stimulated with PMA, ionomycin and brefeldin A for 5 h

to examine cytokine expression. Cells were stained with fluorochrome-conjugated antibodies specific for CD3, CD8, IL-2 and TNF- α , and were analysed by flow cytometry.

CD4⁺IL-2⁺ T cells were significantly increased in Fumaderm™-treated patients compared with untreated patients ($p < 0.01$) (Figure 5.24 A and C). A trend towards increased frequencies of CD4⁺IL-2⁺ T cells was observed in healthy controls compared with untreated psoriasis patients; however this did not reach significance (Figure 5.24 A and C).

The frequency of CD4⁺ T cells expressing TNF- α was significantly decreased in untreated patients ($p < 0.001$) and Fumaderm™-treated patients ($p < 0.05$) compared with healthy controls (Figure 5.24 B and D).

This data collectively demonstrates an increase in IL-2-expressing CD4⁺ T cells in the Fumaderm™-treated patients relative to untreated patients and a decrease in TNF- α -expressing CD4⁺ T cells for both untreated and Fumaderm™-treated patients compared with healthy donors.

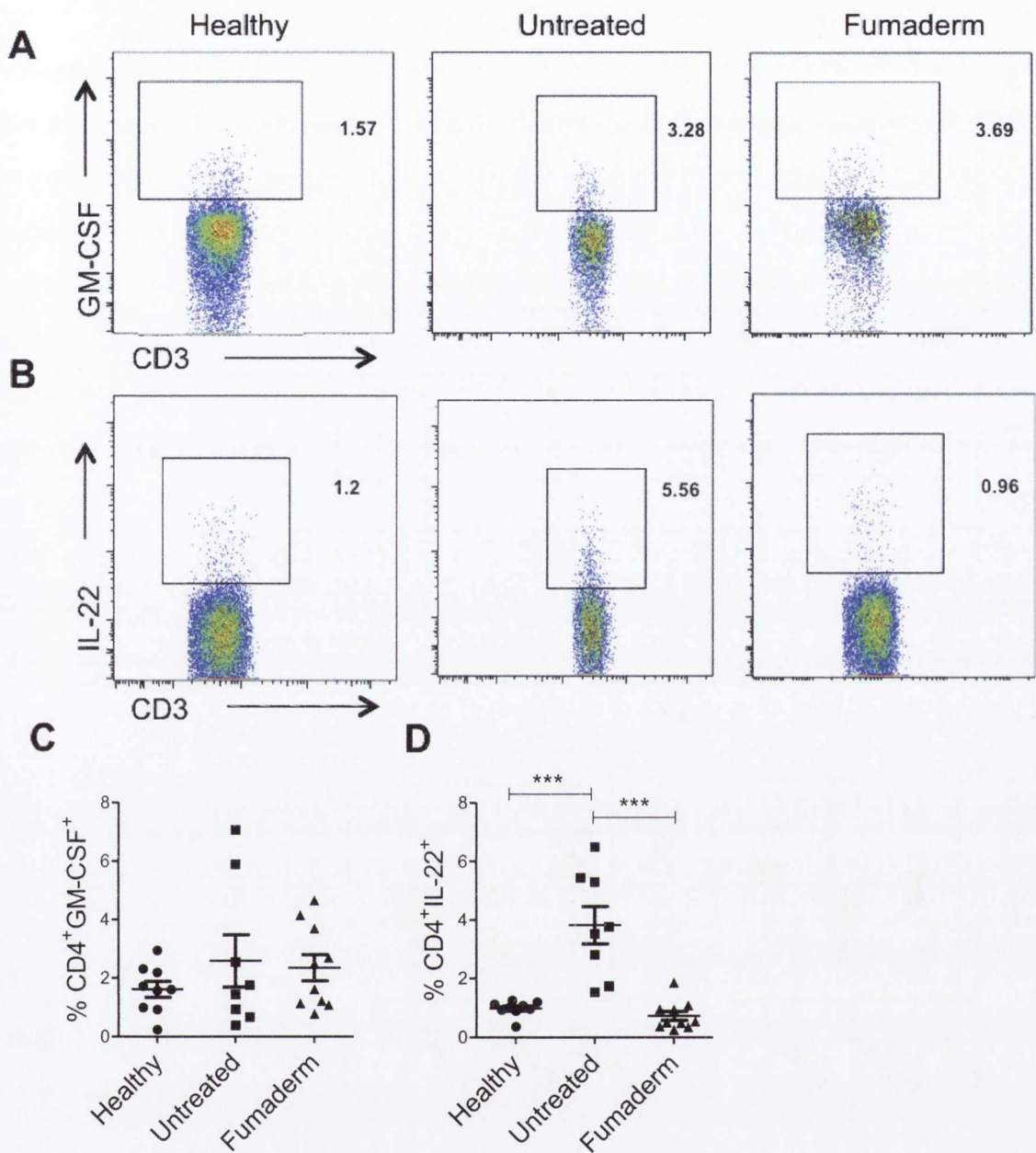


Figure 5.23. Fumaderm™ treatment decreases IL-22⁺ T cell frequencies.

PBMC were isolated from healthy donors, a group of untreated psoriasis patients and a separate group of Fumaderm™-treated psoriasis patients and were stimulated for 5 h with PMA, ionomycin and brefeldin A. Cells were stained with fluorochrome-conjugated antibodies specific for CD3, CD8, GM-CSF and IL-22, and analysed by flow cytometry. Representative dot plots are gated on CD3⁺CD8⁻ (CD4) T cells. The frequencies of CD4⁺GM-CSF⁺ T cells (A) and CD4⁺IL-22⁺ T cells (B) are presented for healthy, untreated psoriasis patients and Fumaderm™-treated psoriasis patients. The graphs represent CD4⁺GM-CSF⁺ T cells (C) and CD4⁺IL-22⁺ T cell (D) frequencies for each group. Statistical differences between groups were determined by one-way ANOVA with Tukey's Multiple Comparison test; ***p<0.001.

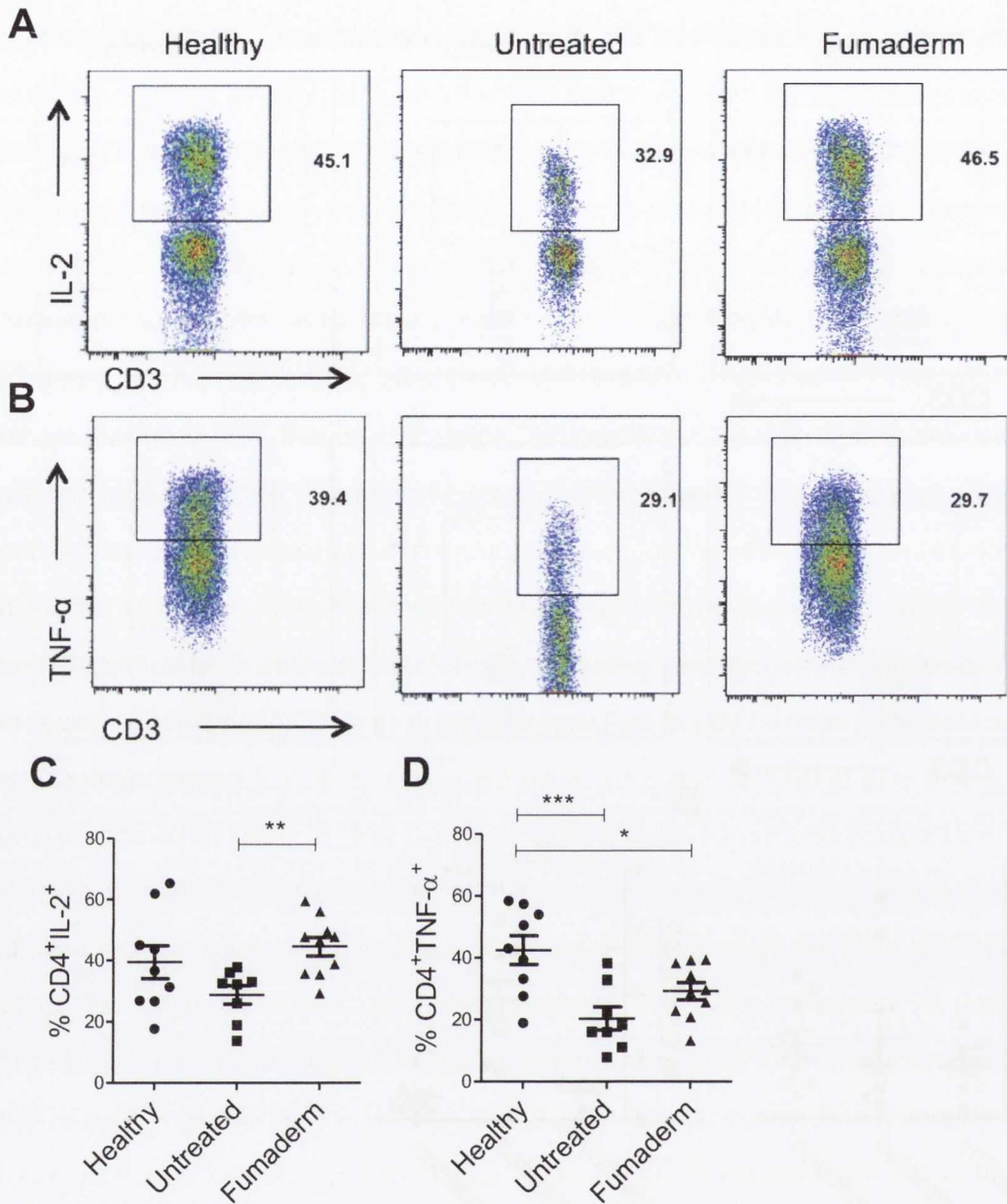


Figure 5.24. The effect of Fumaderm™ treatment on IL-2⁺ and TNF-α⁺ CD4⁺ T cell frequencies.

PBMC were isolated from healthy donors, a group of untreated psoriasis patients and a separate group of Fumaderm™-treated psoriasis patients and stimulated for 5 h with PMA, ionomycin and brefeldin A. Cells were stained with fluorochrome-conjugated antibodies specific for CD3, CD8, IL-2 and TNF-α, and analysed by flow cytometry. Representative dot plots are gated on CD3⁺CD8⁻ (CD4) T cells. The frequencies of CD4⁺IL-2⁺ T cells (A) and CD4⁺TNF-α⁺ T cells (B) are presented for healthy, untreated psoriasis patients and Fumaderm™-treated psoriasis patients. The graphs represent the frequencies of CD4⁺IL-2⁺ T cells (C) and CD4⁺TNF-α⁺ T cells (D) cells for each patient group. Statistical differences between groups were determined by one-way ANOVA with Tukey's Multiple Comparison test; *p<0.05, **p<0.01, ***p<0.001.

5.2.16. The effect of Fumaderm™ treatment on regulatory T cell frequencies in psoriasis.

Regulatory T cells are vital to immunological tolerance and suppression of inappropriate immune responses. Increased numbers of infiltrating Foxp3⁺ T cells were found in psoriatic plaques (Zhang, Yang et al. 2010). Additionally, other studies indicate an increase in Treg cell populations in patient blood compared with healthy controls (Arcese, Aste et al. 2010). The anti-inflammatory effects of Fumaderm™ treatment could be mediated by enhancing Treg cells, and therefore, Treg cell populations were examined in untreated and Fumaderm™ treated psoriasis patients. Blood from healthy donors, psoriasis patients not yet receiving treatment (Untreated) and psoriasis patients receiving Fumaderm™ were processed and PBMC were isolated. Cells were stained with fluorochrome-conjugated antibodies specific for CD4, CD25, CD127 and Foxp3, and analysed by flow cytometry. The gating strategy used to identify Treg cells is shown in Figure 5.25. The frequencies of Treg cells (CD4⁺CD25⁺CD127^{Lo}Foxp3⁺) were significantly increased in Fumaderm™-treated compared with untreated psoriasis patients (p<0.05) (Figure 5.26 A and B).

Foxp3⁺CD39⁺ Treg cells are highly suppressive and were previously shown to suppress IL-17 production by responder cells in MS, whilst CD39⁻Treg cells were unable to do so (Fletcher, Lonergan et al. 2009). The frequency of CD39⁺ Treg cells was investigated in psoriasis patients. Cells were stained for CD4, CD25, CD127, CD39 and Foxp3. The frequency of CD39⁺Treg cells (CD4⁺CD25⁺CD127^{Lo}Foxp3⁺CD39⁺) was unchanged between healthy, untreated patients and total Fumaderm™-treated patients (Figure 5.26 C).

Finally, CTLA-4 expression is required for Treg cell suppression and lack of CTLA-4 results in the development of lethal autoimmunity (Jain, Nguyen et al. 2010). The frequency of CTLA-4 expression by Treg cells was examined in untreated psoriasis patients and following Fumaderm™ treatment. Cells were stained CD4, CD25, CD127, CTLA-4 and Foxp3. The frequency of CTLA-4⁺Treg cells (CD4⁺CD25⁺CD127^{Lo}Foxp3⁺CTLA-4⁺) was unchanged between healthy, untreated patients and total Fumaderm™-treated patients (Figure 5.26 D).

This data together reveals an increase in total Treg cell frequencies in patients treated with Fumaderm™, and these Treg cells did not reveal any deficit in CD39 or CTLA-4 expression. This suggests a role for Treg cells in the anti-inflammatory effects mediated by Fumaderm™ in psoriasis patients.

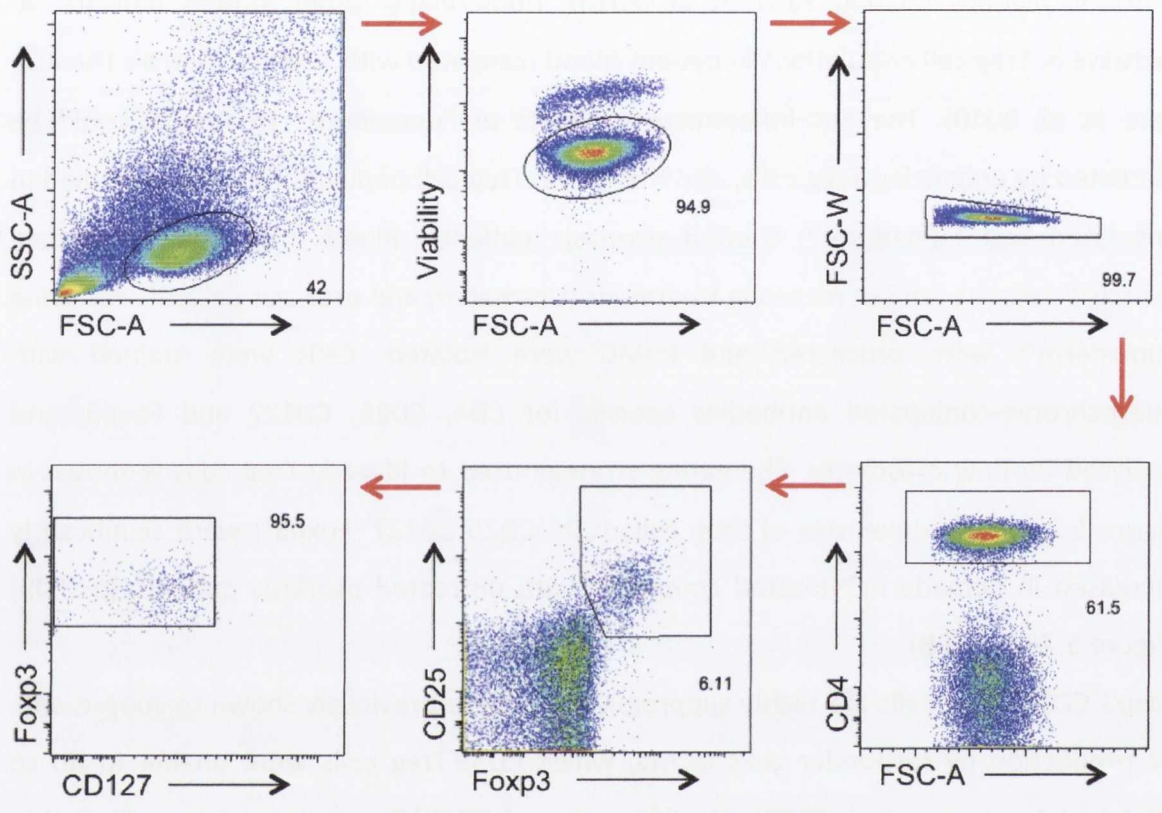


Figure 5.25 The flow cytometry gating strategy for identifying Treg cells

The lymphocyte population was identified from total PBMC on the basis of SSC-A and FSC-A. Viable cells were gated from the lymphocyte population following gating on the basis of Viability dye and FSC-A. Doublets were removed from the population of interest on the basis of FSC-W and FSC-A. CD4⁺ T cells were gated on the basis of CD4 and FSC-A. Expression of CD25 and Foxp3 was examined in the CD4⁺ population. CD25⁺Foxp3⁺ T cells were gated from the CD4⁺ population. CD25⁺Foxp3⁺ T cells were gated on Foxp3 and CD127 to identify Treg cells as being CD4⁺CD25⁺Foxp3⁺CD127^{lo}.

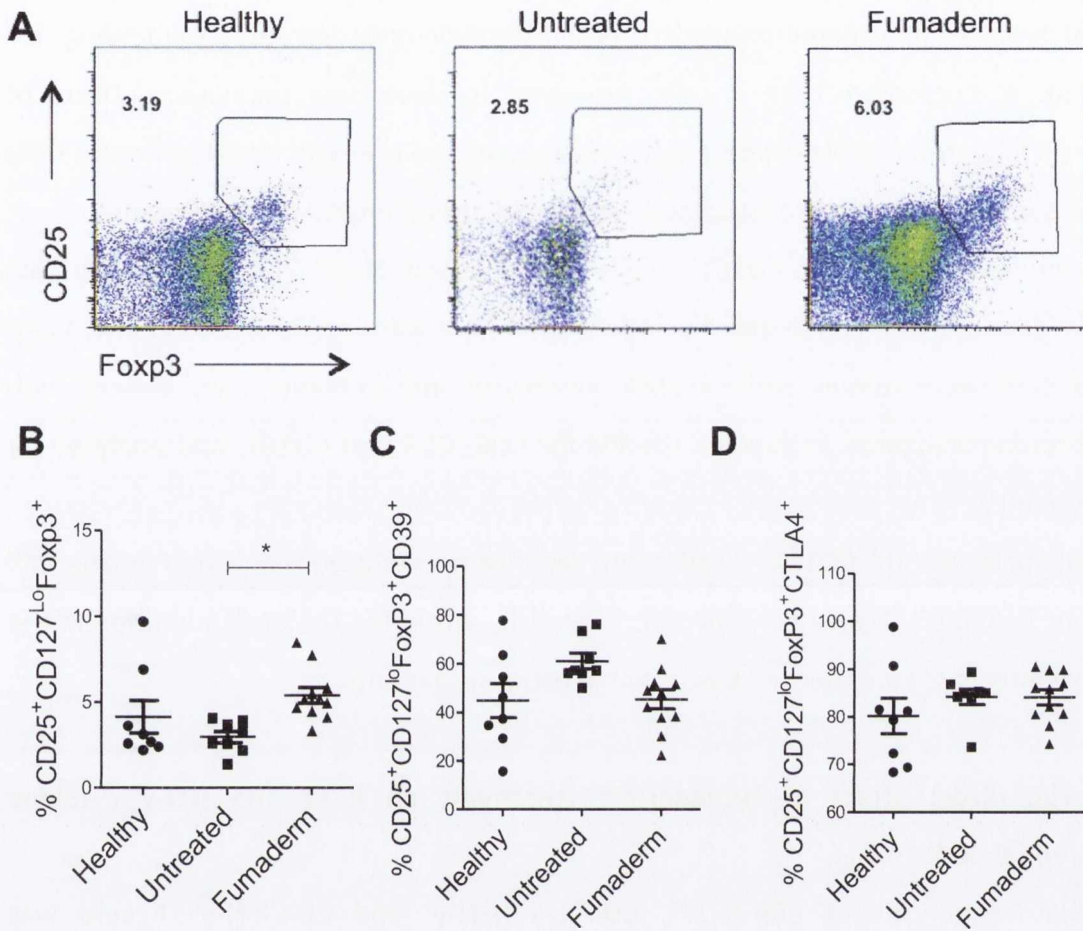


Figure 5.26. Treg cells are increased following Fumaderm™ treatment in psoriasis.

Healthy donor, untreated and Fumaderm™-treated psoriasis patient blood was processed and PBMC were stained with fluorochrome-conjugated antibodies specific for CD4, CD25, CD127, CD39, Foxp3 and CTLA-4. Cells were analysed by flow cytometry and representative dot plots are gated on CD4⁺ T cells. The frequencies of CD4⁺CD25⁺Foxp3⁺ (A) T cells are presented for healthy, untreated psoriasis patients and Fumaderm™-treated psoriasis patients. The graphs represent the frequencies of CD4⁺CD25⁺CD127^{Lo}Foxp3⁺ (B), CD4⁺CD25⁺CD127^{Lo}Foxp3⁺CD39⁺ (C) and CD4⁺CD25⁺CD127^{Lo}Foxp3⁺CTLA-4⁺ (D) T cells are presented for healthy, untreated psoriasis patients and Fumaderm™-treated psoriasis patients. Statistical differences between groups were determined by one-way ANOVA with Tukey's Multiple Comparison test; *p<0.05.

5.2.17 The direct effect of Fumaderm™ on CD4⁺CD161⁺ T cells in psoriasis

Initially, the examination of the effect of Fumaderm on T cell subsets concentrated on comparing healthy donors with a group of untreated psoriasis patients and a separate group of Fumaderm™-treated patients. This investigation provided some key findings for the effect of Fumaderm™ on T cells; however, to determine the direct effects of Fumaderm™, a group of psoriasis patients were examined pre- and post-treatment. Cells from the same individual were examined before and after Fumaderm™ treatment.

Initially the frequency of CD4⁺CD161⁺ T cells was examined. Blood from psoriasis patients prior to treatment with Fumaderm™ and post-treatment were processed and PBMC were isolated. Cells were stimulated with PMA, ionomycin and brefeldin A and stained with fluorochrome-conjugated antibodies specific for CD3, CD8 and CD161, and analysed by flow cytometry.

The frequencies of CD4⁺CD161⁺ T cells were significantly reduced following Fumaderm™ treatment ($p < 0.001$) (Figure 5.27) ($n=10$), suggesting a role for Th17 cell inhibition in the beneficial effects of Fumaderm™ treatment in psoriasis patients.

5.2.18 The direct effect of Fumaderm™ treatment on IL-17 and IFN- γ cytokine expression by CD4⁺ T cells.

Next, the frequencies of CD4⁺IL-17⁺, CD4⁺IL-17⁺IFN- γ ⁺ and CD4⁺IFN- γ ⁺ T cells was examined in psoriasis patients pre- and post-Fumaderm™ treatment. Blood from psoriasis patients prior to treatment with Fumaderm™ and post-treatment were processed and PBMC were isolated. Cells were stimulated with PMA, ionomycin and brefeldin A for 5 h to examine cytokine expression. Cells were stained with fluorochrome-conjugated antibodies specific for CD3, CD8, IL-17 and IFN- γ , and analysed by flow cytometry. Representative dot plots were gated on CD3⁺CD8⁻ T cells (CD4). The frequency of CD4⁺IL-17⁺ T cells (CD3⁺CD8⁻IL-17⁺) was unchanged following Fumaderm™ treatment (Figure 5.28 A). The frequency of transitional exTh17 (CD3⁺CD8⁻IL-17⁺IFN- γ ⁺) cells was unchanged between pre- and post-Fumaderm™-treated patients (Figure 5.28 B). Additionally, the frequency of CD3⁺CD8⁻IFN- γ ⁺ T cells was unchanged following Fumaderm™ treatment (Figure 5.28 C).

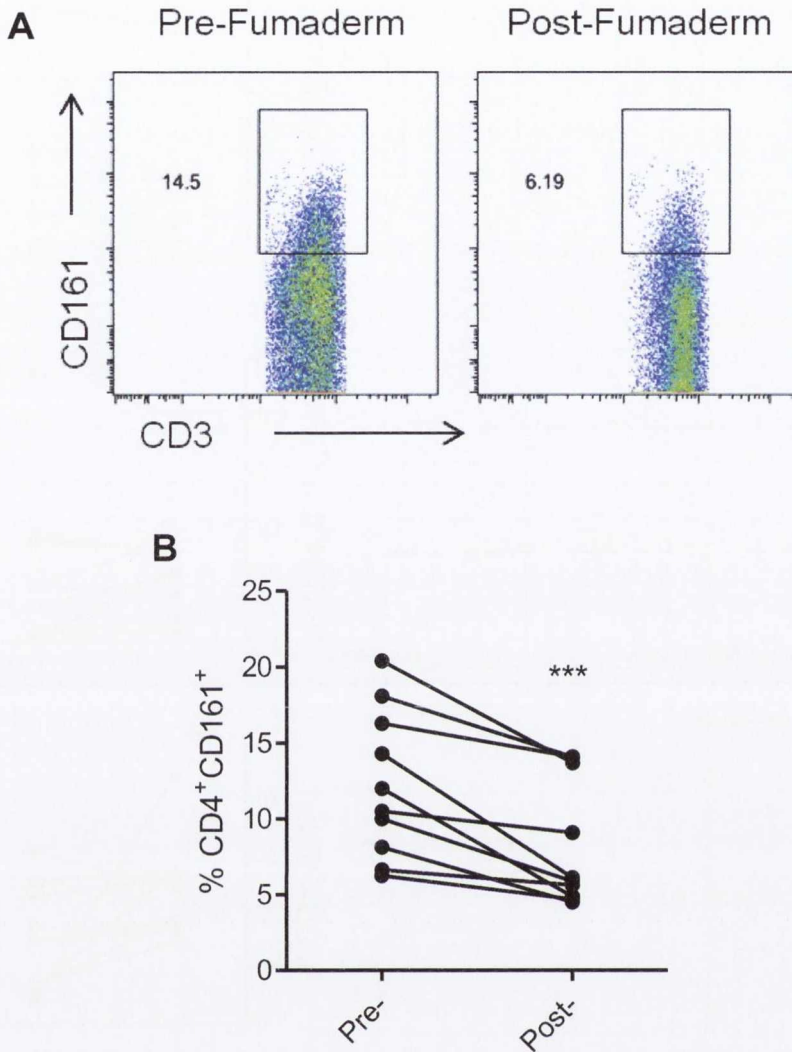


Figure 5.27. The frequencies of CD4⁺CD161⁺ T cells are decreased after Fumaderm[™] treatment.

PBMC were isolated from psoriasis patients pre- and post-Fumaderm[™] treatment and stimulated for 18 h with PMA, ionomycin and brefeldin A. Cells were stained with fluorochrome-conjugated antibodies specific for CD3, CD8 and CD161, and analysed by flow cytometry. Representative dot plots are gated on CD3⁺CD8⁻ (CD4) T cells and represent CD4⁺CD161⁺ cells (A) for pre- and post-Fumaderm[™]-treated psoriasis patients. The graph presents CD4⁺CD161⁺ cells (B) for pre- and post-Fumaderm[™]-treated psoriasis patients. Statistical differences between groups were determined a paired, two-tailed T test; ***p<0.01

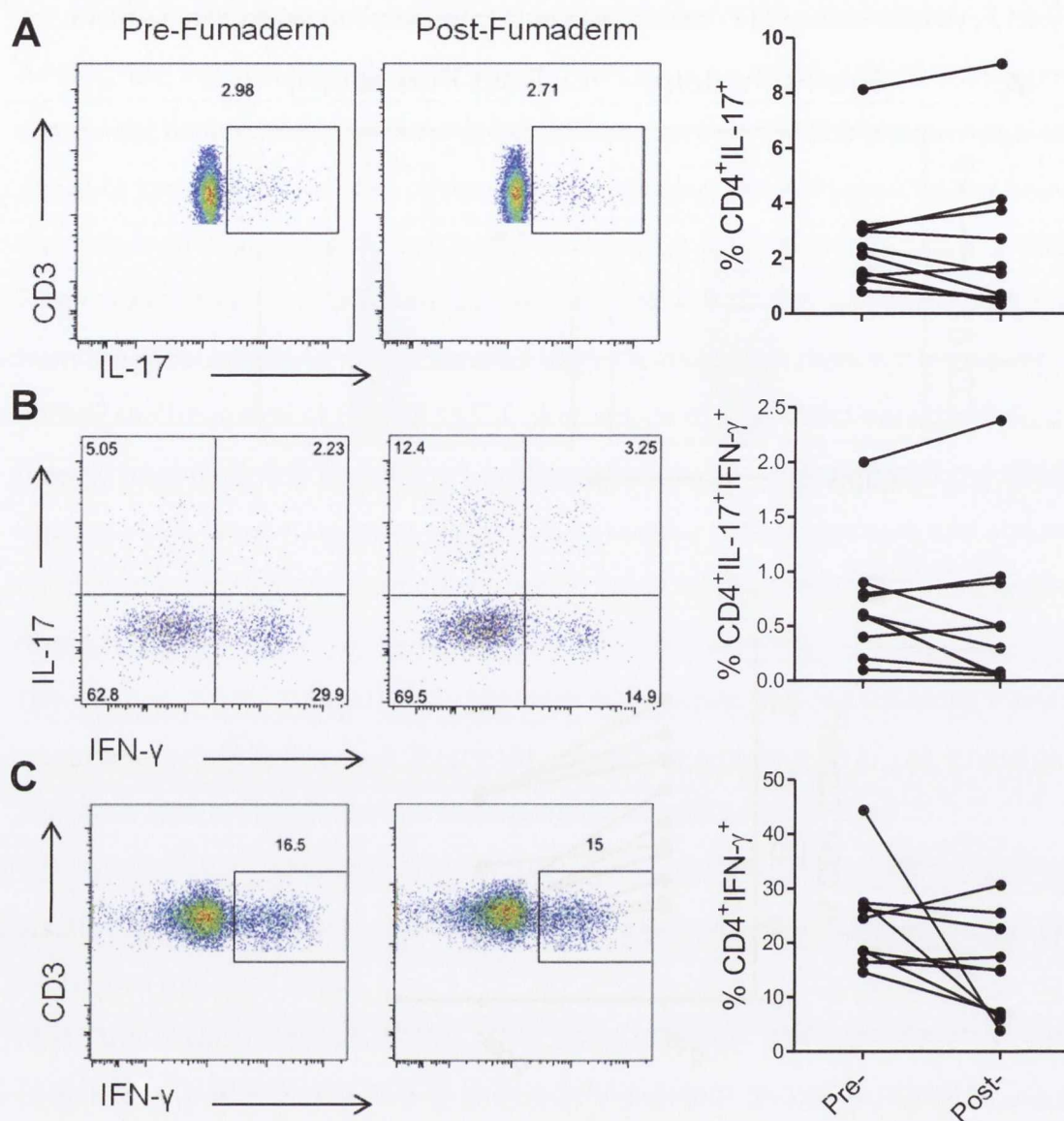


Figure 5.28. Analysis of CD4⁺IL-17⁺, CD4⁺IL-17⁺IFN-γ⁺ and CD4⁺IFN-γ⁺ T cells between pre- and post-Fumaderm™-treated patients.

PBMC were processed from psoriasis patient blood pre- and post-Fumaderm™ treatment and stimulated for 18 h with PMA, ionomycin and brefeldin A. Cells were stained with fluorochrome-conjugated antibodies specific for CD3, CD8, IL-17 and IFN-γ, and analysed by flow cytometry. Representative dot plots are gated on CD3⁺CD8⁻ (CD4) T cells. The frequencies of Th17 (CD4⁺IL-17⁺IFN-γ⁻) (A), exTh17 (CD4⁺CD161⁺IL-17⁺IFN-γ⁺) (B) and Th1 (CD4⁺CD161⁺IFN-γ⁺) T cells (C) are presented for pre- and post-Fumaderm™ treated psoriasis patients.

5.2.19 ExTh17 cells are reduced in psoriasis patients following Fumaderm™ treatment.

Th17 lineage cells (CD161⁺IL-17⁺), exTh17 cells (CD161⁺IFN- γ ⁺) and Th1 cells (CD161⁻IFN- γ ⁺) cells were examined in psoriasis patients pre- and post-Fumaderm™ treatment. Cells were stimulated as stated previously (5.2.18) and stained with CD3, CD8, CD161, IL-17 and IFN- γ . The frequency of bona fide Th17 cells (CD161⁺IL-17⁺) was unchanged between patients pre- and post-Fumaderm™ treatment (Figure 5.29 A). Additionally, Th1 cells (CD4⁺CD161⁻IFN- γ ⁺) were unchanged between psoriasis patients prior to and after Fumaderm™ treatment (Figure 5.29 C). Finally, the frequencies of fully switched exTh17 cells, expressing both CD161 and IFN- γ , were significantly reduced in patients post-Fumaderm™ treatment compared with patients prior to treatment ($p < 0.01$) (Figure 5.29 B). This data demonstrates a direct effect of Fumaderm™ treatment on exTh17 cell inhibition in psoriasis patients.

5.2.20 The direct effect of Fumaderm™ treatment on GM-CSF and IL-22 expressing CD4⁺ T cells.

As mentioned previously, IL-22 and GM-CSF are Th17 cell-related cytokines, which are known to be increased in psoriasis. Therefore, the direct effects of Fumaderm™ treatment on CD4⁺GM-CSF⁺ and CD4⁺IL-22⁺ T cells was examined for psoriasis patients pre- and post-treatment with Fumaderm™. Blood from psoriasis patients prior to treatment with Fumaderm™ and post-treatment were processed and PBMC were isolated. Cells were stimulated with PMA, ionomycin and brefeldin A to examine cytokine expression. Cells were stained with fluorochrome-conjugated antibodies specific for CD3, CD8, GM-CSF and IL-22, and were analysed by flow cytometry. The frequency of CD4⁺GM-CSF⁺ T cells were significantly reduced following Fumaderm™ treatment of psoriasis patients compared with the same patient prior to treatment (Figure 5.30 A). Additionally, the frequency of CD4⁺IL-22⁺ T cells was examined; however, the frequency of this population of cells was unchanged between pre- and post-Fumaderm™ treated patients (Figure 5.30 B).

These results suggest a role for Fumaderm™ in the inhibition of GM-CSF-expressing CD4⁺ T cells in psoriasis patients.

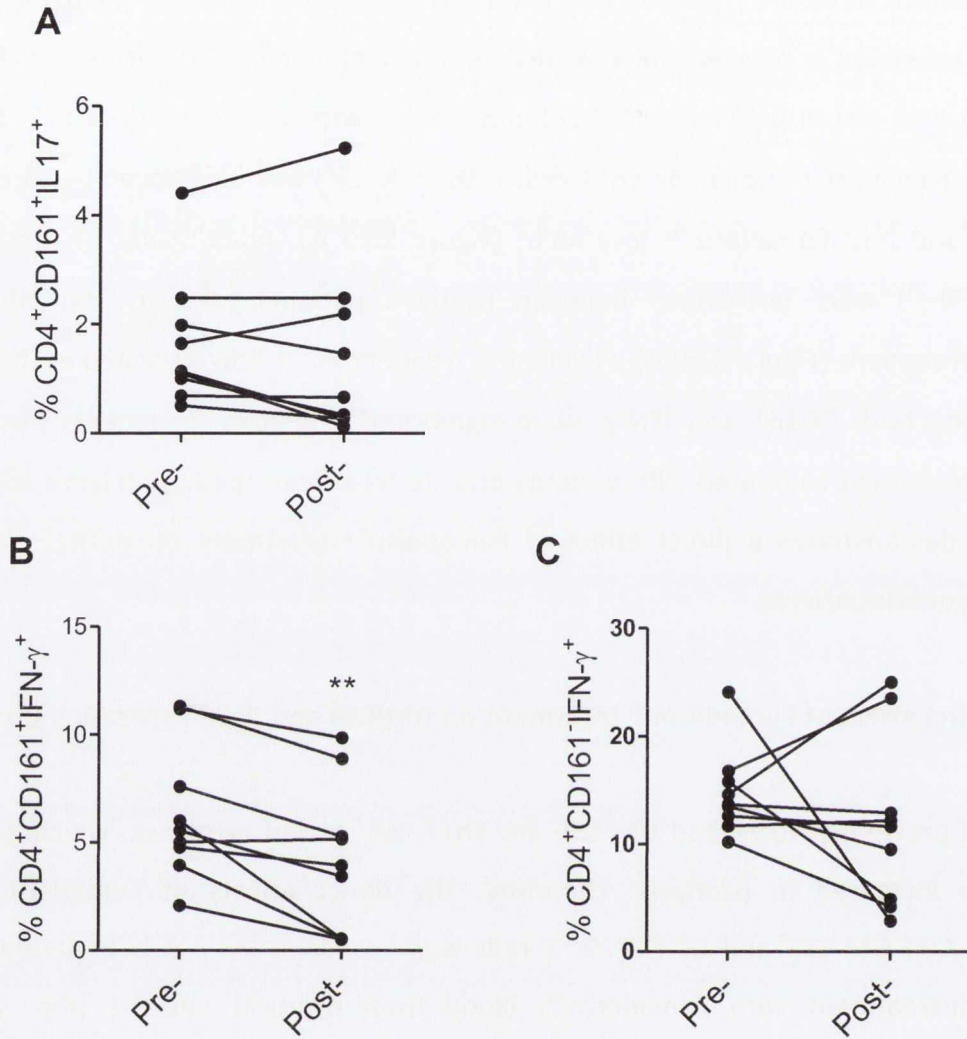


Figure 5.29. CD161⁺IFN- γ ⁺ T cell frequencies are decreased between pre- and post-FumadermTM-treated patients.

PBMC were processed from psoriasis patient blood pre- and post-FumadermTM treatment and stimulated for 18 h with PMA, ionomycin and brefeldin A. Cells were stained with fluorochrome-conjugated antibodies specific for CD3, CD8, CD161, IL-17 and IFN- γ , and analysed by flow cytometry. CD4 T cells are represented as CD3⁺CD8⁻ T cells. The graphs represent the frequency of CD4⁺CD161⁺IL-17⁺ (A), CD4⁺CD161⁺IFN- γ ⁺ (B) and CD4⁺CD161⁻IFN- γ ⁺ T cells (C) for pre- and post-FumadermTM treated psoriasis patients. Statistical differences between groups were determined by a paired, two-tailed T test; **p<0.01.

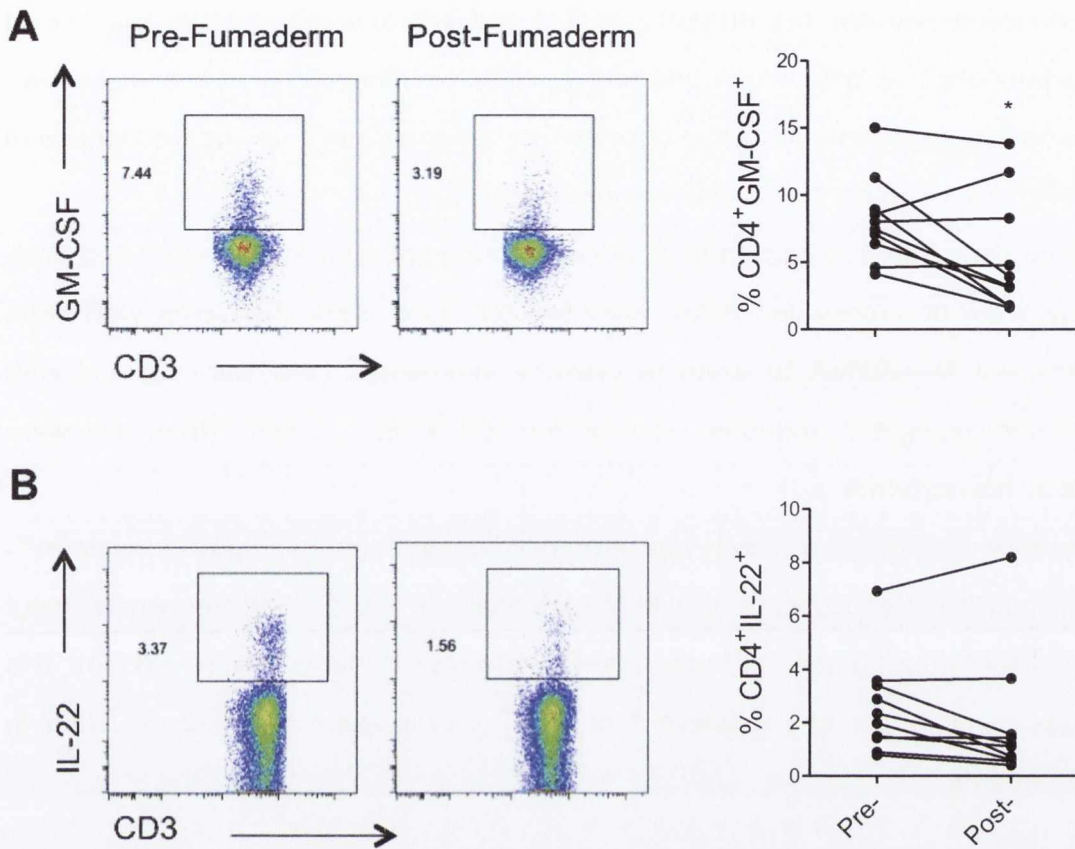


Figure 5.30. The frequency of CD4⁺GM-CSF⁺ T cells is decreased between pre- and post-Fumaderm[™] treated psoriasis patients.

PBMC were processed from psoriasis patient blood pre- and post-Fumaderm[™] treatment and stimulated for 18 h with PMA, ionomycin and brefeldin A. Cells were stained with fluorochrome-conjugated antibodies specific for CD3, CD8, GM-CSF and IL-22, and analysed by flow cytometry. Representative dot plots are gated on CD3⁺CD8⁻ (CD4) T cells. The frequencies of CD4⁺GM-CSF⁺ T cells (A) and CD4⁺IL-22⁺ T cells (B) are presented in the representative dot plots and graphed for pre- and post-Fumaderm[™]-treated psoriasis patients. Statistical differences between groups were determined by paired, tow-tailed T test; *p<0.05.

5.2.21 The direct effect of Fumaderm™ treatment on TNF- α and IL-2 cytokine expressing CD4⁺ T cells.

As mentioned previously, the presence of IL-2 and TNF- α is increased in the skin of psoriasis patients. IL-2 is known to promote T cell activation and TNF- α is a well known pro-inflammatory cytokine. Next, the direct effect of Fumaderm™ on the frequencies of IL-2 and TNF- α -expressing CD4⁺ T cells was examined.

Blood from the same psoriasis patients prior to treatment with Fumaderm™ and post-treatment were processed and PBMC were isolated. Cells were stimulated with PMA, ionomycin and brefeldin-A to examine cytokine expression. Cells were stained with fluorochrome-conjugated antibodies specific for CD3, CD8, IL-2 and TNF- α , and were analysed by flow cytometry.

The frequency of CD4⁺TNF- α ⁺ T cells was unchanged between pre- and post-Fumaderm™-treated psoriasis patients (Figure 5.31 A). Additionally, CD4⁺IL-2⁺ T cell frequencies were unchanged following Fumaderm™ treatment in psoriasis patients (Figure 5.31 B). This data suggests no effect of Fumaderm™ on CD4⁺ T cells expressing IL-2 or TNF- α in psoriasis patients.

5.2.22 Treg cells are enhanced in psoriasis patients post-Fumaderm™ treatment.

Finally the direct effect of Fumaderm™ treatment on Treg cell frequencies was examined for psoriasis patients. Blood from psoriasis patients prior to treatment with Fumaderm™ and post-treatment were processed and PBMC were isolated. Cells were stained with fluorochrome-conjugated antibodies specific for CD4, CD25, CD127 and Foxp3, and analysed by flow cytometry. The frequency of Treg cells (CD4⁺CD25⁺CD127^{Lo}Foxp3⁺) were significantly increased following Fumaderm™ treatment compared with patients prior to treatment with Fumaderm™ ($p < 0.05$) (Figure 5.32 A). The frequency of CD39⁺Treg cells was investigated also as cells were stained for CD4, CD25, CD127, CD39 and Foxp3. The frequency of CD39⁺Treg cells (CD4⁺CD25⁺CD127^{Lo}Foxp3⁺CD39⁺) was unchanged between patients pre- and post-Fumaderm™ treatment (Figure 5.32 B). Finally, CTLA-4 expression by Treg cells was for patients pre- and post-Fumaderm™ treatment. Cells were stained for CD4, CD25, CD127, CTLA-4 and Foxp3. Additionally, the frequency of CTLA-4⁺Treg cells (CD4⁺CD25⁺CD127^{Lo} Foxp3⁺CTLA-4⁺) was unchanged between psoriasis patients prior to and after Fumaderm™ treatment (Figure 5.32 C).

Collectively, this data reveals an increase in Treg cell frequencies following Fumaderm™ treatment, and these Treg cells do not reveal any deficit in CD39 or CTLA-4 expression. This suggests a role for Treg cells in the anti-inflammatory effects observed by Fumaderm™ treatment in psoriasis patients.

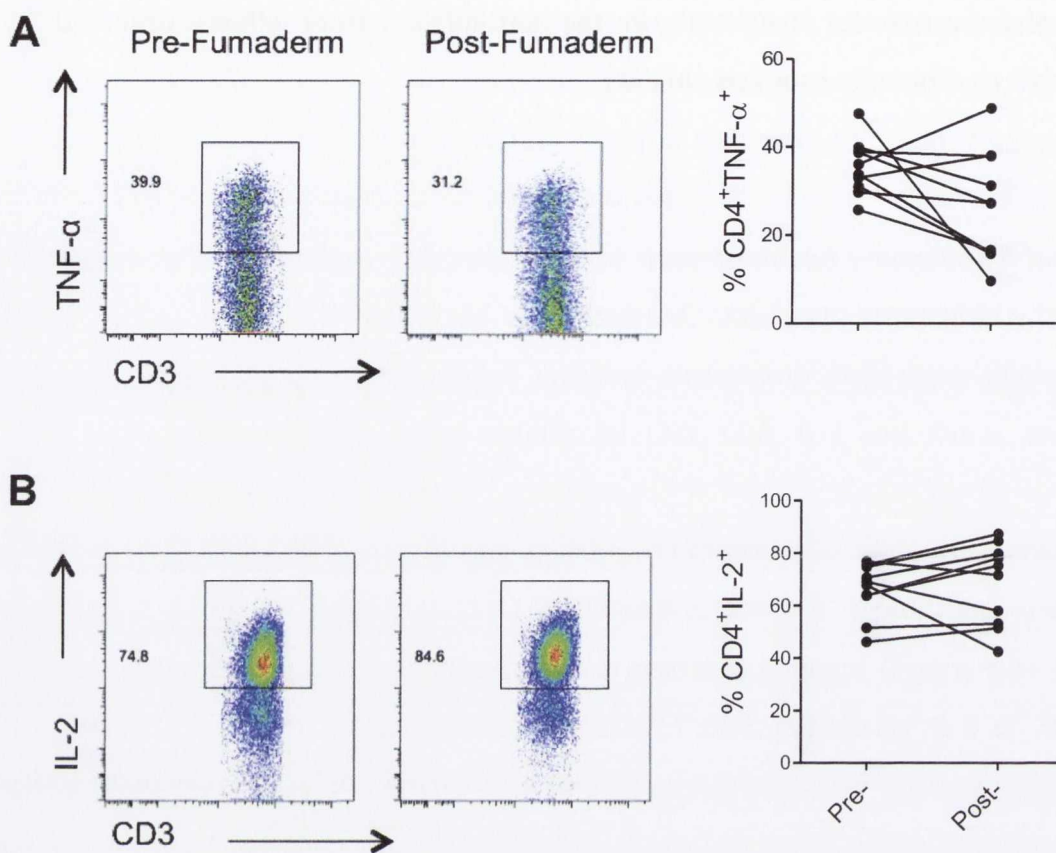


Figure 5.31. Comparing CD4⁺IL-2⁺ and CD4⁺TNF- α ⁺ T cell frequencies between psoriasis patients pre- and post-FumadermTM treatment.

PBMC were processed from psoriasis patient blood pre- and post-FumadermTM treatment and stimulated for 18 h with PMA, ionomycin and brefeldin A. Cells were stained with fluorochrome-conjugated antibodies specific for CD3, CD8, IL-2 and TNF- α , and analysed by flow cytometry. Representative dot plots are gated on CD3⁺CD8⁻ (CD4) T cells. The frequencies of CD4⁺IL-2⁺ T cells (A) and CD4⁺TNF- α ⁺ T cells (B) are for pre- and post-FumadermTM treated psoriasis patients.

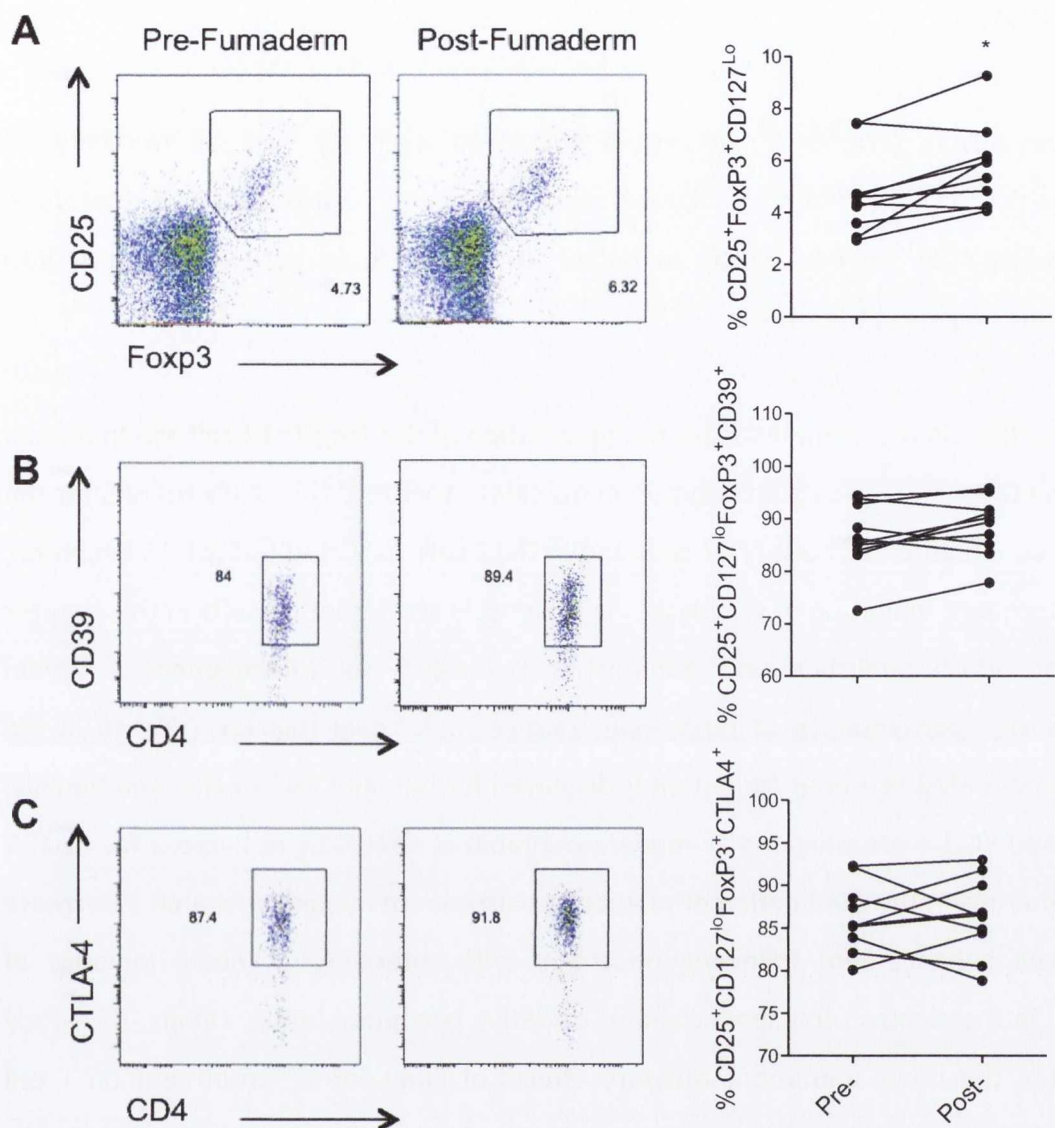


Figure 5.32. Treg cell frequencies are increased between pre- and post-Fumaderm™ treated psoriasis patients.

PBMC were processed from psoriasis patient blood pre- and post-Fumaderm™ treatment and stained with fluorochrome-conjugated antibodies specific for CD4, CD25, CD127, CD39, Foxp3 and CTLA-4. Cells were analysed by flow cytometry and representative dot plots are gated on CD4⁺T cells (A) and CD4⁺CD25⁺CD127^{Lo}Foxp3⁺ T cells (B and C). The dot plots represent CD4⁺CD25⁺Foxp3⁺ (A) CD4⁺CD25⁺CD127^{Lo}Foxp3⁺CD39⁺ (B) and CD4⁺CD25⁺CD127^{Lo}Foxp3⁺CTLA-4⁺ (C) T cell for pre- and post-Fumaderm™ treated psoriasis patients. The graphs present CD4⁺CD25⁺CD127^{Lo}Foxp3⁺ (A) CD4⁺CD25⁺CD127^{Lo}Foxp3⁺CD39⁺ (B) and CD4⁺CD25⁺CD127^{Lo}Foxp3⁺CTLA-4⁺ (C) T cells for pre- and post-Fumaderm™ treated psoriasis patients. Statistical differences between groups were determined by a paired, two-tailed T test; *p<0.05.

5.3 Discussion

A balance in the Treg:Th17 cell axis is critical to maintain optimal immunity. In autoimmune and inflammatory disease, this balance is disrupted; and therefore, understanding the factors which modulate this axis could provide insights into autoimmune targets in the future

The data in this chapter demonstrates the modulation of the Treg:Th17 cell axis in human cells via metabolism, hypoxia and immunomodulatory therapy. This study reveals for the first time an inhibition of both Th17 cells and exTh17 cells as a result of mTOR inhibition, and a subsequent inhibition of glycolysis, via rapamycin treatment. Results in this chapter support previously published data, demonstrating a significant enhancement of human Treg cells as a consequence of rapamycin treatment. A novel role for TEPP-46 in the promotion of PKM2 tetramer formation is displayed for human CD4⁺ T cells. Additionally, TEPP-46 and YC-1 were revealed as moderate inhibitors of HIF-1 α in hypoxia for CD4⁺ T cells. Furthermore, the modulation of metabolic pathways in hypoxia revealed a decrease in Treg cell enhancement following treatment with rotenone, a known inhibitor of complex I in the electron transport chain of oxidative phosphorylation. Finally, this study investigated the novel immunomodulatory effects of FumadermTM treatment on T cell subsets in psoriasis patients demonstrating a direct effect on CD161⁺ T cells, exTh17 cells, GM-CSF-expressing cells and Treg cells.

Rapamycin, the immunosuppressive drug targeting mTOR, inhibits mTOR activity and subsequently pS6 expression. In Chapter 3 it was demonstrated that Th17 lineage cells exhibited increased mTOR activity after T cell activation, compared with non-Th17 lineage cells and Treg cells. mTOR is a key molecule involved in glycolysis and therefore rapamycin indirectly inhibits glycolysis. In order to determine the role of glycolysis in modulating T cell subsets the effect of rapamycin on the frequency of differentiated memory T cell subsets was investigated. The data in this chapter revealed the novel finding that rapamycin selectively inhibited Th17 lineage cells, which was consistent with their increased mTOR activity. The frequency of memory CD4⁺ T cells expressing IL-17 and CD161 was decreased following rapamycin treatment. These data is in agreement with previous murine studies revealing a decrease in Th17 cell differentiation from naïve CD4⁺

T cells under Th17 cell cytokine skewing conditions in the presence of rapamycin (Kopf, de la Rosa et al. 2007, Shi, Wang et al. 2011). IFN- γ -expression by CD4⁺ T cells was decreased following inhibition of mTOR and this is consistent with findings in murine studies following activation of lymph node cells with anti-CD3/28 (Tomasoni, Basso et al. 2011). Effector T cells are clearly affected by inhibition of mTOR. The inhibition of human effector T cell subsets in this study as a result of rapamycin treatment is supported by previous data indicating that T cells from mTOR knockout mice fail to differentiate into Th1, Th2 or Th17 cells (Delgoffe, Kole et al. 2009). Furthermore, effector T cells failed to activate lineage-selective STAT proteins or master transcription factors. In Th17 cells in particular, murine studies have revealed a requirement for the PI3K-Akt-mTORC1 axis in Th17 cell differentiation as treatment with rapamycin resulted in a decreased translocation of the Th17 cell-specific transcription factor ROR γ t to the nucleus (Kurebayashi, Nagai et al. 2012). This, along with the promotion of glycolysis, may be the mechanism by which mTOR favours human Th17 cells.

The frequency of Treg cells is increased as a consequence of rapamycin treatment in this study. This result is in accordance with studies performed in both murine and human cells (Battaglia, Stabilini et al. 2005, Kopf, de la Rosa et al. 2007, Zeiser, Leveson-Gower et al. 2008, Strauss, Czystowska et al. 2009). However, none of the mentioned studies utilized CD127 during Treg cell gating, and therefore Treg cells may not have been properly identified. Rapamycin prevents graft rejection in both mouse and human transplantation, owing to increased Treg cell populations (Saunders, Metcalfe et al. 2001, Taams, Vukmanovic-Stejic et al. 2003). The origin of the increased Treg cell population is suggested to have expanded from an existing thymic Treg cell population, as following the depletion of CD25⁺ cells from total CD4⁺ T cells failed to yield an increase in Foxp3⁺ T cells in the presence of rapamycin (Battaglia, Stabilini et al. 2005). Unfortunately, in this study, all cellular proliferation was hindered following depletion of CD25⁺CD4⁺ T cells from total CD4⁺ T cells via the Aria Fusion sorter, and therefore the origin of the expanded Treg cell populations, in this system, could not be examined. In contrast to the low mTOR activity observed for human Treg cells in this study, in the form of pS6 expression, murine Treg cells display an increased expression of AMPK, known to inhibit mTOR and to drive lipid metabolism via the mitochondria (Michalek, Gerriets et al. 2011). Therefore, the increased frequency of human Treg cells following mTOR inhibition may be due to the

promotion of oxidative phosphorylation and a subsequent inhibition of glycolysis, and may also be orchestrated via AMPK expression; however, AMPK expression in human Treg cells is yet to be investigated.

TEPP-46 promotes the formation of the PKM2 tetramer, known to inhibit HIF-1 α transcriptional activity in murine macrophages (Palsson-McDermott, Curtis et al. 2015). This study uncovers a novel role for TEPP-46 in the tetramerization of PKM2 in human PBMC and CD4⁺ T cells. Having optimized DSS-linking of cell lysates treated with TEPP-46 in the human Jurkat T cell line, TEPP-46 was shown to increase PKM2 tetramer protein levels in both human PBMC and CD4⁺ T cells. In this study, CD161⁺, IL-17⁺, and IL17⁺IFN- γ ⁺ T cells trended towards a decrease following TEPP-46 treatment in normoxia. No trend was observed for CD4⁺IFN- γ ⁺ T cells. As previously shown in chapter 4, Th17 and exTh17 cells display a trend towards increased HIF-1 α expression compared with Th1 cells in normal oxygen levels; therefore, the inhibition of HIF-1 α by TEPP-46 additionally results in an inhibition of Th17 and exTh17 cells compared with Th1 cells. Furthermore, PKM2 is known to regulate metabolism, as the dimeric form promotes glycolysis, whereas the tetrameric form promotes pyruvate formation and the activation of oxidative phosphorylation (Christofk, Vander Heiden et al. 2008, Hitosugi, Kang et al. 2009). This role of TEPP-46 additionally supports the inhibition of Th17 and exTh17 cells, which have been demonstrated to maintain glycolysis for their metabolic demands. Contrastingly, the frequency of Treg cells trended towards an increase after TEPP-46 treatment in normoxia. This is supported by earlier findings in this study, stating a decreased expression of HIF-1 α in Treg cells. Additionally, focusing on the metabolic effects of TEPP-46, this result supports previous data stating a lack of reliance of Treg cells on glycolytic metabolism. Unfortunately, HIF-1 α expression levels in normoxia are insufficient to observe a further decrease following TEPP-46 treatment by flow cytometry; therefore, the effects of TEPP-46 on HIF-1 α was determined in hypoxic conditions.

Investigating the inhibitory effects of TEPP-46 on HIF-1 α in hypoxia revealed a trend towards a decreased expression of HIF-1 α in CD4⁺ T cells. However, TEPP-46 failed to completely inhibit HIF-1 α in hypoxia and its effects as an inhibitor in human cells remains unsatisfactory. Previous data in this study has revealed a significant increase in Treg cell populations in hypoxia, in addition to an increased HIF-1 α expression, even to a higher

extent than Th17 cells. It was hypothesized that HIF-1 α may promote Treg survival in hypoxia, and following TEPP-46 treatment, the enhancement of Treg cell frequencies in hypoxia trended towards a decrease as HIF-1 α was moderately inhibited. However, this observation resulting from decreased HIF-1 α activity is unlikely. Furthermore, concentrating on the metabolic role of the PKM2 tetramer and the inhibition of glycolysis, this implies a possible role for glycolysis in the expansion of Treg cells in hypoxia. Supporting this theory, GLUT1 is significantly increased in Treg cells in hypoxia, whereas GLUT1 is not increased in Th17 cells.

Additionally, YC-1 acts to inhibit HIF-1 α at the transcriptional level and consequently inhibits the transcription factor activity of HIF-1 α . YC-1 is also shown to promote the dissociation of the transcription co-activator p300 from HIF-1 α within the nucleus (Li, Shin et al. 2008). This study reveals no change in cytokine production, CD161 expression or Treg cell frequencies in normoxia following YC-1 treatment. However, YC-1 was shown to decrease the frequency of CD4⁺ T cells expressing HIF-1 α in hypoxia for the first time. Comparable with Tepp-46, YC-1 failed to completely inhibit HIF-1 α and is subsequently observed as a moderate inhibitor in human CD4⁺ T cells. The resulting inability of YC-1 to affect Treg cell frequencies in hypoxia may be as a result of insufficient inhibition of HIF-1 α . However, in contrary to this hypothesis, a study performed in a human hepatoma cell line (Hep3B) demonstrated an increased inhibitory effect of YC-1 on HIF-1 α activity rather than protein levels (Li, Shin et al. 2008). Additionally, One study observed in human T cells following YC-1 treatment resulted in a decreased expression of IL-17 by CD4⁺ T cells pre-treated with a stabilizer of HIF-1 α , dimethylxaloylglycine (DMOG) (Bollinger, Gies et al. 2014). However, YC-1 concentrations in the Bollinger et al. study, beginning at 600 nM, caused a significant decrease in CD4⁺ T cell proliferation in this present study. Perhaps the concentration utilized in this study was not sufficient to inhibit HIF-1 α transcriptional activity.

In order to elucidate the metabolic pathways utilized by Treg and Th17 cells in hypoxia, PBMC were cultured in the presence of metabolic compounds in hypoxic conditions. The frequency of CD4⁺IL-17⁺ T cells in hypoxia were unchanged following culture with glucose, oligomycin A, 2-DG and rotenone. The promotion of glycolysis via oligomycin A, the inhibition of glycolysis with 2-DG or the hindrance of oxidative phosphorylation via

rotenone, did not affect the inhibition of Th17 cells in hypoxia. Additionally, the effect of metabolic compounds on the expansion of Treg cells in hypoxia was examined. Additional glucose was supplemented into the system in order to provide extra sugar for glycolysis. If Treg cells were adapting this process in hypoxia, the speculation was to provide an approach by which the cells could increase their expansion further. In this report, glucose treatment did not affect Treg cell expansion. However, additional glucose may not stimulate glycolysis if sufficient glucose is available. This was also the case for the inhibition of glycolysis with 2-DG. A recent study in cancer cell lines demonstrates that HIF-1 α confers resistance to glycolytic inhibitors (Maher, Wangpaichitr et al. 2007). This study revealed a decreased resistance to 2-DG in cancer cells following HIF-1 α knockdown, an increased toxicity of 2-DG in HIF-deficient cells in hypoxia and the plausible explanation for the resistance to glycolytic inhibition is that increased glycolytic enzymes induced by HIF-1 α require greater concentrations of 2-DG to effectively block glycolysis (Maher, Wangpaichitr et al. 2007). Glycolytic induction by oligomycin A treatment, shown to subsequently decrease oxidative phosphorylation, did not affect the increased Treg cell frequencies in hypoxia. ATP synthase is inhibited by oligomycin A, however, ATP production by the mitochondria is not halted completely as protons diffuse into the mitochondrial matrix via proton leak or mitochondrial uncoupling (Jastroch, Divakaruni et al. 2010). Finally, the inhibition of complex I in the electron transport chain by rotenone treatment results in a significant decrease in Treg cell frequencies compared with those displayed in hypoxia. These results suggest the expansion of Treg cells in hypoxia may be due to the utilization of both glycolysis and mitochondrial respiration pathways. However, previous studies have demonstrated an impairment in oxidative phosphorylation by prolonged hypoxia in breast cancer cells (Rodriguez-Enriquez, Carreno-Fuentes et al. 2010). Additionally, most reports in the literature consider hypoxic conditions occurring in cells at 5-0.5% O₂; however, this range corresponds to 46-4.6 μ M O₂, with studies indicating that oxidative phosphorylation activity is not dependent on oxygen concentration up to at least 20 μ M at a pH 7.4 (Wilson, Rumsey et al. 1988). This study focused on rat liver mitochondria and may not reflect the mitochondrial activity in human CD4⁺ T cells.

The mechanisms by which Treg cell frequencies are increased in hypoxia are not clearly defined. Glycolysis seems to play a role in this expansion and survival, as does HIF-1 α . Mitochondrial respiration may also contribute to Treg cell survival in hypoxia.

This study investigated the role of Fumaderm™ treatment in modulating the Treg:Th17 axis in psoriasis. Fumaderm™ has been approved for the treatment of psoriasis in Germany for many years. However, the mechanism of action by which Fumaderm™ exerts its anti-inflammatory effects is unknown, although it was originally thought to play a role in metabolism (Schweckendiek 1959). This chapter identified the effect of Fumaderm™ on Th17, Th1, exTh17 and Treg cells, including inflammatory cytokine expression by CD4⁺ T cells.

Initially comparing separate groups of healthy donor blood, untreated psoriasis patients and a group of patients receiving Fumaderm™, IL-17-expressing CD4⁺ T cells were shown to be decreased in Fumaderm™-treated patients compared with untreated patients. Transitioning exTh17 cells, IL-17 and IFN- γ double positive cells, and exTh17 cells switched fully to primarily IFN- γ producers were reduced in the Fumaderm™-treated patients compared with untreated patients. Fumaderm™ did not affect Th1 IFN- γ -producing T cells in this study. Fumaderm™-treated patients revealed a reduction in IL-22 expression and an increase in CD4⁺IL-2⁺ T cells. Finally, the examination of Treg cell frequencies in psoriasis patients exposed a significant increase in patients treated with Fumaderm™ compared with untreated patients. These data suggested that Fumaderm™ treatment in psoriasis targets the Treg:Th17 axis. Furthermore, examining the more direct effects of Fumaderm™ treatment in psoriasis patients both pre- and post-treatment (the same individual both before and after treatment) revealed a reduction in CD4⁺CD161⁺ T cells and, in exTh17 cells expressing chiefly IFN- γ , a decrease in CD4⁺ T cells expressing GM-CSF and finally an increase in Treg cell frequencies in patients post-Fumaderm™ treatment. This data demonstrates for the first time a role for Fumaderm™ in manipulating the Treg:Th17 axis by the reduction of Th17 lineage and exTh17 cells, and a corresponding increase in Treg cells, in psoriasis patients.

Evidence for a key role for T cells in the pathogenesis of psoriasis has come from both experimental and clinical data. Th17 cells in particular have been implicated in the propagation of inflammation in psoriasis. In this study, Th17 cell frequencies, characterized by CD161 and IL-17 expression, are reduced to healthy levels in Fumaderm™ treated patients compared with untreated patients. IL-17⁺ T cells are

reduced, as is the frequency of CD161⁺IL-17⁺ T cells in the total FumadermTM-treated group compared with untreated. However, the expression of total CD161 is not significantly changed, although a trend towards a decrease is observed. Human NKT cells express both CD3 and CD161 and studies have revealed an increase in NKT cells expressing the activation marker CD161 in psoriasis (Nickoloff 1999). Therefore, CD161 expression by NKT cells in psoriasis could mask the decrease in CD4⁺CD161⁺ Th17 cells (gated on CD3⁺CD8⁻) following total FumadermTM treatment. However, NKT cells make up only 1% of total peripheral blood, making this scenario unlikely. The inspection of the direct effect of FumadermTM on Th17 lineage cell populations revealed a significant decrease in CD161-expressing T cells, and no change in IL-17- or CD161⁺IL-17-expressing T cells. This result focuses on Fumaderm directly, examining PBMC from the same patients pre- and post-FumadermTM. Although no change is observed for IL-17-expressing T cells, a reduced expression of CD161, known to promote transendothelial migration, could result in decreased migration of Th17 lineage cells to the skin (Poggi, Costa et al. 1997). It is important to note that FumadermTM dosage for these patients is unknown, as is the level of success of treatment. Additionally in murine studies, DMF has demonstrated an inhibition of HIF-1 α expression and function. This may contribute to the inhibitory effects of FumadermTM on Th17 cells, as Th17 cells in vivo in RA have demonstrated a trend towards an increased expression of HIF-1 α . However, Treg cells also displayed this trend and therefore, inhibition of HIF-1 α by FumadermTM may additionally effect Treg cell populations in psoriasis.

ExTh17 cells, as mentioned previously, are highly polyfunctional cells that are enriched in the RA joint and have been shown to resist Treg cell-mediated suppression (Basdeo et al. unpublished data). Their role in psoriasis is yet to be elucidated. In this study, the frequency of transitioning exTh17 cells, IL-17⁺IFN- γ ⁺ T cells, is increased in untreated psoriasis patients compared with healthy donors, and decreased in FumadermTM-treated patients compared with untreated. Additionally, the frequency of fully switched exTh17 cells, CD161⁺IFN- γ ⁺, are markedly enhanced in untreated patients, and decreased in FumadermTM-treated patients. Additionally, examining the direct effect of FumadermTM on exTh17 cells, the frequency of fully switched exTh17 cells are significantly decreased. This result demonstrates the direct negative effect of FumadermTM on exTh17 cell

populations in psoriasis and a possible role for exTh17 cells in the pathogenesis of psoriasis.

This chapter also examined the frequency of Th1 cells in untreated psoriasis patients compared with those following Fumaderm™ treatment. The results demonstrated no significant change in Th1 cells between healthy, untreated or Fumaderm™-treated patients, be it IFN- γ -expressing T cells or those gated as CD161⁺IFN- γ -producing T cells, in order to remove exTh17 cells expressing IFN- γ . Psoriasis was originally thought to be a Th1 cell-mediated disease, as elevated levels of IFN- γ cytokine were observed in psoriasis patients (Schlaak, Buslau et al. 1994). Therefore, the lack of change in IFN- γ -expressing T cells in untreated psoriasis patients was unforeseen and surprising. However, it has emerged that a combination of Th1 and Th17 cells propagate inflammation in psoriasis (Kryczek, Bruce et al. 2008). Kryczek et al. found that IFN- γ is a potent promoter of human IL-17⁺ T-cell trafficking, induction and function (Kryczek, Bruce et al. 2008). As of yet, psoriasis therapies have not targeted Th1 cells, and as results in this chapter demonstrate no effect of Fumaderm™ on Th1 cells, perhaps this will not be an effective target. It is possible that some of the studies described above may have incorrectly identified exTh17 cells as Th1 cells.

This study demonstrates the novel role of Fumaderm™ treatment in cytokine-expression by CD4⁺ T cells. IL-2 is required for T cell activation and levels are increased in psoriatic lesions (Uyemura, Yamamura et al. 1993). In this study, a significant increase in the frequency of IL-2-expressing CD4⁺ T cells was demonstrated in Fumaderm™-treated patients, compared with untreated patients. However, looking directly at Fumaderm™ treatment, no change was observed between pre- and post-Fumaderm™ patients. This result was surprising, however, regulatory T cells, characterized by IL-2R (CD25) expression, require substantial IL-2 signalling to maintain survival and function in the periphery (Maloy and Powrie 2005). This may provide reasoning for an overall increase in IL-2-expressing T cells in Fumaderm™-treated patients compared with untreated. Increased IL-2 may be contributing to the anti-inflammatory effect of Fumaderm™ via Treg cells.

TNF- α is a hallmark of psoriasis. However, the frequency of TNF- α -expressing CD4⁺ T cells were decreased in untreated psoriasis patients compared with healthy controls. Additionally, Fumaderm™ demonstrated no direct or indirect effect on CD4⁺TNF- α ⁺ T cells. This result was unanticipated, as successful therapies for psoriasis have previously targeted TNF- α (Yost and Gudjonsson 2009). TNF- α is produced dominantly by macrophages and antigen-presenting cells, and although CD4⁺TNF- α ⁺ T cell frequencies are unchanged between healthy, untreated and Fumaderm™ treatment in psoriasis, this does not take into account total TNF- α production.

This chapter demonstrates a significant decrease in GM-CSF-expressing CD4⁺ T cells following Fumaderm™ treatment in psoriasis patients. This result is observed between psoriasis patients pre- and post-Fumaderm™ treatment. GM-CSF is produced by numerous cell types, including macrophages and Th17 cells, and is known to promote epidermal growth and the proliferation of keratinocytes in humans in vivo (Braunstein, Kaplan et al. 1994). GM-CSF amplifies inflammation in psoriasis, and therefore, inhibition of GM-CSF in psoriasis by Fumaderm™ could contribute to the anti-inflammatory effects observed in patients.

IL-22, another Th17 cell-related cytokine, is significantly increased from healthy to untreated patients, and reduced from untreated to Fumaderm™-treated patients. IL-22 levels in psoriasis correlate with disease severity (Caproni, Antiga et al. 2009) and it has also been shown to induce psoriasis-like epidermis alterations (Wolk, Witte et al. 2009). Inhibition of IL-22 in murine studies has revealed a reduction in the expression of inflammatory mediators by epithelial cells and keratinocytes, as well as the recruitment and maintenance of inflammatory Th17 cells at the tissue site (Ma, Liang et al. 2008). Decreased IL-22-expressing CD4⁺ T cells may contribute to the anti-inflammatory effects induced by Fumaderm™.

Finally, regulatory T cell frequencies were examined in psoriasis patients. This study revealed for the first time a significant increase in Treg cells between untreated and Fumaderm™-treated patients, and additionally between the same individuals pre- and post-Fumaderm™. Treg cells provide suppression of responder cells; therefore, this result proposes a role for Treg cells in the reduced inflammation observed following

Fumaderm™ treatment. The expression of CD39 and CTLA-4 by Treg cells was investigated, as CTLA-4 is required for Treg cell-mediated suppression and CD39⁺Treg cells have previously been shown to provide enhanced suppression in MS compared with CD39⁻Treg cells (Fletcher, Loneragan et al. 2009). The expression of both proteins was unchanged between healthy controls and patients pre- and post-Fumaderm™ treatment. This suggests no known defect or enhancement, with regards to this study, in the suppressive abilities of Treg cells following Fumaderm™ treatment in psoriasis patients.

In summary, Fumaderm™ treatment of psoriasis patients favourably alters the Treg:Th17 ratio. Although there were some differences between the data from untreated/treated groups and pre-post treatment; broadly speaking Fumaderm™ appeared to inhibit Th17 lineage cells and associated cytokines and promote Treg cells. Fumaderm had a direct effect on the reduction of Th17 lineage cells (CD4⁺CD161⁺) and fully switched exTh17 cells (CD161⁺IFN- γ ⁺). There is no direct effect of Fumaderm™ on CD4⁺ T cells expressing IL-2, TNF α or IL-22. However, GM-CSF-expressing CD4⁺ T cells are reduced following treatment with Fumaderm™. And lastly, Fumaderm™ enhances the frequency of Treg cells in the blood of psoriasis patients, indicating a role for Treg cell-mediated suppression in the anti-inflammatory impact of Fumaderm™ treatment in psoriasis.

Chapter 6

**General Discussion
and
Future Work**

Chapter 6. General discussion and future work

6.1 General discussion

Introduction

The data presented in this study contributes to the understanding of the metabolic pathways utilized by human T cell subsets. Additionally, it contributes to the overall knowledge of T cell survival and expansion in hypoxic and inflamed environments. As outlined in chapter 1, the importance of maintaining a balance between Treg and Th17 cells is established for inflammatory and autoimmune diseases. Th17 cells are known to contribute to autoimmunity and inflammation, as many diseases have implicated an enrichment of Th17 cells in disease pathogenicity. Furthermore, a reduction in Treg cell frequencies or function can also contribute to the same diseases. The discovery of ways in which the Th17/Treg cell balance may be modified to restore immune homeostasis, may therefore provide a therapeutic benefit in autoimmune conditions.

Animal models of disease have provided a significant amount of information elucidating the role of Th17 and Treg cells in autoimmunity. Additionally, significant advances in our understanding of the *in vivo* functions of human cells have resulted from the development of 'humanized' mouse strains that support a functional human immune system. However, such studies are limited by a number of challenges, including a limited development of the lymph nodes, poor adaptive humoral responses and impairment in cell trafficking to non-lymphoid tissue. Furthermore, data generated from animal studies does not always translate to human cells. Therefore, the examination of human blood and tissue are necessary for the further understanding of the Th17:Treg cell axis in a clinical setting. Unfortunately, challenges exist in the execution of human cell studies, including limited access to specific tissues of interest, low cell numbers and reduced cellular viability following extraction from tissue. In addition, *in vivo* mechanistic studies are constrained by ethical issues, and *in vitro* mechanistic studies are hampered by the lack of tools such as knockouts that are available for murine studies. The examination of peripheral blood, although it provides an accessible route to the study of human cells, may not always reflect the environment encountered within the disease-affected tissue. In this study, the accessibility to RA synovial fluid provided an opportunity to directly

examine cells from the disease environment, and to compare this with matched patient blood.

In the last decade, a rejuvenated interest in immunometabolism has emerged, with studies focusing on the ability of metabolism to manipulate murine T cell differentiation. This could provide a mechanism by which the Th17:Treg cell axis may be skewed in autoimmune disease therapy. This study investigated human T cell subset metabolism and the effect of inflammation and hypoxia on the survival of human T cells.

Insights into human Th17 cell metabolism and the effects of hypoxia

The data herein demonstrates a dominant utilization of glycolysis by human Th17 cells in normoxic conditions. In vitro experiments indicate an increased expression of glucose transporters and glucose uptake by CD161⁺ Th17 lineage cells. The Seahorse Analyzer provided further confirmation of the glycolytic profile of Th17 cells. Additionally, CD161⁺ T cells displayed increased mTOR activity, which is confirmed to promote glycolysis, and the inhibition of this subsequently resulted in a reduction in Th17 cell frequencies. Additional manipulation of metabolic pathways, via galactose treatment and promotion of the PKM2 tetramer, validated the requirement of glycolysis for the survival of Th17 cells. These data is in agreement with the current dogma established within murine cells stating a necessity for glycolysis in the differentiation of Th17 cells. Additionally, murine studies demonstrate a role for HIF-1 α in this preferred glycolytic profile. HIF-1 α and glycolysis have been inseparable in terms of linking hypoxia and metabolism, with HIF-1 α promoting glycolytic gene expression and glycolysis enhancing HIF-1 α protein expression (Lu, Forbes et al. 2002, Shi, Wang et al. 2011). Data in this study demonstrated an increase in HIF-1 α for CD161⁺ T cells, providing a possible survival mechanism, in addition to other survival characteristics, for Th17 cells in hypoxia, which is a common feature of inflamed environments. In the examination of exTh17 cells, these cells demonstrated increased expression of the anti-apoptotic protein Bcl-2, a trend towards increased HIF-1 α expression and additionally demonstrate a glycolytic profile determined following the inhibition of glycolysis. ExTh17 cells have been implicated in numerous autoimmune diseases and an understanding of the mechanisms by which they survive in inflamed environments is crucial to understand and treat these specific diseases

CD161⁺ Th17 lineage cells are enhanced in the synovial fluid of RA patients compared with matched peripheral blood, consistent with the proposed role of Th17 cells in the pathogenesis of RA. Th17 lineage cells further increased their HIF-1 α expression in the SFMC. Furthermore, the expression of glucose transporters was increased in total CD4⁺ T cells and Th17 cells in the SFMC, suggesting the utilization of glycolysis by Th17 cells as a means for survival within the inflamed RA joint. However, the investigation of CD4⁺ T cells in hypoxia in vitro demonstrated a discrepancy in Th17 lineage cell frequencies compared with the results in vivo. Th17 cells were inhibited in hypoxia in vitro, despite an increased expression of HIF-1 α . This experiment highlights the variations that can exist between human in vitro and in vivo studies.

The source of this inhibition of Th17 cells may reside with the oxygen concentration defined as hypoxic in this study. In previous studies mimicking the environment surrounding the RA joint, cells are exposed to 3% oxygen levels. Unfortunately, PBMC demonstrated an inadequate proliferation in 3% oxygen in our system and therefore 5% hypoxia was chosen. It is plausible to suggest that, although HIF-1 α expression is increased overall in 5% oxygen, perhaps this is not sufficient to induce a full transition towards glycolysis in Th17 cells. Additionally, the RA joint represents a highly complex inflamed environment inhabited by an extensive range of cell types, some of which are not present in the in vitro system, including osteoclasts, chondrocytes and fibroblast-like synoviocytes (FLCs). These resident joint cells are crucial participants in RA pathogenesis. In particular, activated FLCs have been demonstrated to produce IL-6 and IL-23 cytokines that can act on Th17 cells to promote expansion and propagate inflammation further within the joint (Schmidt-Weber, Akdis et al. 2007). Additionally, FLCs produce the chemokine CCL20 known to recruit CCR6⁺Th17 cells into the affected joint (Hirota, Yoshitomi et al. 2007). The study of metabolites present at the joint is becoming popular for biomarker discovery in RA. Metabolites, which may not be present in abundance in vitro, may contribute to Th17 cell survival within the joint. Lactate, low-density lipoproteins and cholesterol are elevated in the RA joint, all of which have been shown to promote Th17 cells (Li, Wang et al. 2010, Zhang, Zhang et al. 2012, Haas, Smith et al. 2015). Succinate is another metabolite increased in RA and may promote Th17 cells via increased HIF-1 α . The discrepancies observed between in vitro and in vivo investigations in this study have highlighted the requirement for a more complex in vitro system for the

examination of T cell responses in hypoxia, in order to directly compare it to sites of inflammation.

In addition to the examination of Th17 lineage cells in RA, the effect of Fumaderm™ on CD161⁺ T cells was determined for psoriasis patients. This study confirmed an inhibitory effect of Fumaderm™ on total CD161⁺ Th17 lineage cells, exTh17 cells and the Th17 cell-related cytokine GM-CSF. The mechanism of action of Fumaderm™ is thought to promote anti-inflammatory effects via HO-1 and NRF-2; although, Fumaderm™ was originally taken as a metabolic supplement for fumaric acid (Schweckendiek 1959). These data confirms a role for Th17, exTh17 and GM-CSF inhibition in mediating the therapeutic effects of Fumaderm™ in psoriasis patients. However, it is important to consider the possibility that the cell frequencies observed in the blood may not reflect those in the psoriatic skin.

Insights into human Treg cell metabolism and the effects of hypoxia

The data presented in this study demonstrates a utilization of mitochondrial respiration for human Treg cells in normoxic conditions. Seahorse analysis demonstrates an increase in the oxygen consumption rate, relating to mitochondrial respiration, for human Treg cells. Additionally, Treg cell frequencies were enhanced following inhibition of glycolysis via glucose supplementation and rapamycin treatment. This result is in concurrence with the current dogma established in murine studies, indicating the utilisation of oxidative phosphorylation for Treg cell energy metabolism. These data together could provide a pathway to the promotion of Treg cells in inflamed environments via inhibition of glycolysis. However, this theory is short lived as this study has also presented data confirming a utilization of glycolysis by human Treg cells. Seahorse analysis and increased glucose transporter expression confirms this result. This finding could provide insights into the survival of Treg cells within the tumor microenvironment and inflamed sites, which are known to become hypoxic and subsequently promote glycolysis (Lu, Forbes et al. 2002). The employment of both metabolic pathways for energy supply is not uncommon, as total human CD4⁺ T cells have previously been shown to do so upon activation (Renner, Geiselhoringer et al. 2015).

In the inflamed and hypoxic RA joint, Treg cells were enhanced and displayed a trend towards increased HIF-1 α expression. Additionally, Treg cells demonstrated a glycolytic profile in the SFMC of RA patients through increased GLUT1 expression. These data suggests a possible novel mechanism by which Treg cells survive in inflamed environments in vivo. These data correlate with those presented for hypoxia in vitro, demonstrating an enrichment of Treg cells with increased GLUT1 and HIF-1 α . Attempts to elucidate the mechanism of expansion of Treg cells in hypoxia proved challenging. Inhibition of glycolysis with 2-DG failed to clarify the role of metabolism in Treg cell expansion in hypoxia. This may be explained by a previous study demonstrating an overpowering effect of HIF-1 α on glycolytic inhibitor activity (Maher, Wangpaichitr et al. 2007). The use of the PKM2 activator TEPP-46 resulted in a decrease in Treg cell expansion in hypoxia and may prove to inhibit both glycolysis and HIF-1 α in CD4⁺ T cells. This result may provide an insight into a dual role for HIF-1 α and glycolytic metabolism in the survival and expansion of Treg cells in hypoxia in vitro. Furthermore this suggests that caution should be exercised when considering the targeting of glycolysis in autoimmunity and inflammatory disease, as this might inhibit Treg cells.

Increased Treg cell frequencies were evident after culture in hypoxia in vitro and in vivo data in RA patients; however, the origin of Treg cells present in both studies is unknown. Unlike murine cells, thymic and peripheral Treg cells cannot be separately identified in human studies. Additionally, Treg cell suppression, and suppression of Th17 lineage cells (specifically ex-Th17 cells) in particular, is defective in the RA synovial fluid (Basdeo, Moran et al. 2015, Basdeo et al unpublished). The suppressive activity of human Treg cells in hypoxia in vitro is yet to be investigated, and remains challenging in the context of this study as the culture of sorted CD4⁺ T cells in hypoxia resulted in insufficient cellular proliferation.

Treg cells were further examined for their role in mediating the beneficial effects of Fumaderm™ in psoriasis patients. Patients demonstrated a significant increase in Treg cell frequencies as a result of Fumaderm™ treatment, which may enhance Treg cell-mediated suppression in patients. However, the examination of peripheral blood does not inevitably correlate with results gathered from the psoriatic skin. Continued experiments will need to be performed on psoriatic skin lesions and compared with

peripheral blood. Overall, this study implicates an increased frequency of Treg cells in the blood in mediating the beneficial effects demonstrated by Fumaderm™ treatment in psoriasis patients.

Implications for targeting metabolism and HIF-1 α for therapy

As knowledge of the role of energy metabolism in the differentiation of murine T cells emerged, metabolism and hypoxia became topics of interest for autoimmune and inflammatory disease therapy. Any target that could modulate the Treg:Th17 cell axis could potentially be selected for investigation as a drug target in these diseases. However, results in this study suggest that the targeting of glycolysis or HIF-1 α in order to inhibit inflammation may not necessarily be appropriate.

The targeting of glycolysis in cancer has presented some promising results in murine models of sarcomas, adenocarcinomas, leukemias, melanomas, and bladder, colon, lung, and breast tumors (Goldberg, Israeli et al. 2012). Additionally, 2-DG demonstrated some anti-tumor effects in phase 1 of clinical trials against solid state tumors; however, hypoxic cells soon demonstrated chemoresistance against 2-DG (Maher, Wangpaichitr et al. 2007). Lonidamine is an inhibitor of the glycolytic enzyme hexokinase-2 and has completed phase III trial. However its clinical success has so far been impaired by significant pancreatic and hepatic toxicities (Price, Page et al. 1996). These inhibitors aim to target cancer cells specifically, and the glycolytic metabolism that they employ. Additionally, the targeting of glycolysis in cancer may also target Treg cells, which have been shown to utilise glycolysis and act to suppress immune cell killing of tumor cells. In the case of autoimmune and inflammatory disease, inhibition of glycolysis could potentially inhibit both Th17 and Treg cells, decreasing inflammation but additionally inhibiting immune suppression.

In terms of targeting HIF-1 α , numerous drugs have been approved for the use in cancer, with many others in clinical trials. One group of therapies in particular, known as hypoxia-activated prodrugs (HAP), become activated only after encountering a hypoxic environment and provide a more specified target area for treatment (Denny 2000). Hypoxia is a characteristic feature of the tumor environment, as well as inflamed sites. However, as results in this study have demonstrated, the targeting of HIF-1 α may inhibit

both Th17 and Treg cells during inflammation, and therefore HIF-1 α may not necessarily be a favourable target for autoimmune therapy. Furthermore, as inhibition of HIF-1 α with YC-1 treatment and inhibition of glycolysis with 2-DG displayed no effect on Treg cell expansion in hypoxia in vitro, perhaps only a dual target might inhibit Treg cells in vivo. HIF-1 α is not consistently viewed as having negative effects. For example, in murine models of colitis, inhibition of the PHD proteins and consequent stabilization of HIF-1 α correlates with a decrease in clinical symptoms of the disease (Cummins, Seeballuck et al. 2008). Therefore, HIF-1 α may be both harmful, promoting Th17 cell survival, or protective, promoting Treg cell survival in autoimmune and inflammatory disease.

Conclusion

This study demonstrates a utilization of glycolysis by human Th17 cells in vitro and a possible employment of glycolysis by Th17 cells for the survival in the inflamed RA joint. Additionally, human Treg cells demonstrate a use of both glycolysis and mitochondrial respiration in vitro and their survival in inflamed sites may be attributed to a dual action of glycolysis and HIF-1 α . Additionally, this study has demonstrated a role for Fumaderm™ in the modulation of the Th17:Treg cell axis in psoriasis patients. Collectively, this study has provided an increased understanding of human Th17 and Treg cells in general, and has highlighted the challenges associated with potentially targeting glycolysis or hypoxia for the treatment of autoimmune and inflammatory diseases in the future. A summary of the finding in this study are outlined in figure 6.1.

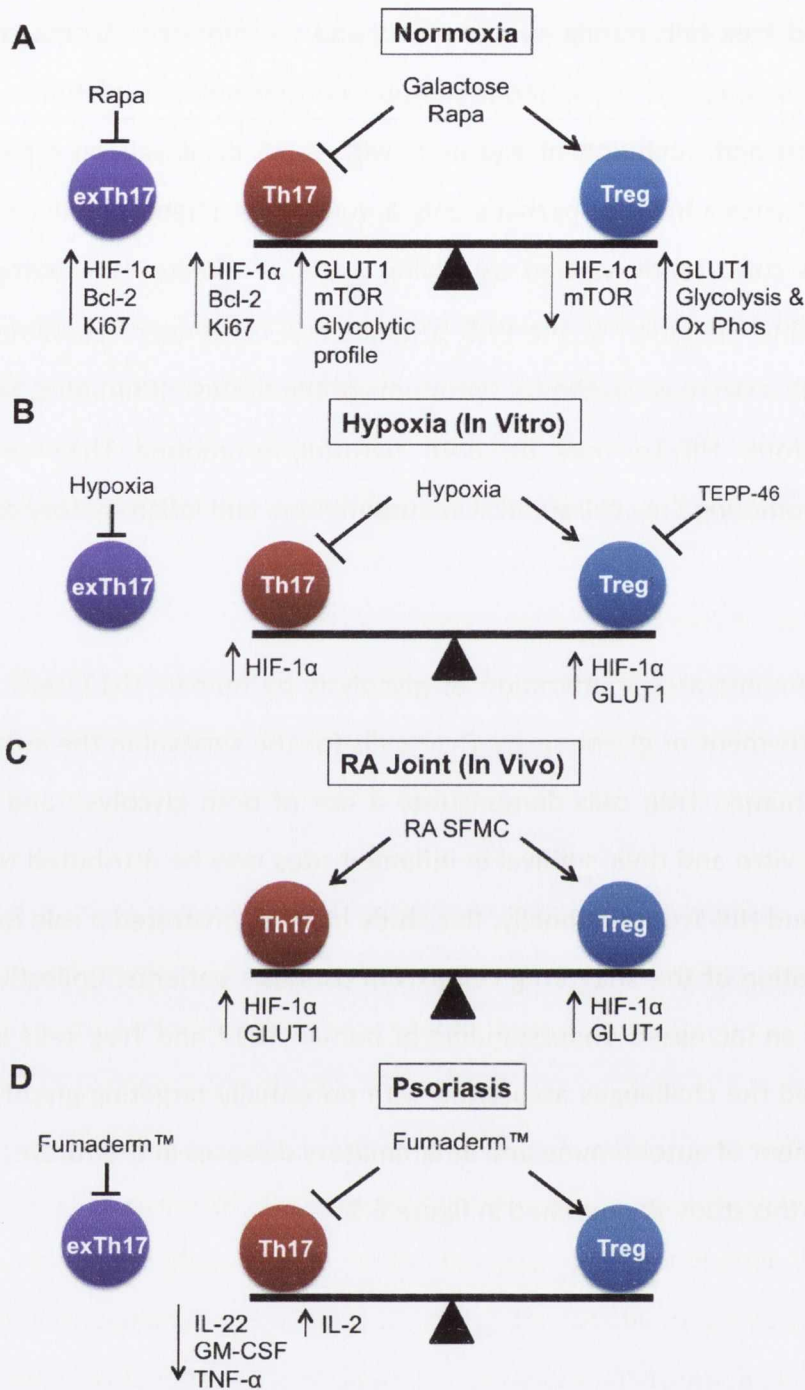


Figure 6.1 Regulation of the Treg:Th17 axis by metabolism, hypoxia and immunomodulatory therapy.

In normoxia (A), Th17 cells and exTh17 cells utilize a glycolytic profile and demonstrate an increase in HIF-1 α , Ki67 and Bcl-2 expression, whereas Treg cells utilize both glycolysis and mitochondrial respiration and can survive during glycolytic inhibition. In hypoxia in vitro (B), Th17 lineage and exTh17 cells are inhibited, although Th17 lineage cells do express increased HIF-1 α . Treg cells are increased in hypoxia and additionally demonstrate an increase in HIF-1 α , but also an increase in GLUT1 expression. Treg cells are inhibited by TEPP-46, suggested to act through an inhibition of both HIF-1 α and glycolysis. In vivo in SFMC of the RA joint (C), an increase in both Th17 and Treg cells is observed, in addition to increased HIF-1 α and GLUT1 expression for both subsets. Finally, Fumaderm™ is shown to manipulate T cells in psoriasis patients, inhibiting Th17 lineage and exTh17 cells and promoting Treg cells (D). This figure summarizes the effect of hypoxia and metabolism on the modulation of the Th17:Treg axis in vitro and in vivo.

6.2 Future experiments

Metabolic profile of T cell subsets

This study provided important new information on the metabolic profile of CD161⁺ Th17 lineage and Treg cells compared with CD161⁻ Th cells. However it would be of great interest in future to carry out a more detailed examination of the metabolic profile of Th1, Th2 and ExTh17 and thymic versus peripheral Treg cells using the approaches established in this thesis. In addition, important insights could be gained from analysing the expression of specific genes involved in glycolysis and mitochondrial respiration in T cell subsets.

The mechanism of Treg induction in hypoxia

In this study culture of PBMC in hypoxia in vitro was found to enhance the frequency of Treg cells although the mechanism for this remains to be elucidated. It would be useful to examine the origin of the Treg cell expansion observed in hypoxia in vitro via depleting PBMC of Treg cells and examining the frequency of Treg cells after activation in hypoxia. Enhancement of Tregs would indicate that Tregs were being induced from non-Treg cells in hypoxia, whereas if there was no enhancement of Treg cells in Treg-depleted PBMC in hypoxia it would indicate that Treg cells had expanded from the existing Treg pool. In addition, it would be of interest to assess the suppressive ability of Treg cells generated in hypoxia.

Mechanism by which Fumaderm™ modulates the Treg:Th17 axis

This study provided novel information on the immunomodulatory effects of Fumaderm™ in vivo. However the molecular mechanism by which it modulates the Treg:Th17 axis is still unknown. Fumarates are known to stabilize the expression of Nrf2, which induces the expression of HO-1 that could potentially exert anti-inflammatory effects. Both RNA and protein extracts from Fumaderm™ treated patients have been stored and will be examined for the expression of HO-1. In addition, further examination of psoriasis patients receiving Fumaderm™ treatment would be performed on skin lesions in comparison with compared with peripheral blood. Finally, the examination of T cell death in Fumaderm™ treated patients is of interest, as instances of progressive multifocal leukoencephalopathy (PML), which occurs as a result of leucopenia, are increasing for psoriasis patients on Fumaderm™ treatment.

Appendices

Appendix 1. Materials

Cell culture medium

Roswell Park Memorial Institute (RPMI)-1640 (BioSera) was supplemented with heat-inactivated (56°C for 30 minutes) Foetal Calf Serum (FCS; 10%, BioSera), 100 mM L-Glutamine and 100 µg/ml penicillin/streptomycin (Sigma).

Complete glucose-free medium

Glucose-free Roswell Park Memorial Institute (RPMI)-1640 (Life Technologies) was supplemented with dialyzed FCS (10%) (Fisher), 2mM L-glutamine (Sigma), 1mM sodium pyruvate (Sigma), penicillin/streptomycin (1%), vitamin cocktail (1:100) (Invivogen) and selenium/insulin cocktail (1:100) (Invivogen).

Seahorse Medium

XF Assay Medium (modified DMEM) (Seahorse Biosciences) supplemented with FCS (10%), sodium pyruvate (1 mM) and L-Glutamine (2 mM).

MACS Buffer

Dulbecco's Phosphate Buffered Saline (PBS; Sigma) supplemented with FCS (2%) and EDTA (2 mM), degassed and maintained at 4°C.

FACS Buffer

PBS (Sigma) supplemented with FCS (2%) and sodium azide (0.02%)

GLUT1 staining buffer A

Complete RPMI supplemented with EDTA (0.2%), and sodium azide (2%) (Sigma).

GLUT1 staining buffer B

PBS supplemented with EDTA (0.2%), sodium azide (2%) and FCS (2%).

PBS-Tween

10X PBS (80 g NaCl, 11.6 g Na₂HPO₄, 2 g KH₂PO₄ and 2 g KCl dissolved in 1 L dH₂O). For a 1X solution, dissolve 1:10 in dH₂O with 1 ml Tween[®] 20 (Sigma)

1 M Tris-HCl (pH7.5)

Dissolve 121.1 g of Tris base (Sigma) in 800 ml of dH₂O. Adjust pH with HCl.

ELISA Reagents

Wash buffer: 1X PBS- Tween[®] 20

Substrate solution: TMB

Stopping solution: Sulphuric Acid (H₂SO₄ ; 1M)

Antibody	Reactivity	Supplier
IFN- γ	Human	eBioscience
IL-10	Human	eBioscience
IL-17A	Human	eBioscience
TGF- β	Human	eBioscience

Fluorochrome-conjugated antibodies for flow cytometry

Antibody	Fluor	Supplier	Vol/ 50µl test (µl)
Bcl-2	FITC	eBioscience	2
CCR4	Alexa 647	BD	2.5
CCR6	FITC	BD	5
CCR7	PE	eBioscience	1.25
CD3	A700	eBioscience	1.25
	V500	BD	1.25
	BV711	BD	1.25
CD4	PerCP-Cy5.5	eBioscience	1.25
	PE-CF594	BD	1.25
	V500	BD	1.25
CD8	APC-e780	eBioscience	1.25
CD25	PE	eBioscience	1.5
	PE-Cy7	eBioscience	1.5
	APC	eBioscience	1.5
CD39	PerCP-e710	eBioscience	1.25
CD45RA	FITC	eBioscience	5
	PE-Cy7	eBioscience	1.25
	V450	eBioscience	1.25
CD45RO	APC-Vio770	Miltenyi	2
	BV650	Biolegend	1.25
CD127	APC-e780	eBioscience	1.5
CD161	PE-Cy7	eBioscience	1.5
	PE	eBioscience	1.5
	PE-Cy5	BD	5
CTLA-4	APC	eBioscience	5
	BV786	BD	1.25
CXCR3	PE	Biolegend	2
Foxp3	FITC	eBioscience	1.5
	PE	eBioscience	1.5
	V450	eBioscience	1.5
GLUT1	GFP	Metfora Biosystems	2.5
GM-CSF	PE	eBioscience	1.25

HIF-1 α	PE	R&D	5
IFN- γ	APC	BD	0.75
	BV605	BD	1.25
	Pacific blue	Biolegend	0.5
IL-2	PE-CF594	BD	1.25
IL-17A	FITC	eBioscience	1.5
	PE	eBioscience	1.5
	A700	BD	1.5
IL-22	PE-Cy7	eBioscience	1.25
Ki67	Alexa-488	BD	1.25
	V450	eBioscience	2
pS6	PE	Cell Signaling	1
TNF- α	PerCP-Cy5.5	eBioscience	1.25
Viability Dye	efluor506	eBioscience	1 μ l/ml

General Reagents

Reagent	Supplier
2-DG	Sigma
2-NBDG	Invivogen
Antimycin A	Sigma
Brefeldin A	Sigma
CFSE	Invivogen
CTV	Invivogen
FCCP	Sigma
Foxp3 Staining Buffers	eBioscience
Glucose	Sigma
Galactose	Sigma
Human anti-CD3 (OKT3 clone)	eBioscience
Ionomycin	Sigma
MACS kits	Miltenyi biotech
Mitotracker Green FM	Invivogen
Oligomycin A	Sigma
PMA	Sigma
Rapamycin	Sigma
rhIL-2	Miltenyi Biotech
rhIL-1 β	Miltenyi Biotech
rhIL-6	Miltenyi Biotech
rhIL-23	Miltenyi Biotech
rhTGF- β	Miltenyi Biotech
Rotenone	Sigma
TGF- β R1 inhibitor	Cambridge Bioscience
Treg expansion kit	Miltenyi biotech

Year	Value	Year	Value
1990	100	1990	100
1991	105	1991	105
1992	110	1992	110
1993	115	1993	115
1994	120	1994	120
1995	125	1995	125
1996	130	1996	130
1997	135	1997	135
1998	140	1998	140
1999	145	1999	145
2000	150	2000	150
2001	155	2001	155
2002	160	2002	160
2003	165	2003	165
2004	170	2004	170
2005	175	2005	175
2006	180	2006	180
2007	185	2007	185
2008	190	2008	190
2009	195	2009	195
2010	200	2010	200
2011	205	2011	205
2012	210	2012	210
2013	215	2013	215
2014	220	2014	220
2015	225	2015	225
2016	230	2016	230
2017	235	2017	235
2018	240	2018	240
2019	245	2019	245
2020	250	2020	250

References

References

- Abrams, J. R., S. L. Kelley, E. Hayes, T. Kikuchi, M. J. Brown, S. Kang, M. G. Lebowitz, C. A. Guzzo, B. V. Jegasothy, P. S. Linsley and J. G. Krueger (2000). "Blockade of T lymphocyte costimulation with cytotoxic T lymphocyte-associated antigen 4-immunoglobulin (CTLA4Ig) reverses the cellular pathology of psoriatic plaques, including the activation of keratinocytes, dendritic cells, and endothelial cells." *J Exp Med* **192**(5): 681-694.
- Acosta-Rodriguez, E. V., G. Napolitani, A. Lanzavecchia and F. Sallusto (2007). "Interleukins 1beta and 6 but not transforming growth factor-beta are essential for the differentiation of interleukin 17-producing human T helper cells." *Nat Immunol* **8**(9): 942-949.
- Agarwal, S., R. Misra and A. Aggarwal (2008). "Interleukin 17 levels are increased in juvenile idiopathic arthritis synovial fluid and induce synovial fibroblasts to produce proinflammatory cytokines and matrix metalloproteinases." *J Rheumatol* **35**(3): 515-519.
- Aggarwal, S., N. Ghilardi, M. H. Xie, F. J. de Sauvage and A. L. Gurney (2003). "Interleukin-23 promotes a distinct CD4 T cell activation state characterized by the production of interleukin-17." *J Biol Chem* **278**(3): 1910-1914.
- Alspaugh, M. A., F. C. Jensen, H. Rabin and E. M. Tan (1978). "Lymphocytes transformed by Epstein-Barr virus. Induction of nuclear antigen reactive with antibody in rheumatoid arthritis." *J Exp Med* **147**(4): 1018-1027.
- Alunno, A., M. Manetti, S. Caterbi, L. Ibba-Manneschi, O. Bistoni, E. Bartoloni, V. Valentini, R. Terenzi and R. Gerli (2015). "Altered immunoregulation in rheumatoid arthritis: the role of regulatory T cells and proinflammatory th17 cells and therapeutic implications." *Mediators Inflamm* **2015**: 751793.
- Anastasiou, D., Y. Yu, W. J. Israelsen, J. K. Jiang, M. B. Boxer, B. S. Hong, W. Tempel, S. Dimov, M. Shen, A. Jha, H. Yang, K. R. Mattaini, C. M. Metallo, B. P. Fiske, K. D. Courtney, S. Malstrom, T. M. Khan, C. Kung, A. P. Skoumbourdis, H. Veith, N. Southall, M. J. Walsh, K. R. Brimacombe, W. Leister, S. Y. Lunt, Z. R. Johnson, K. E. Yen, K. Kunii, S. M. Davidson, H. R. Christofk, C. P. Austin, J. Inglese, M. H. Harris, J. M. Asara, G. Stephanopoulos, F. G. Salituro, S. Jin, L. Dang, D. S. Auld, H. W. Park, L. C. Cantley, C. J. Thomas and M. G. Vander Heiden (2012). "Pyruvate kinase M2 activators promote tetramer formation and suppress tumorigenesis." *Nat Chem Biol* **8**(10): 839-847.
- Annunziato, F., L. Cosmi, F. Liotta, E. Maggi and S. Romagnani (2012). "Defining the human T helper 17 cell phenotype." *Trends Immunol* **33**(10): 505-512.
- Annunziato, F., L. Cosmi, F. Liotta, E. Maggi and S. Romagnani (2013). "Main features of human T helper 17 cells." *Ann N Y Acad Sci* **1284**: 66-70.
- Annunziato, F., L. Cosmi, V. Santarlasci, L. Maggi, F. Liotta, B. Mazzinghi, E. Parente, L. Fili, S. Ferri, F. Frosali, F. Giudici, P. Romagnani, P. Parronchi, F. Tonelli, E. Maggi and S. Romagnani (2007). "Phenotypic and functional features of human Th17 cells." *J Exp Med* **204**(8): 1849-1861.
- Apostolou, I., A. Sarukhan, L. Klein and H. von Boehmer (2002). "Origin of regulatory T cells with known specificity for antigen." *Nat Immunol* **3**(8): 756-763.
- Arcese, A., N. Aste, A. Bettacchi, G. Camplone, F. Cantoresi, M. Caproni, D. D'Amico, P. Fabbri, G. Filosa, A. Galluccio, K. Hansel, P. Lisi, G. Micali, M. L. Musumeci, M. Nicolini, A. Parodi, M. Patania, M. Pezza, C. Potenza, A. Richetta, M. Simonacci, P.

- Trevisan, G. Valenti and S. Calvieri (2010). "Treating psoriasis with etanercept in Italian clinical practice: prescribing practices and duration of remission following discontinuation." Clin Drug Investig **30**(8): 507-516.
- Astry, B., E. Harberts and K. D. Moudgil (2011). "A cytokine-centric view of the pathogenesis and treatment of autoimmune arthritis." J Interferon Cytokine Res **31**(12): 927-940.
- Basdeo, S. A., B. Moran, D. Cluxton, M. Canavan, J. McCormick, M. Connolly, C. Orr, K. H. Mills, D. J. Veale, U. Fearon and J. M. Fletcher (2015). "Polyfunctional, Pathogenic CD161+ Th17 Lineage Cells Are Resistant to Regulatory T Cell-Mediated Suppression in the Context of Autoimmunity." J Immunol **195**(2): 528-540.
- Basdeo, S. A., B. Moran, D. Cluxton, M. Canavan, J. McCormick, M. Connolly, C. Orr, K. H. Mills, D. J. Veale, U. Fearon and J. M. Fletcher (2015). "Polyfunctional, Pathogenic CD161+ Th17 Lineage Cells Are Resistant to Regulatory T Cell-Mediated Suppression in the Context of Autoimmunity." J Immunol.
- Battaglia, M., A. Stabilini, B. Migliavacca, J. Horejs-Hoeck, T. Kaupper and M. G. Roncarolo (2006). "Rapamycin promotes expansion of functional CD4+CD25+FOXP3+ regulatory T cells of both healthy subjects and type 1 diabetic patients." J Immunol **177**(12): 8338-8347.
- Battaglia, M., A. Stabilini and M. G. Roncarolo (2005). "Rapamycin selectively expands CD4+CD25+FoxP3+ regulatory T cells." Blood **105**(12): 4743-4748.
- Battaglia, M., A. Stabilini and E. Tresoldi (2012). "Expanding human T regulatory cells with the mTOR-inhibitor rapamycin." Methods Mol Biol **821**: 279-293.
- Ben-Shoshan, J., S. Maysel-Auslender, A. Mor, G. Keren and J. George (2008). "Hypoxia controls CD4+CD25+ regulatory T-cell homeostasis via hypoxia-inducible factor-1alpha." Eur J Immunol **38**(9): 2412-2418.
- Bettelli, E., Y. Carrier, W. Gao, T. Korn, T. B. Strom, M. Oukka, H. L. Weiner and V. K. Kuchroo (2006). "Reciprocal developmental pathways for the generation of pathogenic effector TH17 and regulatory T cells." Nature **441**(7090): 235-238.
- Bin Dhuban, K., M. Kornete, S. M. E and C. A. Piccirillo (2014). "Functional dynamics of Foxp3(+) regulatory T cells in mice and humans." Immunol Rev **259**(1): 140-158.
- Bollinger, T., S. Gies, J. Naujoks, L. Feldhoff, A. Bollinger, W. Solbach and J. Rupp (2014). "HIF-1alpha- and hypoxia-dependent immune responses in human CD4+CD25high T cells and T helper 17 cells." J Leukoc Biol **96**(2): 305-312.
- Borsellino, G., M. Kleinewietfeld, D. Di Mitri, A. Sternjak, A. Diamantini, R. Giometto, S. Hopner, D. Centonze, G. Bernardi, M. L. Dell'Acqua, P. M. Rossini, L. Battistini, O. Rotzschke and K. Falk (2007). "Expression of ectonucleotidase CD39 by Foxp3+ Treg cells: hydrolysis of extracellular ATP and immune suppression." Blood **110**(4): 1225-1232.
- Bowcock, A. M. and J. G. Krueger (2005). "Getting under the skin: the immunogenetics of psoriasis." Nat Rev Immunol **5**(9): 699-711.
- Brabletz, T., I. Pfeuffer, E. Schorr, F. Siebelt, T. Wirth and E. Serfling (1993). "Transforming growth factor beta and cyclosporin A inhibit the inducible activity of the interleukin-2 gene in T cells through a noncanonical octamer-binding site." Mol Cell Biol **13**(2): 1155-1162.
- Braunstein, S., G. Kaplan, A. B. Gottlieb, M. Schwartz, G. Walsh, R. M. Abalos, T. T. Fajardo, L. S. Guido and J. G. Krueger (1994). "GM-CSF activates regenerative epidermal growth and stimulates keratinocyte proliferation in human skin in vivo." J Invest Dermatol **103**(4): 601-604.

- Bush, K. A., J. S. Walker, C. S. Lee and B. W. Kirkham (2001). "Cytokine expression and synovial pathology in the initiation and spontaneous resolution phases of adjuvant arthritis: interleukin-17 expression is upregulated in early disease." Clin Exp Immunol **123**(3): 487-495.
- Bustamante, E. and P. L. Pedersen (1977). "High aerobic glycolysis of rat hepatoma cells in culture: role of mitochondrial hexokinase." Proc Natl Acad Sci U S A **74**(9): 3735-3739.
- Cao, D., R. van Vollenhoven, L. Klareskog, C. Trollmo and V. Malmstrom (2004). "CD25^{bright}CD4⁺ regulatory T cells are enriched in inflamed joints of patients with chronic rheumatic disease." Arthritis Res Ther **6**(4): R335-346.
- Cao, Y., J. C. Rathmell and A. N. Macintyre (2014). "Metabolic reprogramming towards aerobic glycolysis correlates with greater proliferative ability and resistance to metabolic inhibition in CD8 versus CD4 T cells." PLoS One **9**(8): e104104.
- Caproni, M., E. Antiga, L. Melani, W. Volpi, E. Del Bianco and P. Fabbri (2009). "Serum levels of IL-17 and IL-22 are reduced by etanercept, but not by acitretin, in patients with psoriasis: a randomized-controlled trial." J Clin Immunol **29**(2): 210-214.
- Chalan, P., B. J. Kroesen, K. S. van der Geest, M. G. Huitema, W. H. Abdulahad, J. Bijzet, E. Brouwer and A. M. Boots (2013). "Circulating CD4⁺CD161⁺ T lymphocytes are increased in seropositive arthralgia patients but decreased in patients with newly diagnosed rheumatoid arthritis." PLoS One **8**(11): e79370.
- Cham, C. M., G. Driessens, J. P. O'Keefe and T. F. Gajewski (2008). "Glucose deprivation inhibits multiple key gene expression events and effector functions in CD8⁺ T cells." Eur J Immunol **38**(9): 2438-2450.
- Chang, C. H., J. D. Curtis, L. B. Maggi, Jr., B. Faubert, A. V. Villarino, D. O'Sullivan, S. C. Huang, G. J. van der Windt, J. Blagih, J. Qiu, J. D. Weber, E. J. Pearce, R. G. Jones and E. L. Pearce (2013). "Posttranscriptional control of T cell effector function by aerobic glycolysis." Cell **153**(6): 1239-1251.
- Chaturvedi, P., D. M. Gilkes, C. C. Wong, Kshitiz, W. Luo, H. Zhang, H. Wei, N. Takano, L. Schito, A. Levchenko and G. L. Semenza (2013). "Hypoxia-inducible factor-dependent breast cancer-mesenchymal stem cell bidirectional signaling promotes metastasis." J Clin Invest **123**(1): 189-205.
- Chen, W., W. Jin, N. Hardegen, K. J. Lei, L. Li, N. Marinos, G. McGrady and S. M. Wahl (2003). "Conversion of peripheral CD4⁺CD25⁻ naive T cells to CD4⁺CD25⁺ regulatory T cells by TGF-beta induction of transcription factor Foxp3." J Exp Med **198**(12): 1875-1886.
- Chen, Z., C. M. Tato, L. Muul, A. Laurence and J. J. O'Shea (2007). "Distinct regulation of interleukin-17 in human T helper lymphocytes." Arthritis Rheum **56**(9): 2936-2946.
- Chi, H. (2012). "Regulation and function of mTOR signalling in T cell fate decisions." Nat Rev Immunol **12**(5): 325-338.
- Chiricozzi, A. and J. G. Krueger (2013). "IL-17 targeted therapies for psoriasis." Expert Opin Investig Drugs **22**(8): 993-1005.
- Christofk, H. R., M. G. Vander Heiden, M. H. Harris, A. Ramanathan, R. E. Gerszten, R. Wei, M. D. Fleming, S. L. Schreiber and L. C. Cantley (2008). "The M2 splice isoform of pyruvate kinase is important for cancer metabolism and tumour growth." Nature **452**(7184): 230-233.
- Chun, Y. S., E. J. Yeo, E. Choi, C. M. Teng, J. M. Bae, M. S. Kim and J. W. Park (2001). "Inhibitory effect of YC-1 on the hypoxic induction of erythropoietin and vascular endothelial growth factor in Hep3B cells." Biochem Pharmacol **61**(8): 947-954.

- Chun, Y. S., E. J. Yeo and J. W. Park (2004). "Versatile pharmacological actions of YC-1: anti-platelet to anticancer." Cancer Lett **207**(1): 1-7.
- Clambey, E. T., E. N. McNamee, J. A. Westrich, L. E. Glover, E. L. Campbell, P. Jedlicka, E. F. de Zoeten, J. C. Cambier, K. R. Stenmark, S. P. Colgan and H. K. Eltzschig (2012). "Hypoxia-inducible factor-1 alpha-dependent induction of FoxP3 drives regulatory T-cell abundance and function during inflammatory hypoxia of the mucosa." Proc Natl Acad Sci U S A **109**(41): E2784-2793.
- Cockman, M. E., N. Masson, D. R. Mole, P. Jaakkola, G. W. Chang, S. C. Clifford, E. R. Maher, C. W. Pugh, P. J. Ratcliffe and P. H. Maxwell (2000). "Hypoxia inducible factor-alpha binding and ubiquitylation by the von Hippel-Lindau tumor suppressor protein." J Biol Chem **275**(33): 25733-25741.
- Cosmi, L., R. Cimaz, L. Maggi, V. Santarlaschi, M. Capone, F. Borriello, F. Frosali, V. Querci, G. Simonini, G. Barra, M. P. Piccinni, F. Liotta, R. De Palma, E. Maggi, S. Romagnani and F. Annunziato (2011). "Evidence of the transient nature of the Th17 phenotype of CD4+CD161+ T cells in the synovial fluid of patients with juvenile idiopathic arthritis." Arthritis Rheum **63**(8): 2504-2515.
- Cosmi, L., R. De Palma, V. Santarlaschi, L. Maggi, M. Capone, F. Frosali, G. Rodolico, V. Querci, G. Abbate, R. Angeli, L. Berrino, M. Fambrini, M. Caproni, F. Tonelli, E. Lazzeri, P. Parronchi, F. Liotta, E. Maggi, S. Romagnani and F. Annunziato (2008). "Human interleukin 17-producing cells originate from a CD161+CD4+ T cell precursor." J Exp Med **205**(8): 1903-1916.
- Cosmi, L., F. Liotta, E. Maggi, S. Romagnani and F. Annunziato (2014). "Th17 and non-classic Th1 cells in chronic inflammatory disorders: two sides of the same coin." Int Arch Allergy Immunol **164**(3): 171-177.
- Creagh, E. M. and L. A. O'Neill (2006). "TLRs, NLRs and RLRs: a trinity of pathogen sensors that co-operate in innate immunity." Trends Immunol **27**(8): 352-357.
- Cummins, E. P., F. Seeballuck, S. J. Keely, N. E. Mangan, J. J. Callanan, P. G. Fallon and C. T. Taylor (2008). "The hydroxylase inhibitor dimethyloxalylglycine is protective in a murine model of colitis." Gastroenterology **134**(1): 156-165.
- Czabotar, P. E., G. Lessene, A. Strasser and J. M. Adams (2014). "Control of apoptosis by the BCL-2 protein family: implications for physiology and therapy." Nat Rev Mol Cell Biol **15**(1): 49-63.
- Dahlquist, G. (1998). "The aetiology of type 1 diabetes: an epidemiological perspective." Acta Paediatr Suppl **425**: 5-10.
- Dang, E. V., J. Barbi, H. Y. Yang, D. Jinasena, H. Yu, Y. Zheng, Z. Bordman, J. Fu, Y. Kim, H. R. Yen, W. Luo, K. Zeller, L. Shimoda, S. L. Topalian, G. L. Semenza, C. V. Dang, D. M. Pardoll and F. Pan (2011). "Control of T(H)17/T(reg) balance by hypoxia-inducible factor 1." Cell **146**(5): 772-784.
- Davidson, A. and B. Diamond (2001). "Autoimmune diseases." N Engl J Med **345**(5): 340-350.
- de Boer, O. J., I. M. Wakelkamp, S. T. Pals, N. Claessen, J. D. Bos and P. K. Das (1994). "Increased expression of adhesion receptors in both lesional and non-lesional psoriatic skin." Arch Dermatol Res **286**(6): 304-311.
- Deaglio, S., K. M. Dwyer, W. Gao, D. Friedman, A. Usheva, A. Erat, J. F. Chen, K. Enjoji, J. Linden, M. Oukka, V. K. Kuchroo, T. B. Strom and S. C. Robson (2007). "Adenosine generation catalyzed by CD39 and CD73 expressed on regulatory T cells mediates immune suppression." J Exp Med **204**(6): 1257-1265.
- Dejaco, C., C. Duftner, B. Grubeck-Loebenstien and M. Schirmer (2006). "Imbalance of regulatory T cells in human autoimmune diseases." Immunology **117**(3): 289-300.

- Delgoffe, G. M., T. P. Kole, Y. Zheng, P. E. Zarek, K. L. Matthews, B. Xiao, P. F. Worley, S. C. Kozma and J. D. Powell (2009). "The mTOR kinase differentially regulates effector and regulatory T cell lineage commitment." *Immunity* **30**(6): 832-844.
- Delgoffe, G. M., K. N. Pollizzi, A. T. Waickman, E. Heikamp, D. J. Meyers, M. R. Horton, B. Xiao, P. F. Worley and J. D. Powell (2011). "The kinase mTOR regulates the differentiation of helper T cells through the selective activation of signaling by mTORC1 and mTORC2." *Nat Immunol* **12**(4): 295-303.
- Demaria, M., C. Giorgi, M. Lebedzinska, G. Esposito, L. D'Angeli, A. Bartoli, D. J. Gough, J. Turkson, D. E. Levy, C. J. Watson, M. R. Wieckowski, P. Provero, P. Pinton and V. Poli (2010). "A STAT3-mediated metabolic switch is involved in tumour transformation and STAT3 addiction." *Aging (Albany NY)* **2**(11): 823-842.
- Denny, W. A. (2000). "The role of hypoxia-activated prodrugs in cancer therapy." *Lancet Oncol* **1**(1): 25-29.
- Dolhain, R. J., N. T. ter Haar, S. Hoefakker, P. P. Tak, M. de Ley, E. Claassen, F. C. Breedveld and A. M. Miltenburg (1996). "Increased expression of interferon (IFN)-gamma together with IFN-gamma receptor in the rheumatoid synovial membrane compared with synovium of patients with osteoarthritis." *Br J Rheumatol* **35**(1): 24-32.
- Duvel, K., J. L. Yecies, S. Menon, P. Raman, A. I. Lipovsky, A. L. Souza, E. Triantafellow, Q. Ma, R. Gorski, S. Cleaver, M. G. Vander Heiden, J. P. MacKeigan, P. M. Finan, C. B. Clish, L. O. Murphy and B. D. Manning (2010). "Activation of a metabolic gene regulatory network downstream of mTOR complex 1." *Mol Cell* **39**(2): 171-183.
- Edinger, A. L. and C. B. Thompson (2002). "Akt maintains cell size and survival by increasing mTOR-dependent nutrient uptake." *Mol Biol Cell* **13**(7): 2276-2288.
- Ehrenstein, M. R., J. G. Evans, A. Singh, S. Moore, G. Warnes, D. A. Isenberg and C. Mauri (2004). "Compromised function of regulatory T cells in rheumatoid arthritis and reversal by anti-TNFalpha therapy." *J Exp Med* **200**(3): 277-285.
- Ema, M., S. Taya, N. Yokotani, K. Sogawa, Y. Matsuda and Y. Fujii-Kuriyama (1997). "A novel bHLH-PAS factor with close sequence similarity to hypoxia-inducible factor 1alpha regulates the VEGF expression and is potentially involved in lung and vascular development." *Proc Natl Acad Sci U S A* **94**(9): 4273-4278.
- Eyerich, S., K. Eyerich, D. Pennino, T. Carbone, F. Nasorri, S. Pallotta, F. Cianfarani, T. Odorisio, C. Traidl-Hoffmann, H. Behrendt, S. R. Durham, C. B. Schmidt-Weber and A. Cavani (2009). "Th22 cells represent a distinct human T cell subset involved in epidermal immunity and remodeling." *J Clin Invest* **119**(12): 3573-3585.
- Fantini, M. C., C. Becker, G. Monteleone, F. Pallone, P. R. Galle and M. F. Neurath (2004). "Cutting edge: TGF-beta induces a regulatory phenotype in CD4+CD25- T cells through Foxp3 induction and down-regulation of Smad7." *J Immunol* **172**(9): 5149-5153.
- Fergusson, J. R., V. M. Fleming and P. Klenerman (2011). "CD161-expressing human T cells." *Front Immunol* **2**: 36.
- Fletcher, J. M., S. J. Lalor, C. M. Sweeney, N. Tubridy and K. H. Mills (2010). "T cells in multiple sclerosis and experimental autoimmune encephalomyelitis." *Clin Exp Immunol* **162**(1): 1-11.
- Fletcher, J. M., R. Lonergan, L. Costelloe, K. Kinsella, B. Moran, C. O'Farrelly, N. Tubridy and K. H. Mills (2009). "CD39+Foxp3+ regulatory T Cells suppress pathogenic Th17 cells and are impaired in multiple sclerosis." *J Immunol* **183**(11): 7602-7610.

- Forster, R., A. Schubel, D. Breitfeld, E. Kremmer, I. Renner-Muller, E. Wolf and M. Lipp (1999). "CCR7 coordinates the primary immune response by establishing functional microenvironments in secondary lymphoid organs." Cell **99**(1): 23-33.
- Frauwirth, K. A., J. L. Riley, M. H. Harris, R. V. Parry, J. C. Rathmell, D. R. Plas, R. L. Elstrom, C. H. June and C. B. Thompson (2002). "The CD28 signaling pathway regulates glucose metabolism." Immunity **16**(6): 769-777.
- Galkin, A., A. Higgs and S. Moncada (2007). "Nitric oxide and hypoxia." Essays Biochem **43**: 29-42.
- Germain, C., A. Meier, T. Jensen, P. Knapnougel, G. Poupon, A. Lazzari, A. Neisig, K. Hakansson, T. Dong, N. Wagtmann, E. D. Galsgaard, P. Spee and V. M. Braud (2011). "Induction of lectin-like transcript 1 (LLT1) protein cell surface expression by pathogens and interferon-gamma contributes to modulate immune responses." J Biol Chem **286**(44): 37964-37975.
- Germain, R. N. (2002). "T-cell development and the CD4-CD8 lineage decision." Nat Rev Immunol **2**(5): 309-322.
- Gerriets, V. A., R. J. Kishton, A. G. Nichols, A. N. Macintyre, M. Inoue, O. Ilkayeva, P. S. Winter, X. Liu, B. Priyadarshini, M. E. Slawinska, L. Haerberli, C. Huck, L. A. Turka, K. C. Wood, L. P. Hale, P. A. Smith, M. A. Schneider, N. J. MacIver, J. W. Locasale, C. B. Newgard, M. L. Shinohara and J. C. Rathmell (2015). "Metabolic programming and PDHK1 control CD4+ T cell subsets and inflammation." J Clin Invest **125**(1): 194-207.
- Gerriets, V. A. and J. C. Rathmell (2012). "Metabolic pathways in T cell fate and function." Trends Immunol **33**(4): 168-173.
- Gershon, R. K. (1975). "A disquisition on suppressor T cells." Transplant Rev **26**: 170-185.
- Ghoreschi, K., J. Bruck, C. Kellerer, C. Deng, H. Peng, O. Rothfuss, R. Z. Hussain, A. R. Gocke, A. Respa, I. Glocova, N. Valtcheva, E. Alexander, S. Feil, R. Feil, K. Schulze-Osthoff, R. A. Rupec, A. E. Lovett-Racke, R. Dringen, M. K. Racke and M. Rocken (2011). "Fumarates improve psoriasis and multiple sclerosis by inducing type II dendritic cells." J Exp Med **208**(11): 2291-2303.
- Giatromanolaki, A., E. Sivridis, E. Maltezos, N. Athanassou, D. Papazoglou, K. C. Gatter, A. L. Harris and M. I. Koukourakis (2003). "Upregulated hypoxia inducible factor-1alpha and -2alpha pathway in rheumatoid arthritis and osteoarthritis." Arthritis Res Ther **5**(4): R193-201.
- Goldberg, L., R. Israeli and Y. Kloog (2012). "FTS and 2-DG induce pancreatic cancer cell death and tumor shrinkage in mice." Cell Death Dis **3**: e284.
- Griffiths, C. E. and J. N. Barker (2007). "Pathogenesis and clinical features of psoriasis." Lancet **370**(9583): 263-271.
- Grossman, Z., B. Min, M. Meier-Schellersheim and W. E. Paul (2004). "Concomitant regulation of T-cell activation and homeostasis." Nat Rev Immunol **4**(5): 387-395.
- Haas, R., J. Smith, V. Rocher-Ros, S. Nadkarni, T. Montero-Melendez, F. D'Acquisto, E. J. Bland, M. Bombardieri, C. Pitzalis, M. Perretti, F. M. Marelli-Berg and C. Mauro (2015). "Lactate Regulates Metabolic and Pro-inflammatory Circuits in Control of T Cell Migration and Effector Functions." PLoS Biol **13**(7): e1002202.
- Hao, J. Q. (2014). "Targeting interleukin-22 in psoriasis." Inflammation **37**(1): 94-99.
- Harrington, L. E., R. D. Hatton, P. R. Mangan, H. Turner, T. L. Murphy, K. M. Murphy and C. T. Weaver (2005). "Interleukin 17-producing CD4+ effector T cells develop via a lineage distinct from the T helper type 1 and 2 lineages." Nat Immunol **6**(11): 1123-1132.

- He, S., K. Kato, J. Jiang, D. R. Wahl, S. Mineishi, E. M. Fisher, D. M. Murasko, G. D. Glick and Y. Zhang (2011). "Characterization of the metabolic phenotype of rapamycin-treated CD8+ T cells with augmented ability to generate long-lasting memory cells." *PLoS One* **6**(5): e20107.
- Hegazy, A. N., M. Peine, C. Helmstetter, I. Panse, A. Frohlich, A. Bergthaler, L. Flatz, D. D. Pinschewer, A. Radbruch and M. Lohning (2010). "Interferons direct Th2 cell reprogramming to generate a stable GATA-3(+)T-bet(+) cell subset with combined Th2 and Th1 cell functions." *Immunity* **32**(1): 116-128.
- Henderson, B., L. Bitensky and J. Chayen (1979). "Glycolytic activity in human synovial lining cells in rheumatoid arthritis." *Ann Rheum Dis* **38**(1): 63-67.
- Henson, S. M., A. Lanna, N. E. Riddell, O. Franzese, R. Macaulay, S. J. Griffiths, D. J. Puleston, A. S. Watson, A. K. Simon, S. A. Tooze and A. N. Akbar (2014). "p38 signaling inhibits mTORC1-independent autophagy in senescent human CD8(+) T cells." *J Clin Invest* **124**(9): 4004-4016.
- Hirota, K., H. Yoshitomi, M. Hashimoto, S. Maeda, S. Teradaira, N. Sugimoto, T. Yamaguchi, T. Nomura, H. Ito, T. Nakamura, N. Sakaguchi and S. Sakaguchi (2007). "Preferential recruitment of CCR6-expressing Th17 cells to inflamed joints via CCL20 in rheumatoid arthritis and its animal model." *J Exp Med* **204**(12): 2803-2812.
- Hitosugi, T., S. Kang, M. G. Vander Heiden, T. W. Chung, S. Elf, K. Lythgoe, S. Dong, S. Lonial, X. Wang, G. Z. Chen, J. Xie, T. L. Gu, R. D. Polakiewicz, J. L. Roesel, T. J. Boggon, F. R. Khuri, D. G. Gilliland, L. C. Cantley, J. Kaufman and J. Chen (2009). "Tyrosine phosphorylation inhibits PKM2 to promote the Warburg effect and tumor growth." *Sci Signal* **2**(97): ra73.
- Hori, S., T. Nomura and S. Sakaguchi (2003). "Control of regulatory T cell development by the transcription factor Foxp3." *Science* **299**(5609): 1057-1061.
- Hot, A., S. Zrioual, M. L. Toh, V. Lenief and P. Miossec (2011). "IL-17A- versus IL-17F-induced intracellular signal transduction pathways and modulation by IL-17RA and IL-17RC RNA interference in rheumatoid synoviocytes." *Ann Rheum Dis* **70**(2): 341-348.
- Hsiao, H. W., T. S. Hsu, W. H. Liu, W. C. Hsieh, T. F. Chou, Y. J. Wu, S. T. Jiang and M. Z. Lai (2015). "Deltex1 antagonizes HIF-1alpha and sustains the stability of regulatory T cells in vivo." *Nat Commun* **6**: 6353.
- Huarte, E., J. R. Cubillos-Ruiz, Y. C. Nesbeth, U. K. Scarlett, D. G. Martinez, X. A. Engle, W. F. Rigby, P. A. Pioli, P. M. Guyre and J. R. Conejo-Garcia (2008). "PILAR is a novel modulator of human T-cell expansion." *Blood* **112**(4): 1259-1268.
- Hueber, W., D. D. Patel, T. Dryja, A. M. Wright, I. Koroleva, G. Bruin, C. Antoni, Z. Draelos, M. H. Gold, G. Psoriasis Study, P. Durez, P. P. Tak, J. J. Gomez-Reino, G. Rheumatoid Arthritis Study, C. S. Foster, R. Y. Kim, C. M. Samson, N. S. Falk, D. S. Chu, D. Callanan, Q. D. Nguyen, G. Uveitis Study, K. Rose, A. Haider and F. Di Padova (2010). "Effects of AIN457, a fully human antibody to interleukin-17A, on psoriasis, rheumatoid arthritis, and uveitis." *Sci Transl Med* **2**(52): 52ra72.
- Isaacs, J. S., Y. J. Jung, D. R. Mole, S. Lee, C. Torres-Cabala, Y. L. Chung, M. Merino, J. Trepel, B. Zbar, J. Toro, P. J. Ratcliffe, W. M. Linehan and L. Neckers (2005). "HIF overexpression correlates with biallelic loss of fumarate hydratase in renal cancer: novel role of fumarate in regulation of HIF stability." *Cancer Cell* **8**(2): 143-153.
- Ivanov, I., B. S. McKenzie, L. Zhou, C. E. Tadokoro, A. Lepelletier, J. J. Lafaille, D. J. Cua and D. R. Littman (2006). "The orphan nuclear receptor RORgamma directs the

- differentiation program of proinflammatory IL-17+ T helper cells." Cell **126**(6): 1121-1133.
- James, E. A., M. Rieck, J. Pieper, J. A. Gebe, B. B. Yue, M. Tatum, M. Peda, C. Sandin, L. Klareskog, V. Malmstrom and J. H. Buckner (2014). "Citruiline-specific Th1 cells are increased in rheumatoid arthritis and their frequency is influenced by disease duration and therapy." Arthritis Rheumatol **66**(7): 1712-1722.
- Jantsch, J., D. Chakravorty, N. Turza, A. T. Prechtel, B. Buchholz, R. G. Gerlach, M. Volke, J. Glasner, C. Warnecke, M. S. Wiesener, K. U. Eckardt, A. Steinkasserer, M. Hensel and C. Willam (2008). "Hypoxia and hypoxia-inducible factor-1 alpha modulate lipopolysaccharide-induced dendritic cell activation and function." J Immunol **180**(7): 4697-4705.
- Jastroch, M., A. S. Divakaruni, S. Mookerjee, J. R. Treberg and M. D. Brand (2010). "Mitochondrial proton and electron leaks." Essays Biochem **47**: 53-67.
- Ju, J. H., Y. J. Heo, M. L. Cho, J. Y. Jhun, J. S. Park, S. Y. Lee, H. J. Oh, S. J. Moon, S. K. Kwok, K. S. Park, S. H. Park and H. Y. Kim (2012). "Modulation of STAT-3 in rheumatoid synovial T cells suppresses Th17 differentiation and increases the proportion of Treg cells." Arthritis Rheum **64**(11): 3543-3552.
- Jung, J. E., H. S. Kim, C. S. Lee, Y. J. Shin, Y. N. Kim, G. H. Kang, T. Y. Kim, Y. S. Juhn, S. J. Kim, J. W. Park, S. K. Ye and M. H. Chung (2008). "STAT3 inhibits the degradation of HIF-1alpha by pVHL-mediated ubiquitination." Exp Mol Med **40**(5): 479-485.
- Kagami, S., H. L. Rizzo, J. J. Lee, Y. Koguchi and A. Blauvelt (2010). "Circulating Th17, Th22, and Th1 cells are increased in psoriasis." J Invest Dermatol **130**(5): 1373-1383.
- Kane, L. P. and A. Weiss (2003). "The PI-3 kinase/Akt pathway and T cell activation: pleiotropic pathways downstream of PIP3." Immunol Rev **192**: 7-20.
- Kehlen, A., A. Pachnio, K. Thiele and J. Langner (2003). "Gene expression induced by interleukin-17 in fibroblast-like synoviocytes of patients with rheumatoid arthritis: upregulation of hyaluronan-binding protein TSG-6." Arthritis Res Ther **5**(4): R186-192.
- Kehrl, J. H., A. B. Roberts, L. M. Wakefield, S. Jakowlew, M. B. Sporn and A. S. Fauci (1986). "Transforming growth factor beta is an important immunomodulatory protein for human B lymphocytes." J Immunol **137**(12): 3855-3860.
- Kehrl, J. H., L. M. Wakefield, A. B. Roberts, S. Jakowlew, M. Alvarez-Mon, R. Derynck, M. B. Sporn and A. S. Fauci (1986). "Production of transforming growth factor beta by human T lymphocytes and its potential role in the regulation of T cell growth." J Exp Med **163**(5): 1037-1050.
- Kellner, H. (2013). "Targeting interleukin-17 in patients with active rheumatoid arthritis: rationale and clinical potential." Ther Adv Musculoskelet Dis **5**(3): 141-152.
- Kim, H. L., E. J. Yeo, Y. S. Chun and J. W. Park (2006). "A domain responsible for HIF-1alpha degradation by YC-1, a novel anticancer agent." Int J Oncol **29**(1): 255-260.
- King, C., S. G. Tangye and C. R. Mackay (2008). "T follicular helper (TFH) cells in normal and dysregulated immune responses." Annu Rev Immunol **26**: 741-766.
- Kleinschek, M. A., K. Boniface, S. Sadekova, J. Grein, E. E. Murphy, S. P. Turner, L. Raskin, B. Desai, W. A. Faubion, R. de Waal Malefyt, R. H. Pierce, T. McClanahan and R. A. Kastelein (2009). "Circulating and gut-resident human Th17 cells express CD161 and promote intestinal inflammation." J Exp Med **206**(3): 525-534.
- Kopf, H., G. M. de la Rosa, O. M. Howard and X. Chen (2007). "Rapamycin inhibits differentiation of Th17 cells and promotes generation of FoxP3+ T regulatory cells." Int Immunopharmacol **7**(13): 1819-1824.

- Kryczek, I., A. T. Bruce, J. E. Gudjonsson, A. Johnston, A. Aphale, L. Vatan, W. Szeliga, Y. Wang, Y. Liu, T. H. Welling, J. T. Elder and W. Zou (2008). "Induction of IL-17+ T cell trafficking and development by IFN-gamma: mechanism and pathological relevance in psoriasis." *J Immunol* **181**(7): 4733-4741.
- Kryczek, I., E. Zhao, Y. Liu, Y. Wang, L. Vatan, W. Szeliga, J. Moyer, A. Klimczak, A. Lange and W. Zou (2011). "Human TH17 cells are long-lived effector memory cells." *Sci Transl Med* **3**(104): 104ra100.
- Kurebayashi, Y., S. Nagai, A. Ikejiri, M. Ohtani, K. Ichiyama, Y. Baba, T. Yamada, S. Egami, T. Hoshii, A. Hirao, S. Matsuda and S. Koyasu (2012). "PI3K-Akt-mTORC1-S6K1/2 axis controls Th17 differentiation by regulating Gfi1 expression and nuclear translocation of RORgamma." *Cell Rep* **1**(4): 360-373.
- Lanzavecchia, A. and F. Sallusto (2000). "Dynamics of T lymphocyte responses: intermediates, effectors, and memory cells." *Science* **290**(5489): 92-97.
- Lebwohl, M. (2003). "Psoriasis." *Lancet* **361**(9364): 1197-1204.
- Lee, E., W. L. Trepicchio, J. L. Oestreicher, D. Pittman, F. Wang, F. Chamian, M. Dhodapkar and J. G. Krueger (2004). "Increased expression of interleukin 23 p19 and p40 in lesional skin of patients with psoriasis vulgaris." *J Exp Med* **199**(1): 125-130.
- Lee, Y. K., H. Turner, C. L. Maynard, J. R. Oliver, D. Chen, C. O. Elson and C. T. Weaver (2009). "Late developmental plasticity in the T helper 17 lineage." *Immunity* **30**(1): 92-107.
- Lehmann, J. C., J. J. Listopad, C. U. Rentsch, F. H. Igney, A. von Bonin, H. H. Hennekes, K. Asadullah and W. D. Docke (2007). "Dimethylfumarate induces immunosuppression via glutathione depletion and subsequent induction of heme oxygenase 1." *J Invest Dermatol* **127**(4): 835-845.
- Lew, W., A. M. Bowcock and J. G. Krueger (2004). "Psoriasis vulgaris: cutaneous lymphoid tissue supports T-cell activation and "Type 1" inflammatory gene expression." *Trends Immunol* **25**(6): 295-305.
- Li, Q., Y. Wang, K. Chen, Q. Zhou, W. Wei, Y. Wang and Y. Wang (2010). "The role of oxidized low-density lipoprotein in breaking peripheral Th17/Treg balance in patients with acute coronary syndrome." *Biochem Biophys Res Commun* **394**(3): 836-842.
- Li, S. H., D. H. Shin, Y. S. Chun, M. K. Lee, M. S. Kim and J. W. Park (2008). "A novel mode of action of YC-1 in HIF inhibition: stimulation of FIH-dependent p300 dissociation from HIF-1{alpha}." *Mol Cancer Ther* **7**(12): 3729-3738.
- Liao, F., R. L. Rabin, C. S. Smith, G. Sharma, T. B. Nutman and J. M. Farber (1999). "CC-chemokine receptor 6 is expressed on diverse memory subsets of T cells and determines responsiveness to macrophage inflammatory protein 3 alpha." *J Immunol* **162**(1): 186-194.
- Lin, S. X., L. Lisi, C. Dello Russo, P. E. Polak, A. Sharp, G. Weinberg, S. Kalinin and D. L. Feinstein (2011). "The anti-inflammatory effects of dimethyl fumarate in astrocytes involve glutathione and haem oxygenase-1." *ASN Neuro* **3**(2).
- Linker, R. A., D. H. Lee, S. Ryan, A. M. van Dam, R. Conrad, P. Bista, W. Zeng, X. Hronowsky, A. Buko, S. Chollate, G. Ellrichmann, W. Bruck, K. Dawson, S. Goelz, S. Wiese, R. H. Scannevin, M. Lukashev and R. Gold (2011). "Fumaric acid esters exert neuroprotective effects in neuroinflammation via activation of the Nrf2 antioxidant pathway." *Brain* **134**(Pt 3): 678-692.
- Litjens, N. H., M. Rademaker, B. Ravensbergen, D. Rea, M. J. van der Plas, B. Thio, A. Walding, J. T. van Dissel and P. H. Nibbering (2004). "Monomethylfumarate affects

- polarization of monocyte-derived dendritic cells resulting in down-regulated Th1 lymphocyte responses." Eur J Immunol **34**(2): 565-575.
- Litjens, N. H., M. Rademaker, B. Ravensbergen, H. B. Thio, J. T. van Dissel and P. H. Nibbering (2006). "Effects of monomethylfumarate on dendritic cell differentiation." Br J Dermatol **154**(2): 211-217.
- Lowes, M. A., T. Kikuchi, J. Fuentes-Duculan, I. Cardinale, L. C. Zaba, A. S. Haider, E. P. Bowman and J. G. Krueger (2008). "Psoriasis vulgaris lesions contain discrete populations of Th1 and Th17 T cells." J Invest Dermatol **128**(5): 1207-1211.
- Lu, H., R. A. Forbes and A. Verma (2002). "Hypoxia-inducible factor 1 activation by aerobic glycolysis implicates the Warburg effect in carcinogenesis." J Biol Chem **277**(26): 23111-23115.
- Lubberts, E., M. I. Koenders and W. B. van den Berg (2005). "The role of T-cell interleukin-17 in conducting destructive arthritis: lessons from animal models." Arthritis Res Ther **7**(1): 29-37.
- Lund-Olesen, K. (1970). "Oxygen tension in synovial fluids." Arthritis Rheum **13**(6): 769-776.
- Luo, W., H. Hu, R. Chang, J. Zhong, M. Knabel, R. O'Meally, R. N. Cole, A. Pandey and G. L. Semenza (2011). "Pyruvate kinase M2 is a PHD3-stimulated coactivator for hypoxia-inducible factor 1." Cell **145**(5): 732-744.
- Luo, W. and G. L. Semenza (2011). "Pyruvate kinase M2 regulates glucose metabolism by functioning as a coactivator for hypoxia-inducible factor 1 in cancer cells." Oncotarget **2**(7): 551-556.
- Ma, H. L., S. Liang, J. Li, L. Napierata, T. Brown, S. Benoit, M. Senices, D. Gill, K. Dunussi-Joannopoulos, M. Collins, C. Nickerson-Nutter, L. A. Fouser and D. A. Young (2008). "IL-22 is required for Th17 cell-mediated pathology in a mouse model of psoriasis-like skin inflammation." J Clin Invest **118**(2): 597-607.
- Macintyre, A. N., V. A. Gerriets, A. G. Nichols, R. D. Michalek, M. C. Rudolph, D. Deoliveira, S. M. Anderson, E. D. Abel, B. J. Chen, L. P. Hale and J. C. Rathmell (2014). "The glucose transporter Glut1 is selectively essential for CD4 T cell activation and effector function." Cell Metab **20**(1): 61-72.
- MacIver, N. J., R. D. Michalek and J. C. Rathmell (2013). "Metabolic regulation of T lymphocytes." Annu Rev Immunol **31**: 259-283.
- Maddur, M. S., P. Miossec, S. V. Kaveri and J. Bayry (2012). "Th17 cells: biology, pathogenesis of autoimmune and inflammatory diseases, and therapeutic strategies." Am J Pathol **181**(1): 8-18.
- Maggi, L., V. Santarlasci, M. Capone, A. Peired, F. Frosali, S. Q. Crome, V. Querci, M. Fambrini, F. Liotta, M. K. Levings, E. Maggi, L. Cosmi, S. Romagnani and F. Annunziato (2010). "CD161 is a marker of all human IL-17-producing T-cell subsets and is induced by RORC." Eur J Immunol **40**(8): 2174-2181.
- Maggi, L., V. Santarlasci, M. Capone, M. C. Rossi, V. Querci, A. Mazzoni, R. Cimaz, R. De Palma, F. Liotta, E. Maggi, S. Romagnani, L. Cosmi and F. Annunziato (2012). "Distinctive features of classic and nonclassic (Th17 derived) human Th1 cells." Eur J Immunol **42**(12): 3180-3188.
- Maher, C. O., K. Dunne, R. Comerford, S. O'Dea, A. Loy, J. Woo, T. R. Rogers, F. Mulcahy, P. J. Dunne and D. G. Doherty (2015). "Candida albicans stimulates IL-23 release by human dendritic cells and downstream IL-17 secretion by Vdelta1 T cells." J Immunol **194**(12): 5953-5960.

- Maher, J. C., M. Wangpaichitr, N. Savaraj, M. Kurtoglu and T. J. Lampidis (2007). "Hypoxia-inducible factor-1 confers resistance to the glycolytic inhibitor 2-deoxy-D-glucose." Mol Cancer Ther **6**(2): 732-741.
- Majmundar, A. J., W. J. Wong and M. C. Simon (2010). "Hypoxia-inducible factors and the response to hypoxic stress." Mol Cell **40**(2): 294-309.
- Maloy, K. J. and F. Powrie (2005). "Fueling regulation: IL-2 keeps CD4+ Treg cells fit." Nat Immunol **6**(11): 1071-1072.
- Manel, N., D. Unutmaz and D. R. Littman (2008). "The differentiation of human T(H)-17 cells requires transforming growth factor-beta and induction of the nuclear receptor RORgamma." Nat Immunol **9**(6): 641-649.
- Marroquin, L. D., J. Hynes, J. A. Dykens, J. D. Jamieson and Y. Will (2007). "Circumventing the Crabtree effect: replacing media glucose with galactose increases susceptibility of HepG2 cells to mitochondrial toxicants." Toxicol Sci **97**(2): 539-547.
- McInnes, I. B. and G. Schett (2011). "The pathogenesis of rheumatoid arthritis." N Engl J Med **365**(23): 2205-2219.
- Michalek, R. D., V. A. Gerriets, S. R. Jacobs, A. N. Macintyre, N. J. MacIver, E. F. Mason, S. A. Sullivan, A. G. Nichols and J. C. Rathmell (2011). "Cutting edge: distinct glycolytic and lipid oxidative metabolic programs are essential for effector and regulatory CD4+ T cell subsets." J Immunol **186**(6): 3299-3303.
- Miyamoto, S., A. N. Murphy and J. H. Brown (2008). "Akt mediates mitochondrial protection in cardiomyocytes through phosphorylation of mitochondrial hexokinase-II." Cell Death Differ **15**(3): 521-529.
- Mosmann, T. R., H. Cherwinski, M. W. Bond, M. A. Giedlin and R. L. Coffman (1986). "Two types of murine helper T cell clone. I. Definition according to profiles of lymphokine activities and secreted proteins." J Immunol **136**(7): 2348-2357.
- Mueckler, M. (1994). "Facilitative glucose transporters." Eur J Biochem **219**(3): 713-725.
- Mueller, W. and B. Herrmann (1979). "Cyclosporin A for psoriasis." N Engl J Med **301**(10): 555.
- Munn, D. H., M. D. Sharma, J. R. Lee, K. G. Jhaver, T. S. Johnson, D. B. Keskin, B. Marshall, P. Chandler, S. J. Antonia, R. Burgess, C. L. Slingluff, Jr. and A. L. Mellor (2002). "Potential regulatory function of human dendritic cells expressing indoleamine 2,3-dioxygenase." Science **297**(5588): 1867-1870.
- Muranski, P., Z. A. Borman, S. P. Kerkar, C. A. Klebanoff, Y. Ji, L. Sanchez-Perez, M. Sukumar, R. N. Reger, Z. Yu, S. J. Kern, R. Roychoudhuri, G. A. Ferreyra, W. Shen, S. K. Durum, L. Feigenbaum, D. C. Palmer, P. A. Antony, C. C. Chan, A. Laurence, R. L. Danner, L. Gattinoni and N. P. Restifo (2011). "Th17 cells are long lived and retain a stem cell-like molecular signature." Immunity **35**(6): 972-985.
- Murphy, E., K. Shibuya, N. Hosken, P. Openshaw, V. Maino, K. Davis, K. Murphy and A. O'Garra (1996). "Reversibility of T helper 1 and 2 populations is lost after long-term stimulation." J Exp Med **183**(3): 901-913.
- Murphy, K., P. Travers, M. Walport and C. Janeway (2008). Janeway's immunobiology. New York, Garland Science.
- Nadkarni, S., C. Mauri and M. R. Ehrenstein (2007). "Anti-TNF-alpha therapy induces a distinct regulatory T cell population in patients with rheumatoid arthritis via TGF-beta." J Exp Med **204**(1): 33-39.
- Nakamura, H., Y. Makino, K. Okamoto, L. Poellinger, K. Ohnuma, C. Morimoto and H. Tanaka (2005). "TCR engagement increases hypoxia-inducible factor-1 alpha

- protein synthesis via rapamycin-sensitive pathway under hypoxic conditions in human peripheral T cells." J Immunol **174**(12): 7592-7599.
- Naldini, A. and F. Carraro (1999). "Hypoxia modulates cyclin and cytokine expression and inhibits peripheral mononuclear cell proliferation." J Cell Physiol **181**(3): 448-454.
- Naldini, A., F. Carraro, S. Silvestri and V. Bocci (1997). "Hypoxia affects cytokine production and proliferative responses by human peripheral mononuclear cells." J Cell Physiol **173**(3): 335-342.
- Nestle, F. O., D. H. Kaplan and J. Barker (2009). "Psoriasis." N Engl J Med **361**(5): 496-509.
- Netea, M. G. (2013). "Training innate immunity: the changing concept of immunological memory in innate host defence." Eur J Clin Invest **43**(8): 881-884.
- Newsholme, P., R. Curi, S. Gordon and E. A. Newsholme (1986). "Metabolism of glucose, glutamine, long-chain fatty acids and ketone bodies by murine macrophages." Biochem J **239**(1): 121-125.
- Ng, C. T., M. Biniecka, A. Kennedy, J. McCormick, O. Fitzgerald, B. Bresnihan, D. Buggy, C. T. Taylor, J. O'Sullivan, U. Fearon and D. J. Veale (2010). "Synovial tissue hypoxia and inflammation in vivo." Ann Rheum Dis **69**(7): 1389-1395.
- Nickoloff, B. J. (1999). "The immunologic and genetic basis of psoriasis." Arch Dermatol **135**(9): 1104-1110.
- Nicolas, J. F., N. Chamchick, J. Thivolet, J. Wijdenes, P. Morel and J. P. Revillard (1991). "CD4 antibody treatment of severe psoriasis." Lancet **338**(8762): 321.
- Nistala, K., S. Adams, H. Cambrook, S. Ursu, B. Olivito, W. de Jager, J. G. Evans, R. Cimaz, M. Bajaj-Elliott and L. R. Wedderburn (2010). "Th17 plasticity in human autoimmune arthritis is driven by the inflammatory environment." Proc Natl Acad Sci U S A **107**(33): 14751-14756.
- Noack, M. and P. Miossec (2014). "Th17 and regulatory T cell balance in autoimmune and inflammatory diseases." Autoimmun Rev **13**(6): 668-677.
- Noseworthy, J. H., C. Lucchinetti, M. Rodriguez and B. G. Weinshenker (2000). "Multiple sclerosis." N Engl J Med **343**(13): 938-952.
- Ochs, H. D., E. Gambineri and T. R. Torgerson (2007). "IPEX, FOXP3 and regulatory T-cells: a model for autoimmunity." Immunol Res **38**(1-3): 112-121.
- Ockenfels, H. M., T. Schultewolter, G. Ockenfels, R. Funk and M. Goos (1998). "The antipsoriatic agent dimethylfumarate immunomodulates T-cell cytokine secretion and inhibits cytokines of the psoriatic cytokine network." Br J Dermatol **139**(3): 390-395.
- Oldenhove, G., N. Bouladoux, E. A. Wohlfert, J. A. Hall, D. Chou, L. Dos Santos, S. O'Brien, R. Blank, E. Lamb, S. Natarajan, R. Kastenmayer, C. Hunter, M. E. Grigg and Y. Belkaid (2009). "Decrease of Foxp3+ Treg cell number and acquisition of effector cell phenotype during lethal infection." Immunity **31**(5): 772-786.
- Owen, C. M. and P. V. Harrison (2000). "Successful treatment of severe psoriasis with basiliximab, an interleukin-2 receptor monoclonal antibody." Clin Exp Dermatol **25**(3): 195-197.
- Palsson-McDermott, E. M., A. M. Curtis, G. Goel, M. A. Lauterbach, F. J. Sheedy, L. E. Gleeson, M. W. van den Bosch, S. R. Quinn, R. Domingo-Fernandez, D. G. Johnston, J. K. Jiang, W. J. Israelsen, J. Keane, C. Thomas, C. Clish, M. Vander Heiden, R. J. Xavier and L. A. O'Neill (2015). "Pyruvate kinase M2 regulates Hif-1alpha activity and IL-1beta induction and is a critical determinant of the warburg effect in LPS-activated macrophages." Cell Metab **21**(1): 65-80.
- Parsonage, G., A. Filer, M. Bik, D. Hardie, S. Lax, K. Howlett, L. D. Church, K. Raza, S. H. Wong, E. Trebilcock, D. Scheel-Toellner, M. Salmon, J. M. Lord and C. D. Buckley

- (2008). "Prolonged, granulocyte-macrophage colony-stimulating factor-dependent, neutrophil survival following rheumatoid synovial fibroblast activation by IL-17 and TNF α ." Arthritis Res Ther **10**(2): R47.
- Patel, S. A. and M. C. Simon (2008). "Biology of hypoxia-inducible factor-2 α in development and disease." Cell Death Differ **15**(4): 628-634.
- Paust, S., L. Lu, N. McCarty and H. Cantor (2004). "Engagement of B7 on effector T cells by regulatory T cells prevents autoimmune disease." Proc Natl Acad Sci U S A **101**(28): 10398-10403.
- Pesce, B., L. Soto, F. Sabugo, P. Wurmman, M. Cuchacovich, M. N. Lopez, P. H. Sotelo, M. C. Molina, J. C. Aguillon and D. Catalan (2013). "Effect of interleukin-6 receptor blockade on the balance between regulatory T cells and T helper type 17 cells in rheumatoid arthritis patients." Clin Exp Immunol **171**(3): 237-242.
- Poggi, A., P. Costa, M. R. Zocchi and L. Moretta (1997). "NKR1A molecule is involved in transendothelial migration of CD4+ human T lymphocytes." Immunol Lett **57**(1-3): 121-123.
- Price, G. S., R. L. Page, J. E. Riviere, J. M. Cline and D. E. Thrall (1996). "Pharmacokinetics and toxicity of oral and intravenous lonidamine in dogs." Cancer Chemother Pharmacol **38**(2): 129-135.
- Quaglino, P., M. Ortoncelli, A. Comessatti, R. Ponti, M. Novelli, M. Bergallo, C. Costa, S. Cicchelli, P. Savoia and M. G. Bernengo (2009). "Circulating CD4+CD25 bright FOXP3+ T cells are up-regulated by biological therapies and correlate with the clinical response in psoriasis patients." Dermatology **219**(3): 250-258.
- Raghavan, S., D. Cao, M. Widhe, K. Roth, J. Herrath, M. Engstrom, G. Roncador, A. H. Banham, C. Trollmo, A. I. Catrina and V. Malmstrom (2009). "FOXP3 expression in blood, synovial fluid and synovial tissue during inflammatory arthritis and intra-articular corticosteroid treatment." Ann Rheum Dis **68**(12): 1908-1915.
- Ramsden, D. B., P. W. Ho, J. W. Ho, H. F. Liu, D. H. So, H. M. Tse, K. H. Chan and S. L. Ho (2012). "Human neuronal uncoupling proteins 4 and 5 (UCP4 and UCP5): structural properties, regulation, and physiological role in protection against oxidative stress and mitochondrial dysfunction." Brain Behav **2**(4): 468-478.
- Rathmell, J. C., C. J. Fox, D. R. Plas, P. S. Hammerman, R. M. Cinalli and C. B. Thompson (2003). "Akt-directed glucose metabolism can prevent Bax conformation change and promote growth factor-independent survival." Mol Cell Biol **23**(20): 7315-7328.
- Renner, K., A. L. Geiselhoringer, M. Fante, C. Bruss, S. Farber, G. Schonhammer, K. Peter, K. Singer, R. Andreesen, P. Hoffmann, P. Oefner, W. Herr and M. Kreuz (2015). "Metabolic plasticity of human T cells: Preserved cytokine production under glucose deprivation or mitochondrial restriction, but 2-deoxy-glucose affects effector functions." Eur J Immunol.
- Ricquier, D. and F. Bouillaud (2000). "The uncoupling protein homologues: UCP1, UCP2, UCP3, StUCP and AtUCP." Biochem J **345 Pt 2**: 161-179.
- Robey, E. and B. J. Fowlkes (1994). "Selective events in T cell development." Annu Rev Immunol **12**: 675-705.
- Rodriguez-Enriquez, S., L. Carreno-Fuentes, J. C. Gallardo-Perez, E. Saavedra, H. Quezada, A. Vega, A. Marin-Hernandez, V. Olin-Sandoval, M. E. Torres-Marquez and R. Moreno-Sanchez (2010). "Oxidative phosphorylation is impaired by prolonged hypoxia in breast and possibly in cervix carcinoma." Int J Biochem Cell Biol **42**(10): 1744-1751.

- Roman, J., T. Rangasamy, J. Guo, S. Sugunan, N. Meednu, G. Packirisamy, L. A. Shimoda, A. Golding, G. Semenza and S. N. Georas (2010). "T-cell activation under hypoxic conditions enhances IFN-gamma secretion." Am J Respir Cell Mol Biol **42**(1): 123-128.
- Roncarolo, M. G., R. Bacchetta, C. Bordignon, S. Narula and M. K. Levings (2001). "Type 1 T regulatory cells." Immunol Rev **182**: 68-79.
- Rossignol, R., R. Gilkerson, R. Aggeler, K. Yamagata, S. J. Remington and R. A. Capaldi (2004). "Energy substrate modulates mitochondrial structure and oxidative capacity in cancer cells." Cancer Res **64**(3): 985-993.
- Rubant, S. A., R. J. Ludwig, S. Diehl, K. Hardt, R. Kaufmann, J. M. Pfeilschifter and W. H. Boehncke (2008). "Dimethylfumarate reduces leukocyte rolling in vivo through modulation of adhesion molecule expression." J Invest Dermatol **128**(2): 326-331.
- Sabatini, D. M. (2006). "mTOR and cancer: insights into a complex relationship." Nat Rev Cancer **6**(9): 729-734.
- Saito, C., A. Maeda and A. Morita (2009). "Bath-PUVA therapy induces circulating regulatory T cells in patients with psoriasis." J Dermatol Sci **53**(3): 231-233.
- Sakaguchi, S., N. Sakaguchi, M. Asano, M. Itoh and M. Toda (1995). "Immunologic self-tolerance maintained by activated T cells expressing IL-2 receptor alpha-chains (CD25). Breakdown of a single mechanism of self-tolerance causes various autoimmune diseases." J Immunol **155**(3): 1151-1164.
- Sallusto, F., J. Geginat and A. Lanzavecchia (2004). "Central memory and effector memory T cell subsets: function, generation, and maintenance." Annu Rev Immunol **22**: 745-763.
- Sallusto, F., E. Kremmer, B. Palermo, A. Hoy, P. Ponath, S. Qin, R. Forster, M. Lipp and A. Lanzavecchia (1999). "Switch in chemokine receptor expression upon TCR stimulation reveals novel homing potential for recently activated T cells." Eur J Immunol **29**(6): 2037-2045.
- Sallusto, F. and A. Lanzavecchia (2009). "Human Th17 cells in infection and autoimmunity." Microbes Infect **11**(5): 620-624.
- Sallusto, F., D. Lenig, R. Forster, M. Lipp and A. Lanzavecchia (1999). "Two subsets of memory T lymphocytes with distinct homing potentials and effector functions." Nature **401**(6754): 708-712.
- Santoro, M. G. (2000). "Heat shock factors and the control of the stress response." Biochem Pharmacol **59**(1): 55-63.
- Saunders, R. N., M. S. Metcalfe and M. L. Nicholson (2001). "Rapamycin in transplantation: a review of the evidence." Kidney Int **59**(1): 3-16.
- Scannevin, R. H., S. Chollate, M. Y. Jung, M. Shackett, H. Patel, P. Bista, W. Zeng, S. Ryan, M. Yamamoto, M. Lukashev and K. J. Rhodes (2012). "Fumarates promote cytoprotection of central nervous system cells against oxidative stress via the nuclear factor (erythroid-derived 2)-like 2 pathway." J Pharmacol Exp Ther **341**(1): 274-284.
- Schlaak, J. F., M. Buslau, W. Jochum, E. Hermann, M. Girndt, H. Gallati, K. H. Meyer zum Buschenfelde and B. Fleischer (1994). "T cells involved in psoriasis vulgaris belong to the Th1 subset." J Invest Dermatol **102**(2): 145-149.
- Schmidt-Weber, C. B., M. Akdis and C. A. Akdis (2007). "TH17 cells in the big picture of immunology." J Allergy Clin Immunol **120**(2): 247-254.
- Schofield, C. J. and P. J. Ratcliffe (2004). "Oxygen sensing by HIF hydroxylases." Nat Rev Mol Cell Biol **5**(5): 343-354.

- Schweckendiek, W. (1959). "[Treatment of psoriasis vulgaris]." Med Monatsschr **13**(2): 103-104.
- Selak, M. A., S. M. Armour, E. D. MacKenzie, H. Boulahbel, D. G. Watson, K. D. Mansfield, Y. Pan, M. C. Simon, C. B. Thompson and E. Gottlieb (2005). "Succinate links TCA cycle dysfunction to oncogenesis by inhibiting HIF-alpha prolyl hydroxylase." Cancer Cell **7**(1): 77-85.
- Semenza, G. L. (2009). "Regulation of oxygen homeostasis by hypoxia-inducible factor 1." Physiology (Bethesda) **24**: 97-106.
- Semenza, G. L. (2010). "HIF-1: upstream and downstream of cancer metabolism." Curr Opin Genet Dev **20**(1): 51-56.
- Sempere-Ortells, J. M., V. Perez-Garcia, G. Marin-Alberca, A. Peris-Pertusa, J. M. Benito, F. M. Marco, J. J. Zubcoff and F. J. Navarro-Blasco (2009). "Quantification and phenotype of regulatory T cells in rheumatoid arthritis according to disease activity score-28." Autoimmunity **42**(8): 636-645.
- Sengupta, S., P. M. Chilton and T. C. Mitchell (2005). "Adjuvant-induced survival signaling in clonally expanded T cells is associated with transient increases in pAkt levels and sustained uptake of glucose." Immunobiology **210**(9): 647-659.
- Shahrara, S., S. R. Pickens, A. Dorfleutner and R. M. Pope (2009). "IL-17 induces monocyte migration in rheumatoid arthritis." J Immunol **182**(6): 3884-3891.
- Shay, J. E. and M. Celeste Simon (2012). "Hypoxia-inducible factors: crosstalk between inflammation and metabolism." Semin Cell Dev Biol **23**(4): 389-394.
- Shen, H., J. C. Goodall and J. S. Hill Gaston (2009). "Frequency and phenotype of peripheral blood Th17 cells in ankylosing spondylitis and rheumatoid arthritis." Arthritis Rheum **60**(6): 1647-1656.
- Shi, L. Z., R. Wang, G. Huang, P. Vogel, G. Neale, D. R. Green and H. Chi (2011). "HIF1alpha-dependent glycolytic pathway orchestrates a metabolic checkpoint for the differentiation of TH17 and Treg cells." J Exp Med **208**(7): 1367-1376.
- Silman, A. J. and J. E. Pearson (2002). "Epidemiology and genetics of rheumatoid arthritis." Arthritis Res **4 Suppl 3**: S265-272.
- Strauss, L., M. Czystowska, M. Szajnik, M. Mandapathil and T. L. Whiteside (2009). "Differential responses of human regulatory T cells (Treg) and effector T cells to rapamycin." PLoS One **4**(6): e5994.
- Stritesky, G. L., N. Yeh and M. H. Kaplan (2008). "IL-23 promotes maintenance but not commitment to the Th17 lineage." J Immunol **181**(9): 5948-5955.
- Sugiyama, H., R. Gyulai, E. Toichi, E. Garaczi, S. Shimada, S. R. Stevens, T. S. McCormick and K. D. Cooper (2005). "Dysfunctional blood and target tissue CD4+CD25high regulatory T cells in psoriasis: mechanism underlying unrestrained pathogenic effector T cell proliferation." J Immunol **174**(1): 164-173.
- Symmons, D. P., C. R. Bankhead, B. J. Harrison, P. Brennan, E. M. Barrett, D. G. Scott and A. J. Silman (1997). "Blood transfusion, smoking, and obesity as risk factors for the development of rheumatoid arthritis: results from a primary care-based incident case-control study in Norfolk, England." Arthritis Rheum **40**(11): 1955-1961.
- Szabo, S. J., N. G. Jacobson, A. S. Dighe, U. Gubler and K. M. Murphy (1995). "Developmental commitment to the Th2 lineage by extinction of IL-12 signaling." Immunity **2**(6): 665-675.
- Szabo, S. J., S. T. Kim, G. L. Costa, X. Zhang, C. G. Fathman and L. H. Glimcher (2000). "A novel transcription factor, T-bet, directs Th1 lineage commitment." Cell **100**(6): 655-669.

- Taams, L., M. Vukmanovic-Stejic, M. Salmon and A. Akbar (2003). "Immune regulation by CD4+CD25+ regulatory T cells: implications for transplantation tolerance." Transpl Immunol **11**(3-4): 277-285.
- Tandon, P., C. A. Gallo, S. Khatri, J. F. Barger, H. Yepiskoposyan and D. R. Plas (2011). "Requirement for ribosomal protein S6 kinase 1 to mediate glycolysis and apoptosis resistance induced by Pten deficiency." Proc Natl Acad Sci U S A **108**(6): 2361-2365.
- Taylor, A., J. Verhagen, K. Blaser, M. Akdis and C. A. Akdis (2006). "Mechanisms of immune suppression by interleukin-10 and transforming growth factor-beta: the role of T regulatory cells." Immunology **117**(4): 433-442.
- Telfer, N. R., R. J. Chalmers, K. Whale and G. Colman (1992). "The role of streptococcal infection in the initiation of guttate psoriasis." Arch Dermatol **128**(1): 39-42.
- Teng, C. M., C. C. Wu, F. N. Ko, F. Y. Lee and S. C. Kuo (1997). "YC-1, a nitric oxide-independent activator of soluble guanylate cyclase, inhibits platelet-rich thrombosis in mice." Eur J Pharmacol **320**(2-3): 161-166.
- Tobin, A. M. and B. Kirby (2005). "TNF alpha inhibitors in the treatment of psoriasis and psoriatic arthritis." BioDrugs **19**(1): 47-57.
- Tomasoni, R., V. Basso, K. Pilipow, G. Sitia, S. Sacconi, A. Agresti, F. Mietton, G. Natoli, S. Colombetti and A. Mondino (2011). "Rapamycin-sensitive signals control TCR/CD28-driven Ifng, Il4 and Foxp3 transcription and promoter region methylation." Eur J Immunol **41**(7): 2086-2096.
- Towler, M. C. and D. G. Hardie (2007). "AMP-activated protein kinase in metabolic control and insulin signaling." Circ Res **100**(3): 328-341.
- Treumer, F., K. Zhu, R. Glaser and U. Mrowietz (2003). "Dimethylfumarate is a potent inducer of apoptosis in human T cells." J Invest Dermatol **121**(6): 1383-1388.
- Usui, T., J. C. Preiss, Y. Kanno, Z. J. Yao, J. H. Bream, J. J. O'Shea and W. Strober (2006). "T-bet regulates Th1 responses through essential effects on GATA-3 function rather than on IFNG gene acetylation and transcription." J Exp Med **203**(3): 755-766.
- Uyemura, K., M. Yamamura, D. F. Fivenson, R. L. Modlin and B. J. Nickoloff (1993). "The cytokine network in lesional and lesion-free psoriatic skin is characterized by a T-helper type 1 cell-mediated response." J Invest Dermatol **101**(5): 701-705.
- Valencia, X., G. Stephens, R. Goldbach-Mansky, M. Wilson, E. M. Shevach and P. E. Lipsky (2006). "TNF downmodulates the function of human CD4+CD25hi T-regulatory cells." Blood **108**(1): 253-261.
- van Amelsfort, J. M., K. M. Jacobs, J. W. Bijlsma, F. P. Lafeber and L. S. Taams (2004). "CD4(+)CD25(+) regulatory T cells in rheumatoid arthritis: differences in the presence, phenotype, and function between peripheral blood and synovial fluid." Arthritis Rheum **50**(9): 2775-2785.
- van Amelsfort, J. M., J. A. van Roon, M. Noordegraaf, K. M. Jacobs, J. W. Bijlsma, F. P. Lafeber and L. S. Taams (2007). "Proinflammatory mediator-induced reversal of CD4+,CD25+ regulatory T cell-mediated suppression in rheumatoid arthritis." Arthritis Rheum **56**(3): 732-742.
- van der Windt, G. J., B. Everts, C. H. Chang, J. D. Curtis, T. C. Freitas, E. Amiel, E. J. Pearce and E. L. Pearce (2012). "Mitochondrial respiratory capacity is a critical regulator of CD8+ T cell memory development." Immunity **36**(1): 68-78.
- Vandermeeren, M., S. Janssens, M. Borgers and J. Geysen (1997). "Dimethylfumarate is an inhibitor of cytokine-induced E-selectin, VCAM-1, and ICAM-1 expression in human endothelial cells." Biochem Biophys Res Commun **234**(1): 19-23.

- Veldhoen, M., C. Uyttenhove, J. van Snick, H. Helmbj, A. Westendorf, J. Buer, B. Martin, C. Wilhelm and B. Stockinger (2008). "Transforming growth factor-beta 'reprograms' the differentiation of T helper 2 cells and promotes an interleukin 9-producing subset." Nat Immunol **9**(12): 1341-1346.
- Volpe, E., N. Servant, R. Zollinger, S. I. Bogiatzi, P. Hupe, E. Barillot and V. Soumelis (2008). "A critical function for transforming growth factor-beta, interleukin 23 and proinflammatory cytokines in driving and modulating human T(H)-17 responses." Nat Immunol **9**(6): 650-657.
- Wang, G. L. and G. L. Semenza (1993). "Desferrioxamine induces erythropoietin gene expression and hypoxia-inducible factor 1 DNA-binding activity: implications for models of hypoxia signal transduction." Blood **82**(12): 3610-3615.
- Warburg, O. (1956). "On the origin of cancer cells." Science **123**(3191): 309-314.
- Warburg, O., K. Gawehn and A. W. Geissler (1958). "[Metabolism of leukocytes]." Z Naturforsch B **13B**(8): 515-516.
- Wei, G., L. Wei, J. Zhu, C. Zang, J. Hu-Li, Z. Yao, K. Cui, Y. Kanno, T. Y. Roh, W. T. Watford, D. E. Schones, W. Peng, H. W. Sun, W. E. Paul, J. J. O'Shea and K. Zhao (2009). "Global mapping of H3K4me3 and H3K27me3 reveals specificity and plasticity in lineage fate determination of differentiating CD4+ T cells." Immunity **30**(1): 155-167.
- Weiner, H. L. (2001). "Induction and mechanism of action of transforming growth factor-beta-secreting Th3 regulatory cells." Immunol Rev **182**: 207-214.
- Wilms, H., J. Sievers, U. Rickert, M. Rostami-Yazdi, U. Mrowietz and R. Lucius (2010). "Dimethylfumarate inhibits microglial and astrocytic inflammation by suppressing the synthesis of nitric oxide, IL-1beta, TNF-alpha and IL-6 in an in-vitro model of brain inflammation." J Neuroinflammation **7**: 30.
- Wilson, D. F., W. L. Rumsey, T. J. Green and J. M. Vanderkooi (1988). "The oxygen dependence of mitochondrial oxidative phosphorylation measured by a new optical method for measuring oxygen concentration." J Biol Chem **263**(6): 2712-2718.
- Wilson, N. J., K. Boniface, J. R. Chan, B. S. McKenzie, W. M. Blumenschein, J. D. Mattson, B. Basham, K. Smith, T. Chen, F. Morel, J. C. Lecron, R. A. Kastelein, D. J. Cua, T. K. McClanahan, E. P. Bowman and R. de Waal Malefyt (2007). "Development, cytokine profile and function of human interleukin 17-producing helper T cells." Nat Immunol **8**(9): 950-957.
- Wolk, K., E. Witte, K. Warszawska, G. Schulze-Tanzil, K. Witte, S. Philipp, S. Kunz, W. D. Docke, K. Asadullah, H. D. Volk, W. Sterry and R. Sabat (2009). "The Th17 cytokine IL-22 induces IL-20 production in keratinocytes: a novel immunological cascade with potential relevance in psoriasis." Eur J Immunol **39**(12): 3570-3581.
- Xinqiang, S., L. Fei, L. Nan, L. Yuan, Y. Fang, X. Hong, T. Lixin, L. Juan, Z. Xiao, S. Yuying and X. Yongzhi (2010). "Therapeutic efficacy of experimental rheumatoid arthritis with low-dose methotrexate by increasing partially CD4+CD25+ Treg cells and inducing Th1 to Th2 shift in both cells and cytokines." Biomed Pharmacother **64**(7): 463-471.
- Yan, K. X., X. Fang, L. Han, Z. H. Zhang, K. F. Kang, Z. Z. Zheng and Q. Huang (2010). "Foxp3+ regulatory T cells and related cytokines differentially expressed in plaque vs. guttate psoriasis vulgaris." Br J Dermatol **163**(1): 48-56.
- Yang, L., D. E. Anderson, C. Baecher-Allan, W. D. Hastings, E. Bettelli, M. Oukka, V. K. Kuchroo and D. A. Hafler (2008). "IL-21 and TGF-beta are required for differentiation of human T(H)17 cells." Nature **454**(7202): 350-352.

- Yost, J. and J. E. Gudjonsson (2009). "The role of TNF inhibitors in psoriasis therapy: new implications for associated comorbidities." F1000 Med Rep **1**.
- Zeiser, R., D. B. Leveson-Gower, E. A. Zambricki, N. Kambham, A. Beilhack, J. Loh, J. Z. Hou and R. S. Negrin (2008). "Differential impact of mammalian target of rapamycin inhibition on CD4+CD25+Foxp3+ regulatory T cells compared with conventional CD4+ T cells." Blood **111**(1): 453-462.
- Zhang, L., H. Li, X. Hu, D. M. Benedek, C. S. Fullerton, R. D. Forsten, J. A. Naifeh, X. Li, H. Wu, K. N. Benevides, T. Le, S. Smerin, D. W. Russell and R. J. Ursano (2015). "Mitochondria-focused gene expression profile reveals common pathways and CPT1B dysregulation in both rodent stress model and human subjects with PTSD." Transl Psychiatry **5**: e580.
- Zhang, L., X. Q. Yang, J. Cheng, R. S. Hui and T. W. Gao (2010). "Increased Th17 cells are accompanied by FoxP3(+) Treg cell accumulation and correlated with psoriasis disease severity." Clin Immunol **135**(1): 108-117.
- Zhang, W., J. Zhang, L. Fang, L. Zhou, S. Wang, Z. Xiang, Y. Li, B. Wisely, G. Zhang, G. An, Y. Wang, S. Leung and Z. Zhong (2012). "Increasing human Th17 differentiation through activation of orphan nuclear receptor retinoid acid-related orphan receptor gamma (RORgamma) by a class of aryl amide compounds." Mol Pharmacol **82**(4): 583-590.
- Zhao, M., M. Schlame, D. Rua and M. L. Greenberg (1998). "Cardiolipin synthase is associated with a large complex in yeast mitochondria." J Biol Chem **273**(4): 2402-2408.
- Zheng, Y., D. M. Danilenko, P. Valdez, I. Kasman, J. Eastham-Anderson, J. Wu and W. Ouyang (2007). "Interleukin-22, a T(H)17 cytokine, mediates IL-23-induced dermal inflammation and acanthosis." Nature **445**(7128): 648-651.
- Zoghi, S., Z. Amirghofran, A. Nikseresht, N. Ashjazadeh, E. Kamali-Sarvestani and N. Rezaei (2011). "Cytokine secretion pattern in treatment of lymphocytes of multiple sclerosis patients with fumaric acid esters." Immunol Invest **40**(6): 581-596.